UiT The Arctic University of Norway

Faculty of Science and Technology
Department of Chemistry

Exploring fluorination in MBL inhibitor design

Alexandra Kondratieva

A dissertation for the degree of Philosophiae Doctor   May 2024

UiT The Arctic University of Norway

"There is nothing more deceptive than an obvious fact."

Acknowledgements

Embarking on this journey, if someone would have told me what the coming years would bring, I would have been in a state of utter disbelief. Yet here we are. It has been quite the experience. At times I have enjoyed it, at times I have endured it, but one thing is for sure, it would not have been possible without a particular group of people.

First and foremost, I would like to express my immense gratitude to Annette. Thank you for providing me with this opportunity, for your encouragement and guidance, for always finding time, for your patience and belief in me. I appreciate all the lengthy project-related discussions (well beyond the allocated meeting time) as well as your understanding and advice concerning any other problems I happened to encounter. You have helped me come a long way and it has been a great pleasure to work under your supervision.

Thank you to my co-supervisor Hanna-Kirsti for sharing your expertise and guidance throughout my research. I would also like to thank all of my co-authors for their contributions to the project. A special thanks to Kate for coming all the way to Tromsø and making this collaboration possible. Thank you to Prof. Máté Erdélyi for your insights and input. I would also like to thank Phil for joining in on the fun, all the great discussions and helping out with the NMR. Additionally, I would like to express my gratitude to Prof. Nathaniel Martin and his group for the warm welcome and sharing their knowledge on conjugates.

I would like to express my gratefulness to all the past and present group members of the Bayer and CHOCO groups for all the help and friendly working environment. Thank you to Aya for welcoming me into the group. A shout-out to Manuel for being the best labmate and helping me out on innumerable occasions, including the cumbersome task of proof reading. I guess this calls for at least one cake, maybe two tops. I am extremely grateful for everything and I am going to miss all the chats, scientific discussions and the music.

Thank you to all my fellow co-workers at the department: Yngve, Anna, Bjørn, Tone, Floriane, just to name a few, for all the shared laughs and experiences. A special thanks to the engineers, Jostein Johansen and Truls Ingebrigsten, for providing assistance in the day-to-day research life.

To all the friends made during the past years. Hanna and Manuel, thanks to you I managed to discover Tromsø from a different aspect and find out that I am capable of way more than I thought. I genuinely appreciate all the good times spent with you guys and am beyond grateful for the support in overcoming the hardships of the few past years. A special thanks for introducing me to climbing. On this topic, cheers to all the wonderful people I have met through this activity. Thanks to Swantje for our friendship, understanding, countless conversations and dog walks. Thank you for your encouragement and Tromsø would have been very different without you. Danielle and Johan, thanks to you guys for all the laughs and good times, hopefully there are more to come.

Lastly, I would like to express my gratitude to my family, relatives and friends left behind. I appreciate the continuous support from all of you during these challenging past few years and all the great memories shared during my brief, but anticipated visits. I miss you all and wish we could see each other

more often. A separate thanks to my sister for the extensive phone call conversations, being there for me and sharing my interests.

Once again, a big thank you to everyone mentioned above and to anyone, whose name was not listed, but was still part of my PhD journey.

<div align="right">

Alexandra Kondratieva
May 2024, Tromsø, Norway

</div>

Abstract

Antimicrobial resistance (AMR) achieved through, among others, β-lactamase activity, remains an ongoing challenge for the treatment of infections caused by antibiotic-resistant pathogens. Metallo-β-lactamase (MBL)-expressing bacteria, resistant to most β-lactam antibiotics, are of growing clinical relevance with currently no approved treatment options available. The most common approaches to combating AMR include the modification of existing compounds or the development of new drugs and inhibitors. Alternative strategies are also being explored, including novel drug delivery systems. Recently, an approach based on exploiting the ability of MBLs to hydrolyze β-lactams has been investigated using cephalosporin prodrugs. The reported conjugates consisted of aromatic thiol-based MBL inhibitors linked to a cephalosporin scaffold that was designed to release the inhibitors upon enzymatic hydrolysis.

The goal of the current work was to extend the concept of thiol-releasing conjugates to aliphatic thiol-based MBL inhibitors, as aliphatic thiols have been described to lack the required leaving group properties. The work is based on the hypothesis that fluorination in the vicinity of the thiol moiety can be used as a tool in the design of aliphatic thiol-releasing conjugates.

Thus, the initial focus was on designing fluorinated captopril analogues, exhibiting inhibitory activity against relevant MBLs, and investigating the influence of fluorination on their inhibitory effect. A library of fluorinated thiols, of which several exhibited IC_{50} values in the low micromolar region against NDM-1, was developed. Furthermore, the use of fluorinated inhibitors as probes for NMR-based binding studies was demonstrated on a representative compound.

Among the active thiols, a few were selected for attachment to the cephalosporin core, resulting in a series of conjugates. The hydrolysis of the conjugates was examined and the inhibitory activity against several MBLs was determined. The conjugates were shown to release the thiols, as determined by LC-MS and NMR. In addition, IC_{50} values of the conjugates were found to be in a similar range to the respective thiol inhibitors.

In summary, the obtained conjugates verified that fluorination facilitates the release of aliphatic thiol-based inhibitors and provide directions for future conjugate development. Moreover, fluorinated thiol inhibitors can assist in studies of inhibitor-enzyme interactions and conjugate hydrolysis utilizing ^{19}F NMR methods.

Summary of papers and author contributions

Paper I

Fluorinated Captopril Analogues Inhibit Metallo-β-Lactamases and Facilitate Structure Determination of NDM-1 Binding Pose.

Alexandra Kondratieva, Katarzyna Palica, Christopher Frøhlich, Rebekka Rolfsnes Hovd, Hanna-Kirsti S. Leiros, Mate Erdelyi, Annette Bayer, *Eur. J. Med. Chem.* **2024**, *266*, 116140.

Paper Summary:

In paper I we developed a small library of trifluoromethylated captopril analogues as MBL inhibitors. The compounds were designed to act as probes for structural studies of enzyme-inhibitor binding poses. The inhibitory activity and synergistic effect of the fluorinated thiols were investigated and found to be comparable to the non-fluorinated inhibitors. We demonstrated that fluorinated analogues of inhibitors can be used to determine the binding pose.

My contribution:

I contributed to the planning and development of the synthetic strategy. I synthesized all the compounds and analyzed all analytical data. I contributed to the analysis and contextualization of IC_{50} and MIC values. I wrote the first draft of the manuscript, with the exception of the sections regarding NMR and molecular docking binding pose determination. I did not carry out the biological and NMR titration experiments.

Paper II

The Use of Fluorinated Aliphatic Thiols in the Design of Cephalosporin Conjugates – Manuscript

Alexandra Kondratieva, Philip Rainsford, Perwez Bakht, Hanna-Kirsti S. Leiros, Ranjana Pathania, Annette Bayer.

Paper Summary

In paper II we studied the release of thiol MBL inhibitors from cephalosporin conjugates. For that, conjugates containing trifluoromethylated thiols were designed and synthesized. The β-lactam ring cleavage of the conjugates under basic and enzymatic conditions was examined. We demonstrated that fluorination could facilitate release of aliphatic thiol inhibitors. The inhibitory activity of the conjugates was evaluated.

My contribution:

I contributed to the planning and development of the synthetic strategy. I synthesized all the compounds and analyzed all analytical data. I carried out the kinetic hydrolysis studies and contributed to the interpretation of the obtained results. I contributed to the analysis and contextualization of IC_{50} values. I wrote the first draft of the manuscript. I did not carry out the biological experiments.

Table of Contents

Abbreviations

ACE	Angiotensin-converting enzyme
AIM	Adelaide imipenemase
AmpC	Class C β-lactamases
AMR	Antimicrobial resistance
BcII	*Bacillus cereus* type II
BL	β-Lactam
BTZ	Bisthiazolidine
CDI	Carbonyl diimidazole
CMPI	2-Chloro-1-methylpyridinium iodide
COMU	(1-Cyano-2-ethoxy-2-oxoethylidenaminooxy)dimethylamino-morpholino-carbenium hexafluorophosphate
CphA	Carbapenem-hydrolyzing metallo-β-lactamase
DABCO	1,4-Diazabicyclo[2.2.2]octane
DBU	1,8-Diazabicyclo[5.4.0]undec-7-ene
DCE	Dichloroethane
DCM	Dichloromethane
DIPEA	*N*,*N*-Diisopropylethylamine
DMAP	4-(Dimethylamino)pyridine
DMF	Dimethylformamide
DPA	Dipicolinic acid
EDC/EDC HCl	1-Ethyl-3-(3-dimethylaminopropyl)carbodiimide hydrochloride
ESBL	Extended-spectrum β-lactamase
GCLE	4-Methoxybenzyl 3-chloromethyl-7-(2-phenylacetamido)-3-cephem-4-carboxylate
GIM	German imepenemase
GOB	*Elizabethkingia meningoseptica* class B
HATU	Hexafluorophosphate azabenzotriazole tetramethyl uronium
HBTU	Hexafluorophosphate benzotriazole tetramethyl uronium
HEPES	4-(2-Hydroxyethyl)-1-piperazineethanesulfonic acid
HOAt	1-Hydroxy-7-azabenzotriazole
HOBt	1-Hydroxybenzotriazole

HPLC	High-performance liquid chromatography
IBCF	Isobutyl chloroformate
IC_{50}	Half-maximal inhibitory concentration
IMP	Imepenemase
KPC	*Klebsiella pneumoniae* carbapenemase
L1	Labile β-lactamase from *S. maltophilia*
LC-MS	Liquid chromatography–mass spectrometry
MBL	Metallo-β-lactamase
*m*CPBA	*m*-Chloroperoxybenzoic acid
MIC	Minimum inhibitory concentration
MMC	7-Mercapto-4-methylcoumarin
MPLC	Medium-pressure liquid chromatography
MW	Microwave
NDM	New Delhi metallo-β-lactamase
NMM	*N*-Methylmorpholine
NMR	Nuclear magnetic resonance
o/n	Overnight
OXA	Oxacillinase
PMB	*p*-Methoxybenzyl
PyBOP	Benzotriazole-1-yl-oxy-tris-pyrrolidino-phosphonium hexafluorophosphate
rt	Room temperature
SBL	Serine-β-lactamase
SFH	*Serratia fonticola* carbapenem hydrolase
SMB	*Serratia* metallo-β-lactamase
SPM	Sao Paulo metallo-β-lactamase
TBTA	*tert*-Butyl 2,2,2-trichloroacetimidate
TFA	Trifluoroacetic acid
TFFH	Tetramethylfluoroformamidinium hexafluorophosphate
THF	Tetrahydrofuran
TLC	Thin layer chromatography
TMB	Tripoli metallo-β-lactamase
TMS	Tetramethylsilane
TMU	Tetramethylurea
T3P	Propylphosphonic anhydride

VIM	Verona integron-encoded metallo-β-lactamase
7-ACA	7-Aminocephalosporanic acid
8-TQ	8-Thioquinoline

1 Introduction

Antibiotics have played a significant role in opposing infectious diseases and prolonging the average life expectancy. Nonetheless, the growing resistance towards these drugs has threatened the successful treatment of bacterial infections. Although there are many factors influencing antimicrobial resistance (AMR), overuse and misuse of antibiotics remain the leading causes.[1] Thus, there is a simultaneous need for both new effective treatment options to counteract resistant pathogens and the establishment of appropriate antibiotic consumption practices.

β-Lactams are the most prescribed class of antibiotics due to their broad spectrum of activity.[2] β-Lactam resistance is mainly realized through the expression of β-lactamases, enzymes which can cleave the β-lactam ring, inactivating the antibiotics. Of particular concern are extended spectrum β-lactamases (ESBLs) and carbapenemases. The development of resistance towards carbapenems, also known as last-resort antibiotics, leaving no other options for the treatment of bacterial infections, poses a global health issue.[3] Metallo-β-lactamases (MBLs) are the clinically most threatening carbapenemases, due to their ability to hydrolyze a wide range of β-lactams.

From a medicinal chemistry perspective, to overcome β-lactamase-mediated resistance two tactics have been identified: 1) development of new drugs as alternatives to those rendered ineffective or 2) preservation of the longevity of antibiotics currently in use.[4] Since the "golden age" of antibiotic discovery, very few new classes of drugs have managed to reach the market and the focus has shifted to the derivatization of already approved drugs.[5] The slow rate at which new antibiotics are developed alongside the rapid proliferation of antibiotic-resistant strains have forced the investigation of alternative strategies. Combining a β-lactam antibiotic with a small-molecule inhibitor, capable of counteracting β-lactamase activity, has shown to be successful in overcoming AMR.[6]

The development of new antibiotics or inhibitors, especially those effective against multidrug-resistant bacteria, is highly challenging.[7] This is partially due to incomplete knowledge on the permeability of bacterial membranes and efflux mechanisms. In order to develop new active molecules, it is crucial to gain further insight into the binding sites and modes. Furthermore, due to the structural variety and constant evolution of MBL enzymes, novel strategies are necessary to advance drug and inhibitor design. With less than 20% sequence identity between subclasses, the structural diversity of MBLs, represented by varying zinc content and low homology among the active site residues, necessitates the demanding task of developing broad-spectrum inhibitors.[8-9]

Although there are currently no MBL inhibitors approved for clinical use, scientific advancement has been focused on the development of zinc-binding and zinc-chelating molecules. Compounds containing thiol, carboxylic acid, pyridine and, more recently, cyclic boronate moieties have received the most attention as potential MBL inhibitors.[10-11] Aliphatic thiol inhibitors have demonstrated a broad spectrum of activity towards MBLs, thus having an advantage over other compound classes for MBL inhibitor design.[12-13] Nevertheless, use of thiols as MBL inhibitors is impeded by their tendency to oxidize and form disulfides or interact with other metalloenzymes.

A more recent approach to combating resistance, utilizes β-lactam (BL) conjugates as prodrugs, in which a thiol inhibitor is attached to a β-lactam scaffold. There are several reports illustrating that, upon β-lactamase-mediated hydrolysis, specifically designed BL conjugates can release various moieties.[14] In

a similar manner, MBL-mediated cleavage of the β-lactam ring can be used for intracellular release of inhibitors. This approach allows for the selective delivery of inhibitors to MBL-producing pathogens. Furthermore, the usage of conjugates could help reduce the risk of off-target effects and protect the thiol functionality from unwanted reactions.

1.1 Aim of the thesis

The overall aim of the thesis was to develop BL conjugates releasing, upon β-lactamase-mediated hydrolysis, an alkyl thiol-based MBL inhibitor (Fig. 1). Previously reported conjugates demonstrated that release of alkyl thiol inhibitors is problematic, due to their leaving group ability. Alkyl thiols are an important component of MBL inhibitor development, therefore the design of thiols with altered leaving group ability is of relevance. We hypothesized that the incorporation of an electron withdrawing group, such as fluorine, in the vicinity of the thiol moiety would facilitate the release of alkyl thiol inhibitors.

The conjugates can be divided into two structural parts – the β-lactam core and the thiol inhibitor. In this work, the cephalosporin core and fluorinated captopril derivatives were chosen as the β-lactam part and the thiol inhibitors, respectively. Cephalosporin-based conjugates have been shown to successfully release various moieties upon MBL-mediated hydrolysis. Moreover, various synthetic pathways to these conjugates are described in literature, making the cephalosporin core a feasible and accessible scaffold. Captopril and reported analogues, which have shown inhibitory activity towards various MBLs, served as the starting point for the fluorinated thiol inhibitors.
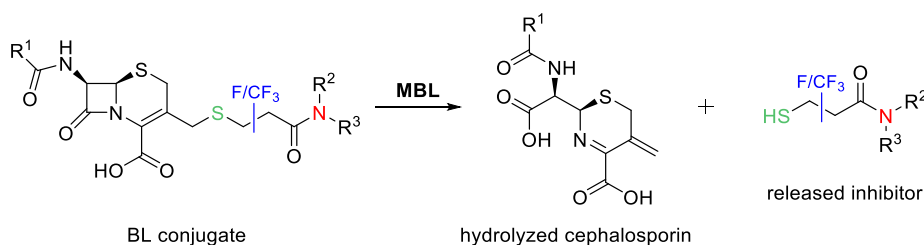
Figure 1. General structure of the envisioned conjugates and the released inhibitors.

In order to achieve the goal of designing a conjugate with a releasable alkyl thiol inhibitor, the following objectives were set:

- Synthesis and evaluation of a library of fluorinated thiol-based compounds as inhibitors against MBLs.
- Assessment of the influence of fluorination on inhibitory activity and gaining insight into the inhibitor binding mode using NMR spectroscopy.
- Synthesis of cephalosporin conjugates with fluorinated alkyl thiols and exploration of the release of the active inhibitor.

1.2 Outline

The thesis consists of several chapters. A brief introduction to the topic of the thesis as well as the aim are described in Chapter 1. Chapter 2 is composed of the relevant background information, providing an overview of the research topic from a broader perspective. Subchapters 2.1 and 2.2 present further insight into the issue of AMR and MBL-based hydrolysis of β-lactams. One of the most pursued methods of overcoming antimicrobial resistance, development of β-lactamase inhibitors, is discussed in subchapter 2.3. Subchapter 2.4 introduces the concept of β-lactamase-activated conjugates, highlighting the applications and synthetic strategies towards BL probes. The synthetic approaches to relevant thiol-

containing MBL inhibitors are reviewed in subchapter 2.5. Chapter 3 provides the summarized findings of the thesis, including those presented in papers I and II. The discussion of the overall result and future prospects are provided in Chapter 4. The conclusion is outlined in Chapter 5. The appendix with experimental procedures that are not included in the papers and references constitute Chapters 6 and 7, respectively.

2 Background relevant for this thesis

2.1 β-Lactam antibiotics and AMR

Ever since penicillin had been introduced for the treatment of bacterial infections, β-lactam antibiotics have become the most frequently prescribed antibacterial compounds. This antibiotic group shares the common structural feature of 2-azetidinone, more commonly known as the β-lactam ring.[15]

β-Lactam antibiotics are divided into the following classes: penicillins, cephalosporins, carbapenems and monobactams (Fig. 2).[2] The classification is based on the structure of the ring fused to the β-lactam scaffold. For penicillins and cephalosporins the β-lactam ring is fused to a five and six-membered ring containing sulfur, respectively. Carbapenems have a cyclopentene attached to the β-lactam core, while monobactams are the only group without a ring fused to the β-lactam ring.[16]
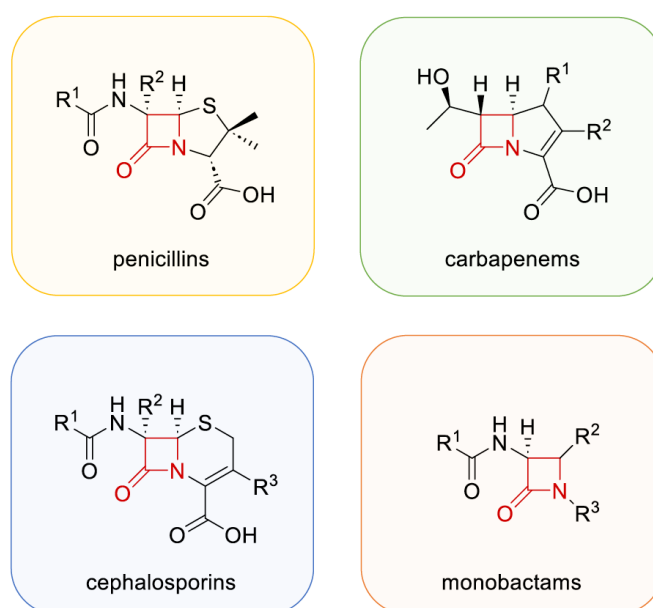
Figure 2. Chemical structures of the different classes of β-lactam antibiotics. The β-lactam ring is shown in red.

However, the flourishing of β-lactam antibiotics has been overshadowed by the emergence of resistant bacteria. Antimicrobial resistance is a threat to global health, challenging the treatment of a variety of infections. While there exist various mechanisms of resistance, hydrolysis of β-lactam antibiotics by β-lactamases (BLases) is considered the most common and worrying among them.[17]

2.2 β-Lactamases

According to the Ambler classification, β-lactamases are divided into classes A, C, D, which comprise serine β-lactamases (SBLs), and class B or metallo-β-lactamases (MBLs) (Fig. 3).[18-19] The distinction between SBLs and MBLs is based on the mechanism of the β-lactam ring hydrolysis. SBLs utilize a serine residue in the active site to hydrolyze a β-lactam, while MBL-mediated hydrolysis occurs via a hydroxide ion, stabilized by zinc in the active site.[20]
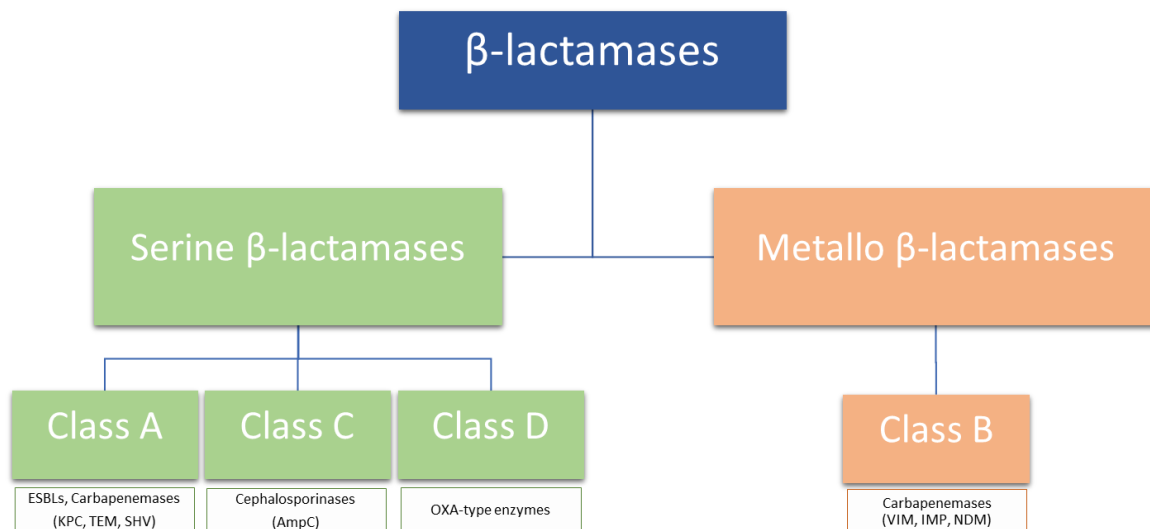
Figure 3. Ambler classification of β-lactamases.

MBLs demonstrate a broad range of structural diversity, making comparison of different proteins difficult. Nevertheless, as mentioned previously, all MBLs require zinc ions for catalytic activity. Based on the number of zinc ions and the amino acid sequences, MBLs are further separated into three subclasses: B1, B2 and B3.[11] Both B1 and B3 subclasses are di-zinc enzymes, whereas B2 MBLs contain only one zinc ion in the active site.
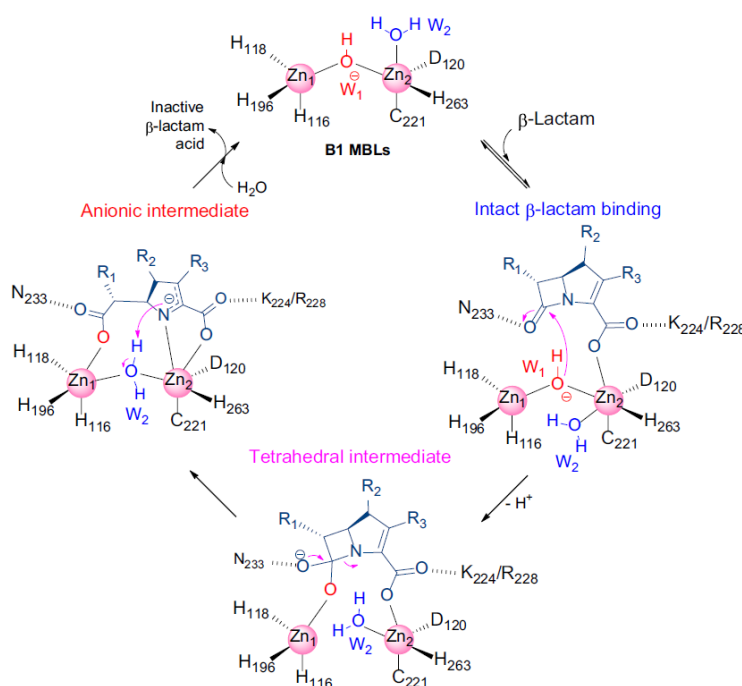

Figure 4. The proposed mechanism of β-lactam hydrolysis mediated by B1 MBLs. Reproduced with permission from Yang Y. et al. *Trends Microbiol.* **2023**, *8*, 735-748. Copyright 2024 Elsevier.[21]

There is a plethora of published studies devoted to MBL-mediated hydrolysis of β-lactams.[22-24] Although the exact mechanisms of hydrolysis as well as the appropriate intermediates depend on the

subclass of the MBL and the substrate, certain common features can be discussed (Fig. 4). First, substrate binding occurs, establishing interactions with the metal in the active site and surrounding residues. The following nucleophilic attack on the carbonyl group of the β-lactam ring results in the formation of a tetrahedral intermediate. Subsequent β-lactam ring opening generates an anionic intermediate, as demonstrated by experimental evidence.[25-27] Delocalization of the negative charge within the antibiotic structure and the interaction with zinc lead to stabilization of the formed negative charge. Lastly, protonation of this intermediate yields the inactive β-lactam acid and subsequent recovery of the unbound enzyme.

The clinically most relevant MBLs are considered to be New Delhi metallo-β-lactamases (NDMs), Verona integron-encoded metallo-β-lactamases (VIMs) and imepenemases (IMPs), all belonging to the B1 subclass.[28] The aforementioned enzymes hydrolyze a broad range of β-lactams, the exception being monobactams.[29] Thus, they present a major challenge to public health, making it the more important to find ways of overcoming this resistance.

2.3 β-Lactamase inhibitors

A promising strategy to combat bacterial resistance is the development of small-molecule inhibitors. The first clinically approved inhibitors were sulbactam, tazobactam and clavulanic acid (Fig. 5), which exhibited a limited spectrum of activity towards some SBLs.[30-31] All of the aforementioned inhibitors appear to be similar to β-lactam antibiotics, with two fused rings present in the structure. However, since then inhibitor development has shifted to structures that do not contain a β-lactam ring. Furthermore, a selection of SBL inhibitors is available for the treatment of bacterial infections, while no MBL inhibitor has been successful in passing clinical trials so far.[21, 32] Currently there are three drug candidates, which are all dual SBL/MBL inhibitors, undergoing clinical studies: VNRX-5133 (taniborbactam), QPX7728 (xeruborbactam) and QPX7831 (Fig. 5).[21, 33-34] Thus, the development of new MBL inhibitors remains a relevant challenge in the field of AMR.[35]
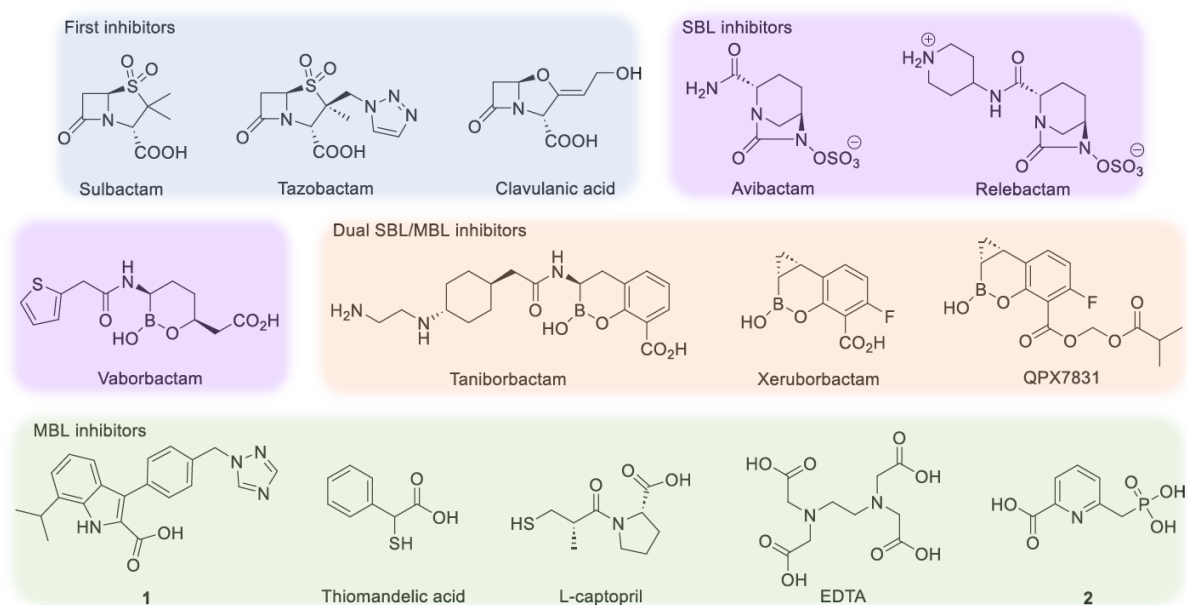
Figure 5. Examples of BLase inhibitors.

7

Typically, SBL and MBL inhibitors do not display antibacterial activity by themselves, therefore they are paired with BLs for clinical application. The combination of β-lactamase inhibitors and β-lactam antibiotics has proven to be a successful approach in overcoming AMR.[36] The efficacy and susceptibility of such combinations greatly depend on the used ratios. Currently, there are several combinations approved for clinical use (Table 1). The combinations used in clinic are only active against SBLs and contain the following inhibitors: clavulanic acid, sulbactam, tazobactam, avibactam, relebactam and vaborbactam.[15, 37-38] Until now, no combination is available for MBL-producing pathogens, however, recent progress in this area demonstrates promising results. The combinations of avibactam with aztreonam (a monobactam) and taniborbactam with cefepime, both used for treatment of MBL-harboring infections, have reached phase III of clinical trials.[39] The recently published data from the phase III trials of the cefepime-taniborbactam combination is especially promising.[40] However, as of February 2024, these clinical studies have been halted due to FDA requesting additional information on the drug, testing methods and manufacturing process.[41]

Table 1. β-Lactam/β-lactamase inhibitor combinations.[15, 39]

Inhibitor	β-Lactam partner	Development stage	Spectrum of application				
			ESBL	AmpC	KPC	OXA-48	MBL
Clavulanic acid	Amoxicillin Ticarcillin	Approved Approved	+	-	-	-	-
Sulbactam	Ampicillin	Approved	+	-	-	-	-
Tazobactam	Piperacilin Cefepime Ceftolozane	Approved Approved Approved	+	-	-	-	-
Enmetazobactam	Cefepime	Phase III	+	+	-	-	-
Avibactam	Ceftazidime Aztreonam	Approved Phase III	+ +	+ +	+ +	+ +	- +
Relebactam	Imipenem	Approved	+	+	+	-	-
Nacubactam	Meropenem	Phase II	+	+	+	-	-
Zidebactam	Cefepime	Phase III	+	+	+	+	-
ETX2514	Sulbactam	Phase II	+	+	+	+	-
Vaborbactam	Meropenem	Approved	+	+	+	-	-
Taniborbactam	Cefepime	Phase III	+	+	+	+	+

+ = antimicrobial activity, - = no antimicrobial activity

MBL inhibitors are usually separated into those that bind directly to the zinc ions in the active site, preventing substrate binding, and those that interfere with the stability of the enzyme via zinc deprivation.[42] In a recent review,[21] the authors proposed to divide MBL inhibitors into five types, with some inhibitors belonging to more than one type. Inhibitors of the first type contain metal-binding pharmacophores and coordinate zinc instead of the bridging water molecule W_1 or hydroxide (Fig. 4). The second and third types of MBL inhibitors mimic the initial binding mode of the intact β-lactam antibiotic and the tetrahedral intermediate, respectively. Inhibitors that imitate the binding of the anionic intermediate or the hydrolyzed products constitute the fourth type of MBLs. The last type of MBLs act via degradation or alteration of the metal ion binding site by replacing or removing zinc ions or through covalent interactions. It should be noted that the dual SBL/MBL inhibitors, currently under clinical evaluation, are representative examples of the third type of inhibitors.

The first type of inhibitors, which act via replacement of the catalytically active water molecule, is represented by the majority of the reported MBL inhibitors. Various chemotypes that are able to inhibit MBLs have been renowned in literature, including but not limited to, thiols, carboxylates, sulfonamides, triazoles and phosphonates (Fig. 5).[11, 42] Among the functionalities linked to zinc binding, sulfur-containing molecules are among the most studied.[43-45] Discovery of the inhibitory activity of thiomandelic acid[46] and captopril[47] towards MBLs has led to the development of a selection of thiol-containing inhibitors. Since L-captopril is a clinically approved drug for hypertension,[48] implying its toxicity and bioavailability standards are deemed satisfactory, the scaffold is a promising starting point for the design of molecules as potential MBL inhibitors.
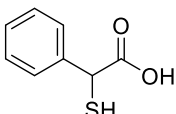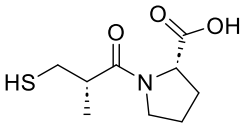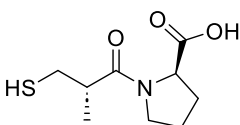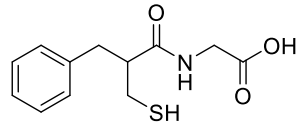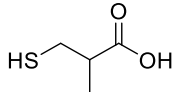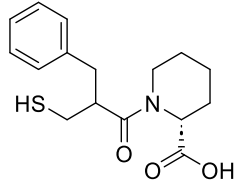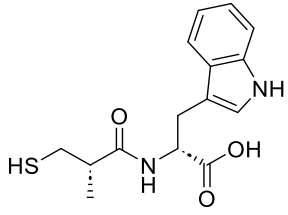
While there are many prospective MBL inhibitors described in literature, the studied compounds are often only active against one subclass of MBLs or even one specific enzyme.[49] Nevertheless, thiol compounds have been reported to coordinate zinc in the active site of MBLs from different subclasses, demonstrating the potential of broad-spectrum inhibition.[50] In 2001, thiomandelic acid (Table 2, entry 1) was found to exhibit a wide spectrum of activity against B1 and B3 subclasses, giving rise to the heightened interest in thiols as MBL inhibitors.[46] The subsequent finding that L-captopril, a known angiotensin converting enzyme (ACE) inhibitor, and its stereoisomer, D-captopril (entries 2 and 3), inhibit several B1 MBLs further encouraged investigation of thiol-based compounds.[51] Klingler et al. succeeded in finding three compounds that inhibit clinically relevant B1 MBLs, while screening already approved drugs containing thiols.[45] For example, thiorphan, an enkephalin inhibitor, displayed IC_{50} values in the low micromolar region when tested against NDM-1, IMP-7 and VIM-1 (entry 4).
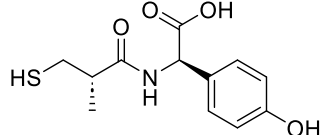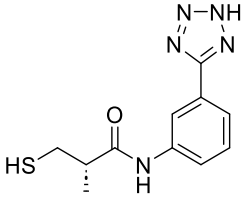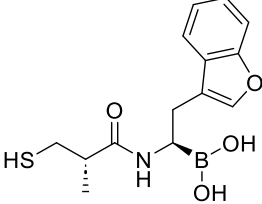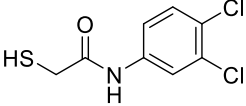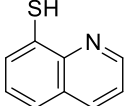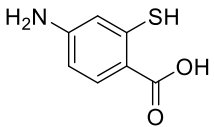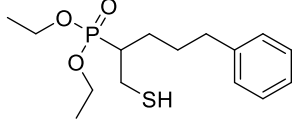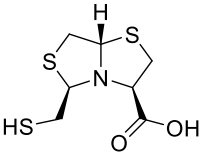
In an attempt to simplify the structure of captopril and locate the chemical moieties necessary for binding to NDM-1, Li et al. demonstrated that the thiol and the carboxylic acid groups are essential for inhibitory activity using 3-mercapto-2-methylpropanoic acid (entry 5).[52] In another study, modification of both the pyrrolidine ring and the methyl group of captopril identified the piperidine scaffold as a promising motif for the inhibition of clinically relevant MBLs (entry 6). Combining the (S)-3-mercapto-2-methylpropanal moiety of captopril with tryptophan resulted in a potent broad-spectrum inhibitor of B1 and B3 MBLs (entry 7).[53] Members of a captopril-inspired library of 2-substituted ((S)-3-mercapto-2-methylpropanamido)acetic acid analogues demonstrated low micromolar IC_{50} values for NDM-1 and VIM-2 (entry 8), suggesting that the D-amino acid-containing compounds are more potent inhibitors than the respective L-amino acid derivatives.[54] Yan et al. investigated the structure-activity relationship of mercaptopropionamide substituted aryl tetrazoles and identified that the meta-derivative (entry 9) exhibited the strongest inhibitory activity against representative B1 MBLs.[55] Using a pharmacophore fusion strategy in order to achieve dual MBL/SBL inhibition, Wang et al. synthesized (1-(3´-mercaptopropanamido)methyl)boronic acid derivatives and managed to find a potent inhibitor of all three MBL subclasses (entry 10).[56] In a search for dual inhibitors of MBLs and the extracellular virulence factor elastase, an N-mercaptoacetamide derivative, inspired by the structural similarity to mercaptopropionamide compounds, was shown to inhibit several B1 MBLs.[57]

While a wide variety of thiol-based MBL inhibitors share the common aliphatic thiol motif of captopril with some alterations (such as the previously discussed entries 1-11), instances of other thiol-based scaffolds can be found in literature. Two aromatic thiols, 8-thioquinoline[58] and 4-amino-2-sulfanylbenzoic acid[59] (entries 12 and 13), have been reported to inhibit various B1 and B3 MBLs, respectively. Among the reported inhibitors many have not only a thiol but also a carboxylic acid moiety

incorporated into the structure. Thus, Skagseth *et al.* investigated bioisosters of the carboxylic group and found that compounds containing a mercapto group and a phosphonic acid successfully inhibited NDM-1, VIM-2, GIM-1 and TMB-1 (entry 14).[60-61] Also worth mentioning are bisthiazolidines (BTZs), bicyclic compounds with a free thiol moiety, capable of inhibiting MBLs of all subclasses (entry 15). Their wide spectrum of activity is attributed to the ability of the scaffold to bind in multiple ways due to the resemblance in structure and binding to β-lactams, in addition to the zinc-coordinating thiol and carboxylic acid groups.[62]

Table 2. Examples of thiol-containing MBL inhibitors with inhibitory data.

Entry	Structure	Inhibitory data	Reference
1	Thiomandelic acid	B1 IMP-1 (IC_{50} = 0.023 µM) B1 NDM-1 (IC_{50} = 3.17 µM) B1 BcII (K_i = 0.34 µM) B1 VIM-1 (K_i = 0.23 µM) B3 L1 (K_i = 0.081 µM) B3 FEZ-1 (K_i = 0.27 µM)	[10, 46]
2	L-captopril	B1 IMP-1 (IC_{50} = 23.3 µM) B1 BcII (IC_{50} = 80.4 µM) B1 VIM-2 (IC_{50} = 4.4 µM) B1 NDM-1 (IC_{50} = 157.4 µM)	[51]
3	D-captopril	B1 IMP-1 (IC_{50} = 7.2 µM) B1 BcII (IC_{50} = 10.7 µM) B1 VIM-2 (IC_{50} = 0.072 µM) B1 NDM-1 (IC_{50} = 20.1 µM) B2 CphA (K_i = 72 µM)	[47, 51]
4	Thiorphan	B1 NDM-1 (IC_{50} = 1.8 µM) B1 IMP-7 (IC_{50} = 5.3 µM) B1 VIM-1 (IC_{50} = 5.8 µM)	[45]
5		B1 NDM-1 (IC_{50} = 56 µM)	[52]
6		B1 NDM-1 (IC_{50} = 0.7 µM) B1 IMP-7 (IC_{50} = 0.9 µM) B1 VIM-1 (IC_{50} = 4.6 µM)	[12]
7		B1 VIM-5 (IC_{50} = 0.175 µM) B1 VIM-2 (IC_{50} = 0.055 µM) B1 VIM-1 (IC_{50} = 0.526 µM) B1 NDM-1 (IC_{50} = 24.81 µM) B1 SPM-1 (IC_{50} = 0.89 µM) B1 BcII (IC_{50} = 1.63 µM) B1 IMP-1 (IC_{50} = 0.041 µM) B3 L1 (IC_{50} = 16.21 µM)	[53]

#	Structure	Activity	Ref
8		B1 VIM-2 (IC$_{50}$ = 0.0137 µM) B1 NDM-1 (IC$_{50}$ = 3.57 µM)	[54]
9		B1 VIM-2 (IC$_{50}$ = 0.044 µM) B1 NDM-1 (IC$_{50}$ = 0.396 µM) B1 IMP-1 (IC$_{50}$ = 0.71 µM)	[55]
10		B1 VIM-2 (K$_i$ = 0.44 µM) B1 NDM-1 (K$_i$ = 37.95 µM) B2 SFH-1 (K$_i$ = 0.26 µM) B3 GOB-18 (K$_i$ = 0.13 µM)	[56]
11		B1 NDM-1 (IC$_{50}$ = 0.65 µM) B1 IMP-7 (IC$_{50}$ = 0.86 µM) B1 VIM-1 (IC$_{50}$ = 2.2 µM)	[57]
12		B1 NDM-1 (IC$_{50}$ = 2.99 µM) B1 VIM-2 (IC$_{50}$ = 4.2 µM) B1 IMP-1 (IC$_{50}$ = 4.42 µM) B1 IMP-28 (IC$_{50}$ = 4.2 µM)	[58]
13		B1 IMP-1 (IC$_{50}$ = 11.3 µM) B1 VIM-2 (IC$_{50}$ = 42.1 µM) B3 SMB-1 (IC$_{50}$ = 0.22 µM) B3 AIM-1 (IC$_{50}$ = 1.9 µM) B3 L1 (IC$_{50}$ = 0.51 µM)	[59]
14		B1 VIM-2 (IC$_{50}$ = 0.38 µM) B1 GIM-1 (IC$_{50}$ = 0.31 µM) B1 NDM-1 (IC$_{50}$ = 1.8 µM) B1 TMB-1 (IC$_{50}$ = 0.62 µM)	[60-61]
15		B1 NDM-1 (K$_i$ = 7 µM) B1 VIM-2 (K$_i$ = 2.9 µM) B1 IMP-1 (K$_i$ = 8 µM) B1 BcII (K$_i$ = 36 µM) B2 SFH-1 (K$_i$ = 0.26 µM) B3 L1 (K$_i$ = 12 µM) B3 GOB-18 (K$_i$ = 41 µM)	[62]

Although, there are advances in MBL inhibition and some promising compounds have been reported, the development of an effective broad-spectrum MBL inhibitor has proven to be an elusive and cumbersome task. Several reasons as to why it is such a challenge have been recognized.[35, 63] The active sites of MBLs are located in a shallow groove with limited contact points available for inhibitor binding. Furthermore, the structural similarity among the subclasses is very low, characterized by varying zinc content and active site residues. Additionally, MBLs are part of a superfamily of metalloproteins, the active sites of which share certain similarities, explaining why, for example, L-captopril inhibits both ACE and MBLs. Therefore, achieving specificity for MBLs while maintaining broad-spectrum inhibition remains a continuing challenge. The aforementioned issues as well as the dissemination of

MBL-harboring bacteria emphasizes the need for new inhibitors or alternative methods of overcoming MBL-based resistance.[64]

2.4 BL conjugates

Another strategy, as opposed to attempting to combat AMR with inhibitors, is to exploit the resistance. The concept concerns the design of BL probes susceptible to β-lactamase hydrolysis, producing a selective delivery method to target resistant organisms.[14] Upon BLase cleavage of the β-lactam ring, subsequent fragmentation of the molecules leads to the release of a bioactive species, chromophore or fluorophore (Fig. 6). This approach has been utilized for diagnostics, imaging and the design of pro- and co-drugs.
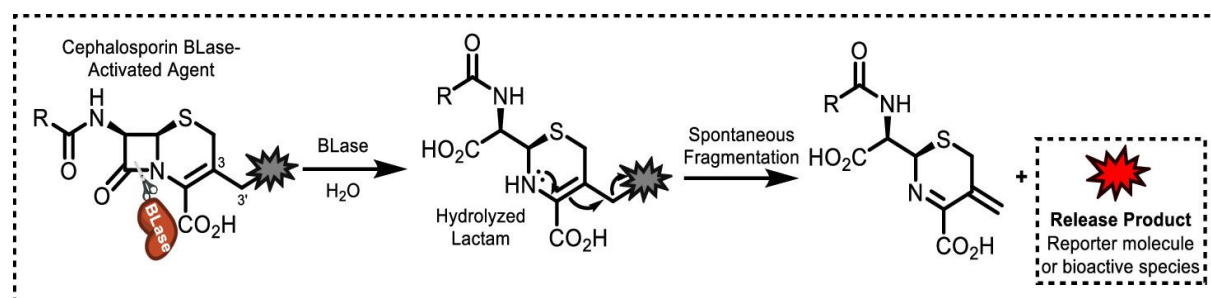
Figure 6. Mechanism of release for β-lactamase-activated cephalosporin conjugates. Reprinted with permission from Cole M. S. et al. *ACS Infect. Dis.* **2022**, *8*, 1992-2018. Copyright 2024 American Chemical Society.[14]

2.4.1 Applications

Early detection of BLases is crucial for the successful treatment of infected patients and requires effective methods of identification of BLase expression. The application of BL fragmentation in diagnostics was initially based on chromogenic molecules such as nitrocefin, PADAC and CENTA (Fig. 7). When these compounds are exposed to β-lactamases, a visible colour change can be detected. In the cases of PADAC and CENTA, fragmentation results in the release of a chromogenic azopyridine species or thionitrobenzoic acid, respectively.[65-66] However, there is no elimination occurring after nitrocefin hydrolysis and the shift in absorbance is attributed to conjugation of the dinitrophenyl group and the nitrogen lone pair.[67]

Further development in this field has led to the replacement of chromogenic cephalosporin-based substrates with fluorescence-based assays, increasing the sensitivity and convenience of BLase detection. For example, fluorogenic substrates **FC4** and **FC5** that release 7-hydroxycoumarin upon hydrolysis, generating an increased fluorescence signal, have been developed.[68] These cephalosporin-based substrates demonstrated high sensitivity and efficiency towards clinically relevant MBLs (NDM-1, VIM-2, IMP-1).

While detection of a broad range of BLases is an important achievement, designing BL probes specific towards individual enzymes or classes can help with the prescription of medication and treatment of an infection. For instance, replacement of the cephalosporin core, susceptible to hydrolysis by a wide variety of β-lactamases, by a carbapenem scaffold would lead to the selective detection of carbapenemases. Utilizing the same fluorophore, 7-hydroxycoumarin, as in the aforementioned cephalosporin-based BL probes, the fluorescent probe **CPC-1** was shown to be MBL-specific.[69]

BL probes have also found application in non-clinical settings, in the field of chemical biology for monitoring biological processes and various interactions. They have been used for imaging of β-lactamase expression in transfected cells, protein-protein interactions as well as visualization of mycobacteria *in vivo*.[14]
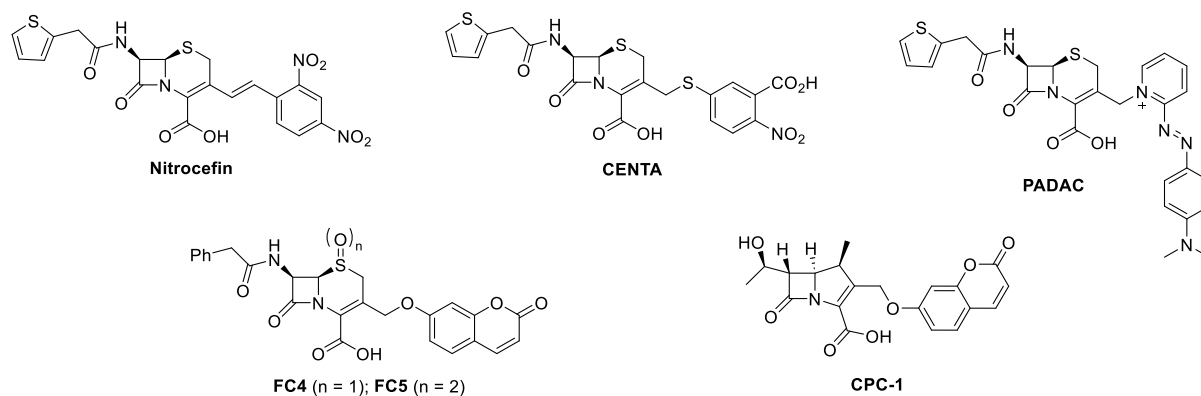

Figure 7. Examples of BL-based probes used in diagnostics.

β-Lactam conjugates have been reported as pro- and co-drugs, with the majority of examples being a combination of a cephalosporin with an antibiotic of a different class. Prodrugs releasing ciprofloxacin, a fluoroquinolone antibiotic, have been proposed as potential anti-tuberculosis agents as well as for the treatment of bacterial infections (compounds **3** and **4**, Fig. 8).[70-71] A cephalosporin conjugate with pyrazinoic acid (compound **5**, Fig. 8) demonstrated a successful co-drug strategy, with both the released drug and the β-lactam moiety contributing to the selective activity against mycobacteria.[72] Cleavable β-lactam motifs have also been explored as prodrugs in cancer therapy, such as compound **6**.[73] Further advancements in this field involve the design and synthesis of three component conjugates to circumvent, for example, obstacles regarding membrane permeability. In a recent study, a siderophore-cephalosporin-oxazolidinone **7** was envisioned to deliver an antibiotic to Gram-negative bacteria via β-lactamase-mediated cleavage, while exhibiting reduced susceptibility to antibiotic efflux mechanisms.[74]
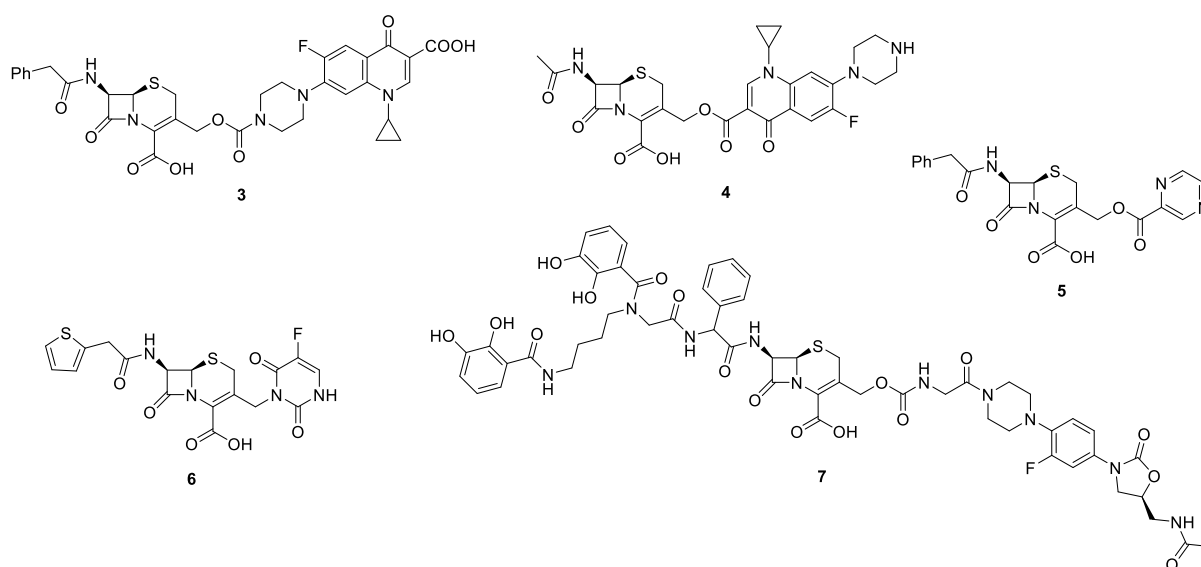
Figure 8. Examples of cephalosporin-based pro- and co-drugs.

13

Moreover, BL-fragmentation has proven to be a valuable tool in recent approaches towards the development of novel MBL inhibitors. A cephalosporin-chelator conjugate releasing a pyrithione moiety (compound **8**, Fig. 9) was among the first to be reported.[75] The compound was able to restore the antibacterial activity of meropenem against NDM-1-producing *E. coli*, presumably inhibiting the enzyme through ternary complex formation.[76] Another study incorporated zinc-binding compounds 8-thioquinoline (8-TQ) and dipicolinic acid (DPA) into the cephalosporin scaffold.[58] The resulting conjugates (compounds **9** and **10**, Fig. 9) demonstrated inhibitory activity against several MBLs, including NDM-1, VIM-2, IMP-1 and IMP-28. NMR and LC-MS studies confirmed the release of the leaving group, indicating this strategy can be applied for selective inhibitor delivery to MBL-expressing bacteria.
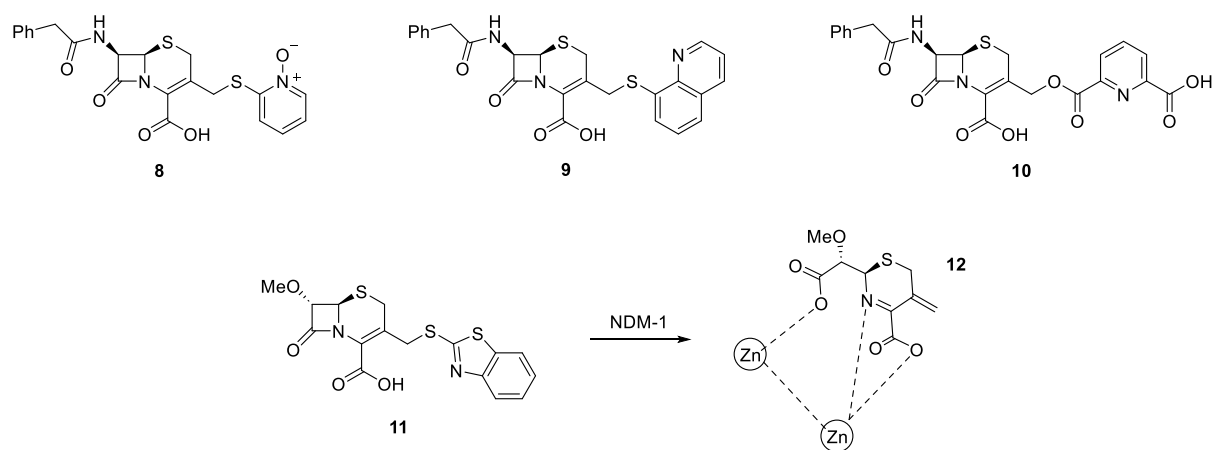
Figure 9. Examples of cephalosporin-based conjugates releasing inhibitors.

All of the aforementioned examples utilize β-lactamase cleavage, with the active inhibitor being released as the leaving group. However, in a study of stereochemically altered cephalosporins, the crystal structure of NDM-1 in complex with one of the compounds revealed that the α,β-unsaturated imine **12**, formed as a result of 3'-benzothiazolethiol elimination, acts as an inhibitor, binding the zinc in the active site, instead of compound **11** (Fig. 9).[77] Formerly it had only been shown that hydrolyzed cephalosporins, with the leaving group remaining attached, can act as the zinc-binding moiety.[78-79]

As can be seen from the examples above, there is an assortment of conjugates designed to release, upon β-lactam hydrolysis, bioactive molecules, including aromatic thiols, phenols, quinolones, pyridines and others.[58, 68-71, 76, 80-81] Furthermore, the rate of β-lactam ring cleavage has been shown to depend on the electron-withdrawing character of the leaving group. In a study of the degradation mechanisms of oxacephem derivatives **13** in alkaline solution two types of degradation products were detected (Fig. 10).[82] Depending on the substituent X, the compounds were divided into three groups. In the case of the first group (X = H, CN), no release was observed and the obtained products **14** were a result of β-lactam ring cleavage. While for compounds from the second group (X = acetate, carbamate, pyridinium, 1-methylthiotetrazole) alkaline hydrolysis led to the exclusive formation of **15**, the product of both hydrolysis and elimination. The last group of compounds, bearing a hydroxy, methoxy or thiomethyl group, was shown to form mixtures of the two products (**14** and **15**) of various composition. Seemingly, formation of the vinylic elimination product **15** happened via the corresponding intermediate **14**, as the direct transformation from **13** to **15** was concluded not to take place. Thus, the leaving group ability of the substituents influences the extent of formation of the vinylic elimination product.

Furthermore, in two recent studies, cephalosporin conjugates with aliphatic thiols showed very slow release or no release of the thiol inhibitor.[83-84] Therefore, incorporation of a suitable leaving group is necessary in order to achieve release of the bioactive molecule.
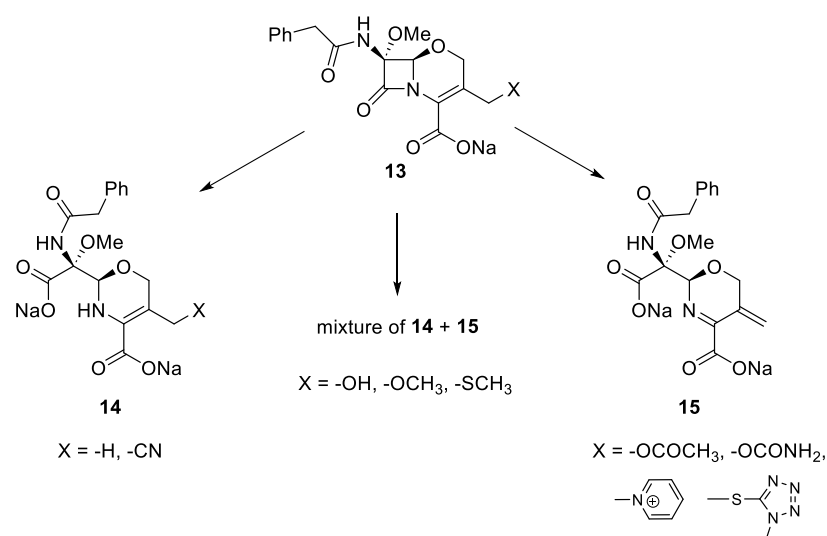

Figure 10. Hydrolysis of oxacephem derivatives bearing various substituents.
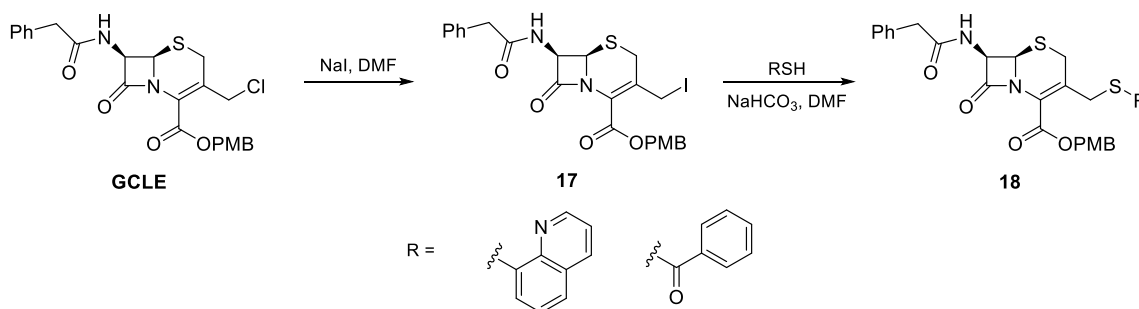
2.4.2 Synthesis

In general, the cephalosporin scaffold is the most prominent in BL probe research. This is partially due to the synthetic availability of such compounds. The most common starting materials for cephalosporin derivative preparation are 7-aminocephalosporanic acid (7-ACA) and 4-methoxybenzyl 3-chloromethyl-7-(2-phenylacetamido)-3-cephem-4-carboxylate (GCLE). Various synthetic strategies towards cephalosporin conjugates have been reported in literature.[71, 73-74, 77, 84] Synthesis of such compounds usually includes several steps, such as *N*-acylation, incorporation and removal of protecting groups as well as other modifications. However, the method of attachment of the cephalosporin core to the bioactive species or reporter molecule is of utmost interest. Two most common approaches can be highlighted, both of them involving substitution reactions.

The first approach requires Lewis acid catalysis of the nucleophilic displacement of the acetoxy group of 7-ACA (Scheme 1). While several Lewis acids had been tested (SnCl$_4$, ZnCl$_2$, TFA and H$_2$SO$_4$), the best results were achieved using BF$_3$.[85] This method has been used to introduce aromatic and aliphatic thiols into the cephalosporin scaffold.[83-84, 86] The thiols reacted with 7-ACA in the presence of boron trifluoride diethyl etherate in anhydrous acetonitrile (MeCN) at slightly elevated temperatures. The advantage of this synthetic route is that it does not require protection of the carboxylic group of the cephem ring, which is necessary when using other reagents.

15
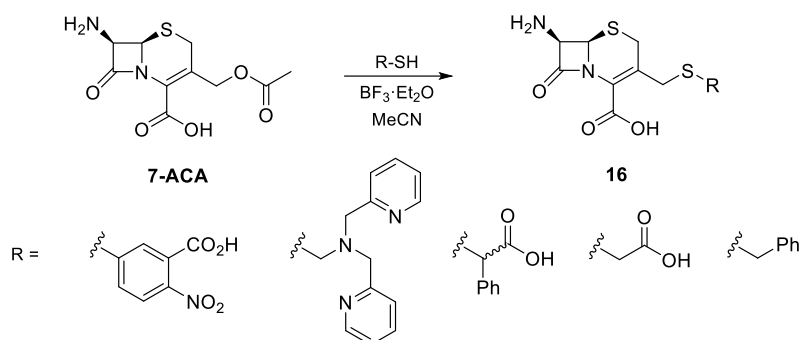
Scheme 1. Lewis acid catalyzed synthesis of cephalosporin conjugates.

The second approach is a two-step one-pot method based on transforming the starting material (7-ACA or GCLE) into the corresponding activated iodocephalosporin, followed by thioether or thioester formation (Scheme 2). The most frequently described method in literature employs sodium iodide for the first step[58, 70, 73, 77], however, there are instances when a different source of iodine is utilized such as trimethylsilyl iodide[71]. Both steps are carried out in dimethylformamide (DMF), with the thioalkylation additionally requiring use of a base, such as sodium bicarbonate.[58, 77] Furthermore, protection of the carboxylic group of the cephem ring is necessary for this approach, thus, depending on the starting material, an additional synthetic step may be required. In the case of GCLE as the starting reagent, the acid is already protected with a *p*-methoxybenzyl (PMB) group, which is generally removed using TFA.

Scheme 2. Synthesis of conjugates via formation of iodocephalosporins.

A major difficulty in the synthesis of cephalosporin derivatives is isomerization of the cephem core. In the presence of a base, cephalosporins, bearing a protecting group on the carboxylate (such as PMB in GCLE), undergo $\Delta^3 \rightarrow \Delta^2$ isomerization of the dihydrothiazine ring. Formation of the undesirable isomer is observed when using bases such as carbonates, tertiary amines as well as pyridine.[73] A possible solution to this issue is oxidation of the sulfur to retain the Δ^3 isomer, followed by reduction of the sulfoxide back to the thioether.[87] For example, in the synthesis of a fluorogenic cephalosporin, GCLE was reacted with 7-mercapto-4-methylcoumarin (MMC) in the presence of DIPEA, resulting in the formation of both Δ^3 and Δ^2 isomers (Scheme 3, A).[68] In order to avoid the isomeric mixture, the cephem sulfur was oxidized to the sulfoxide using *m*CPBA prior to the substitution reaction. An alternative way to overcome isomerization of the cephem scaffold has been proposed.[88] Employing potassium trimethylsilanolate (KOSiMe₃) as the base in the reaction of GCLE with 2-mercaptopyridine N-oxide (pyrithione), prevented the formation of the undesirable Δ^2 isomer with no additional synthesis steps being necessary (Scheme 3, B).[75]
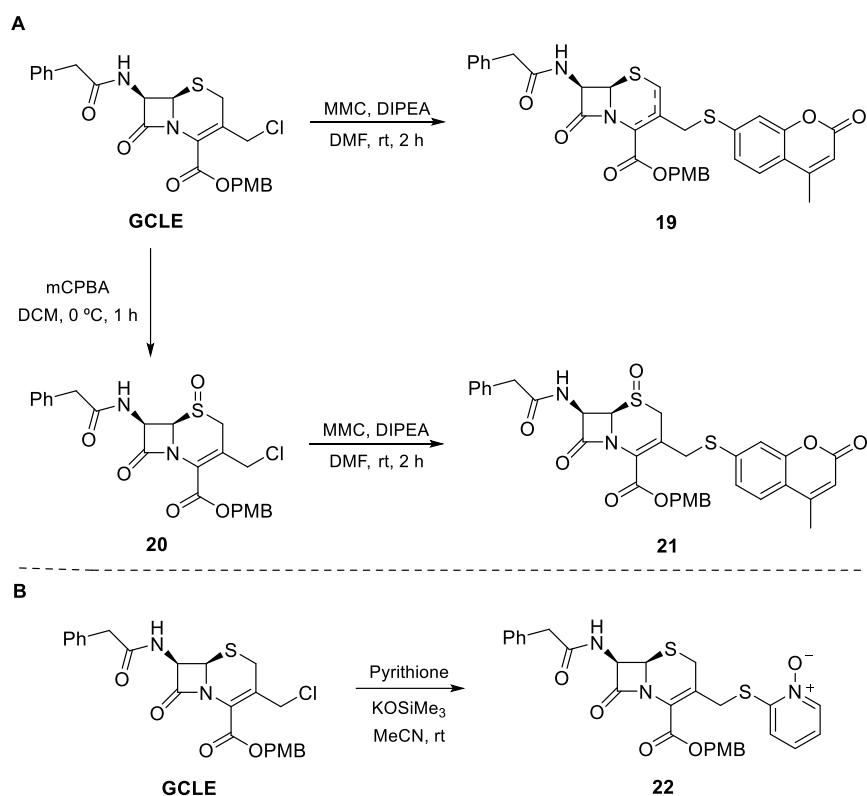
Scheme 3. Synthetic strategies for overcoming cephem isomerization.

Among the less common methods of cephalosporin conjugate synthesis, a few reports using the Wittig reaction can be found.[88-89] In this instance, the chlorocephalosporin was first converted to the iodo derivative, using NaI, followed by the addition of triphenylphosphine (Scheme 4). Subsequent reaction with an aldehyde in the presence of a base, such as NaOH or the aforementioned KOSiMe$_3$ to avoid isomerization, provided the conjugate.
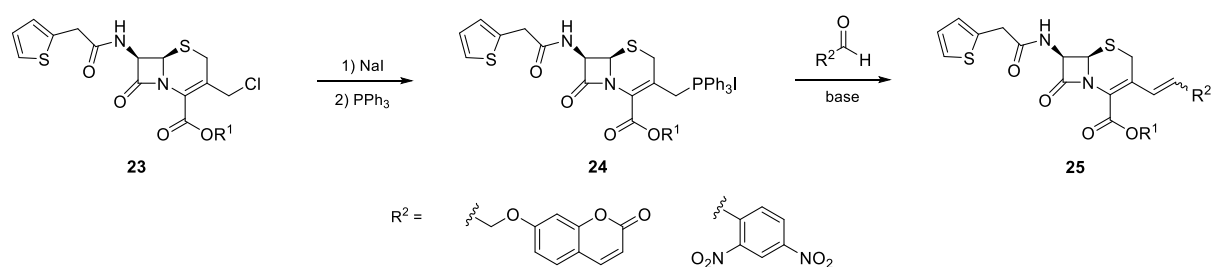
Scheme 4. Examples of the Wittig reaction in conjugate synthesis.

In a recent study, Pd-catalyzed *S*-allylation, also known as the Tsuji-Trost allylation, was used to demonstrate the possibility of utilizing this reaction for late-stage diversification of cephalosporin-based antibiotics.[90] A representative antibiotic, cefalotin (**26**), was chosen to test the applicability of the reaction conditions in combination with several thiols (Scheme 5). Employing Pd/BIPHEPHOS as the catalyst system, the *S*-allylation proved to be successful when using aromatic and aliphatic thiols. Interestingly, in the case of the aliphatic thiol, the resulting thioether **28** additionally underwent decarboxylation. The application of this reaction can be extended to conjugates bearing thioether derivatives.
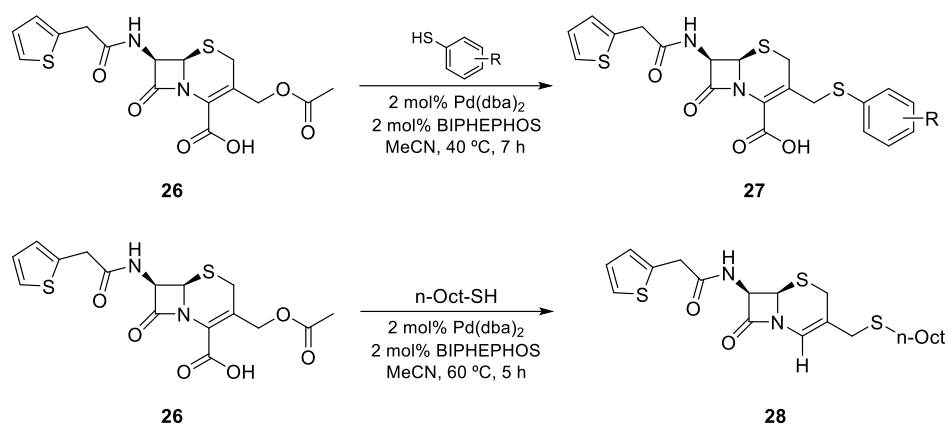
Scheme 5. Pd-catalyzed activation of the allylic acetate moiety of the antibiotic cefalotin (**26**).

2.5 Synthesis of captopril and analogues

One of the objectives of the thesis was to synthesize fluorinated analogues of previously reported thiol MBL inhibitors. As previously mentioned, captopril is considered a relevant starting point for the design of new inhibitors. Therefore, the analysis of synthetic pathways already published for the aforementioned compounds is of relevance. Three synthetic routes to captopril can be highlighted based on literature analysis.

The first synthesis, illustrated by Heinz *et al.* for the synthesis of D-captopril, consists of three steps (Scheme 6, A).[47] To obtain the corresponding acid chloride **30**, chlorination of (2*S*)-3-(acetylthio)-2-methylpropanoic acid was carried out, using thionyl chloride and pyridine in toluene. Next, coupling with D-proline with triethylamine as base in a mixture of THF and water resulted in the mercaptopropionamide derivative **31**. Hydrolysis using sodium hydroxide yielded D-captopril. More than a decade later, Brem *et al.* managed to extend the application of this approach to the synthesis of the other captopril stereoisomers: L-captopril, *epi*-L-captopril, *epi*-D-captopril.[51]
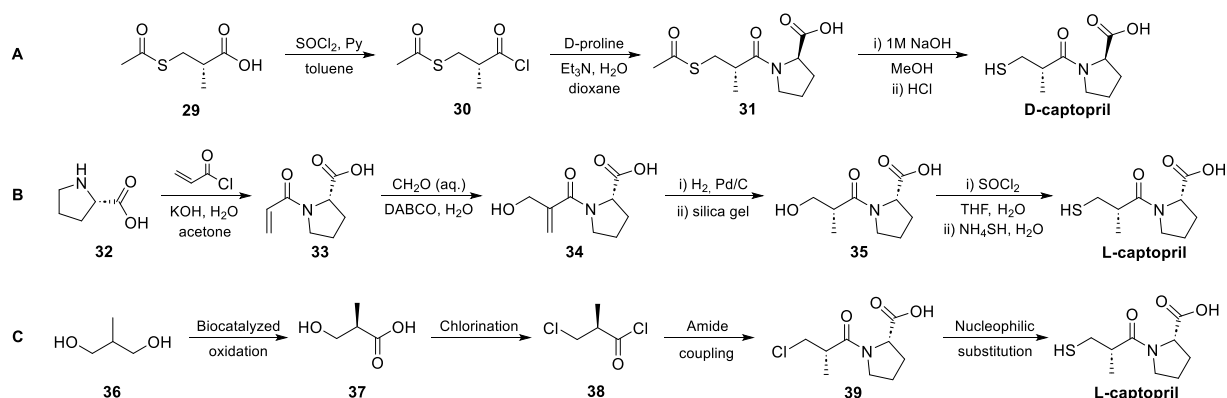
Scheme 6. Synthetic pathways to captopril.

An alternative route to prepare captopril utilizing the Baylis-Hillman reaction has been described in literature (Scheme 6, B).[91] Treatment of L-proline with acryloyl chloride in the presence of potassium hydroxide afforded *N*-acryloylproline **33**. The subsequent DABCO catalyzed Baylis-Hillman reaction between **33** and formaldehyde was used to obtain amide **34**. Next, diastereoselective hydrogenation of

the double bond yielded compound **35**, which was treated with thionyl chloride, followed by ammonium hydrosulfide to produce L-captopril.

In a more recent report, preparation of captopril was achieved via a chemoenzymatic synthesis in flow reactors, utilizing simple, readily available reagents.[92] The reactions were devised in a way that the excess of reagents or any formed by-products would not interfere with the subsequent transformations due to the synthesis being carried out under continuous flow conditions. Starting with a biocatalyzed regio- and stereoselective oxidation of 2-methyl-1,3-propandiol, carboxylic acid **37** was obtained (Scheme 6, C). The acid was then converted to the acid chloride **38** using thionyl chloride, followed by an amide coupling with L-proline that afforded amide **39**. Lastly, nucleophilic substitution of the chlorine with the thiol group using sodium hydrosulfide led to the formation of L-captopril.

Several MBL inhibitors have been designed based on the structure of captopril, with the key functionalities being the thiol and the amide parts of the molecule.[12, 52, 54, 57, 93-96] For the majority of the reported analogues, the synthesis is similar to the first method of captopril synthesis (Scheme 6, A). However, the first two steps are reduced to one by utilizing peptide coupling reagents. In this case, the carboxylic acid is usually activated *in-situ*, thus there is no need for an additional step before the addition of the corresponding amine. Consequently, the synthesis consists of two steps (Scheme 7): amide coupling using reagents such as EDC, HBTU, CDI or HATU in the presence of a base (Et$_3$N, DIPEA, NMM or DBU) and deprotection under basic conditions (NaOH, LiOH, NaHCO$_3$ or Na$_2$CO$_3$). EDC[52, 54, 93-94] and HBTU[95-96] seem to be the most popular choices for the synthesis of captopril analogues, possibly due to the low cost of these coupling reagents.
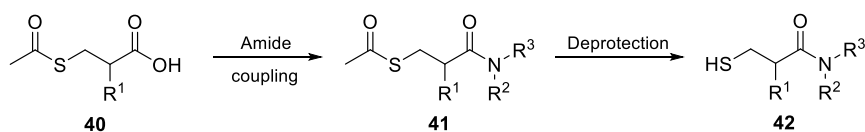
Scheme 7. General approach to the synthesis of mercaptopropionamide derivatives.

The aforementioned method is applicable if the corresponding 3-mercaptopropionic acid derivatives **40** are readily available. Otherwise, some additional transformations or an alternative synthetic method are necessary in order to obtain the mercaptopropionamide derivatives. For instance, acrylic ester derivatives **43**, obtained from the corresponding aldehydes, were hydrolyzed to the corresponding acids using aqueous NaOH under microwave irradiation (Scheme 8).[12] The activation of acrylic acids **44** was performed using thionyl chloride, followed by coupling to *tert*-butyl L-prolinate to yield acrylic amides **45**. Conjugate addition of thioacetic acid and subsequent deprotection, employing trifluoroacetic acid and aqueous ammonia, afforded derivatives **47**.
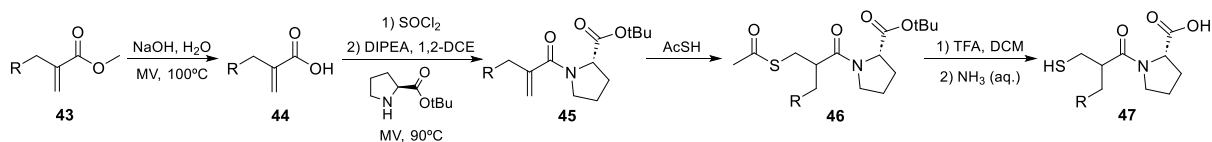
*Scheme 8.* Synthesis of mercaptopropionamide derivatives from acrylic esters.

An alternative three-step synthetic route was reported for the synthesis of *N*-aryl mercaptoacetamides **51** (Scheme 9).[57] First, amide coupling was performed using chloroacetyl chloride and aniline

derivatives in the presence of DIPEA in THF or DCM. Employing potassium thioacetate, nucleophilic substitution of the alkyl chlorides resulted in thioacetates **50**, which were hydrolyzed by KOH in methanol to obtain thiols **51**.
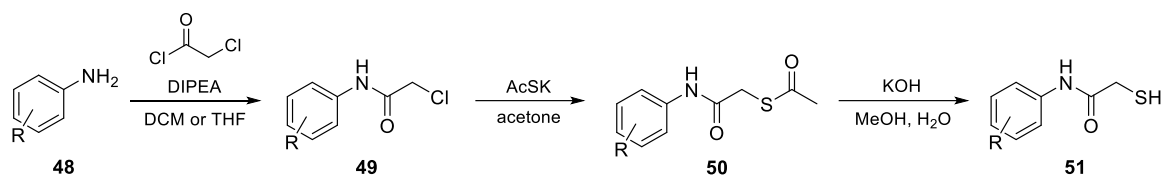
Scheme 9. Synthesis of mercaptopropionamide derivatives from aromatic amines.

To date and to the best of my knowledge, the only example of fluorine incorporation into the captopril scaffold and similar analogues was reported by Ojima *et al.*[97] They described the synthesis of a trifluoromethylated captopril analogue that was more potent than captopril as an ACE inhibitor, demonstrating the positive effect of fluorination of biologically active molecules. Acrylic amide **52** (Scheme 10) was obtained by coupling *tert*-butyl L-prolinate with α-trifluoromethylacrylic acid via acid chloride activation. Reaction of **52** with thioacetic acid (AcSH) in THF resulted in a diastereomeric mixture that was separated using medium pressure liquid chromatography (MPLC), affording **53** as the major stereoisomer. Next, trimethylsilyl iodide was used to remove the *tert*-butyl group, followed by cleavage of the acetyl group with ammonia in methanol. The target thiol **55** was isolated after treatment with sodium borohydride.
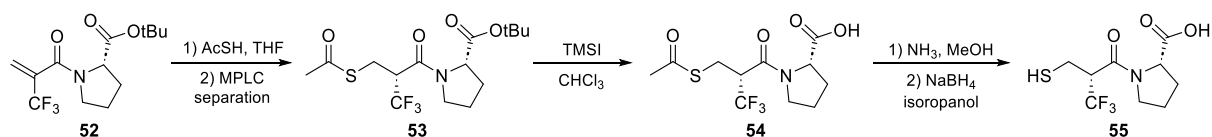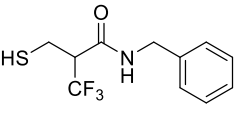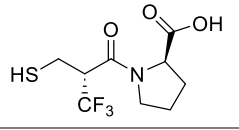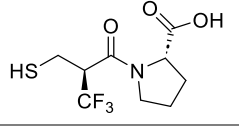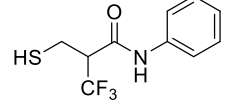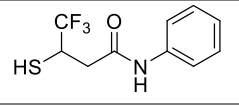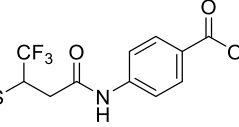
Scheme 10. Synthesis of a trifluoromethylated captopril derivative.

3 Results

*In the following chapters all of the structures that can be found in papers I and II are referred to by using the same code as in the corresponding paper with the addition of the prefix **PI** or **PII**, indicating which paper they belong to. Additionally, an overview of compounds that appear in both papers is provided in Table 3.*

Table 3. Compound structures and respective codes from papers I and II.

Structure	Code corresponding to paper I	Code corresponding to paper II
	PI-rac-5αA	**PII-9**
	PI-(2R,2′R)-5αC	**PII-14**
	PI-(2S,2′S)-5αD	**PII-13**
	PI-5αG	**PII-10**
	PI-5βG	**PII-11**
	PI-5βH	**PII-12**

3.1 Summary of Paper I

Fluorinated Captopril Analogues Inhibit Metallo-β-Lactamases and Facilitate Structure Determination of NDM-1 Binding Pose.

Alexandra Kondratieva, Katarzyna Palica, Christopher Frøhlich, Rebekka Rolfsnes Hovd, Hanna-Kirsti S. Leiros, Mate Erdelyi, Annette Bayer, *Eur. J. Med. Chem.* **2024**, *266*, 116140.

In this study, fluorinated thiol-containing MBL inhibitors as probes for NMR-based structural studies were investigated as an alternative to crystallography. For that, a series of 3-mercaptopropanamide derivatives, containing an α- or β-trifluoromethyl group, was designed and synthesized. The inhibitory activity of the compounds was evaluated against a selection of B1 MBLs.

The synthetic strategy consisted of three steps: conjugate addition of thioacetic acid, peptide coupling and deprotection of the thiol and acid moieties (Scheme 11). This method afforded compounds **PI-4αA**, **PI-4βA** and **PI-4αB**. For the other derivatives the synthetic steps were reversed. Amide coupling was

carried out first followed by conjugate addition, resulting in **PI-4α(C-G)** and **PI-4β(B-H)**. The final compounds **PI-5α(A-G)** and **PI-5β(A-H)** were obtained in moderate to excellent yields (41-98%).
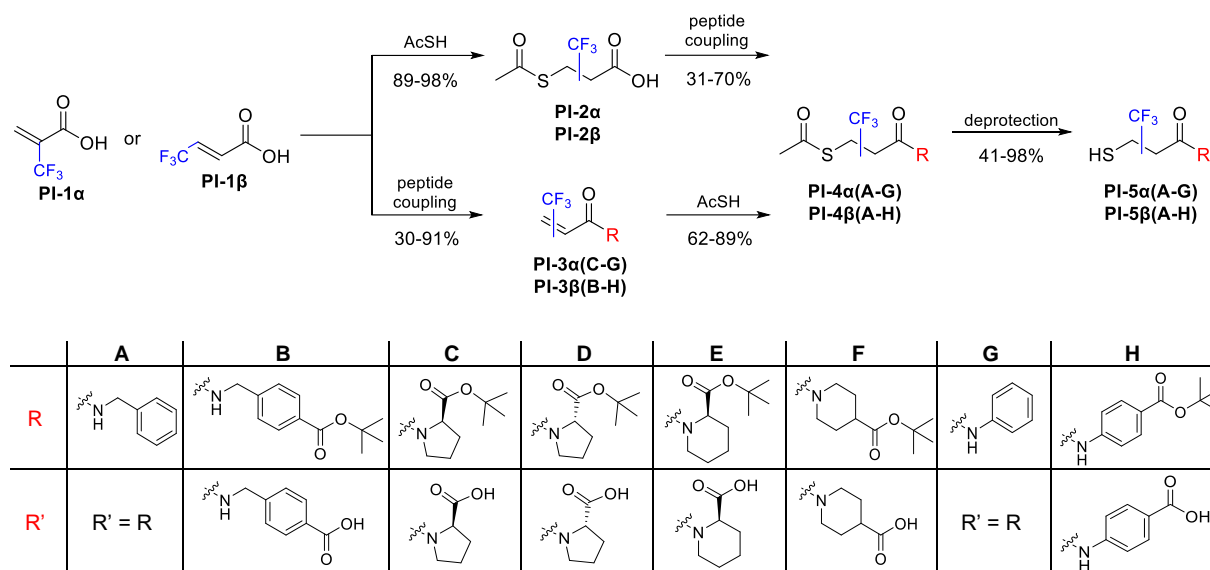
Scheme 11. Synthetic strategy towards thiols **PI-5α(A-G)** and **PI-5β(A-H)**.

To assess the inhibitory activity of the final compounds **PI-5α(A-G)** and **PI-5β(A-H)** against NDM-1, their half maximal inhibitory concentration (IC_{50}) values were measured in an enzyme assay. Several compounds demonstrated low-micromolar inhibition, with the lowest obtained value ($IC_{50} = 0.3$ μM) belonging to the trifluoromethylated-analogue of D-captopril. In general, the derivatives containing an α-CF$_3$ group demonstrated lower IC_{50} values than the corresponding β-CF$_3$ compounds.

The compounds that displayed activity against NDM-1 were further tested in a synergy assay with meropenem in an NDM-1-harboring *Escherichia coli*. The most potent synergists **PI-5αE**, **PI-5αF** as well as the trifluoromethylated analogues of D- and L-captopril (**PI-(2R,2'R)-5αC** and **PI-(2S,2'R)-5αD**) were evaluated against VIM-2 and IMP-26. The inhibitors were able to repotentiate meropenem up to 64-fold in NDM-1 and up to 8-fold in VIM-2 and IMP-26.

Separating the enantiomers of **PI-rac-5αA**, using preparative chiral HPLC, allowed for solution-state NMR studies of the binding of both enantiomers to NDM-1. Both enantiomers demonstrated binding in the slow exchange regime. Furthermore, docking calculations of both enantiomers to NDM-1 were performed.

Although direct comparison of the inhibitory activities of fluorinated and non-fluorinated compounds is challenging, substitution of the α-CH$_3$ with an α-CF$_3$ did not seem to significantly alter the IC_{50} values against NDM-1. However, the fluorinated analogues are slightly less potent synergists when compared to the non-fluorinated inhibitors.

The binding pose of one representative compound in the active site of NDM-1 was identified, using NMR spectroscopy and molecular docking, and was found to resemble the binding pose observed in the crystal structure obtained for L-captopril. Thus, the results indicate that fluorine-containing molecules can be used as probes for the structural studies of enzyme-inhibitor complexes.

3.2 Summary of Paper II

The Use of Fluorinated Aliphatic Thiols in the Design of Cephalosporin Conjugates.

Alexandra Kondratieva, Philip Rainsford, Perwez Bakht, Hanna-Kirsti S. Leiros, Ranjana Pathania, Annette Bayer, *Manuscript.*

Herein we describe the synthesis and evaluation of a series of novel cephalosporin prodrugs, designed to release thiol-based inhibitors upon MBL hydrolysis (Fig. 11). In an attempt to overcome the previously reported limitations of aliphatic thiol conjugates, trifluoromethylated thiol-based inhibitors were utilized.

	1	2	3	4	5	6	7	8
R								
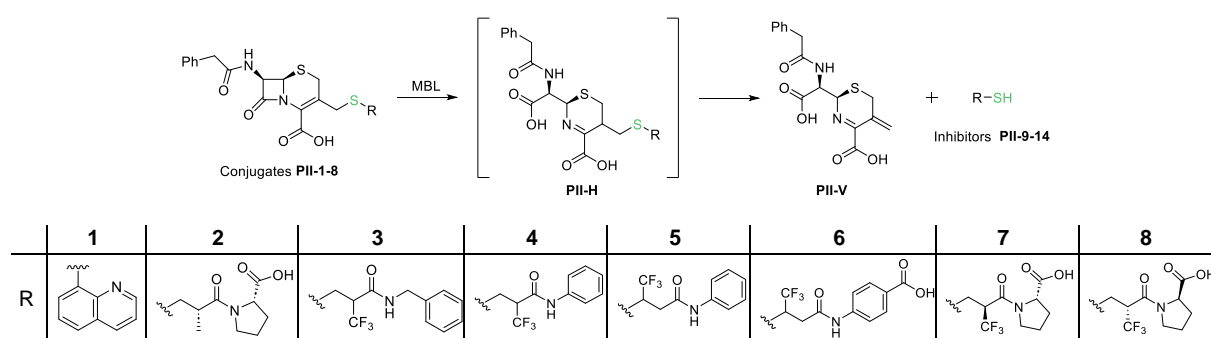
Figure 11. Proposed mechanism of MBL-mediated hydrolysis of conjugates **PII-1-8**.

The thiols were linked to the cephalosporin scaffold via a BF$_3$-catalyzed substitution reaction, followed by acylation of the cephalosporin amino group, resulting in conjugates **PII-2-8** (yields of 23-65% over two steps). Additionally, compounds **PII-1**, **PII-15** and **PII-16** were synthesized to be used as reference compounds for hydrolysis analysis and biological evaluation.

The release of the thiols was first investigated using basic conditions. The conjugates were incubated in an aqueous solution of Na$_2$CO$_3$ or (NH$_4$)$_2$CO$_3$ and the obtained mixtures were analyzed with LC-MS over time. For all of the fluorinated conjugates, the vinylic elimination product (**PII-V**) was detected, indicating that hydrolysis led to inhibitor release. However, compounds with the β-lactam ring hydrolyzed and the thioethers intact (**PII-H**) were also observed.

The thiol release of conjugates **PII-4**, **PII-5** and **PII-6** was further examined in an enzyme-catalyzed hydrolysis experiment. NDM-1-mediated degradation of all three compounds resulted in thiol release, as detected by LC-MS. Although initial release of the inhibitor was determined, in subsequent measurements no significant changes were observed, suggesting no further release or degradation of the thiols. The amount of released inhibitor could not be quantified due to the formation of the intermediates of the general structure **PII-H**.

MBL-mediated hydrolysis of the conjugates was also studied using an *in-situ* NMR assay. The appearance of vinylic proton signals of the vinylic elimination product (**PII-V**) was observed in the ^{1}H NMR spectra. Full consumption of compound **PII-5** was shown to occur faster than that of **PII-4**, demonstrating that the position of the CF$_3$-group or, in general, the electron-withdrawing character of the attached inhibitor, influences the rate of hydrolysis. Despite the disappearance of the peaks

corresponding to the conjugates, the peaks of **PII-V** remained broad and low in intensity, obscuring analysis of the obtained data and suggesting that the system might be more complicated, with simultaneous processes occurring upon hydrolysis.

The inhibitory activity of conjugates **PII-2-8** against a selection of B1 MBLs was investigated in an enzyme assay. Conjugates **PII-3-8** demonstrated similar IC_{50} values as the free thiols, while **PII-2** was less active than the corresponding thiol, L-captopril, further corroborating the release of the fluorinated thiols upon enzymatic hydrolysis.

In conclusion, the release of the fluorinated thiol inhibitors and formation of the vinylic elimination product were verified using LC-MS and NMR, supporting the hypothesis that the leaving group ability of aliphatic thiols is improved by the introduction of an electron-withdrawing moiety.

3.3 Additional results not included in the papers

3.3.1 Synthesis

Our initial approach to the synthesis of fluorinated thiol inhibitors consisted of three steps (Scheme 12): conjugate addition of thioacetic acid, amide coupling and deprotection. Starting from three fluorinated acrylates (**1f**, **PI-1α** and **PI-1β**), a small library of fluorinated thiols was envisioned, with diversification being introduced at the coupling stage by using various amines.
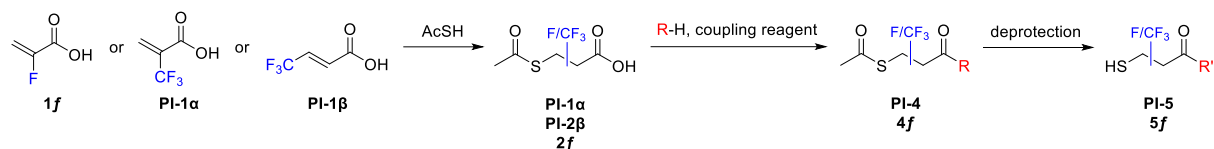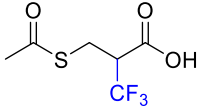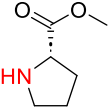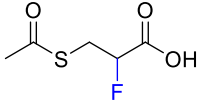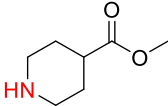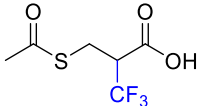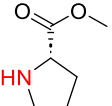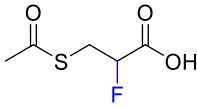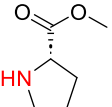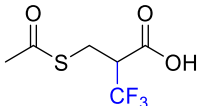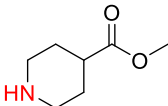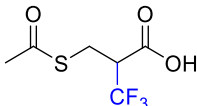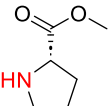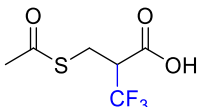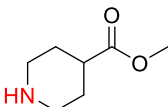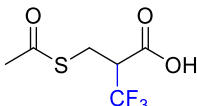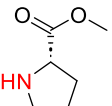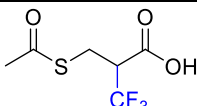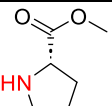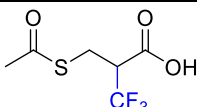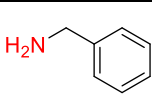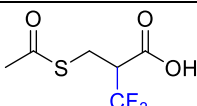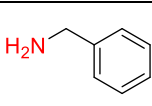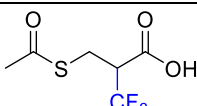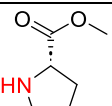
Scheme 12. Proposed synthetic route to fluorinated mercaptopropionamide derivatives.

The first major problem with the aforementioned synthetic approach was uncovered at the coupling stage. The first amine employed for coupling was benzylamine. The reaction was carried out in DCM overnight at ambient temperature with EDC as the coupling reagent and *N*-methylmorpholine (NMM) as the base. Compounds **PI-4αA**, **PI-4βA** and **4fA** were obtained in moderate to good yields (41-70%) using these conditions. However, transferring these conditions to other amines proved to be impossible with no product formation being detected.

At a first glance, the compounds used in this work did not contain any sensitive functionalities, demanding for a specific coupling reagent, or causing potential problems for coupling reactions. Thus, it was challenging to hypothesize which of the existing coupling methods could be effective or, on the contrary, problematic. Due to the plethora of coupling reagents and procedures available, the employed conditions were chosen based on literature procedures, published for acids or amines similar to those utilized in this study. The results of the tested conditions are 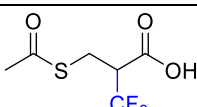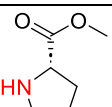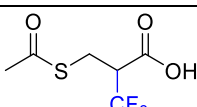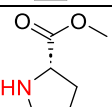summarized in Tables 4-8. Detection of product formation was conducted by MS and NMR analysis of the crude mixtures. Determining if the substrates had been consumed in the course of the reaction, using standard laboratory techniques (TLC, MS, NMR) proved to be challenging, although in some cases unreacted amine was isolated. Therefore, efforts were mainly focused on detection of the product in the crude mixtures without tracking the consumption of the starting materials.
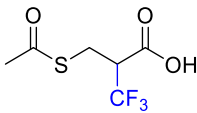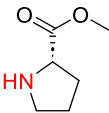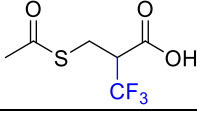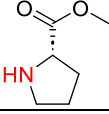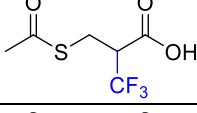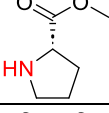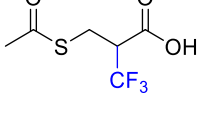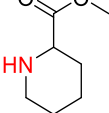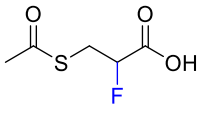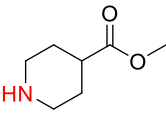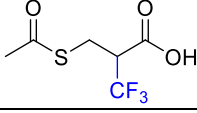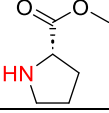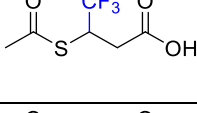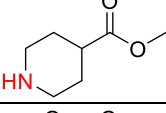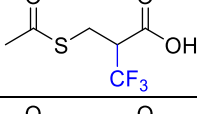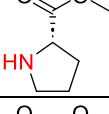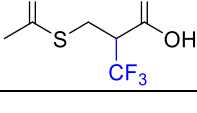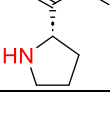
The synthetic procedure used for the coupling with benzylamine served as the starting point for the development of synthetic conditions applicable to a wider substrate range (Table 4, entries 1 and 2). Substituting NMM with DIPEA as the base resulted in product formation, although in very small quantities (entries 3 and 4). Both changing the base to DMAP and the solvent to acetonitrile did not result in any product formation (entries 5-7). Exchanging HOBt for its more reactive counterpart HOAt, slightly improved the yield (entry 8), with the best result (18%) being achieved when the base and solvent were changed to NMM and DMF, respectively (entry 9). Further efforts to increase the yield were directed at using microwave irradiation to accelerate the rate of the reaction. Test reactions with benzylamine provided an adequate yield (entries 10-11), nonetheless, reactions employing L-proline methyl ester did not result in any satisfactory results (entries 12-14).

Table 4. Attempts at peptide coupling reaction optimization using EDC.

Entry	Acid	Amine	Conditions	Result
1	(thioacetate acid, CF₃)	(proline methyl ester)	EDC HCl (2.0 eq), HOBt (1.2 eq), NMM (1.1 eq), DCM, 0 °C – rt	No product formation observed
2	(thioacetate acid, F)	(methyl piperidine-4-carboxylate)	EDC HCl (2.0 eq), HOBt (1.2 eq), NMM (1.1 eq), DCM, 0 °C – rt	No product formation observed
3	(thioacetate acid, CF₃)	(proline methyl ester)	EDC HCl (1.2 eq), HOBt (1.2 eq), DIPEA (3.0 eq), DCM, 0 °C – rt	Product formation observed. Isolated trace amounts.
4	(thioacetate acid, F)	(proline methyl ester)	EDC HCl (1.2 eq), HOBt (1.2 eq), DIPEA (3.0 eq), DCM, 0 °C – rt	Product formation observed. Isolated yield 5%
5	(thioacetate acid, CF₃)	(methyl piperidine-4-carboxylate)	EDC HCl (1.0 eq), HOBt (0.1 eq), DMAP (1.0 eq), DIPEA (5.0 eq), MeCN, 0 °C – rt	No product formation observed
6	(thioacetate acid, CF₃)	(proline methyl ester)	EDC HCl (1.0 eq), HOBt (0.1 eq), DMAP (1.0 eq), DIPEA (5.0 eq), MeCN, 0 °C – rt	No product formation observed
7	(thioacetate acid, CF₃)	(methyl piperidine-4-carboxylate)	EDC HCl (2.0 eq), DMAP (2.2 eq), DCM, 0 °C – rt	No product formation observed
8	(thioacetate acid, CF₃)	(proline methyl ester)	EDC HCl (1.2 eq), HOAt (1.2 eq), DIPEA (3.0 eq), DCM, 0 °C – rt	Product formation observed. Isolated yield 8%
9	(thioacetate acid, CF₃)	(proline methyl ester)	EDC HCl (1.5 eq), HOAt (1.2 eq), NMM (5.0 eq), DMF, 0 °C – rt	Product formation observed. Isolated yield 18%
10	(thioacetate acid, CF₃)	(benzylamine, H_2N)	EDC HCl (2.0 eq), HOBt (1.2 eq), NMM (1.1 eq), DCM, 110 °C, MW, 1 h	Yield 51%
11	(thioacetate acid, CF₃)	(benzylamine, H_2N)	EDC HCl (2.0 eq), HOBt (1.2 eq), NMM (1.1 eq), DCM, 110 °C, MW, 2 h	Yield 51%
12	(thioacetate acid, CF₃)	(proline methyl ester)	EDC HCl (1.2 eq), HOBt (1.2 eq), DIPEA (3.0 eq), DCM, 110 °C, MW, 1 h	No product formation observed
13	(thioacetate acid, CF₃)	(proline methyl ester)	EDC HCl (2.0 eq), HOBt (1.2 eq), NMM (1.1 eq), DCM, 110 °C, MW, 1 h	Product formation observed. Isolated trace amounts.
14	(thioacetate acid, CF₃)	(proline methyl ester)	EDC HCl (2.0 eq), HOAt (1.2 eq), NMM (5.0 eq), DCM, 110 °C, MW, 1 h	Product formation observed. Isolated yield 6%
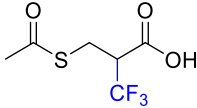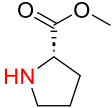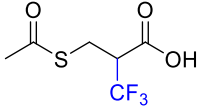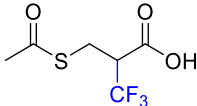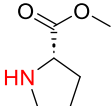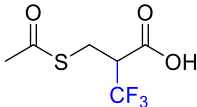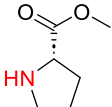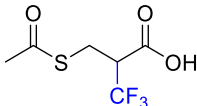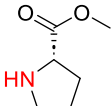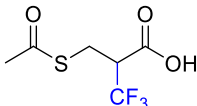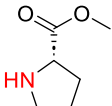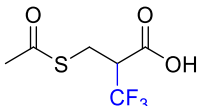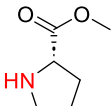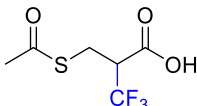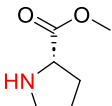
The attention was then turned to aminium coupling reagents, such as HBTU, HATU and COMU (Table 5). Varying both the acid (**PI-2α**, **PI-2β** and **2f**) and amine (L-proline methyl ester, methyl piperidine-4-carboxylate and methyl piperidine-2-carboxylate) components, as well as the reaction solvent (DMF, DCM and THF) did not lead to any promising results. The highest yield (9%) was obtained for the reaction between **2f** and methyl piperidine-4-carboxylate, using HBTU as the coupling reagent, DIPEA as the base and THF as the solvent (entry 5).

Table 5. Attempts at peptide coupling reaction optimization using aminium/uronium salts.

Entry	Acid	Amine	Conditions	Result
1	(acetyl-thio, CF₃, OH acid)	(L-proline methyl ester, HN)	HBTU (1.5 eq), DIPEA (3.0 eq), DMF, -10 °C – rt	No product formation observed
2	(acetyl-thio, CF₃, OH acid)	(L-proline methyl ester, HN)	HBTU (1.5 eq), DIPEA (3.0 eq), DCM, 0 °C – rt	Product formation observed. Isolated trace amounts.
3	(acetyl-thio, CF₃, OH acid)	(L-proline methyl ester, HN)	HBTU (1.5 eq), DIPEA (10 eq), THF, rt	No product formation observed
4	(acetyl-thio, CF₃, OH acid)	(methyl piperidine-2-carboxylate, HN)	HBTU (1.5 eq), DIPEA (5.0 eq), THF, rt	No product formation observed
5	(acetyl-thio, F, OH acid)	(methyl piperidine-4-carboxylate, HN)	HBTU (1.5 eq), DIPEA (4.0 eq), THF, rt	Product formation observed. Isolated yield 9%
6	(acetyl-thio, CF₃, OH acid)	(L-proline methyl ester, HN)	HATU (1.5 eq), DIPEA (3.0 eq), DCM, 0 °C – rt	No product formation observed
7	(acetyl-thio, CF₃, OH acid)	(methyl piperidine-4-carboxylate, HN)	HATU (1.0 eq), DIPEA (1.5 eq), THF, 0 °C – rt	No product formation observed
8	(acetyl-thio, CF₃, OH acid)	(L-proline methyl ester, HN)	COMU (1.5 eq), DIPEA (5.0 eq), THF, rt	No product formation observed
9	(acetyl-thio, CF₃, OH acid)	(L-proline methyl ester, HN)	HATU (1.05 eq), DIPEA (10 eq), DCM, DMF, 0 °C – rt	No product formation observed
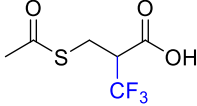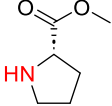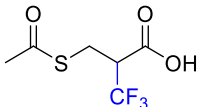
Several other tested coupling procedures are highlighted in Table 6. In the case of a phosphonium coupling reagent – PyBOP (entries 1-3), the product was detected during analysis of the crude, however, only traces were isolated. A similar result was obtained with tetramethylfluoroformamidinium hexafluorophosphate (TFFH) as the coupling reagent, which is used to in situ convert acids to the respective acid fluorides (entry 6). Reagents such as carbonyldiimidazole (CDI), dichlorotriphenylphosphorane and isobutyl chloroformate (IBCF) did not lead to product formation (entries 4, 7 and 8). The best result (11%) was obtained when using 2-chloro-1-methylpyridinium iodide (CMPI) as the coupling reagent (entry 5).
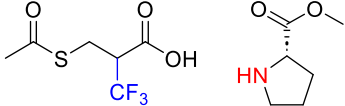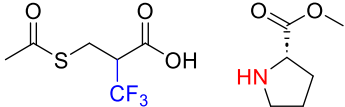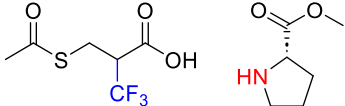
Table 6. Attempts at peptide coupling reaction optimization using other coupling reagents.

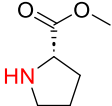| Entry	Acid	Amine	Conditions	Result
1	(acid structure with CF$_3$)	(proline ester amine)	PyBOP (1.1 eq), DIPEA (3.0 eq), DMF, 60 °C, MW, 1 h	No product formation observed
2	(acid structure with CF$_3$)	(proline ester amine)	PyBOP (1.0 eq), DIPEA (3.0 eq), rt, DCM, o/n	Product formation observed. Isolated trace amounts.
3	(acid structure with CF$_3$)	(proline ester amine)	PyBOP (1.0 eq), NMM (3.0 eq), DCM, rt, 48 h	Product formation observed. Isolated trace amounts.
4	(acid structure with CF$_3$)	(proline ester amine)	CDI (1.5 eq), CuBr (0.1 eq), HOBt (0.1 eq), DCM, 0 °C – rt	No product formation observed
5	(acid structure with CF$_3$)	(proline ester amine)	CMPI (1.1 eq), Et$_3$N (3.0 eq), DCM, 0 °C – rt	Product formation observed. Isolated yield 11%
6	(acid structure with CF$_3$)	(proline ester amine)	TFFH (1.5 eq), DIPEA (4.5 eq), DCM, 80 °C, o/n	Product formation observed. Isolated trace amounts.
7	(acid structure with CF$_3$)	(proline ester amine)	Ph$_3$PCl$_2$ (1.5 eq), CHCl$_3$, 100 °C, MW, 1 h	No product formation observed
8	(acid structure with CF$_3$)	(proline ester amine)	IBCF (1.0 eq), NMM (3.0 eq), DCM, 0 °C – rt	No product formation observed

Further optimization attempts were focused on converting **PI-2α** into the corresponding acid chloride (Table 7). Using a two-step one-pot procedure with thionyl chloride as the chloride source, no product was observed after 16 h reaction time (entry 1), while reducing the time to 1 h afforded traces of the product (entry 2). Prolonging the second step from 4 h to an overnight reaction produced a yield of 20% (entry 3). Further attempts to improve the yield by increasing and decreasing the duration of the first step were unsuccessful with the yield declining to 3 and 5%, respectively (entries 4-5).

Table 7. Attempts at peptide coupling reaction optimization via acid chloride formation.
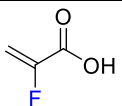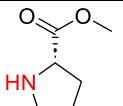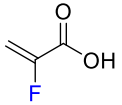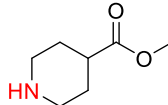
Entry	Acid	Amine	Conditions	Result
1	(acid structure with CF$_3$)	(proline ester amine)	1) SOCl$_2$ (1.1 eq), DCM, 0 °C – rt, 16 h 2) Et$_3$N (4.0 eq), DCM, 0 °C – rt	No product formation observed
2	(acid structure with CF$_3$)	(proline ester amine)	1) SOCl$_2$ (10 eq), DCM, 60 °C, 1 h 2) Et$_3$N (10 eq), DCM, 0 °C – rt, 4 h	Product formation observed. Isolated trace amounts.
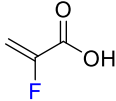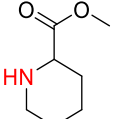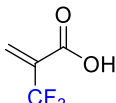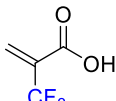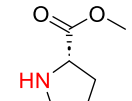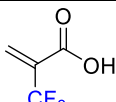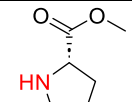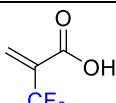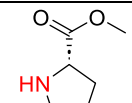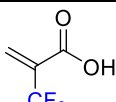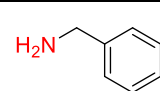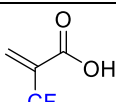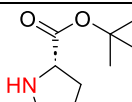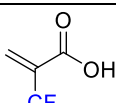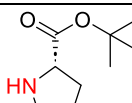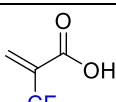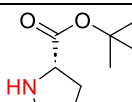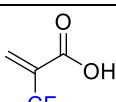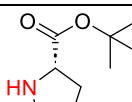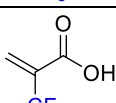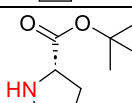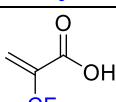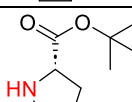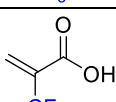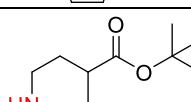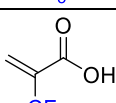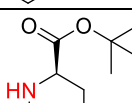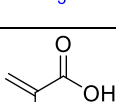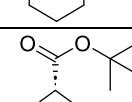
#	Acid	Amine	Conditions	Result
3	(structure: CH₃C(O)S–CH₂–CH(CF₃)–C(O)OH)	(L-proline methyl ester)	1) SOCl₂ (10 eq), DCM, 60 °C, 1 h 2) Et₃N (10 eq), DCM, 0 °C – rt, o/n	Product formation observed. Isolated yield 20%
4	(structure: CH₃C(O)S–CH₂–CH(CF₃)–C(O)OH)	(L-proline methyl ester)	1) SOCl₂ (10 eq), DCM, 60 °C, 2 h 2) Et₃N (10 eq), DCM, 0 °C – rt, o/n	Product formation observed. Isolated yield 3%
5	(structure: CH₃C(O)S–CH₂–CH(CF₃)–C(O)OH)	(L-proline methyl ester)	1) SOCl₂ (10 eq), DCM, 60 °C, 30 min 2) Et₃N (10 eq), DCM, 0 °C – rt, o/n	Product formation observed. Isolated yield 5%

At this point, the best isolated yield was 20%, which, with an additional issue of reproducibility, required further improvement. A decision was then made to try changing the order of the synthetic steps: first carrying out the coupling reaction with the acrylic acids followed by the conjugate addition of thioacetic acid. The summary of the reaction conditions for couplings with acrylic acids is provided in Table 8. Starting with 2-fluoroacrylic acid (**1f**) and L-proline methyl ester, coupling using HBTU provided the product in a yield of 57% (entry 1). The procedure was successfully extended to other amines (entries 2 and 3). However, no product formation was detected when applying the same conditions to the coupling of **PI-1α** (entry 4), also with an increased reaction time (entry 5). Reactions with thionyl chloride and oxalyl chloride were also not successful (entries 6-8). Substituting HBTU with the more reactive HATU, resulted in the desired product although with an unsatisfactory yield of 11% (entry 9). Coupling with EDC provided an even lower yield (entry 11), while reaction in the presence of CMPI afforded a yield of 28% (entry 12). Next, coupling with PyBOP was attempted and resulted in the most promising result thus far (41%, entry 13). This coupling procedure, although seemingly the most efficient, produced an inseparable by-product, which according to MS analysis, had an extra molecule of the amine incorporated into the structure. Presumably, conjugate addition of the amine to the double bond of the acrylate occurred in addition to the coupling of the amine and the acrylic acid. The same issue arose when carrying out the coupling with other amines (entries 15 and 16).

Luckily, in one of what appeared to be the last attempts to improve the coupling of the fluorinated acrylates, T3P was utilized (entry 17). While the resulting yield was not high (36%), the reaction did not produce the same by-product as the PyBOP-based coupling. This method was further applied with some optimization to all the other amines and the results and exact procedures can be found in the supporting information of paper I.

Table 8. Attempts at peptide coupling reaction optimization for acrylates.

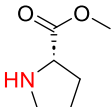| Entry	Acid	Amine	Conditions	Result
1	(2-fluoroacrylic acid)	(L-proline methyl ester)	HBTU (1.5 eq), DIPEA (3.0 eq), DCM, 0 °C – rt, 2 h	Product formation observed. Isolated yield 57%
2	(2-fluoroacrylic acid)	(methyl piperidine-4-carboxylate)	HBTU (1.5 eq), DIPEA (1.5 eq), DCM, 0 °C – rt, 2 h	Product formation observed. Isolated yield 47%

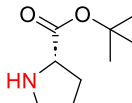| #	Acid	Amine	Conditions	Result
3	2-fluoroacrylic acid (F, OH, O)	proline methyl ester (O, O, HN)	HBTU (1.5 eq), DIPEA (1.5 eq), DCM, 0 °C – rt, 2 h	Product formation observed. Isolated yield 59%
4	2-(trifluoromethyl)acrylic acid (CF_3, OH, O)	proline tert-butyl ester (O, O, HN)	HBTU (1.5 eq), DIPEA (1.5 eq), DCM, 0 °C – rt, 3 h	No product formation observed
5	2-(trifluoromethyl)acrylic acid (CF_3, OH, O)	proline methyl ester (O, O, HN)	HBTU (1.5 eq), DIPEA (3.0 eq), DCM, 0 °C – rt, o/n	No product formation observed
6	2-(trifluoromethyl)acrylic acid (CF_3, OH, O)	proline methyl ester (O, O, HN)	1) $SOCl_2$ (2.5 eq), DCM, 40 °C, 3 h 2) DIPEA (3.0 eq), 1,2-DCE, 90 °C, MW, 1 h	No product formation observed
7	2-(trifluoromethyl)acrylic acid (CF_3, OH, O)	proline methyl ester (O, O, HN)	1) $(COCl)_2$ (2.0 eq), DMF, DCM, rt, 1 h 2) Et_3N (4.0 eq), DCM, 0 °C – rt	No product formation observed
8	2-(trifluoromethyl)acrylic acid (CF_3, OH, O)	benzylamine (H_2N, phenyl)	1) $(COCl)_2$ (2.0 eq), DMF, DCM, rt, 1 h 2) Et_3N (4.0 eq), DCM, 0 °C – rt	No product formation observed
9	2-(trifluoromethyl)acrylic acid (CF_3, OH, O)	proline tert-butyl ester (O, O, HN)	HATU (1.0 eq), DIPEA (1.5 eq), THF, 0 °C – rt, o/n	Product formation observed. Isolated yield 11%
10	2-(trifluoromethyl)acrylic acid (CF_3, OH, O)	proline tert-butyl ester (O, O, HN)	HATU (1.1 eq), Et_3N (1.1 eq), DMF, rt, o/n	No product formation observed
11	2-(trifluoromethyl)acrylic acid (CF_3, OH, O)	proline tert-butyl ester (O, O, HN)	EDC HCl (1.5 eq), DMAP (0.2 eq), DCM, 0 °C – rt, o/n	Product formation observed. Isolated yield 3%
12	2-(trifluoromethyl)acrylic acid (CF_3, OH, O)	proline tert-butyl ester (O, O, HN)	CMPI (1.2 eq), Et_3N (2.5 eq), DCM, 0 °C – rt, o/n	Product formation observed. Isolated yield 28%
13	2-(trifluoromethyl)acrylic acid (CF_3, OH, O)	proline tert-butyl ester (O, O, HN)	PyBOP (1.1 eq), DIPEA (4.0 eq), DCM, 0 °C – rt, 1 h	Product formation observed. Isolated yield 41% (mixture)
14	2-(trifluoromethyl)acrylic acid (CF_3, OH, O)	proline tert-butyl ester (O, O, HN)	PyBOP (2.0 eq), Et_3N (2.0 eq), DMF, rt, o/n	Product formation observed. Isolated yield 18%
15	2-(trifluoromethyl)acrylic acid (CF_3, OH, O)	piperidine-4-carboxylic acid tert-butyl ester (O, O, HN)	PyBOP (1.1 eq), DIPEA (4.0 eq), DCM, 0 °C – rt, 1 h	Product formation observed. Isolated yield 33% (mixture)
16	2-(trifluoromethyl)acrylic acid (CF_3, OH, O)	pipecolic acid tert-butyl ester (O, O, HN)	PyBOP (1.1 eq), DIPEA (4.0 eq), DCM, 0 °C – rt, 1 h	Product formation observed. Isolated yield 52% (mixture)
17	2-(trifluoromethyl)acrylic acid (CF_3, OH, O)	proline tert-butyl ester (O, O, HN)	T3P (1.3 eq), Et_3N (1.5 eq), DCM, 0 °C – rt, 1 h	Product formation observed. Isolated yield 36%

With the coupling starting from **1f** being the least troublesome, the subsequent synthetic steps were carried out on these derivatives (Scheme 13), in parallel with the optimization of coupling reactions with **PI-1α**. Using the formerly established coupling procedure with HBTU, compounds **3fA**, **3fD** and **3fF** were obtained in moderate to good yields (47-82%). Conjugate addition of thioacetic acid, carried out at 60 ˚C for 60 h, afforded compounds **4fA**, **4fD** and **4fF** in moderate to good yields (49-83%). The next step, according to the plan, was supposed to be removal of the acetate from the thiol group. Here the second major issue with the synthetic strategy was discovered.
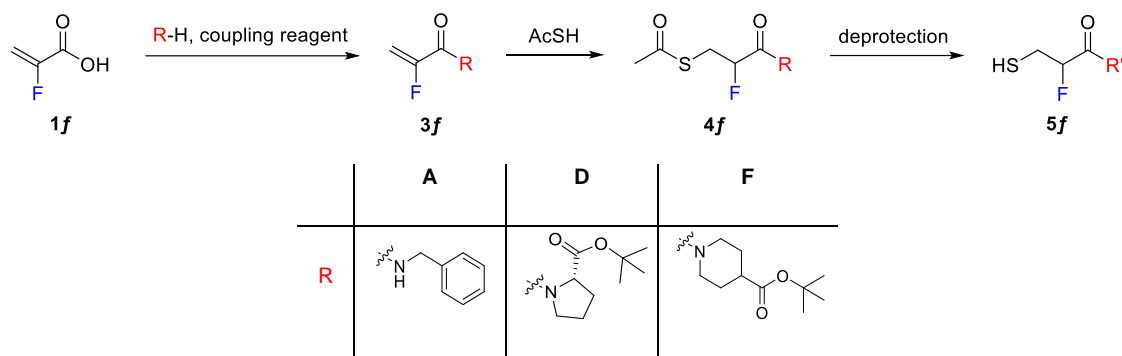
Scheme 13. Attempted synthesis of mercaptopropionamide derivatives from 2-fluoroacrylic acid.

The majority of reported procedures for converting thioacetates into the thiol moiety utilizes basic conditions.[52, 60, 95-96] However, applying these conditions to fluorine derivatives **4f** proved to be difficult. As a result of the reaction of **4fA** and sodium hydroxide, *N*-benzylacrylamide (**56**) was obtained instead of the anticipated **5fA** (Scheme 14). A variety of other conditions were then tested, including aqueous ammonia, sodium thiomethoxide and sodium borohydride, all of which resulted in the defluorinated product. Although it is not clear how defluorination occurs and how the product is formed, NMR analysis of one of the crude mixtures revealed the presence of two compounds. Aside from compound **56**, a compound with aliphatic proton signals, but not containing fluorine, was observed in the crude NMR, suggesting that defluorination occurs before elimination. Furthermore, carrying out the deprotection in boiling hydrochloric acid also led to formation of the defluorinated product.
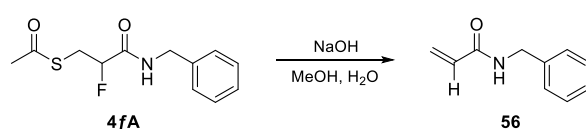
Scheme 14. The result of **4fA** deprotection under basic conditions.

With both basic and acidic conditions causing defluorination of the thioacetates, it was decided to change the protecting group to one that is removed under milder acidic conditions. The trityl protecting group was chosen, which is usually removed via treatment with trifluoroacetic acid. To test the applicability of this method, it was first applied to the trifluoromethylated derivatives (Scheme 15). Starting from **PI-1α**, conjugate addition of triphenylmethanethiol in the presence of triethylamine yielded compound **57**. Compound **58** was then obtained by coupling **57** with benzylamine, using EDC as the coupling reagent. Removal of the trityl protecting group was carried out using TFA in the presence of triethylsilane and resulted in the free thiol **PI-5α**. Unfortunately, transferring this strategy to **1f** proved to be unsuccessful. The presence of triethylamine in the first step of the synthesis also caused

31

defluorination and compound **59** was not obtained. With that, attempts to obtain compounds **5f** were abandoned.
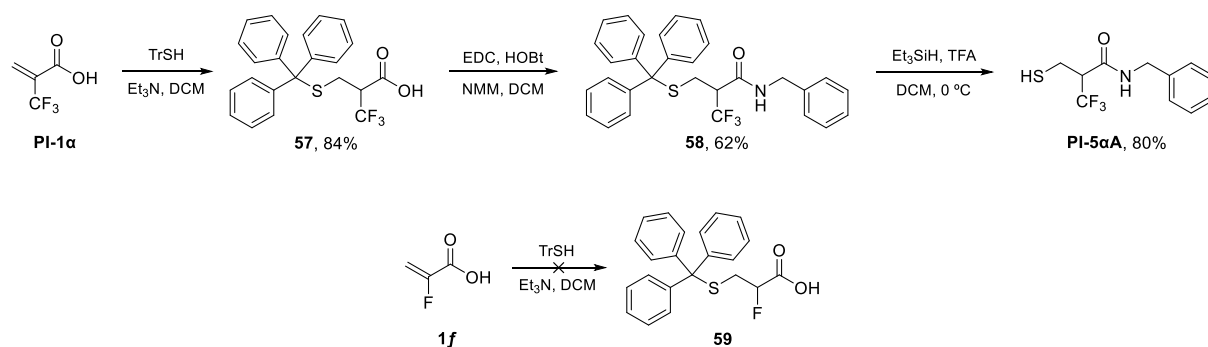
Scheme 15. Trityl protecting group approach.

As mentioned in chapter 2, there are several synthetic strategies used to obtain thiol-containing conjugates, some of which were utilized in this work (Scheme 16). 4-Methoxythiophenol was used as a readily available thiol to test the reactions before applying them to the synthesized thiols. Among published procedures, the two-step one-pot method via an activated iodocephalosporin is a popular choice (Scheme 16, A). Successfully reproducing a published procedure[58], using GCLE and 8-TQ as the starting materials, conjugate **PII-1** was synthesized. Changing the thiol to 4-methoxythiophenol resulted in a 1.3:1 mixture of two compounds that were difficult to separate. Presumably, alongside the desired product an isomer was formed, as indicated by double sets of proton signals in the NMR of the mixture. Next, Pd-catalyzed *S*-allylation was selected (Scheme 16, B). In order to test the reaction, first the free amine and acid of 7-ACA were protected using acetic anhydride and *tert*-butyl 2,2,2-trichloroacetimidate, respectively. Using reported conditions[90], compound **63** was obtained with an unsatisfactory yield of 3%. Lastly, an approach utilizing Lewis acid catalysis was tested (Scheme 16, C), which proved to be successful and was further used to synthesize the conjugates in paper II.
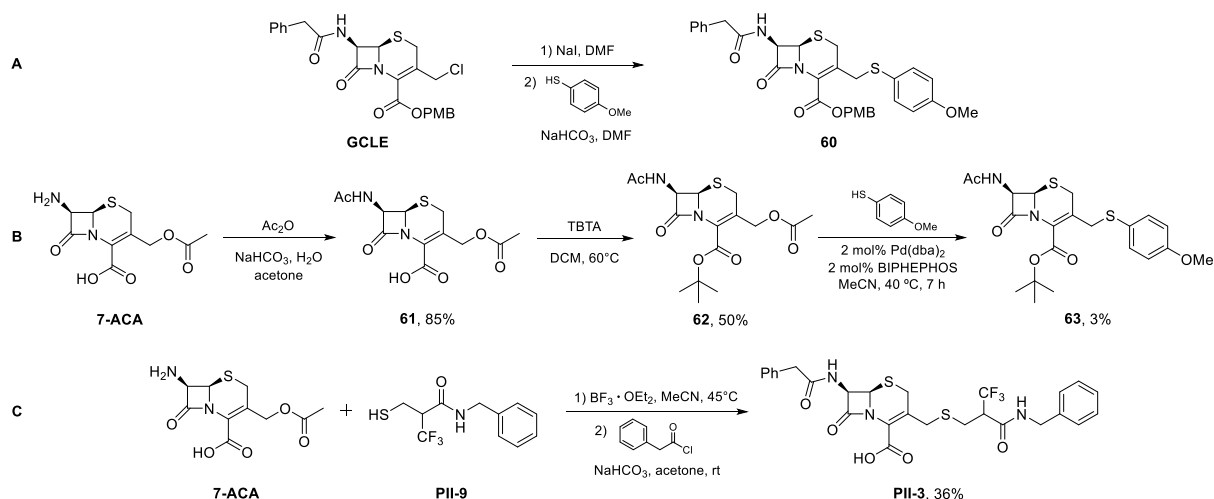
Scheme 16. Various approaches to conjugate synthesis.

3.3.2 Analysis

Initially, to establish a working NMR assay for monitoring the MBL-mediated release of the aliphatic thiols, the set up and conditions reported by van Haren *et al.* were tested on the conjugate of 8-TQ (**PII-1**).[58] The conditions were as follows: to an NMR tube containing the conjugate (2 mM), 20 mM HEPES and 0.5 mM zinc sulfate in D_2O, NDM-1 was added at a final concentration of 374 nM. Interestingly, while the appearance of the vinylic proton signals was observed (at ca 5.55 ppm as in Fig. 12, 3´, marked blue), the release occurred at a faster rate than reported, demonstrating the impact of utilizing a differently produced enzyme. In order to observe the course of hydrolysis (Fig. 12), the NDM-1 concentration was decreased from the published 374 nM to 125 nM. Having established the conditions of the assay, the hydrolyses of the novel conjugates were carried out.
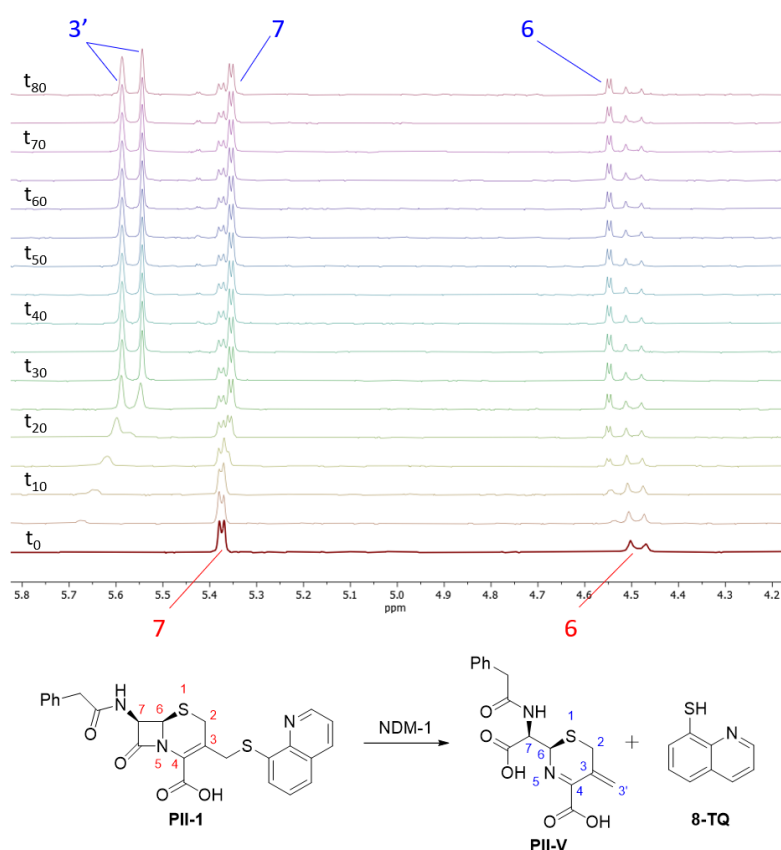
Figure 12. ^{1}H NMR analysis of NDM-1-mediated degradation of **PII-1**.

Next, **PII-5** was subjected to the hydrolysis experiment (Fig. 13, A). The observed proton signals around 5.70 ppm confirmed the formation of the vinylic elimination product (**PII-V**), but the initial low intensity and broad peaks did not significantly change during the course of the kinetic experiment. While the conjugate (**PII-5**) was being consumed, assessed based on the disappearing proton signals of the β-lactam ring (6 and 7, marked red), the intensity of the product peaks was not seen to increase correspondingly (3´, 6 and 7, marked blue). This could be interpreted as **PII-V** being involved in some kind of binding in the active site of the enzyme.

Due to such a difference in the observations for **PII-1** and **PII-5**, the influence of the enzyme concentration was tested again for **PII-5**. Decreasing the amount of added NDM-1, to a final concentration of 63 nM, resulted in the partial hydrolysis of **PII-5** before stalling (Fig. 13, B). The

halting of hydrolysis could, presumably, be attributed to the inhibition of the enzyme by the released thiol inhibitor **PII-11**. In contrast, doubling the enzyme concentration did not enhance the rate of conjugate consumption and did not seem to affect the release significantly (Fig. 13, C).
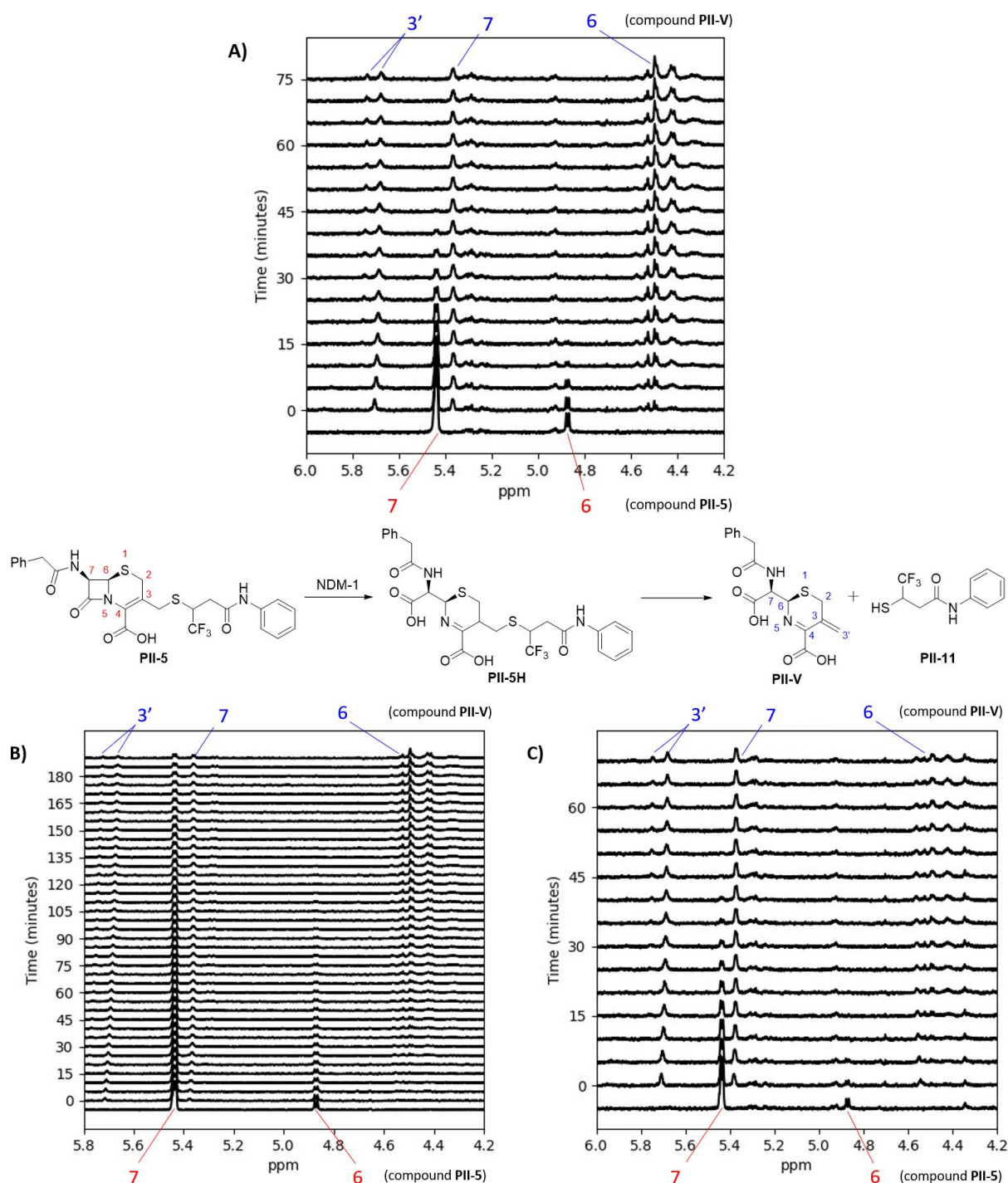
Figure 13. ^{1}H NMR analysis of NDM-1-mediated degradation of **PII-5**. Addition of 2 μl (**A**), 1 μl (**B**) and 4 μl (**C**) of NDM-1 (final concentrations of 125, 63 and 250 nM, respectively).

To test the hypothesis of **PII-V** being trapped in the binding site of the enzyme and to explore the influence of excess zinc on the degradation of the conjugates two experiments were executed. First, after full consumption of conjugate **PII-4**, more of the starting material was added, followed by 5 mM of zinc

sulfate (Fig. 14). As can be seen from the ^{1}H NMR data, the proton signals corresponding to the β-lactam ring of **PII-4** remained unaffected by the addition of zinc ions. The signals corresponding to **PII-V**, however, were found to sharpen and experience a change in the chemical shift. Furthermore, the signals corresponding to the vinylic protons seemingly resulted in two sets of peaks under the influence of additional zinc. A similar observation could be made about one of the β-lactam protons at ca 5.38 ppm, while the signals around 4.50 ppm were more difficult to analyze. These results demonstrated that the conjugate is not significantly influenced by excess zinc and indicated the binding between the vinylic elimination product and zinc ions. Furthermore, the two sets of signals could suggest the formation of two isomers as a result of hydrolysis, producing overlapping protons signals that become distinguishable once the isomers are coordinating to the zinc ions. Although in the starting molecule **PII-4**, the stereocenters of C-6 and C-7 are defined, during the course of the β-lactam ring cleavage, possibly, epimerization occurs. The hydrolysis products of cephalosporin β-lactam antibiotics have been shown to undergo reversible opening of the six-membered dihydrothiazine ring, resulting in epimerization at C-6.[98] Nevertheless, this phenomenon has not been reported for other cephalosporin-inhibitor conjugates and does not seem to occur in the case of compound **PII-1**, perhaps due to faster hydrolysis or differences in the mechanism.
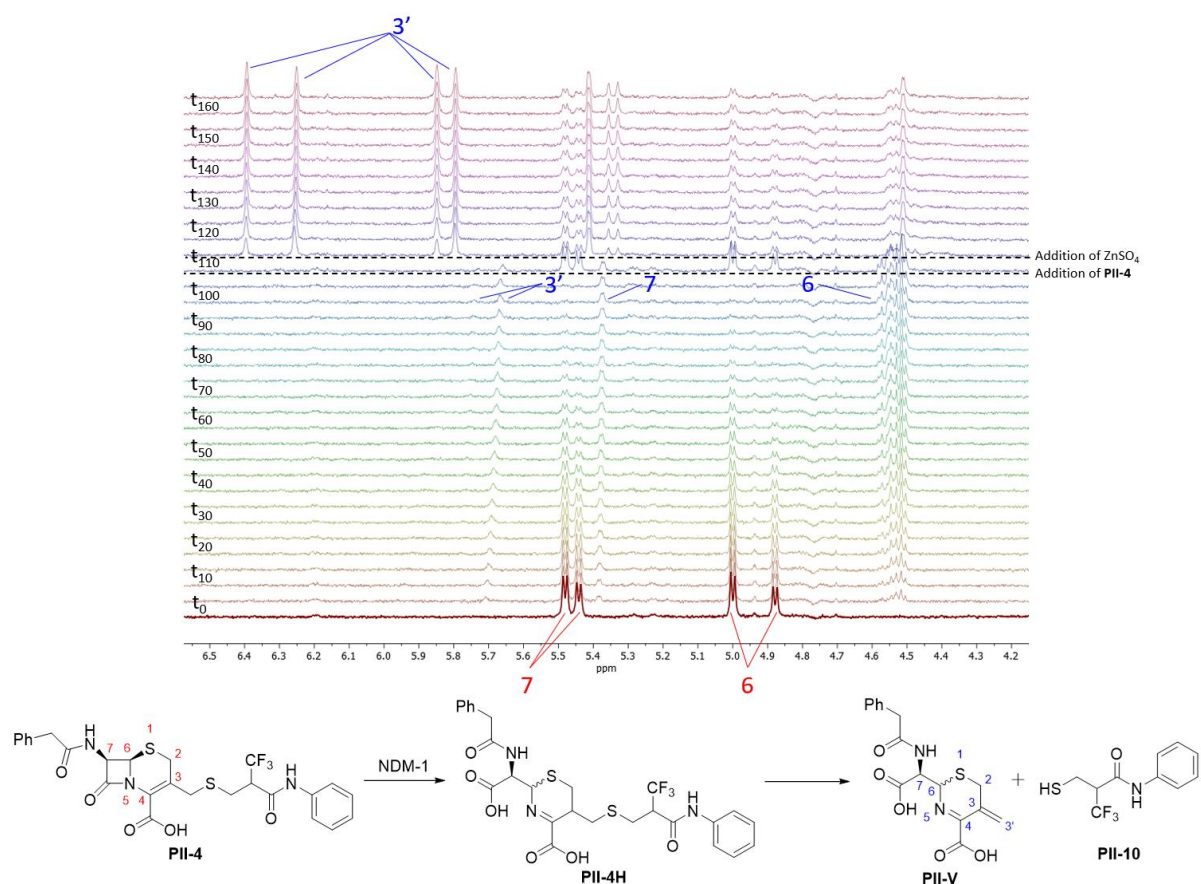
Figure 14. ^{1}H NMR analysis of NDM-1-mediated degradation of **PII-4**. Addition of conjugate and zinc sulfate after full consumption of **PII-4**.

The next experiment involved increasing the initial concentration of zinc sulfate from 0.5 mM to 5mM. The obtained ^{1}H NMR data demonstrated the gradual increase of the two sets of vinylic proton signals, suggesting thiol release during the course of hydrolysis (Fig. 15). However, the disappearance of the

peaks corresponding to the conjugate was shown to occur at a much slower rate when compared to hydrolysis in the presence of less zinc ions in the solution (Fig. 13, A). This could possibly be attributed to the denaturation of NDM-1, which has been reported to be accelerated by higher zinc ion concentrations.[99]
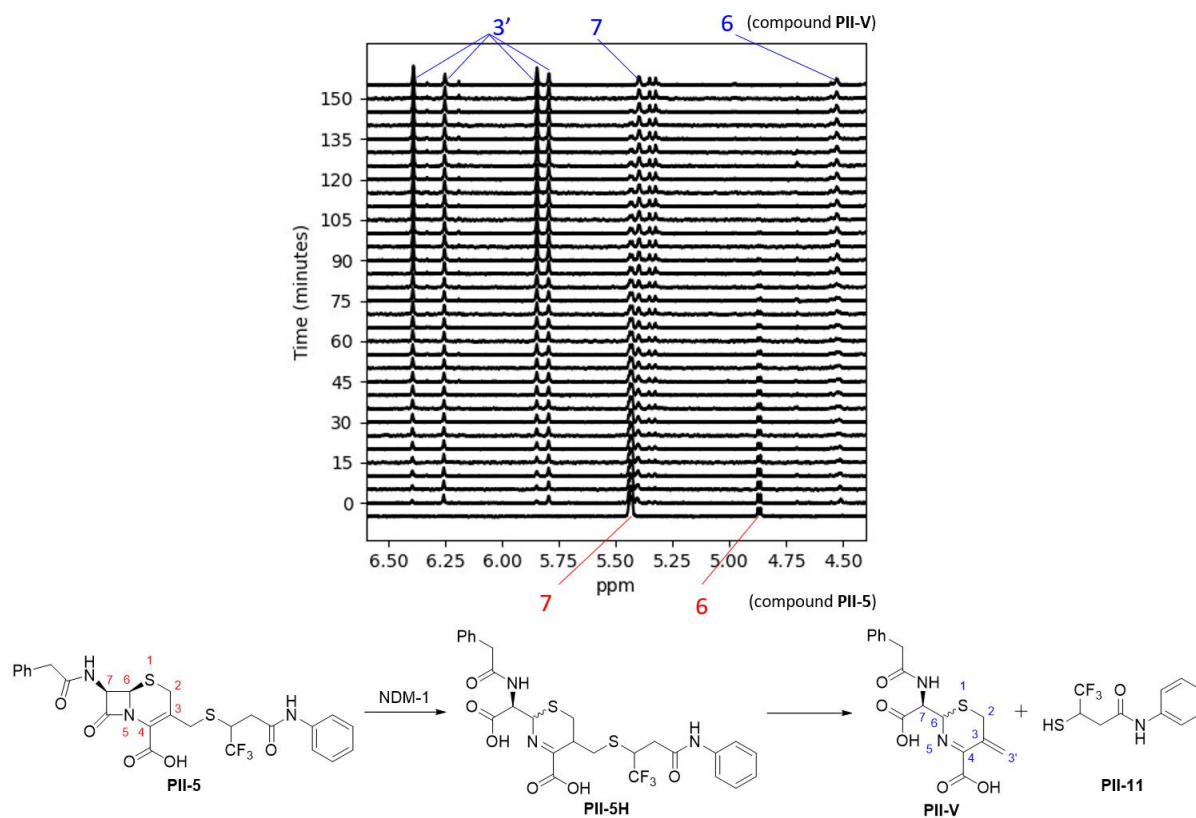
Figure 15. ^{1}H NMR analysis of NDM-1-mediated degradation of **PII-5** in the presence of an excess of zinc sulfate.

4 Discussion and outlook

The overall goal of this study was to develop BL conjugates releasing alkyl thiol-based MBL inhibitors, upon β-lactamase-mediated hydrolysis. For that, a library of fluorinated captopril analogues was synthesized and their activity as inhibitors of MBLs was explored (paper I). A selection of the fluorinated thiols exhibited inhibitory activity against NDM-1 and several α-CF$_3$-containing compounds restored the activity of meropenem against MBL-harboring *E. coli*. The findings showed that fluorination did not deteriorate the inhibitory activity, providing fluorinated inhibitors for further studies. However, derivatives fluorinated in the α-position demonstrated reduced stability as increased disulfide formation was observed.

Out of the thiols from paper I, **PI-rac-5αA**, **PI-**(2*R*,2′*R*)**-5αC**, **PI-**(2*S*,2′*S*)**-5αD**, **PI-5αG**, **PI-5βG**, and **PI-5βH** were selected for conjugate synthesis (paper II), based on the observed activity and synthetic accessibility. Cephalosporin-inhibitor conjugates **PII-3-8** were synthesized, the release of the thiols **PII-9-14** and the inhibitory activity were studied and compared to conjugates of 8-TQ and L-captopril (**PII-1** and **PII-2**, respectively). Using both NMR and LC-MS, the conjugates containing the fluorinated thiols were shown to release the inhibitor upon β-lactam hydrolysis alongside formation of the product of only β-lactam ring cleavage (**PII-H**). For most experiments in the hydrolysis studies a mixture of compounds was obtained, which complicated direct quantification of the release and comparison in between the conjugates. Nevertheless, the inhibitory activity of the conjugates was found to be in correlation with the respective thiols.

Additionally, the use of fluorine containing inhibitors as tools for NMR analysis was demonstrated. In paper I, the potential application of **PI-rac-5αA** and related compounds in solution-state NMR binding studies was illustrated. Furthermore, in paper II, the possibility of using fluorine-containing compounds to monitor enzymatic hydrolysis via ^{19}F NMR was investigated on conjugates **PII-4** and **PII-5**.

Although the studied conjugates demonstrated that fluorination facilitates the release of the aliphatic thiols, the compounds appear to be in between non-fluorinated aliphatic and aromatic thiols in terms of release of the leaving group. Liberation of the thiols might be occurring only to a certain extent, based on the stalling of the release as seen in the LC-MS-monitored experiments. Therefore, further refinement of the conjugate structure to improve thiol release is necessary. Presumably, introduction of an additional trifluoromethyl into the structure of thiols **PI-5** (Fig. 16, left) could lead to enhancement of the release due to better stabilization of the thiolate. However, the synthesis and analysis of such compounds (**64**) would pose a significant challenge. The approach used for fluorinated thiols in the current study included conjugate addition of thioacetic acid, the rate of which is much slower for sterically hindered substrates. In the event that a synthetic pathway is successful the obtained compounds would contain at least two stereocenters, generating mixtures of isomers that would be difficult to separate and analyze.

Within the framework of this study, synthesis of compound **5f** was not successful due to defluorination. Obtaining such compounds and evaluating the release of the respective conjugates remains an open question. Development of a synthetic route that does not result in fluorine expulsion is one of the apparent approaches. Alternatively, elongating the carbon chain would result in a non-conjugated system, possibly overcoming the problem of defluorination (Fig. 16, right). Incidentally, Yusof *et al.*

explored the influence of the length of the mercaptoalkanoyl chain of captopril analogues on inhibitory activity.[96] Compounds containing a three-carbon chain (**66** and **67**) displayed inhibition in a similar range to the corresponding two carbon chain derivatives, indicating that compounds **65** would be a relevant scaffold for fluorination.
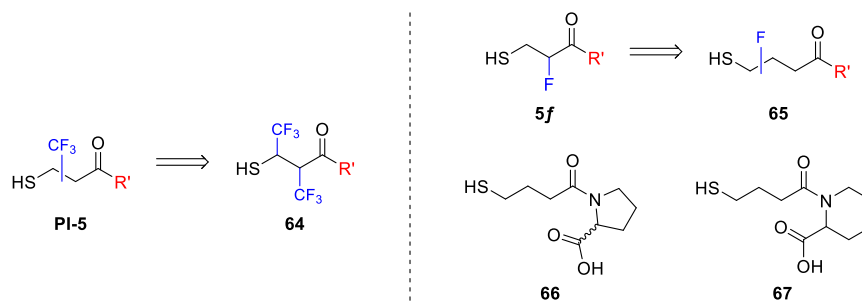
Figure 16. Potential strategies for fluorinated thiol inhibitors.

The two aforementioned approaches are both tied to fluorinated aliphatic inhibitors. While it is evident that fluorination offers certain advantages, it is not always synthetically possible to achieve. Consequently, an alternative strategy independent of the leaving group ability of the aliphatic thiols would be advantageous. A linker, cleavable upon hydrolysis of the β-lactam ring, such as depicted in Figure 17, would rely less on the electronic properties of the attached thiol. This concept has been utilized, for example, in the design of compound **7**, a dual drug conjugate of a siderophore attached to a cephalosporin linked to an oxazolidinone.[74]
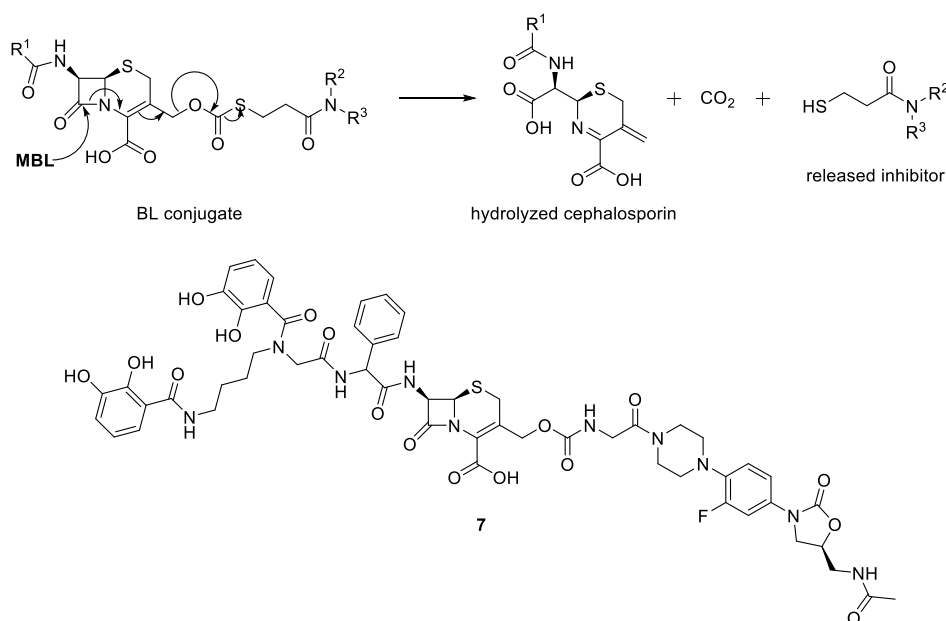
Figure 17. Conjugates with cleavable linkers.

38

5 Conclusion

This thesis describes the development of novel fluorinated alkyl thiol-based MBL inhibitors and cephalosporin conjugates thereof, which release the former upon MBL-mediated hydrolysis.

Initially, fluorinated captopril analogues were synthesized and established to be potent MBL inhibitors, with several compounds exhibiting inhibitory activity in the low micromolar region. The position of the fluorination site was shown to influence the stability towards oxidation and inhibitory activity of the compounds. β-CF$_3$-containing compounds were found to be more stable, while derivatives with an α-CF$_3$ group were more active. The most potent compound was determined to be a CF$_3$-derivative of captopril. Substitution of an α-CH$_3$ with an α-CF$_3$ group proved to have little influence on the inhibitory activity. The binding pose of one fluorine-labelled inhibitor was determined, demonstrating that fluorinated analogues of inhibitors can be used as probes for structural studies of MBL-inhibitor complexes.

A few of the trifluoromethylated thiols were further employed in the synthesis of cephalosporin-based conjugates. The conjugates containing the fluorinated thiol inhibitors were shown to release the thiols upon enzymatic hydrolysis and exhibited inhibitory activity against several MBLs. In addition, ^{19}F NMR was shown to be a sensitive tool for monitoring enzyme-mediated hydrolysis. Comparison of conjugates with α- and β-CF$_3$ groups proved to be challenging due to the formation of other intermediates. However, the results indicate that the β-CF$_3$-positioning is more beneficial for the rate of hydrolysis and release.

The developed compounds provide proof of concept, confirming that incorporation of an electron-withdrawing group into aliphatic thiols can facilitate release. As the conjugates demonstrated accumulation of unwanted intermediates, additional studies on the release could provide insight into structural adjustments to suppress alternative chemical pathways and further enhance the release of aliphatic thiol-based inhibitors from the conjugate.

To my mind, thiol-based inhibitors will continue to be compounds of interest in future MBL inhibitor design. Due to the evolution and spread of resistant bacteria thus far, the dire need for new drugs is not expected to decline anytime soon. Furthermore, the conjugate approach to inhibition of MBLs, facilitating targeted release, thereby limiting unwanted side-reactions, is advantageous over the direct use of inhibitors. With a variety of potent inhibitors being represented by aliphatic thiols, the present study can provide a starting point for future development of aliphatic thiol-containing cephalosporin conjugates.

6 Appendix

This chapter includes additional experimental procedures and NMR spectra for compounds not included in the manuscripts.

6.1 Experimental details

General methods

All reagents were purchased from commercial sources and used as supplied without further purification unless otherwise stated. 2-Fluoroacrylic acid (**1f**)[100], (6R,7R)-7-acetamido-3-(acetoxymethyl)-8-oxo-5-thia-1-azabicyclo[4.2.0]oct-2-ene-2-carboxylic acid (**61**) and *tert*-butyl (6R,7R)-7-acetamido-3-(acetoxymethyl)-8-oxo-5-thia-1-azabicyclo[4.2.0]oct-2-ene-2-carboxylate (**62**) were synthesized as described in literature and the analytical data was found to be in accordance with that reported. Solvents were dried according to standard procedures over appropriately sized molecular sieves.

For thin layer chromatography (TLC) analysis, aluminium plates pre-coated with silica gel (Merck silica gel 60 F_{254}) were used and visualized using either ultraviolet light or by treatment with an appropriate stain. Normal phase chromatography was carried out using Redisep Gold® silica gel columns on a CombiFlash® EZ Prep system.

^{1}H and ^{13}C NMR spectra for assignment were obtained on a 400 MHZ Bruker Advance III HD spectrometer equipped with a 5 mm SmartProbe BB/1H (BB = 19F, 31P-15N) at 20 ˚C. Chemical shifts are reported in ppm relative to the solvent residual peak (CDCl$_3$: δH 7.26 and δC 77.16; Acetone-*d6*: δH 2.05 and δC 206.26; Methanol-*d4*: δH 3.31 and δC 49.00). Coupling constants *J* are reported in Hertz (Hz). The ^{13}C NMR spectra were ^{1}H decoupled. The following abbreviations were used to indicate the multiplicities: s = singlet, d = doublet, t = triplet, q = quartet, dd = doublet of doublets, dq = doublet of quartets, ddd = doublet of doublet of doublets, tt = triplet of triplets, m = multiplet, app = appearing and br = broad. When possible, for compounds obtained as rotameric mixtures, chemical shifts of minor rotamers are reported separately, enclosed in square brackets.

Spectroscopic data
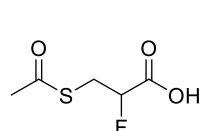
3-(acetylthio)-2-fluoropropanoic acid (**2f**).

2-Fluoroacrylic acid (**1f**) (172 mg, 1.91 mmol, 1.0 eq) was dissolved in THF (2 mL). Thioacetic acid (202 µl, 2.87 mmol, 1.5 eq) was added and the reaction mixture was stirred at 60 ˚C for 60 h. After the mixture cooled down to ambient temperature, the volatiles were removed under reduced pressure to yield **2f** (242 mg, 1.46 mmol, 76%) as a white solid. **^{1}H NMR** (400 MHz, CDCl$_3$) δ 10.10 (br s, 1H), 5.07 (ddd, *J* = 48.0, 7.0, 4.3 Hz, 1H), 3.58 (ddd, *J* = 23.3, 14.6, 4.3 Hz,

1H), 3.35 (ddd, J = 21.7, 14.6, 7.0 Hz, 1H), 2.39 (s, 3H). ^{13}**C NMR** (101 MHz, CDCl$_3$) δ 194.4, 173.0 (d, J = 24.2 Hz), 86.7 (d, J = 188.6 Hz), 30.7 (d, J = 21.9 Hz), 30.6.

N-benzyl-2-fluoroacrylamide (3*f*A).
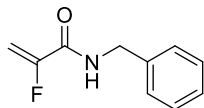
A solution of 2-fluoroacrylic acid (**1***f*) (330 mg, 3.66 mmol, 1.0 eq) in DCM (10 mL) was treated with HBTU (2.09 g, 5.50 mmol, 1.5 eq). The resulting mixture was cooled down to 0 ˚C and DIPEA (1.27 mL, 7.33 mmol, 2.0 eq) and benzylamine (480 μl, 4.40 mmol, 1.2 eq) were sequentially added. After removal of the ice bath, the reaction was stirred at ambient temperature for 2 h. The solvent was removed under reduced pressure and the crude product was purified on an automated flash system equipped with a silica column, using heptane/EtOAc as the eluent, to yield **3***f***A** (306 mg, 1.71 mmol, 47%) as a white solid. ^{1}**H NMR** (400 MHz, CDCl$_3$) δ 7.38 – 7.27 (m, 5H), 6.66 (br s, 1H), 5.72 (dd, J = 47.8, 3.2 Hz, 1H), 5.13 (dd, J = 15.3, 3.2 Hz, 1H), 4.52 (d, J = 5.9 Hz, 2H). *Note: Residual tetramethylurea (TMU) was observed (2.79, s).* ^{13}**C NMR** (101 MHz, CDCl$_3$) δ *Not recorded.*

Tert-butyl (2-fluoroacryloyl)-L-prolinate (3*f*D).
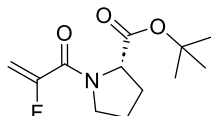
A solution of 2-fluoroacrylic acid (**1***f*) (100 mg, 1.11 mmol, 1.0 eq) in DCM (7 mL) was treated with HBTU (632 mg, 1.67 mmol, 1.5 eq). The resulting mixture was cooled down to 0 ˚C and DIPEA (288 μl, 1.67 mmol, 1.5 eq) and *tert*-butyl L-prolinate (228 mg, 1.33 mmol, 1.2 eq) were sequentially added. After removal of the ice bath, the reaction was stirred at ambient temperature for 2 h. The solvent was removed under reduced pressure and the crude product was purified on an automated flash system equipped with a silica column, using heptane/EtOAc as the eluent, to yield **3***f***D** (222 mg, 0.91 mmol, 82%) as a yellow oil. ^{1}**H NMR** (400 MHz, CDCl$_3$) (a 1.3:1 mixture of rotamers*) δ 5.53 (dd, J = 46.6, 3.1 Hz, 1H) [5.60 (J = 47.4, 3.0 Hz)], 5.12 (dd, J = 16.1, 3.1 Hz, 1H) [5.08 (J = 16.5, 3.0 Hz)], 4.46 – 4.37 (m, 1H) [4.61 – 4.53], 3.86 – 3.58 (m, 2H), 2.32 – 1.80 (m, 4H), 1.46 (s, 9H) [1.44]. *Note: Residual tetramethylurea (TMU) was observed (2.79, s).* ^{13}**C NMR** (101 MHz, CDCl$_3$) δ *Not recorded.*

---

* Chemical shifts of minor rotamer are enclosed in square brackets.
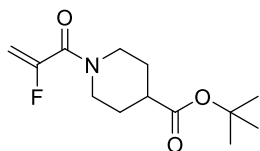
Tert-butyl 1-(2-fluoroacryloyl)piperidine-4-carboxylate (**3fF**).

A solution of 2-fluoroacrylic acid (**1f**) (130 mg, 1.44 mmol, 1.0 eq) in DCM (7 mL) was treated with HBTU (821 mg, 2.17 mmol, 1.5 eq). The resulting mixture was cooled down to 0 ˚C and DIPEA (500 µl, 2.89 mmol, 2.0 eq) and *tert*-butyl piperidine-4-carboxylate hydrochloride (384 mg, 1.73 mmol, 1.2 eq) were sequentially added. After removal of the ice bath, the reaction was stirred at ambient temperature for 2 h. The solvent was removed under reduced pressure and the crude product was purified on an automated flash system equipped with a silica column, using heptane/EtOAc as the eluent, to yield **3fF** (240 mg, 0.93 mmol, 65%) as a colourless oil. **^{1}H NMR** (400 MHz, CDCl$_3$) δ 5.18 (dd, *J* = 54.0, 3.5 Hz, 1H), 5.09 (dd, *J* = 23.5, 3.5 Hz, 1H), 4.39 – 3.70 (m, 2H), 3.28 – 2.83 (m, 2H), 2.47 (app tt, *J* = 10.5, 4.1 Hz, 1H), 1.99 – 1.85 (m, 2H), 1.75 – 1.61 (m, 2H), 1.44 (s, 9H). *Note: Residual tetramethylurea (TMU) was observed (2.79, s).* **^{13}C NMR** (101 MHz, CDCl$_3$) δ 173.4, 161.3 (d, *J* = 30.3 Hz), 157.8 (d, *J* = 271.9 Hz), 99.2 (d, *J* = 15.3 Hz), 80.9, 45.9, 42.1, 41.9, 28.2 (3C), 27.9 (2C). *Note: Carbon signals of the CH$_2$ groups of the piperidine ring (45.9, 42.1, 27.9) are reported based on the cross-peaks observed in the HMBC and HSQC.*
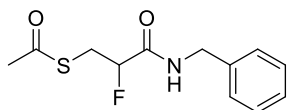
S-(3-(benzylamino)-2-fluoro-3-oxopropyl) ethanethioate (**4fA**).

Compound **2f** (190 mg, 1.14 mmol, 1.0 eq), EDCl (438 mg, 2.29 mmol, 2.0 eq), HOBt (185 mg, 1.37 mmol, 1.2 eq) and *N*-methylmorpholine (138 µl, 1.26 mmol, 1.1 eq) were taken up in DCM (15 mL). The mixture was cooled down to 0 ˚C and benzylamine (137 µl, 1.26 mmol, 1.1 eq) was added. The reaction mixture was stirred at 0 ˚C for 30 min and overnight at ambient temperature. The reaction was quenched with a saturated NaCl$_{(aq)}$ solution and the aqueous layer was extracted three times with EtOAc. The combined organic layers were washed three times with a 5% citric acid$_{(aq)}$ solution, dried over MgSO$_4$, filtered and the solvent was removed under reduced pressure. The crude was purified on an automated flash system equipped with a silica column, using heptane/EtOAc as the eluent, to yield **4fA** (144 mg, 0.56 mmol, 49%) as a white solid. **^{1}H NMR** (400 MHz, CDCl$_3$) δ 7.38 – 7.27 (m, 5H), 6.62 (br s, 1H), 5.07 (ddd, *J* = 49.0, 6.6, 3.7 Hz, 1H), 4.56 – 4.42 (m, 2H), 3.63 (ddd, *J* = 24.0, 14.7, 3.8 Hz, 1H), 3.40 (ddd, *J* = 25.7, 14.6, 6.6 Hz, 1H), 2.36 (s, 3H). **^{13}C NMR** (101 MHz, CDCl$_3$) δ 193.9, 167.8 (d, *J* = 19.4 Hz), 137.4, 129.0 (2C), 128.0 (2C), 127.95, 89.9 (d, *J* = 190.7 Hz), 43.4, 31.0 (d, *J* = 21.2 Hz), 30.6.

Tert-butyl (3-(acetylthio)-2-fluoropropanoyl)-L-prolinate (**4*f*D**).
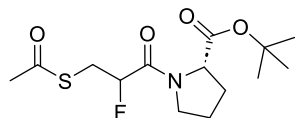
Compound **3*f*D** (100 mg, 0.41 mmol, 1.0 eq) was dissolved in THF (5 mL). Thioacetic acid (58 µl, 0.82 mmol, 2.0 eq) was added and the reaction mixture was stirred at 60 ˚C for 60 h. After the mixture cooled down to ambient temperature, the volatiles were removed under reduced pressure. The crude was purified on an automated flash system equipped with a silica column, using heptane/EtOAc as the eluent, to yield **4*f*D** (109 mg, 0.34 mmol, 83%) as a colourless oil. The title compound was obtained as a diastereomeric mixture, with each diastereomer being present as two rotamers. NMR data is reported for the mixture of four isomers. **¹H NMR** (400 MHz, CDCl₃) (a 3:2:1:1 mixture of isomers) δ 5.14 – 4.86 (m, 1H), 4.63 – 4.30 (m, 1H), 3.81 – 3.15 (m, 4H), 2.38 – 2.27 (m, 3H), 2.26 – 1.74 (m, 4H), 1.47 – 1.35 (m, 9H). **¹³C NMR** (101 MHz, CDCl₃) δ *No suitable data could be acquired due to a mixture of isomers and impurities*.

Tert-butyl 1-(3-(acetylthio)-2-fluoropropanoyl)piperidine-4-carboxylate (**4*f*F**).
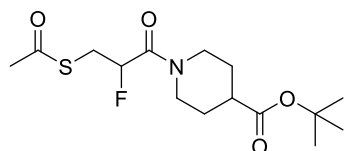
Compound **3*f*F** (240 mg, 0.93 mmol, 1.0 eq) was dissolved in THF (10 mL). Thioacetic acid (132 µl, 1.87 mmol, 2.0 eq) was added and the reaction mixture was stirred at 60 ˚C for 60 h. After the mixture cooled down to ambient temperature, the volatiles were removed under reduced pressure. The crude was purified on an automated flash system equipped with a silica column, using heptane/EtOAc as the eluent, to yield **4*f*F** (229 mg, 0.69 mmol, 74%) as a colourless oil. **¹H NMR** (400 MHz, CDCl₃) (a 1.1:1 mixture of rotamers[*]) δ 5.09 (dd, *J* = 7.7, 5.0 Hz, 1H) [5.21], 4.30 – 4.22 (m, 1H) [4.40 – 4.31], 3.98 – 3.87 (m, 1H), 3.50 – 3.35 (m, 1H), 3.34 – 3.08 (m, 2H), 3.02 – 2.92 (m, 1H) [2.91 – 2.81], 2.52 – 2.41 (m, 1H), 2.36 (s, 3H) [2.35], 1.98 – 1.85 (m, 2H), 1.78 – 1.56 (m, 2H), 1.43 (s, 9H) [1.43]. **¹³C NMR** (101 MHz, CDCl₃) δ 195.7 [195.65], 173.3 [173.4], 165.1 [165.2] (d, *J* = 20.1 Hz), 86.8 [86.75] (d, *J* = 182.4 Hz), 80.85 [80.9], 45.0 [44.6] (d, *J* = 4.4 Hz), 42.0 [41.8], 41.9 [41.6], 30.5, 30.4 [30.6] (d, *J* = 24.9 Hz), 28.7 [28.8], 28.2 (3C), 27.9 [27.85].

N-benzylacrylamide (**56**).
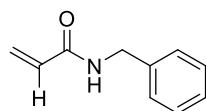
Compound **4*f*A** (36 mg, 0.14 mmol, 1.0 eq) was dissolved in MeOH (1 mL) under an argon atmosphere. A 2 M aqueous solution of NaOH (212 µl, 0.42 mmol, 3.0 eq) was added. The reaction was stirred at ambient temperature for 2 h. The solvent was removed under

---

[*] Chemical shifts of minor rotamer are enclosed in square brackets.

reduced pressure and water was added to the residue. The mixture was acidified to pH = 2 with 1 M HCl and the aqueous layer was extracted three times with EtOAc. The combined organic layers were dried over Na_2SO_4, filtered and the solvent was removed under reduced pressure. The crude product was purified on an automated flash system equipped with a silica column, using heptane/EtOAc as the eluent, to yield **56** (7 mg, 0.04 mmol, 31%) as a white solid. **^{1}H NMR** (400 MHz, Acetone-*d6*) δ 7.69 (br s, 1H), 7.35 – 7.20 (m, 5H), 6.33 (dd, *J* = 17.0, 9.9 Hz, 1H), 6.22 (dd, *J* = 17.0, 2.4 Hz, 1H), 5.59 (dd, *J* = 9.9, 2.4 Hz, 1H), 4.46 (d, *J* = 6.0 Hz, 2H). **^{13}C NMR** (101 MHz, Acetone-*d6*) δ 165.9, 140.6, 132.8, 129.3 (2C), 128.6 (2C), 127.9, 125.8, 43.6.
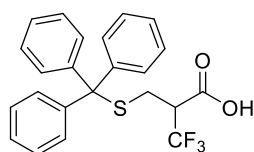
3,3,3-trifluoro-2-((tritylthio)methyl)propanoic acid (**57**).

2-(trifluoromethyl)acrylic acid (70 mg, 0.50 mmol, 1.0 eq) was dissolved in DCM (5 mL). Triphenylmethyl mercaptan (415 mg, 1.50 mmol, 3.0 eq) and triethylamine (279 μl, 2.00 mmol, 4.0 eq) were added and the reaction mixture was stirred at ambient temperature overnight. The reaction mixture was diluted with DCM, washed with water and brine. The organic layer was dried over Na_2SO_4, filtered and the solvent was removed under reduced pressure. The crude product was purified on an automated flash system equipped with a silica column, using DCM/MeOH as the eluent, to yield **57** (175 mg, 0.42 mmol, 84%) as a white solid. **^{1}H NMR** (400 MHz, CDCl$_3$) δ *No suitable data could be acquired due to impurities*. **^{13}C NMR** (101 MHz, CDCl$_3$) δ *No suitable data could be acquired due to impurities*.
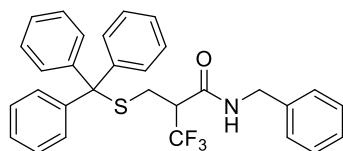
N-benzyl-3,3,3-trifluoro-2-((tritylthio)methyl)propanamide (**58**).

Compound **57** (290 mg, 0.70 mmol, 1.0 eq), EDCl (267 mg, 1.39 mmol, 2.0 eq), HOBt (113 mg, 0.84 mmol, 1.2 eq) and *N*-methylmorpholine (84 μl, 0.77 mmol, 1.1 eq) were taken up in DCM (15 mL). The mixture was cooled down to 0 ˚C and benzylamine (84 μl, 0.77 mmol, 1.1 eq) was added. The reaction mixture was stirred at 0 ˚C for 30 min and overnight at ambient temperature. The reaction was quenched with a saturated NaCl$_{(aq)}$ solution and the aqueous layer was extracted three times with EtOAc. The combined organic layers were washed three times with a 5% citric acid$_{(aq)}$ solution, dried over MgSO$_4$, filtered and the solvent was removed under reduced pressure. The crude was purified on an automated flash system equipped with a silica column, using heptane/EtOAc as the eluent, to yield **58** (219 mg, 0.43 mmol, 62%) as a white solid. **^{1}H NMR** (400 MHz, CDCl$_3$) δ 7.46 – 7.40 (m, 6H), 7.34 – 7.26 (m, 10H), 7.25 – 7.20 (m, 4H), 5.43 (br s, 1H), 4.49, 4.38 (ABdq, *J* = 15.0, 5.9 Hz, 2H), 3.17 (dd, *J* = 13.7, 10.9 Hz, 1H), 2.47 (dd, *J* = 13.8, 4.0 Hz, 1H), 1.76 – 1.63 (m, 1H). *Note: Residual EtOAc was observed.* **^{13}C NMR** (101 MHz, CDCl$_3$) δ *No suitable data could be acquired due to impurities*.
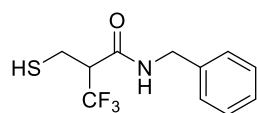
N-benzyl-3,3,3-trifluoro-2-(mercaptomethyl)propanamide (**PI-5αA**).

Compound **58** (207 mg, 0.41 mmol, 1.0 eq) was suspended in DCM (5 mL) and triethylsilane (131 μl, 0.82 mmol, 2.0 eq) was added. The mixture was cooled down to 0 ˚C and TFA (236 μl, 3.07 mmol, 7.5 eq) was added dropwise. The reaction mixture was gradually warmed up and stirred for 1.5 h at ambient temperature. The crude product was purified on an automated flash system equipped with a silica column, using heptane/EtOAc as the eluent, to yield **PI-5αA** (86 mg, 0.33 mmol, 80%) as a white solid. *Analytical data in agreement with the published data (See supporting information of Paper I).*

45

6.2 NMR spectra

3-(acetylthio)-2-fluoropropanoic acid (**2f**)
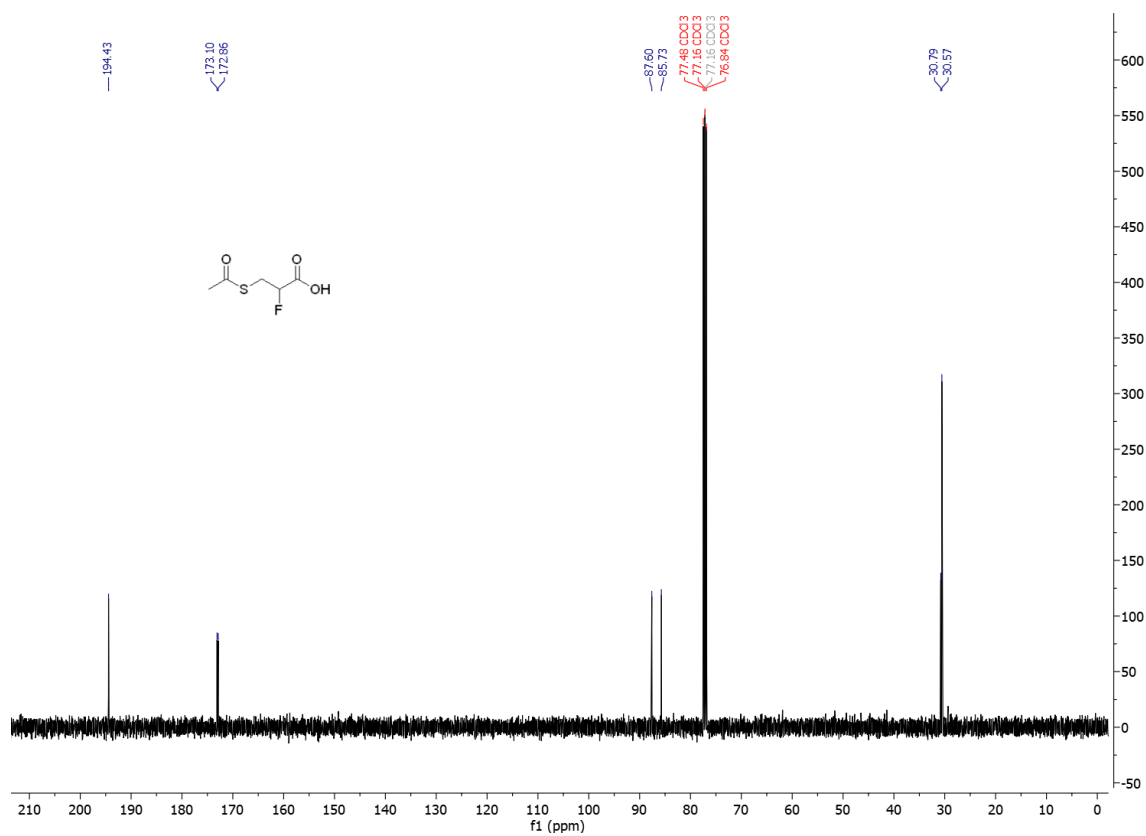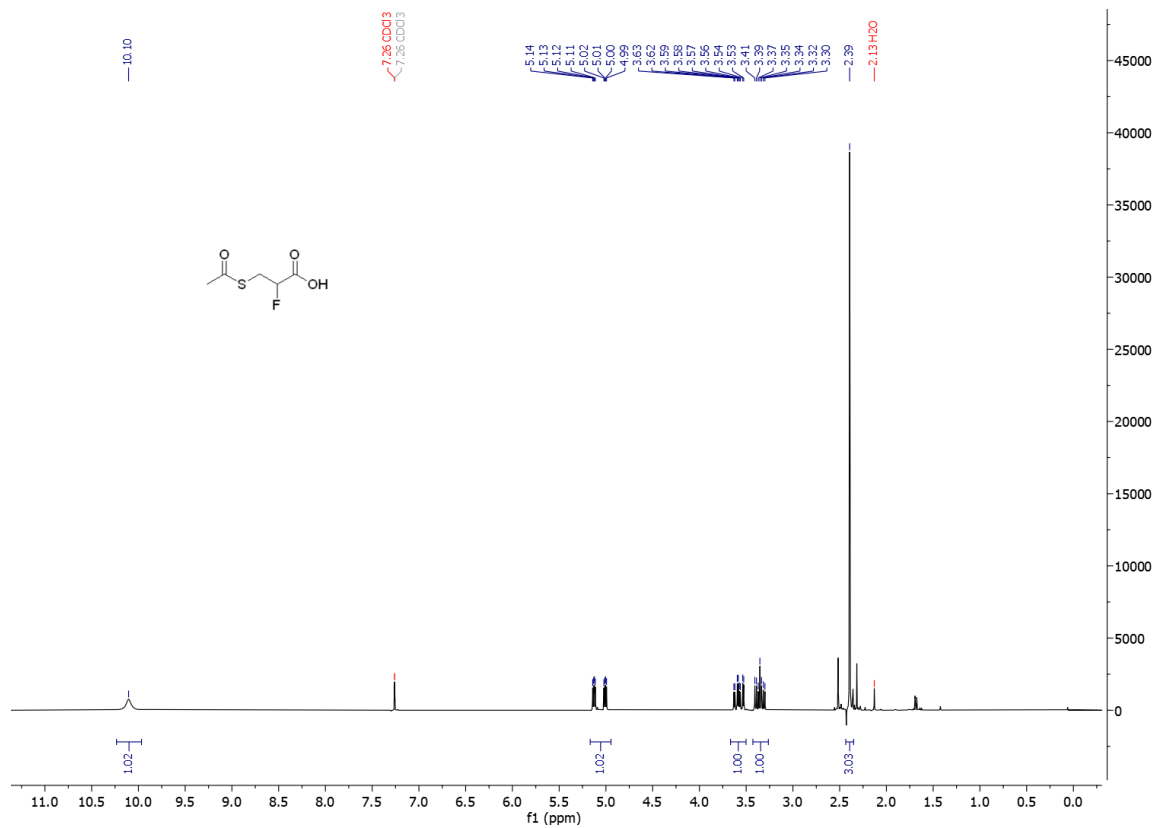
N-benzyl-2-fluoroacrylamide (**3𝑓A**)
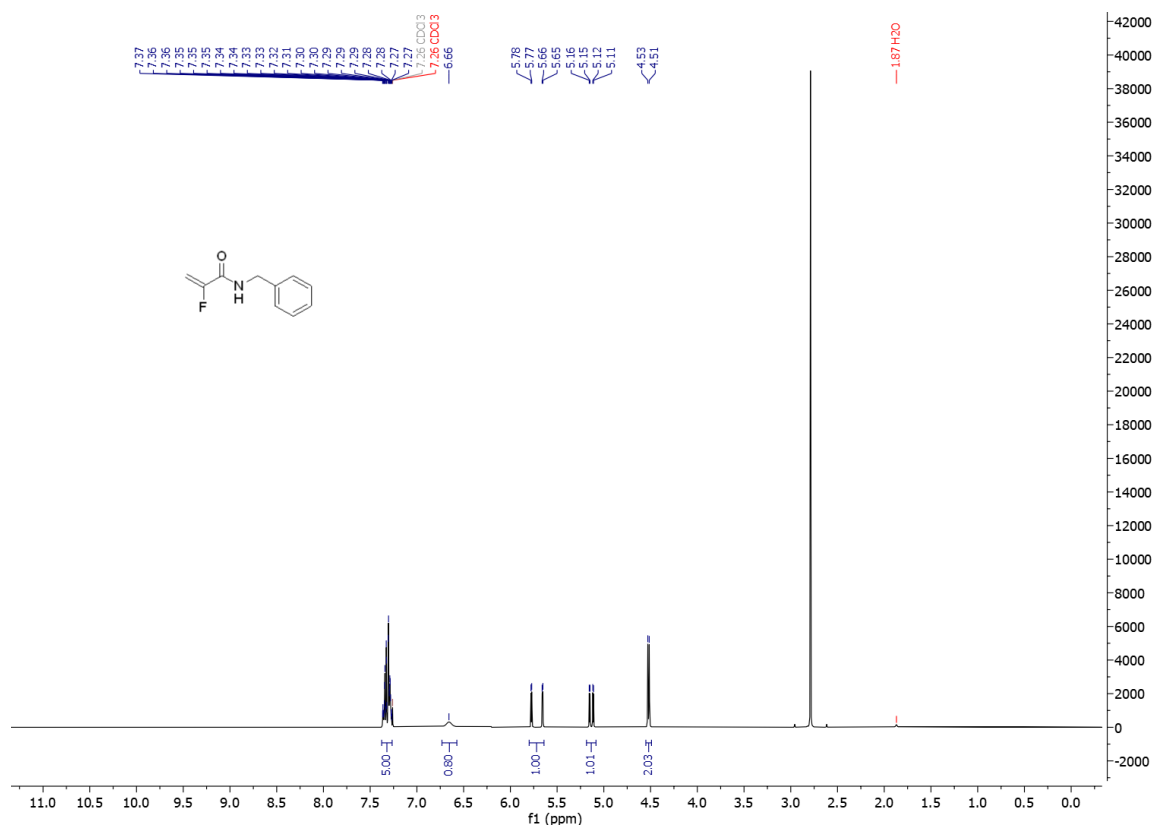
Tert-butyl (2-fluoroacryloyl)-L-prolinate (**3𝑓D**)
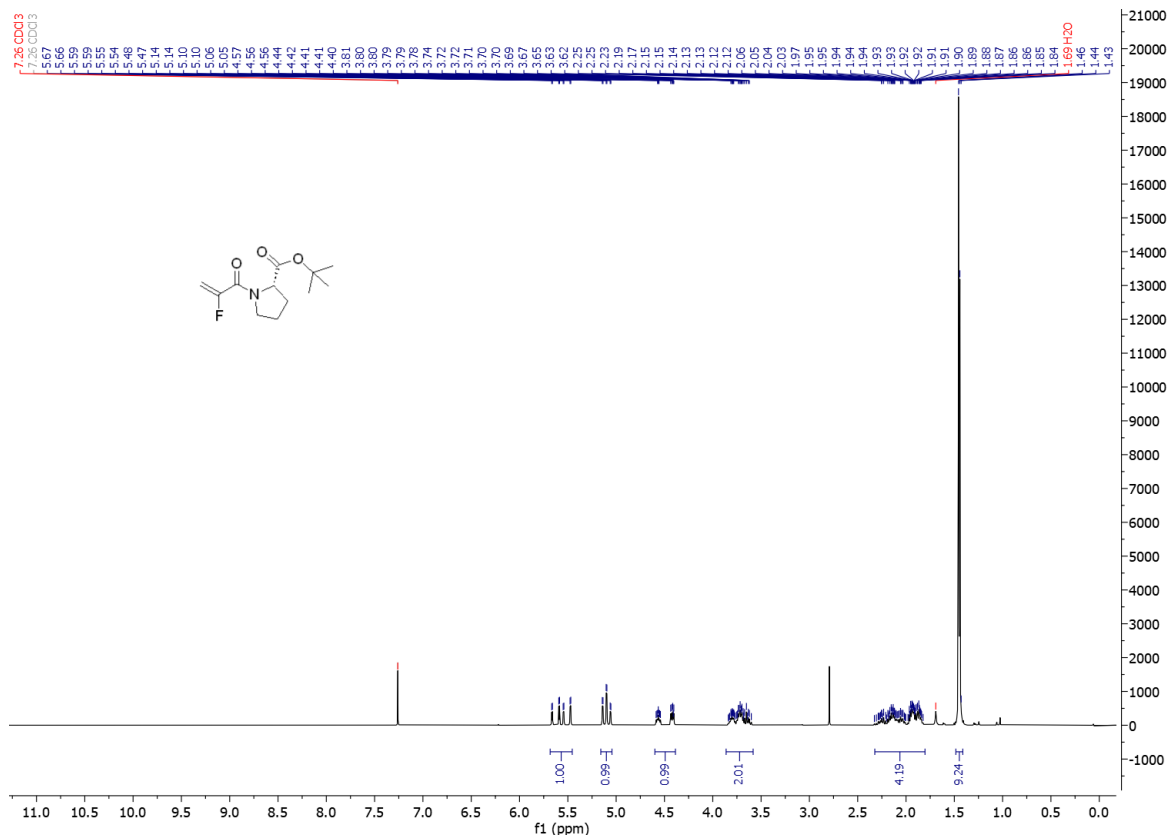
Tert-butyl 1-(2-fluoroacryloyl)piperidine-4-carboxylate (**3fF**)
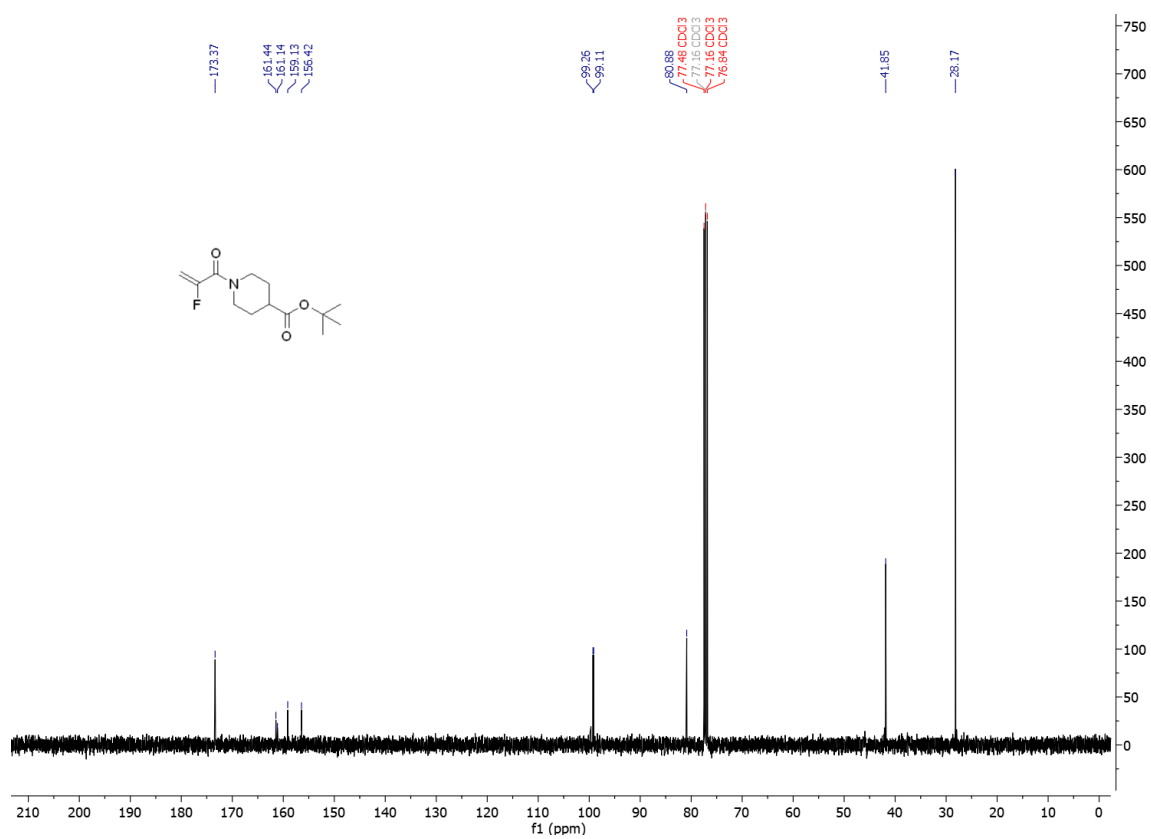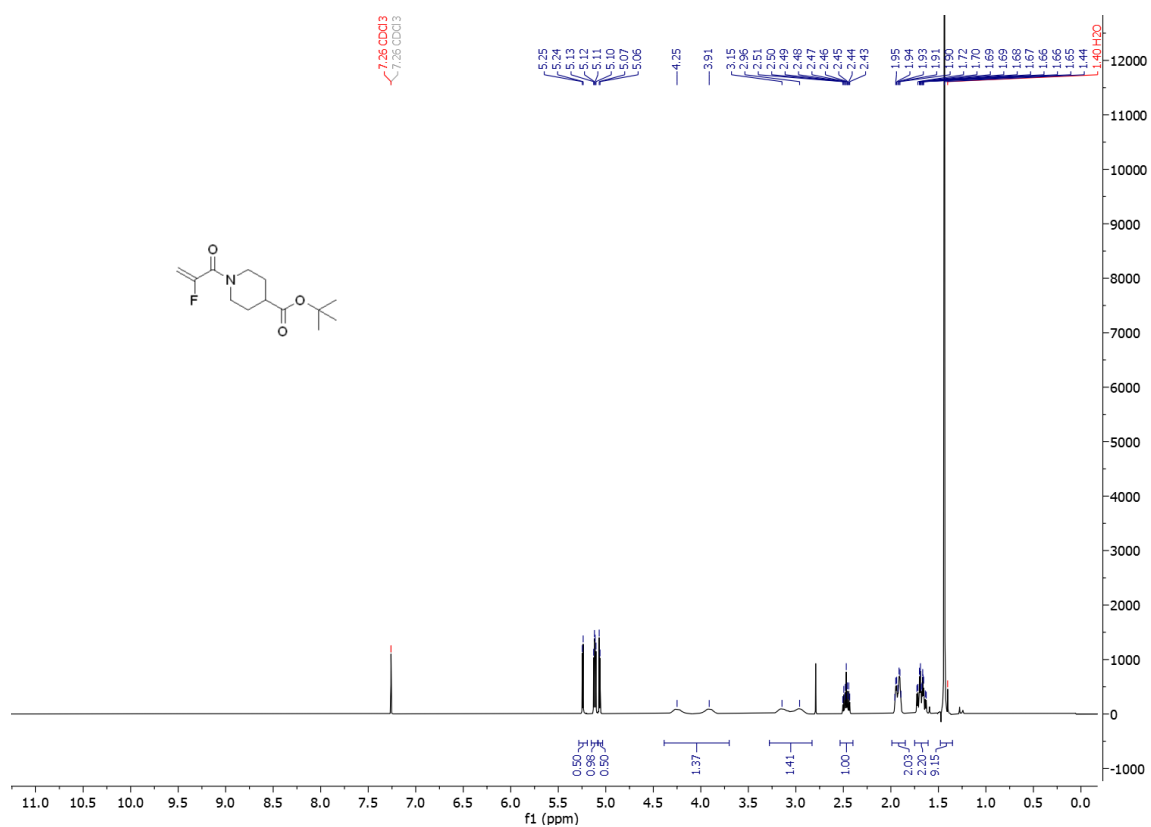
S-(3-(benzylamino)-2-fluoro-3-oxopropyl) ethanethioate (**4*f*A**)
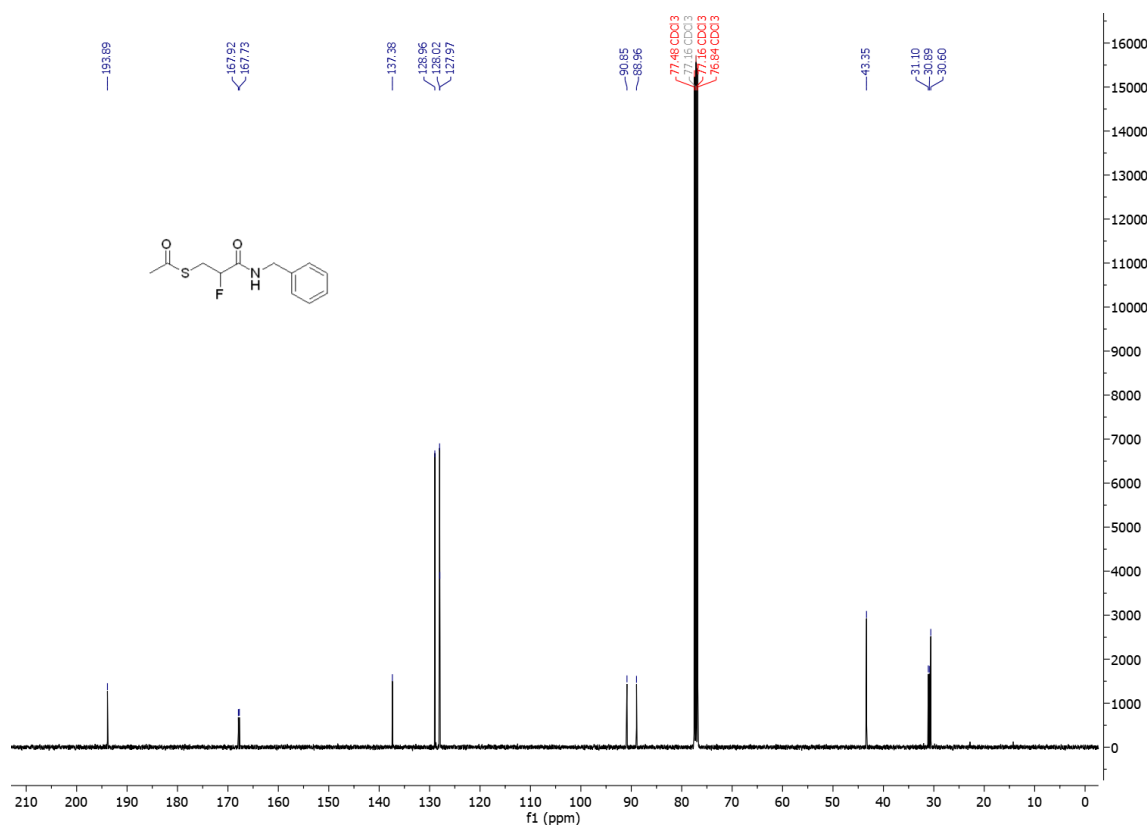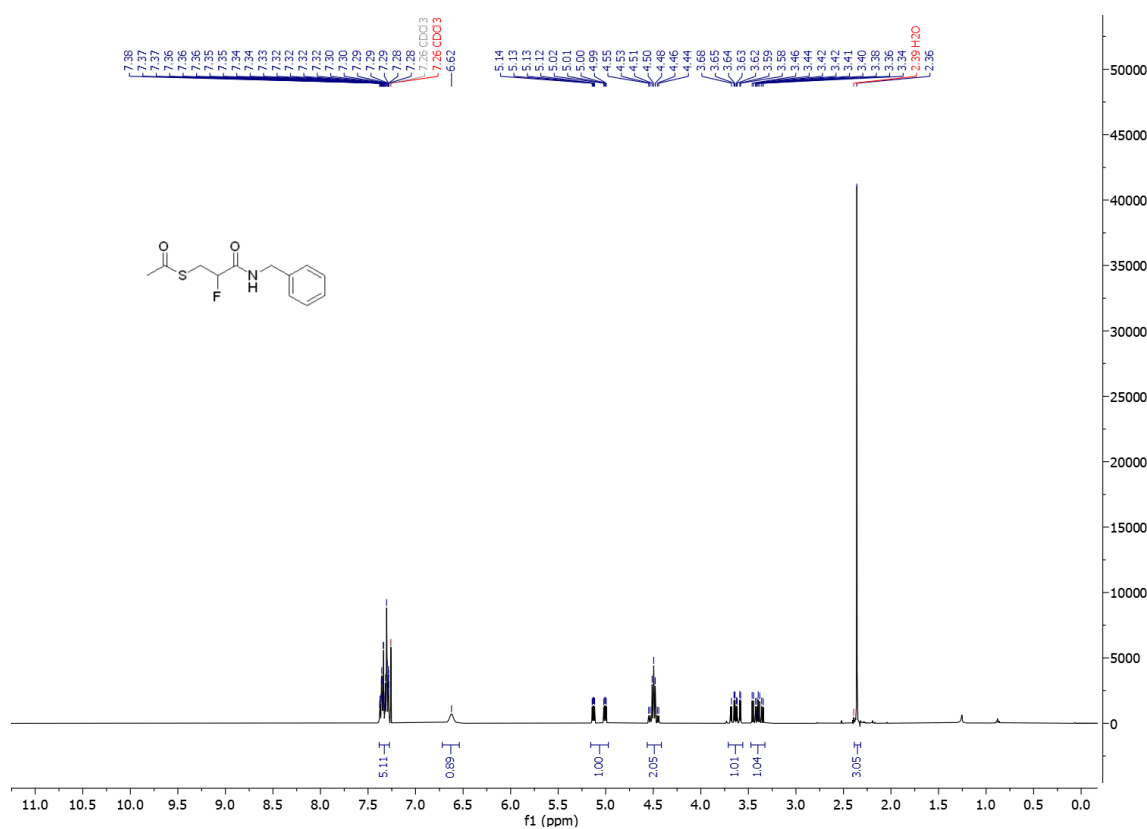
Tert-butyl (3-(acetylthio)-2-fluoropropanoyl)-L-prolinate (**4*f*D**)
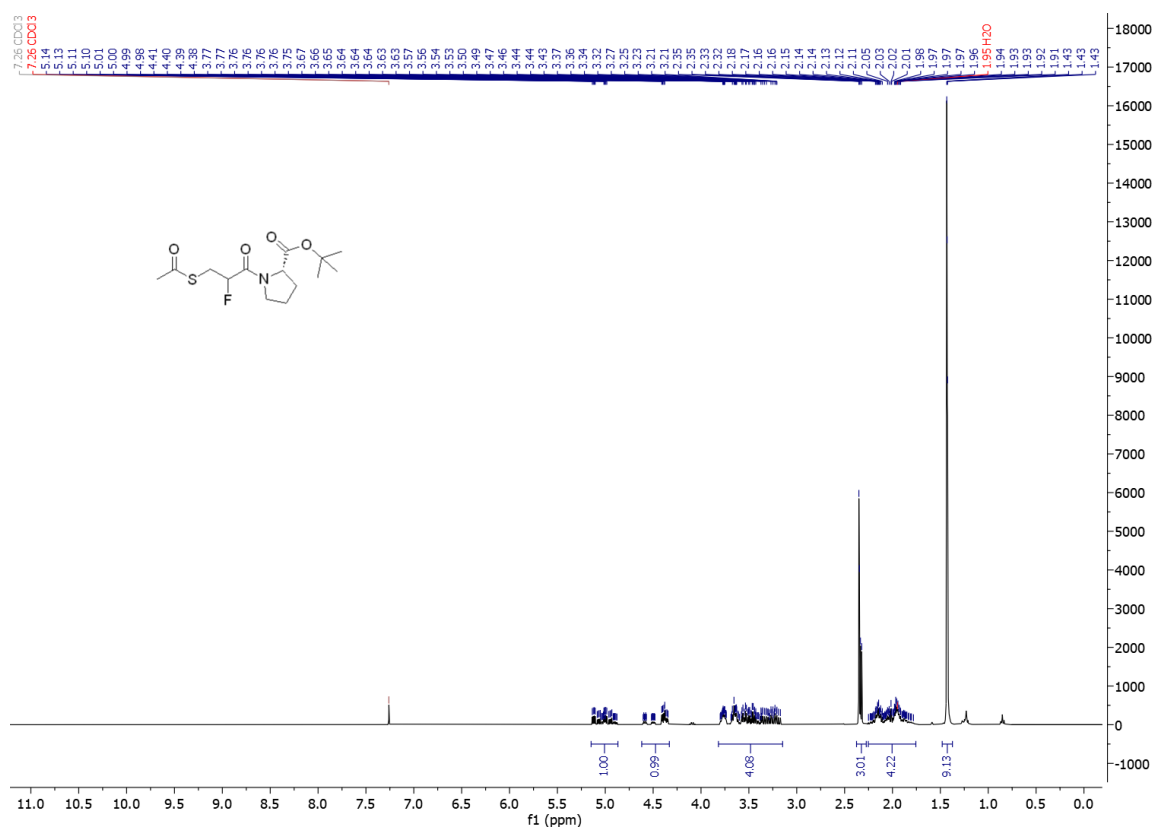
Tert-butyl 1-(3-(acetylthio)-2-fluoropropanoyl)piperidine-4-carboxylate (**4*f*F**)
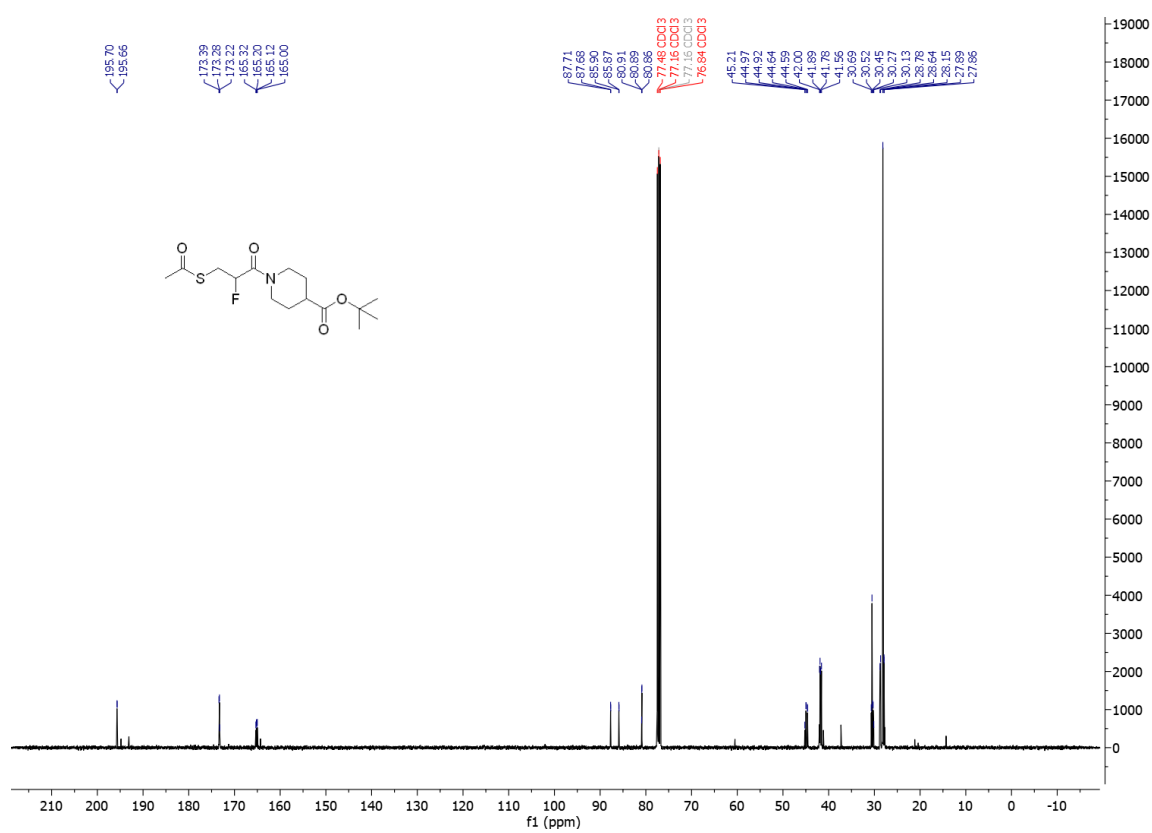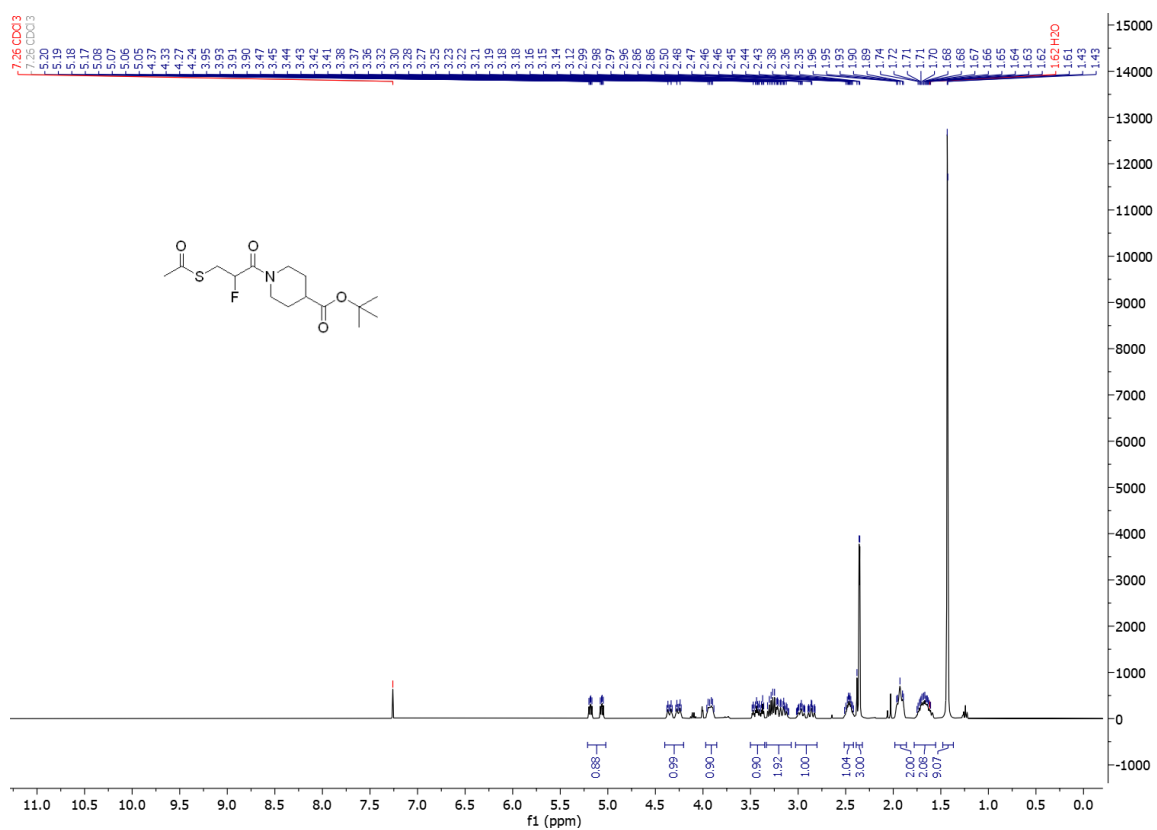
N-benzylacrylamide (**56**)
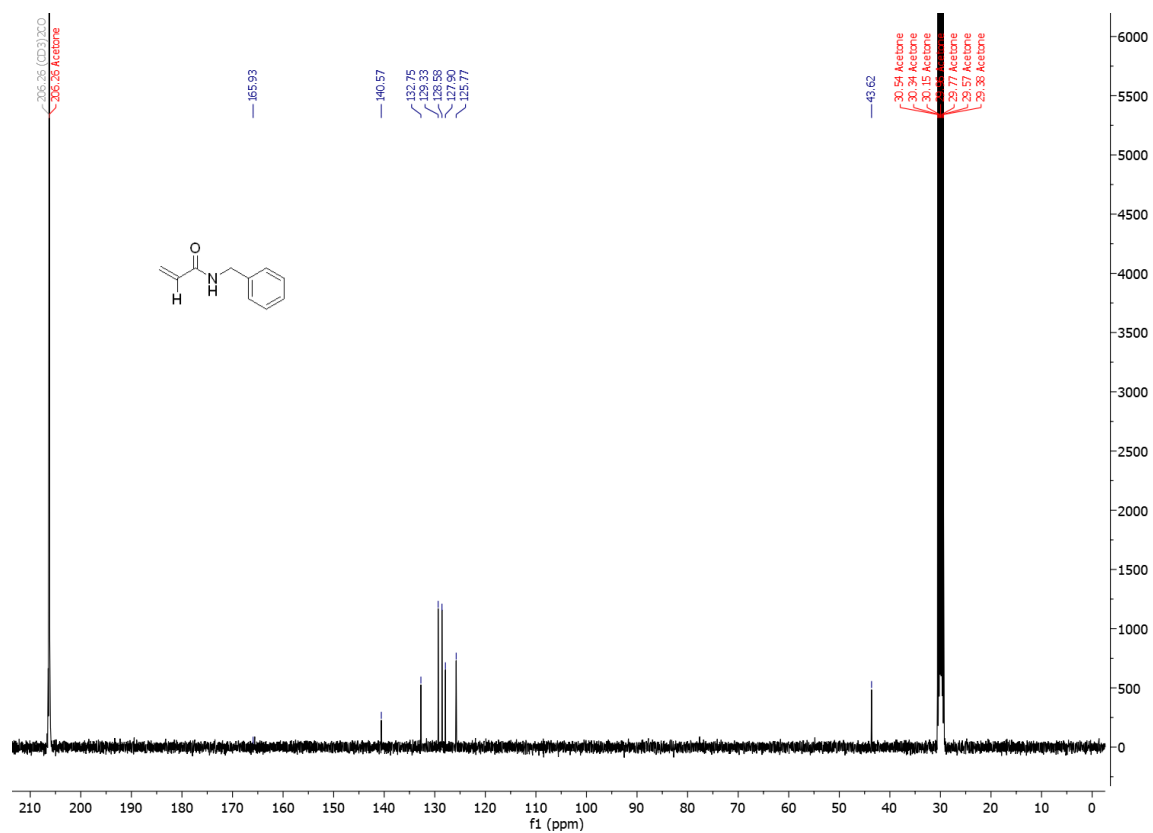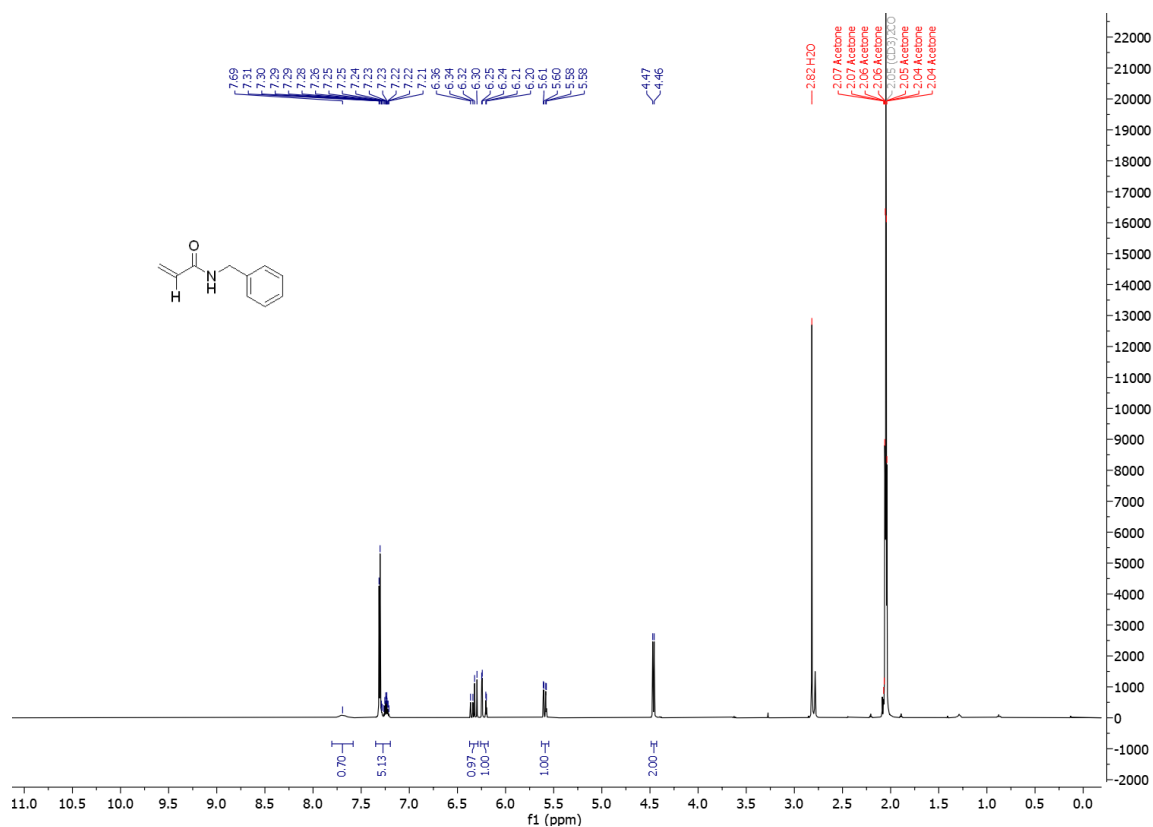
N-benzyl-3,3,3-trifluoro-2-((tritylthio)methyl)propanamide (**58**)
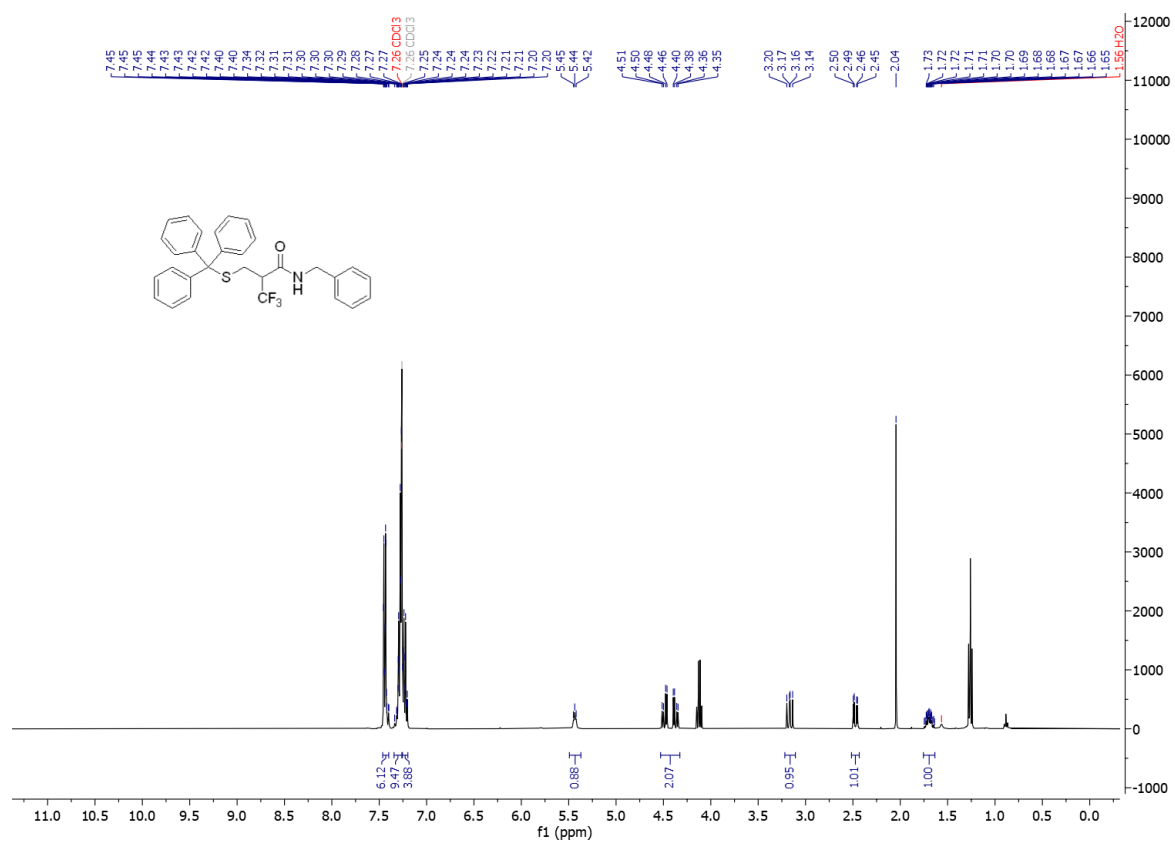
7 References

[1] WHO report on surveillance of antibiotic consumption: 2016-2018 early implementation, World Health Organization, Geneva, **2018**.

[2] Bush, K.; Bradford, P. A., β-Lactams and β-Lactamase Inhibitors: An Overview. *Cold Spring Harb. Perspect. Med.* **2016**, *6*, a025247.

[3] Halat, D. H.; Moubareck, C. A., The Current Burden of Carbapenemases: Review of Significant Properties and Dissemination among Gram-Negative Bacteria. *Antibiotics* **2020**, *9*, 186.

[4] Annunziato, G., Strategies to Overcome Antimicrobial Resistance (AMR) Making Use of Non-Essential Target Inhibitors: A Review. *Int. J. Mol. Sci.* **2019**, *20*, 5844.

[5] Laxminarayan, R.; Duse, A.; Wattal, C.; Zaidi, A. K. M.; Wertheim, H. F. L.; Sumpradit, N.; Vlieghe, E.; Hara, G. L.; Gould, I. M.; Goossens, H.; Greko, C.; So, A. D.; Bigdeli, M.; Tomson, G.; Woodhouse, W.; Ombaka, E.; Peralta, A. Q.; Qamar, F. N.; Mir, F.; Kariuki, S.; Bhutta, Z. A.; Coates, A.; Bergstrom, R.; Wright, G. D.; Brown, E. D.; Cars, O., Antibiotic Resistance — The Need for Global Solutions. *Lancet Infect. Dis.* **2013**, *13*, 1057-1098.

[6] Toussaint, K. A.; Gallagher, J. C., β-Lactam/β-Lactamase Inhibitor Combinations: From Then to Now. *Ann. Pharmacother.* **2014**, *49*, 86-98.

[7] Li, X.; Zhao, J.; Zhang, B.; Duan, X.; Jiao, J.; Wu, W.; Zhou, Y.; Wang, H., Drug Development Concerning Metallo-β-Lactamases in Gram-Negative Bacteria. *Front. Microbiol.* **2022**, *13*, 959107.

[8] Garau, G.; García-Sáez, I.; Bebrone, C.; Anne, C.; Mercuri, P.; Galleni, M.; Frère, J.; Dideberg, O., Update of the Standard Numbering Scheme for Class B β-Lactamases. *Antimicrob. Agents Chemother.* **2004**, *48*, 2347-2349.

[9] Boyd, S. E.; Livermore, D. M.; Hooper, D. C.; Hope, W. W., Metallo-β-Lactamases: Structure, Function, Epidemiology, Treatment Options, and the Development Pipeline. *Antimicrob. Agents Chemother.* **2020**, *64*, 10.1128/aac.00397-00320.

[10] Wade, N.; Tehrani, K. H. M. E.; Brüchle, N. C.; van Haren, M. J.; Mashayekhi, V.; Martin, N. I., Mechanistic Investigations of Metallo-β-lactamase Inhibitors: Strong Zinc Binding Is Not Required for Potent Enzyme Inhibition. *ChemMedChem* **2021**, *16*, 1651-1659.

[11] Bahr, G.; González, L. J.; Vila, A. J., Metallo-β-Lactamases in the Age of Multidrug Resistance: From Structure and Mechanism to Evolution, Dissemination, and Inhibitor Design. *Chem. Rev.* **2021**, *121*, 7957-8094.

[12] Buttner, D.; Kramer, J. S.; Klingler, F. M.; Wittmann, S. K.; Hartmann, M. R.; Kurz, C. G.; Kohnhauser, D.; Weizel, L.; Bruggerhoff, A.; Frank, D.; Steinhilber, D.; Wichelhaus, T. A.; Pogoryelov, D.; Proschak, E., Challenges in the Development of a Thiol-Based Broad-Spectrum Inhibitor for Metallo-β-Lactamases. *ACS Infect. Dis.* **2018**, *4*, 360-372.

[13] Lienard, B. M.; Garau, G.; Horsfall, L.; Karsisiotis, A. I.; Damblon, C.; Lassaux, P.; Papamicael, C.; Roberts, G. C.; Galleni, M.; Dideberg, O.; Frere, J. M.; Schofield, C. J., Structural Basis for the Broad-Spectrum Inhibition of Metallo-β-Lactamases by Thiols. *Org. Biomol. Chem.* **2008**, *6*, 2282-2294.

[14] Cole, M. S.; Hegde, P. V.; Aldrich, C. C., β-Lactamase-Mediated Fragmentation: Historical Perspectives and Recent Advances in Diagnostics, Imaging, and Antibacterial Design. *ACS Infect. Dis.* **2022**, *8*, 1992-2018.

[15] Bush, K.; Bradford, P. A., Interplay Between β-Lactamases and New β-Lactamase Inhibitors. *Nat. Rev. Microbiol.* **2019**, *17*, 295-306.

[16] Lima, L. M.; Silva, B. N. M. D.; Barbosa, G.; Barreiro, E. J., β-Lactam Antibiotics: An Overview from a Medicinal Chemistry Perspective. *Eur. J. Med. Chem.* **2020**, *208*, 112829.

[17] Bush, K.; Jacoby, G. A., Updated Functional Classification of β-Lactamases. *Antimicrob. Agents Chemother.* **2010**, *54*, 969-976.

[18] Tooke, C. L.; Hinchliffe, P.; Bragginton, E. C.; Colenso, C. K.; Hirvonen, V. H. A.; Takebayashi, Y.; Spencer, J., β-Lactamases and β-Lactamase Inhibitors in the 21st Century. *J. Mol. Biol.* **2019**, *431*, 3472-3500.

[19] Ambler, R. P.; Baddiley, J.; Abraham, E. P., The Structure of β-Lactamases. *Philos. Trans. R. Soc. B* **1980**, *289*, 321-331.

[20] Mora-Ochomogo, M.; Lohans, C. T., β-Lactam Antibiotic Targets and Resistance Mechanisms: from Covalent Inhibitors to Substrates. *RSC Med. Chem.* **2021**, *12*, 1623-1639.

[21] Yang, Y.; Yan, Y.-H.; Schofield, C. J.; McNally, A.; Zong, Z.; Li, G.-B., Metallo-β-Lactamase-Mediated Antimicrobial Resistance and Progress in Inhibitor Discovery. *Trends Microbiol.* **2023**, *31*, 735-748.

[22] Meini, M.-R.; Llarrull, L. I.; Vila, A. J., Overcoming Differences: The Catalytic Mechanism of Metallo-β-Lactamases. *FEBS Lett.* **2015**, *589*, 3419-3432.

[23] Lisa, M. N.; Palacios, A. R.; Aitha, M.; González, M. M.; Moreno, D. M.; Crowder, M. W.; Bonomo, R. A.; Spencer, J.; Tierney, D. L.; Llarrull, L. I.; Vila, A. J., A General Reaction Mechanism for Carbapenem Hydrolysis by Mononuclear and Binuclear Metallo-β-Lactamases. *Nat. Commun.* **2017**, *8*, 538.

[24] Palacios, A. R.; Rossi, M.-A.; Mahler, G. S.; Vila, A. J., Metallo-β-Lactamase Inhibitors Inspired on Snapshots from the Catalytic Mechanism. *Biomolecules* **2020**, *10*, 854.

[25] Yang, H.; Aitha, M.; Marts, A. R.; Hetrick, A.; Bennett, B.; Crowder, M. W.; Tierney, D. L., Spectroscopic and Mechanistic Studies of Heterodimetallic Forms of Metallo-β-Lactamase NDM-1. *J. Am. Chem. Soc.* **2014**, *136*, 7273-7285.

[26] Wang, Z.; Fast, W.; Benkovic, S. J., On the Mechanism of the Metallo-β-Lactamase from *Bacteroides fragilis*. *Biochemistry* **1999**, *38*, 10013-10023.

[27] Tioni, M. F.; Llarrull, L. I.; Poeylaut-Palena, A. A.; Martí, M. A.; Saggu, M.; Periyannan, G. R.; Mata, E. G.; Bennett, B.; Murgida, D. H.; Vila, A. J., Trapping and Characterization of a Reaction Intermediate in Carbapenem Hydrolysis by *B. cereus* Metallo-β-Lactamase. *J. Am. Chem. Soc.* **2008**, *130*, 15852-15863.

[28] Farhat, N.; Khan, A. U., Evolving Trends of New Delhi Metallo-Beta-Lactamse (NDM) Variants: A Threat to Antimicrobial Resistance. *Infect. Genet. Evol.* **2020**, *86*, 104588.

[29] Palzkill, T., Metallo-β-Lactamase Structure and Function. *Ann. N. Y. Acad. Sci.* **2013**, *1277*, 91-104.

[30] Payne, D. J.; Cramp, R.; Winstanley, D. J.; Knowles, D. J., Comparative Activities of Clavulanic Acid, Sulbactam, and Tazobactam Against Clinically Important Beta-Lactamases. *Antimicrob. Agents Chemother.* **1994**, *38*, 767-772.

[31] Drawz, S. M.; Bonomo, R. A., Three Decades of β-Lactamase Inhibitors. *Clin. Microbiol. Rev.* **2010**, *23*, 160-201.

[32] Denakpo, E.; Naas, T.; Iorga, B. I., An Updated Patent Review of Metallo-β-Lactamase Inhibitors (2020–2023). *Expert Opin. Ther. Pat.* **2023**, 1-16.

[33] Reddy, K. R.; Parkinson, J.; Sabet, M.; Tarazi, Z.; Boyer, S. H.; Lomovskaya, O.; Griffith, D. C.; Hecker, S. J.; Dudley, M. N., Selection of QPX7831, an Orally Bioavailable Prodrug of Boronic Acid β-Lactamase Inhibitor QPX7728. *J. Med. Chem.* **2021**, *64*, 17523-17529.

[34] Jacobs, L. M. C.; Consol, P.; Chen, Y., Drug Discovery in the Field of β-Lactams: An Academic Perspective. *Antibiotics* **2024**, *13*, 59.

[35] Mojica, M. F.; Rossi, M. A.; Vila, A. J.; Bonomo, R. A., The Urgent Need for Metallo-β-Lactamase Inhibitors: an Unattended Global Threat. *Lancet Infect. Dis.* **2022**, *22*, e28-e34.

[36] Lee, N.; Yuen, K.-Y.; Kumana, C. R., Clinical Role of β-Lactam/β-Lactamase Inhibitor Combinations. *Drugs* **2003**, *63*, 1511-1524.

[37] Yahav, D.; Giske, C. G.; Grāmatniece, A.; Abodakpi, H.; Tam, V. H.; Leibovici, L., New β-Lactam–β-Lactamase Inhibitor Combinations. *Clin. Microbiol. Rev.* **2020**, *34*, 10.1128/cmr.00115-00120.

[38] Bush, K., Game Changers: New β-Lactamase Inhibitor Combinations Targeting Antibiotic Resistance in Gram-Negative Bacteria. *ACS Infect. Dis.* **2018**, *4*, 84-87.

[39] Principe, L.; Lupia, T.; Andriani, L.; Campanile, F.; Carcione, D.; Corcione, S.; De Rosa, F. G.; Luzzati, R.; Stroffolini, G.; Steyde, M.; Decorti, G.; Di Bella, S., Microbiological, Clinical, and PK/PD Features of the New Anti-Gram-Negative Antibiotics: β-Lactam/β-Lactamase Inhibitors in Combination and Cefiderocol—An All-Inclusive Guide for Clinicians. *Pharmaceuticals* **2022**, *15*, 463.

[40] Wagenlehner, F. M.; Gasink, L. B.; McGovern, P. C.; Moeck, G.; McLeroth, P.; Dorr, M.; Dane, A.; Henkel, T., Cefepime–Taniborbactam in Complicated Urinary Tract Infection. *N. Engl. J. Med.* **2024**, *390*, 611-622.

[41] Venatorx Pharmaceuticals. News release. https://venatorx.com/press-releases/venatorx-and-melinta-provide-update-on-status-of-u-s-new-drug-application-for-cefepime-taniborbactam/ (accessed 02.05.2024)

[42] Li, R.; Chen, X.; Zhou, C.; Dai, Q.-Q.; Yang, L., Recent Advances in β-Lactamase Inhibitor Chemotypes and Inhibition Modes. *Eur. J. Med. Chem.* **2022**, *242*, 114677.

[43] Fast, W.; Sutton, L. D., Metallo-β-Lactamase: Inhibitors and Reporter Substrates. *Biochim. Biophys. Acta* **2013**, *1834*, 1648-1659.

[44] Tehrani, K. H. M. E.; Martin, N. I., Thiol-Containing Metallo-β-Lactamase Inhibitors Resensitize Resistant Gram-Negative Bacteria to Meropenem. *ACS Infect. Dis.* **2017**, *3*, 711-717.

[45] Klingler, F. M.; Wichelhaus, T. A.; Frank, D.; Cuesta-Bernal, J.; El-Delik, J.; Muller, H. F.; Sjuts, H.; Gottig, S.; Koenigs, A.; Pos, K. M.; Pogoryelov, D.; Proschak, E., Approved Drugs Containing Thiols as Inhibitors of Metallo-β-Lactamases: Strategy To Combat Multidrug-Resistant Bacteria. *J. Med. Chem.* **2015**, *58*, 3626-3630.

[46] Mollard, C.; Moali, C.; Papamicael, C.; Damblon, C.; Vessilier, S.; Amicosante, G.; Schofield, C. J.; Galleni, M.; Frère, J. M.; Roberts, G. C. K., Thiomandelic Acid, a Broad Spectrum Inhibitor of Zinc β-Lactamases: Kinetic and Spectroscopic Studies. *J. Biol. Chem.* **2001**, *276*, 45015-45023.

[47] Heinz, U.; Bauer, R.; Wommer, S.; Meyer-Klaucke, W.; Papamichaels, C.; Bateson, J.; Adolph, H. W., Coordination Geometries of Metal Ions in D- or L-Captopril-Inhibited Metallo-β-Lactamases. *J. Biol. Chem.* **2003**, *278*, 20659-20666.

[48] Cushman, D. W.; Ondetti, M. A., Design of Angiotensin Converting Enzyme Inhibitors. *Nat. Med.* **1999**, *5*, 1110-1112.

[49] González, M. M.; Vila, A. J. (2017). An Elusive Task: A Clinically Useful Inhibitor of Metallo-β-Lactamases. In: Supuran, C. T.; Capasso, C. (eds.) Zinc Enzyme Inhibitors. Topics in Medicinal Chemistry, *Vol. 22*. Springer, Cham.

[50] Chen, C.; Wang, D.; Yang, K.-W. (2023). Chapter 14 - Thiols as a Privileged Scaffold Against Metallo-β-Lactamases. In: Yu, B.; Li, N.; Fu, C. (eds.) Privileged Scaffolds in Drug Discovery, Academic Press, 301-318.

[51] Brem, J.; van Berkel, S. S.; Zollman, D.; Lee, S. Y.; Gileadi, O.; McHugh, P. J.; Walsh, T. R.; McDonough, M. A.; Schofield, C. J., Structural Basis of Metallo-β-Lactamase Inhibition by Captopril Stereoisomers. *Antimicrob. Agents Chemother.* **2016**, *60*, 142-150.

[52] Li, N.; Xu, Y.; Xia, Q.; Bai, C.; Wang, T.; Wang, L.; He, D.; Xie, N.; Li, L.; Wang, J.; Zhou, H. G.; Xu, F.; Yang, C.; Zhang, Q.; Yin, Z.; Guo, Y.; Chen, Y., Simplified Captopril Analogues as NDM-1 Inhibitors. *Bioorg. Med. Chem. Lett.* **2014**, *24*, 386-389.

[53] Li, G. B.; Brem, J.; Lesniak, R.; Abboud, M. I.; Lohans, C. T.; Clifton, I. J.; Yang, S. Y.; Jimenez-Castellanos, J. C.; Avison, M. B.; Spencer, J.; McDonough, M. A.; Schofield, C. J., Crystallographic analyses of isoquinoline complexes reveal a new mode of metallo-beta-lactamase inhibition. *Chem Commun (Camb)* **2017**, *53*, 5806-5809.

[54] Liu, S.; Jing, L.; Yu, Z. J.; Wu, C.; Zheng, Y.; Zhang, E.; Chen, Q.; Yu, Y.; Guo, L.; Wu, Y.; Li, G. B., ((*S*)-3-Mercapto-2-methylpropanamido)acetic Acid Derivatives as Metallo-β-Lactamase Inhibitors: Synthesis, Kinetic and Crystallographic Studies. *Eur. J. Med. Chem.* **2018**, *145*, 649-660.

[55] Yan, Y. H.; Chen, J.; Zhan, Z.; Yu, Z. J.; Li, G.; Guo, L.; Li, G. B.; Wu, Y.; Zheng, Y., Discovery of Mercaptopropanamide-Substituted Aryl Tetrazoles as New Broad-Spectrum Metallo-beta-Lactamase Inhibitors. *RSC Adv.* **2020**, *10*, 31377-31384.

[56] Wang, Y. L.; Liu, S.; Yu, Z. J.; Lei, Y.; Huang, M. Y.; Yan, Y. H.; Ma, Q.; Zheng, Y.; Deng, H.; Sun, Y.; Wu, C.; Yu, Y.; Chen, Q.; Wang, Z.; Wu, Y.; Li, G. B., Structure-Based Development of (1-(3'-Mercaptopropanamido)methyl)boronic Acid Derived Broad-Spectrum, Dual-Action Inhibitors of Metallo- and Serine-β-Lactamases. *J. Med. Chem.* **2019**, *62*, 7160-7184.

[57] Yahiaoui, S.; Voos, K.; Haupenthal, J.; Wichelhaus, T. A.; Frank, D.; Weizel, L.; Rotter, M.; Brunst, S.; Kramer, J. S.; Proschak, E.; Ducho, C.; Hirsch, A. K. H., *N*-Aryl Mercaptoacetamides as Potential Multi-Target Inhibitors of Metallo-β-Lactamases (MBLs) and the Virulence Factor LasB from *Pseudomonas Aeruginosa*. *RSC Med. Chem.* **2021**, *12*, 1698-1708.

[58] van Haren, M. J.; Tehrani, K. H. M. E.; Kotsogianni, I.; Wade, N.; Bruchle, N. C.; Mashayekhi, V.; Martin, N. I., Cephalosporin Prodrug Inhibitors Overcome Metallo-β-Lactamase Driven Antibiotic Resistance. *Chemistry* **2021**, *27*, 3806-3811.

[59] Wachino, J.-I.; Kanechi, R.; Nishino, E.; Mochizuki, M.; Jin, W.; Kimura, K.; Kurosaki, H.; Arakawa, Y., 4-Amino-2-Sulfanylbenzoic Acid as a Potent Subclass B3 Metallo-β-Lactamase-Specific Inhibitor Applicable for Distinguishing Metallo-β-Lactamase Subclasses. *Antimicrob. Agents Chemother.* **2019**, *63*, 10.1128/aac.01197-01119.

[60] Skagseth, S.; Akhter, S.; Paulsen, M. H.; Muhammad, Z.; Lauksund, S.; Samuelsen, Ø.; Leiros, H.-K. S.; Bayer, A., Metallo-β-Lactamase Inhibitors by Bioisosteric Replacement: Preparation, Activity and Binding. *Eur. J. Med. Chem.* **2017**, *135*, 159-173.

[61] Skagseth, S.; Christopeit, T.; Akhter, S.; Bayer, A.; Samuelsen, Ø.; Leiros, H.-K. S., Structural Insights into TMB-1 and the Role of Residues 119 and 228 in Substrate and Inhibitor Binding. *Antimicrob. Agents Chemother.* **2017**, *61*, 10.1128/aac.02602-02616.

[62] Hinchliffe, P.; González, M. M.; Mojica, M. F.; González, J. M.; Castillo, V.; Saiz, C.; Kosmopoulou, M.; Tooke, C. L.; Llarrull, L. I.; Mahler, G.; Bonomo, R. A.; Vila, A. J.; Spencer, J., Cross-Class Metallo-β-Lactamase Inhibition by Bisthiazolidines Reveals Multiple Binding Modes. *Proc. Natl. Acad. Sci. USA* **2016**, *113*, E3745-E3754.

[63] Kang, S.-J.; Kim, D.-H.; Lee, B.-J., Metallo-β-Lactamase Inhibitors: A Continuing Challenge for Combating Antibiotic Resistance. *Biophys. Chem.* **2024**, *309*, 107228.

[64] Somboro, A. M.; Osei Sekyere, J.; Amoako, D. G.; Essack, S. Y.; Bester, L. A., Diversity and Proliferation of Metallo-β-Lactamases: a Clarion Call for Clinically Effective Metallo-β-Lactamase Inhibitors. *Appl. Environ. Microbiol.* **2018**, *84*, e00698-00618.

[65] Jones, R. N.; Wilson, H. W.; Novick, W. J.; Barry, A. L.; Thornsberry, C., In Vitro Evaluation of CENTA, a New β-Lactamase-Susceptible Chromogenic Cephalosporin Reagent. *J. Clin. Microbiol.* **1982**, *15*, 954-958.

[66] Jorgensen, J. H.; Crawford, S. A.; Alexander, G. A., Pyridinium-2-azo-p-dimethylaniline Chromophore, a New Chromogenic Cephalosporin for Rapid β-Lactamase Testing. *Antimicrob. Agents Chemother.* **1982**, *22*, 162-164.

[67] O'Callaghan, C. H.; Morris, A.; Kirby, S. M.; Shingler, A. H., Novel Method for Detection of β-Lactamases by Using a Chromogenic Cephalosporin Substrate. *Antimicrob. Agents Chemother.* **1972**, *1*, 283-288.

[68] van Berkel, S. S.; Brem, J.; Rydzik, A. M.; Salimraj, R.; Cain, R.; Verma, A.; Owens, R. J.; Fishwick, C. W. G.; Spencer, J.; Schofield, C. J., Assay Platform for Clinically Relevant Metallo-β-Lactamases. *J. Med. Chem.* **2013**, *56*, 6945-6953.

[69] Mao, W.; Wang, Y.; Qian, X.; Xia, L.; Xie, H., A Carbapenem-Based Off–On Fluorescent Probe for Specific Detection of Metallo-β-Lactamase Activities. *ChemBioChem* **2019**, *20*, 511-515.

[70] Zhao, G.; Miller, M. J.; Franzblau, S.; Wan, B.; Möllmann, U., Syntheses and Studies of Quinolone-Cephalosporins as Potential Anti-Tuberculosis Agents. *Bioorg. Med. Chem. Lett.* **2006**, *16*, 5534-5537.

[71] Evans, L. E.; Krishna, A.; Ma, Y.; Webb, T. E.; Marshall, D. C.; Tooke, C. L.; Spencer, J.; Clarke, T. B.; Armstrong, A.; Edwards, A. M., Exploitation of Antibiotic Resistance as a Novel Drug Target: Development of a β-Lactamase-Activated Antibacterial Prodrug. *J. Med. Chem.* **2019**, *62*, 4411-4425.

[72] Cole, M. S.; Howe, M. D.; Buonomo, J. A.; Sharma, S.; Lamont, E. A.; Brody, S. I.; Mishra, N. K.; Minato, Y.; Thiede, J. M.; Baughn, A. D.; Aldrich, C. C., Cephem-Pyrazinoic Acid Conjugates: Circumventing Resistance in *Mycobacterium tuberculosis*. *Chemistry* **2022**, *28*, e202200995.

[73] Phelan, R. M.; Ostermeier, M.; Townsend, C. A., Design and Synthesis of a β-Lactamase Activated 5-Fluorouracil Prodrug. *Bioorg. Med. Chem. Lett.* **2009**, *19*, 1261-1263.

[74] Liu, R.; Miller, P. A.; Vakulenko, S. B.; Stewart, N. K.; Boggess, W. C.; Miller, M. J., A Synthetic Dual Drug Sideromycin Induces Gram-Negative Bacteria To Commit Suicide with a Gram-Positive Antibiotic. *J. Med. Chem.* **2018**, *61*, 3845-3854.

[75] Zaengle-Barone, J. M.; Jackson, A. C.; Besse, D. M.; Becken, B.; Arshad, M.; Seed, P. C.; Franz, K. J., Copper Influences the Antibacterial Outcomes of a β-Lactamase-Activated Prochelator against Drug-Resistant Bacteria. *ACS Infect. Dis.* **2018**, *4*, 1019-1029.

[76] Jackson, A. C.; Zaengle-Barone, J. M.; Puccio, E. A.; Franz, K. J., A Cephalosporin Prochelator Inhibits New Delhi Metallo-β-lactamase 1 without Removing Zinc. *ACS Infect. Dis.* **2020**, *6*, 1264-1272.

[77] Hu, L.; Yang, H.; Yu, T.; Chen, F.; Liu, R.; Xue, S.; Zhang, S.; Mao, W.; Ji, C.; Wang, H.; Xie, H., Stereochemically Altered Cephalosporins as Potent Inhibitors of New Delhi Metallo-β-Lactamases. *Eur. J. Med. Chem.* **2022**, *232*, 114174.

[78] Feng, H.; Ding, J.; Zhu, D.; Liu, X.; Xu, X.; Zhang, Y.; Zang, S.; Wang, D.-C.; Liu, W., Structural and Mechanistic Insights into NDM-1 Catalyzed Hydrolysis of Cephalosporins. *J. Am. Chem. Soc.* **2014**, *136*, 14694-14697.

[79] King, D. T.; Worrall, L. J.; Gruninger, R.; Strynadka, N. C. J., New Delhi Metallo-β-Lactamase: Structural Insights into β-Lactam Recognition and Inhibition. *J. Am. Chem. Soc.* **2012**, *134*, 11362-11365.

[80] Qian, X.; Zhang, S.; Xue, S.; Mao, W.; Xu, M.; Xu, W.; Xie, H., A Carbapenem-Based Fluorescence Assay for the Screening of Metallo-β-Lactamase Inhibitors. *Bioorg. Med. Chem. Lett.* **2019**, *29*, 322-325.

[81] Xing, B.; Rao, J.; Liu, R., Novel Beta-Lactam Antibiotics Derivatives: Their New Applications as Gene Reporters, Antitumor Prodrugs and Enzyme Inhibitors. *Mini-Rev. Med. Chem.* **2008**, *8*, 455-471.

[82] Nishikawa, J.; Watanabe, F.; Shudou, M.; Terui, Y.; Narisada, M., Proton NMR Study of Degradation Mechanisms of Oxacephem Derivatives with Various 3'-Substituents in Alkaline Solution. *J. Med. Chem.* **1987**, *30*, 523-527.

[83] Tehrani, K. H. M. E.; Wade, N.; Mashayekhi, V.; Bruchle, N. C.; Jespers, W.; Voskuil, K.; Pesce, D.; van Haren, M. J.; van Westen, G. J. P.; Martin, N. I., Novel Cephalosporin Conjugates Display Potent and Selective Inhibition of Imipenemase-Type Metallo-β-Lactamases. *J. Med. Chem.* **2021**, *64*, 9141-9151.

[84] Tian, H.; Wang, Y.; Dai, Y.; Mao, A.; Zhou, W.; Cao, X.; Deng, H.; Lu, H.; Ding, L.; Shen, H.; Wang, X., A Cephalosporin-Tripodalamine Conjugate Inhibits Metallo-β-Lactamase with High Efficacy and Low Toxicity. *Antimicrob. Agents Chemother.* **2022**, *66*, e00352-00322.

[85] Saikawa, I.; Takano, S.; Momonoi, K.; Takakura, I.; Tanaka, K.; Kutani, C., An Efficient Method for the Preparation of 3-(Substituted thiomethyl)-7-aminocephalosporins. *Chem. Pharm. Bull.* **1985**, *33*, 5534-5538.

[86] Quotadamo, A.; Linciano, P.; Davoli, P.; Tondi, D.; Costi, M. P.; Venturelli, A., An Improved Synthesis of CENTA, a Chromogenic Substrate for β-Lactamases. *Synlett* **2016**, *27*, 2447-2450.

[87] Kaiser, G. V.; Cooper, R. D. G.; Koehler, R. E.; Murphy, C. F.; Webber, J. A.; Wright, I. G.; Van Heyningen, E. M., Chemistry of Cephalosporin Antibiotics. XIX. Transformation of Δ^2-Cephem to Δ^3-Cephem by Oxidation-Reduction at Sulfur. *J. Org. Chem.* **1970**, *35*, 2430-2433.

[88] Lee, M.; Hesek, D.; Mobashery, S., A Practical Synthesis of Nitrocefin. *J. Org. Chem.* **2005**, *70*, 367-369.

[89] Gao, W.; Xing, B.; Tsien, R. Y.; Rao, J., Novel Fluorogenic Substrates for Imaging β-Lactamase Gene Expression. *J. Am. Chem. Soc.* **2003**, *125*, 11146-11147.

[90] Schlatzer, T.; Schröder, H.; Trobe, M.; Lembacher-Fadum, C.; Stangl, S.; Schlögl, C.; Weber, H.; Breinbauer, R., Pd/BIPHEPHOS is an Efficient Catalyst for the Pd-Catalyzed *S*-Allylation of Thiols with High *n*-Selectivity. *Adv. Synth. Catal.* **2020**, *362*, 331-336.

[91] Feltrin, M. P.; Almeida, W. P., A Synthesis of Captopril Through a Baylis–Hillman Reaction. *Synth. Commun.* **2003**, *33*, 1141-1146.

[92] De Vitis, V.; Dall'Oglio, F.; Pinto, A.; De Micheli, C.; Molinari, F.; Conti, P.; Romano, D.; Tamborini, L., Chemoenzymatic Synthesis in Flow Reactors: A Rapid and Convenient Preparation of Captopril. *ChemistryOpen* **2017**, *6*, 668-673.

[93] Kaya, C.; Konstantinović, J.; Kany, A. M.; Andreas, A.; Kramer, J. S.; Brunst, S.; Weizel, L.; Rotter, M. J.; Frank, D.; Yahiaoui, S.; Müller, R.; Hartmann, R. W.; Haupenthal, J.; Proschak, E.; Wichelhaus, T. A.; Hirsch, A. K. H., *N*-Aryl Mercaptopropionamides as Broad-Spectrum Inhibitors of Metallo-β-Lactamases. *J. Med. Chem.* **2022**, *65*, 3913-3922.

[94] Meng, Z.; Tang, M. L.; Yu, L.; Liang, Y.; Han, J.; Zhang, C.; Hu, F.; Yu, J. M.; Sun, X., Novel Mercapto Propionamide Derivatives with Potent New Delhi Metallo-β-Lactamase-1 Inhibitory Activity and Low Toxicity. *ACS Infect. Dis.* **2019**, *5*, 903-916.

[95] Ma, G.; Wang, S.; Wu, K.; Zhang, W.; Ahmad, A.; Hao, Q.; Lei, X.; Zhang, H., Structure-Guided Optimization of D-Captopril for Discovery of Potent NDM-1 Inhibitors. *Bioorg. Med. Chem.* **2021**, *29*, 115902.

[96] Yusof, Y.; Tan, D. T. C.; Arjomandi, O. K.; Schenk, G.; McGeary, R. P., Captopril Analogues as Metallo-β-Lactamase Inhibitors. *Bioorg. Med. Chem. Lett.* **2016**, *26*, 1589-1593.

[97] Ojima, I.; Jameison, F. A., A New Potent Inhibitor for Angiotensin Converting Enzyme: (*R*,*S*)-Captopril-F3. *Bioorg. Med. Chem. Lett.* **1991**, *1*, 581-584.

[98] Badarau, A.; Llinás, A.; Laws, A. P.; Damblon, C.; Page, M. I., Inhibitors of Metallo-β-Lactamase Generated from β-Lactam Antibiotics. *Biochemistry* **2005**, *44*, 8578-8589.

[99] Rivière, G.; Oueslati, S.; Gayral, M.; Créchet, J.-B.; Nhiri, N.; Jacquet, E.; Cintrat, J.-C.; Giraud, F.; van Heijenoort, C.; Lescop, E.; Pethe, S.; Iorga, B. I.; Naas, T.; Guittet, E.; Morellet, N., NMR Characterization of the Influence of Zinc(II) Ions on the Structural and Dynamic Behavior of the New Delhi Metallo-β-Lactamase-1 and on the Binding with Flavonols as Inhibitors. *ACS Omega* **2020**, *5*, 10466-10480.

[100] Cogswell, T. J.; Donald, C. S.; Long, D. L.; Marquez, R., Short and Efficient Synthesis of Fluorinated δ-Lactams. *Org. Biomol. Chem.* **2015**, *13*, 717-728.

Paper I

Fluorinated Captopril Analogues Inhibit Metallo-β-Lactamases and Facilitate Structure Determination of NDM-1 Binding Pose

Alexandra Kondratieva, Katarzyna Palica, Christopher Frøhlich, Rebekka Rolfsnes Hovd, Hanna-Kirsti S. Leiros, Mate Erdelyi, Annette Bayer

Research paper

Fluorinated captopril analogues inhibit metallo-β-lactamases and facilitate structure determination of NDM-1 binding pose

Alexandra Kondratieva [a], Katarzyna Palica [b], Christopher Frøhlich [c], Rebekka Rolfsnes Hovd [d], Hanna-Kirsti S. Leiros [a], Mate Erdelyi [b], Annette Bayer [a,*]

[a] Department of Chemistry, UiT The Arctic University of Norway, NO-9037, Tromsø, Norway
[b] Department of Chemistry – BMC, Organic Chemistry, Uppsala University, 752 37, Uppsala, Sweden
[c] Department of Pharmacy, UiT The Arctic University of Norway, NO-9037, Tromsø, Norway
[d] AdjuTec Pharma, NO-0165 Oslo, Norway

ARTICLE INFO

ABSTRACT

Bacterial resistance to the majority of clinically used β-lactam antibiotics is a global health threat and, consequently, the driving force for the development of metallo-β-lactamase (MBL) inhibitors. The rapid evolution of new MBLs calls for new strategies and tools for inhibitor development. In this study, we designed and developed a series of trifluoromethylated captopril analogues as probes for structural studies of enzyme-inhibitor binding. The new compounds showed activity comparable to the non-fluorinated inhibitors against the New Delhi Metallo-β-lactamase-1 (NDM-1). The most active compound, a derivative of D-captopril, exhibited an IC_{50} value of 0.3 μM. Several compounds demonstrated synergistic effects, restoring the effect of meropenem and reducing the minimum inhibitory concentration (MIC) values in NDM-1 (up to 64-fold), VIM-2 (up to 8-fold) and IMP-26 (up to 8-fold) harbouring *Escherichia coli*. NMR spectroscopy and molecular docking of one representative inhibitor determined the binding pose in NDM-1, demonstrating that fluorinated analogues of inhibitors are a valuable tool for structural studies of MBL-inhibitor complexes.

1. Introduction

Antimicrobial resistance presents a worldwide challenge to global health, threatening the effective treatment of an increasing range of infections as well as holding back advances in medicine and drug development [1]. Although there are several mechanisms through which bacterial resistance to β-lactam antibiotics arises, the production of β-lactamase enzymes is considered the most common and worrying in Gram-negative pathogens [2]. These enzymes mediate the hydrolysis of the β-lactam ring, which deactivates penicillins, cephalosporins and even carbapenems, the so-called last-resort antibiotics.

β-Lactamases can be divided into two main groups, based on the mechanism of hydrolysis: serine β-lactamases (SBLs) and metallo-β-lactamases (MBLs) [3]. SBLs constitute Ambler classes A, C and D and bind covalently to a β-lactam antibiotic via a nucleophilic serine moiety. Ambler class B, or MBLs, rely on zinc ions in the active site to activate a water molecule for the cleavage of the β-lactam ring. At present (December 2023), around 940 MBLs have been identified according to the Beta Lactamase Database (BLDB, http://www.bldb.eu/), whereof

around 600 belong to the B1 subgroup [4]. The B1 subgroup contains the clinically most relevant MBLs, such as New Dehli metallo-β-lactamases (NDMs), Verona integron-encoded metallo-β-lactamases (VIMs) and imipenemases (IMPs) [5]. Many B1 MBLs are structurally diverse due to their low sequence identity [5b], e.g. the sequence identity of NDM-1 and IMP-26 is 34 %.

One way to oppose the resistance caused by β-lactamases is the development of small molecule β-lactamase inhibitors to be administered together with the antibiotic. While SBLs are inhibited by a variety of clinically approved inhibitors such as tazobactam, avibactam and relebactam [6], there are none available for MBLs [7]. Currently three dual SBL/MBL inhibitors: VNRX-5133 (taniborbactam), QPX7728 (xeruborbactam) and QPX7831 are under evaluation in clinical studies [8], hopefully leading to the first clinically approved MBL inhibitor after over 30 years of research [9]. However, due to the continuous evolution of MBL enzymes and their structural diversity, new inhibitors as well as new strategies for inhibitor development are needed.

Thiols are a compound class known to broadly inhibit MBLs due to the ability of sulfur to coordinate zinc, thus a number of thiol-based

inhibitors have been reported [10]. (2S)-1-((2S)-2-methyl-3-sulfanyl-propanoyl)pyrrolidine-2-carboxylic acid, more commonly known as L-captopril (Fig. 1), is a thiol-containing molecule developed to target the angiotensin-converting enzyme (ACE) and is a clinically approved drug used for controlling high blood pressure [11]. It has been shown that L-captopril (the (2S,2′S)-stereoisomer), as well as its three stereoisomers, could be of interest for the development of new MBL inhibitors [12]. Initially, clinically used L-captopril was reported to be less active than D-captopril (the (2R,2′S)-stereoisomer) against some MBLs [14]. However, L-captopril has lately been shown to be of similar effectivity against NDM-1, with half maximal inhibitory concentration (IC$_{50}$) values in the low micromolar region [15]. Based on these findings, several captopril analogues have been developed that exhibit inhibitory activity against MBLs (Fig. 1) [13].

The development of thiol-based inhibitors has been limited by their tendency to oxidize to the corresponding disulfides, thus losing zinc binding and MBL inhibitory properties [16]. Recent attempts to overcome this limitation have focused on the development of prodrugs that release the thiol inhibitor directly in the cell. However, so far, prodrugs designed for the release of aliphatic thiol inhibitors were shown to cleave the inhibitor very slowly or not at all due to the poor leaving group ability of the aliphatic thiols [17]. Thus, structurally more diverse thiol-based inhibitors are necessary. The bioisostere replacement of H to F to manage properties of drug candidates such as bioactivity, membrane permeability, and pKa of proximal functionalities is well established [18]. However, to our knowledge, fluorinated aliphatic thiols such as trifluoromethylated captopril analogues have only been studied as ACE inhibitors [19].

The development of broad-spectrum MBL inhibitors has been strongly dependent on understanding of the binding site and binding mode. The primary source of structural information on enzyme-inhibitor complexes has been X-ray crystallography. However, according to the BLDB (status December 2023) [4], for the approximately 600 reported B1 MBLs, crystal structures of less than 10 % (40 structures) have been deposited, and even fewer of enzyme-inhibitor complexes. Solution-state NMR can serve as an alternative and provide structural insights, as demonstrated recently in the investigation of the active sites of NDM-1 and VIM-2 [20]. However, signal overlaps in the ^{1}H NMR dimension remain a serious challenge [21].

As native proteins lack fluorine atoms, fluorine labelling of potent MBL-inhibitors is expected to provide valuable probes for studying inhibitor binding poses, in particular when X-ray crystallography is not feasible, and when standard NMR experiments do not provide sufficient information. The ^{19}F NMR signal of fluorine-labelled ligands provides a highly sensitive handle to locate the binding site and binding mode using 3D HOESY-HSQC (^{1}H,[19]F,[13]C). ^{19}F NMR has a wider chemical shift scale (800 ppm) compared to ^{1}H NMR (15 ppm) and, consequently, ^{19}F NMR chemical shift changes induced by binding are more pronounced and hence easier to detect. The use of ^{19}F NMR diminishes the risk of overlaps between the signals of the protein and the binding ligand. The ^{19}F-labelling of drug candidates [22] or of the target protein [23] has accordingly been shown to facilitate the determination of the protein-ligand binding pose as well as the mechanism of enzyme-inhibition.

We aimed for fluorinated MBL inhibitors as probes for solution-state NMR studies of MBLs as an alternative to crystallography. In this study, we describe the design and synthesis of a series of fluorinated thiol inhibitors and demonstrate their inhibitory activity against a panel of

structurally diverse B1 MBLs (NDM-1, VIM-2 and IMP-26). Finally, solution-state NMR spectroscopy directed molecular docking is used to identify the binding pose of a fluorinated inhibitor with NDM-1.

2. Results and discussion

2.1. Design and synthesis

Starting from the structure of captopril (Fig. 1), we aimed to obtain compounds with the general structure **5** (Scheme 1). From a synthetic point of view, it was most feasible to expand the compound library by varying the amine part of the molecule (R′), while having a fixed fluorinated scaffold. We envisioned trifluoromethylation in the α- or β-position of the 3-mercaptopropionamide substructure of captopril as the fluorinated scaffold. By changing the position of the CF$_3$ moiety, we intended to study the effect on inhibitory activity as well as its influence on the stability of the thiol moiety towards oxidation. Direct captopril analogues of all four stereoisomers with methyl replaced by a trifluoromethyl group were synthesized. Moreover, we modified the amine part of the scaffold, inspired by previously reported compounds [13b,c].

The synthetic route towards trifluoromethyl-containing mercaptopropionamide derivatives is shown in Scheme 1. Starting with the commercially available regioisomers 2-(trifluoromethyl)acrylic acid (**1α**) or (E)-4,4,4-trifluorobut-2-enoic acid (**1β**) and thioacetic acid, compounds **2α** and **2β** were prepared according to published procedures [24]. The next step was envisioned to be a coupling reaction between the obtained acids and different amines to obtain a diverse library of fluorinated mercaptopropionamide derivatives. Using **2α** or **2β**, the corresponding amines and EDC as the coupling reagent, compounds **4αA**, **4βA** and **4αB** were obtained. No product formation was observed for coupling of **2α** or **2β** to aliphatic amines, even when using other coupling reagents and conditions. The order of the synthetic steps was therefore reversed for the remaining desired compounds.

Starting with the acrylic acids **1α** or **1β**, amide coupling was performed with various amines, followed by conjugate addition of thioacetic acid to the previously obtained amides. This approach afforded compounds **4α(C-G)** and **4β(B–H)**. For compounds with a β-CF$_3$ group, previously reported reaction conditions using HBTU as the coupling reagent and DIPEA as the base [13c] were successful, providing compounds **3βC**, **3βD**, **3βF** and **3βG** in moderate to excellent yields (45–91 %). For compounds containing an α-CF$_3$ group, the same conditions proved to be unsuccessful, resulting in mixtures of the desired product and a compound with two amines attached, according to MS. This is presumably the product of a conjugate addition of the amine to the desired α,β-unsaturated amide. The two products had similar R$_f$ values, which hampered purification by flash column chromatography. However, we discovered that using propanephosphonic acid anhydride (T3P) as the coupling reagent did not lead to formation of the problematic side-product. Further coupling reactions were carried out using T3P, affording compounds **3αC**, **3αD**, **3αE**, **3βE**, **3αF**, **3αG**, **3βH** and **3βB** in low to very good yields (30–85 %). It is noteworthy that **3C**, **3D** and **3E** were obtained as a mixture of rotamers. The conjugate addition step with thioacetic acid for α–CF$_3$–containing compounds proceeded overnight at ambient temperature, while for derivatives with a β-CF$_3$ group 60 h reaction time at 60 °C was necessary.

Compounds **4C**, **4D** and **4E** were acquired as diastereomeric mixtures, which were difficult to separate using column chromatography. For **4αD**, the separation of diastereomers using medium pressure liquid
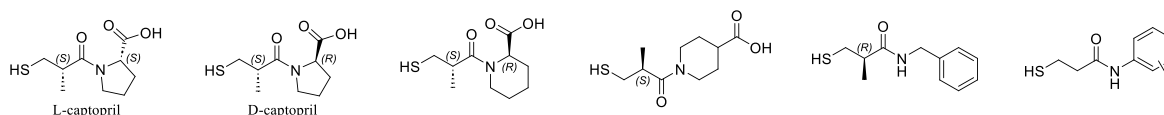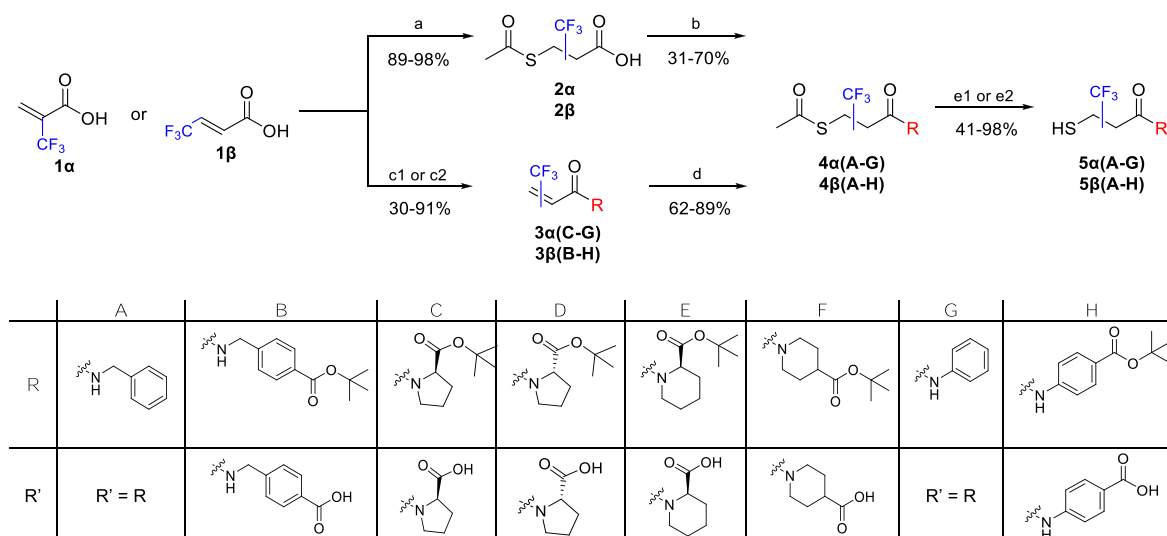

Fig. 1. D- and L-captopril and some structurally related thiol derivatives reported in literature [13] as potential MBL inhibitors.

Scheme 1. Synthetic strategy towards thiols **5α(A-G)** and **5β(A-H)**. Reaction conditions: (a) AcSH, neat, room temperature (r.t.), overnight (o.n.) or 60 °C, 60 h; (b) R–H, EDC·HCl, HOBt, *N*-methylmorpholine, DCM, 0 °C to r.t., o.n.; (c1) amine, HBTU, DIPEA or T3P, Et₃N, DCM, 0 °C to r.t., 1–4 h; (c2) amine, T3P, DIPEA, EtOAc, 0 °C to r.t., o.n.; (d) AcSH, THF, r.t., o.n. or 60 °C, 60 h; (e1) NaSMe, MeOH, −20 °C, 30 min; (e2) TFA, DCM, 50 °C, o.n. and NH₃ (aq), r.t., 3 h.

chromatography (MPLC) has previously been reported as well as the assignment of stereocenters using X-ray crystallography [19a]. Based on this data, we were able to separate the diastereomers and determine the configuration of the stereoisomers of **4αD** as well as **4αC**. For the rest of the derivatives, the diastereomers were not separated, and they were further used and analyzed as mixtures.

The last step of the synthesis was the deprotection of the thiol and, where relevant, acid moieties. For compounds requiring only a thiol deprotection (**4αA**, **4βA**, **4αG**, **4βG**), an adapted previously established procedure [25], employing sodium thiomethoxide, was used. For the rest of the derivatives, ester hydrolysis was accomplished using trifluoroacetic acid (TFA) in methylene chloride at 50 °C overnight. Subsequent removal of the acetate by treatment with aqueous ammonia for 3 h at room temperature afforded compounds **5B–F** and **5H** [26]. Compounds **5B**, **5G** and **5H** precipitated upon using the standard work-up procedure and were used for analysis without further purification. Use of normal phase column chromatography for some of the final compounds led to oxidation of the thiol moieties, resulting in disulfide formation. Primary thiols have been shown to exhibit relatively short half-lives and form disulfides faster than secondary, thus hindering synthesis and analysis [16b]. Following the same trend, compounds with an α-CF₃ group were noticeably more prone to oxidation than β-CF₃ derivatives, which complicates purification and storage of these compounds. To limit formation of the undesired disulfides, the final compounds were all purified by preparative reversed-phase HPLC. The final compounds **5α(A-G)** and **5β(A-H)** were obtained in moderate to excellent yields (41–98 %).

2.2. Inhibitory activities

The inhibitory activity of all final compounds (**5α(A-G)** and **5β(A-H)**) against NDM-1 was evaluated in an enzyme assay in terms of their half maximal inhibitory concentration (IC_{50}) values (Table 1), measured using meropenem as the reporter substrate. Initial rates of the reactions with various concentrations of the inhibitors in a 2-fold dilution series were measured and the IC_{50} values were derived from the fitted dose-response curves. To validate our assay, commercially available L-captopril was included in our compound library. The reported IC_{50} values for L-captopril vary from 9.4 to 157.4 μM [14,15], with the spread of the values being attributed to differences in assay buffers, reporter substrates and protein constructs. We obtained an IC_{50} value of 7 μM, which is in good agreement with previous reports.

The tested compounds **5α(A-G)** and **5β(A-H)** showed IC_{50} values ranging from 0.3 to >300 μM. Interestingly, the position of the CF₃ group plays a vital role in the activity of the studied inhibitors. In all cases, the compounds with an α-CF₃ group showed lower IC_{50} values than the respective β-CF₃ derivative. Furthermore, compounds containing a β-CF₃ group exhibited no significant inhibitory activity (IC_{50} >300 μM), with the exception of **5βE** (IC_{50} = 145 μM) and **5βH** (IC_{50} = 5.6 μM). It has been previously shown that a carboxylic acid moiety may be important for binding to the active site of NDM-1 [13b]. This hypothesis is corroborated by the activity of compounds **5βG** (IC_{50} = 22 μM) and **5βH** (IC_{50} = 5.6 μM), yet is contradicted by the deterioration of activity of **5αA** (IC_{50} = 20 μM) upon carboxylation (**5αB**, IC_{50} = 65 μM). This may be due to the inhibitor becoming too large to be accommodated by the active site with this modification. For piperidine-based derivatives **5αF** (IC_{50} = 2.2 μM) and **5αE** (IC_{50} = 3.2 μM), the position of the carboxylic acid has little influence on the activity.

Brem et al. carried out a study of the inhibitory activity of the four captopril stereoisomers (Fig. 2) against several MBLs, including NDM-1 [14a]. They showed that D-captopril (IC_{50} = 22 μM) was the most potent of the four possible captopril stereoisomers, followed by *epi*-D-captopril, L-captopril and *epi*-L-captopril with IC_{50} values of 64, 157 and >500 μM, respectively. In general, captopril derivatives containing the D-proline motif (*2R* configuration) showed better inhibition than those derived from L-proline (*2S* configuration). In the current study, the same trend can be seen for the trifluoromethyl-containing analogues: (2R,2′R)-**5αC** (IC_{50} = 0.3 μM), (2R,2′S)-**5αC** (IC_{50} = 4.5 μM), (2S,2′R)-**5αD** (IC_{50} = 6.1 μM), and (2S,2′S)-**5αD** (IC_{50} = 60 μM). Comparing L-captopril and its trifluoromethyl-derivative ((2S,2′R)-**5αD**), the inhibitory activity seems unaffected by the structural modification of the methyl group (IC_{50} values of 7 and 6 μM, respectively). For other compounds, replacement of the CH₃ group with a CF₃ group provided IC_{50} values in a similar range to those reported for the non-fluorinated inhibitors (Table 1, entries 3, 4, 8, 9, 12, 15, 17), but a direct comparison is challenging due to different assay conditions.

Additionally, a selection of inhibitors was tested for synergistic activity with meropenem in an NDM-1-producing *Escherichia coli* (Fig. S3, Supporting Information). The production of NDM-1 increased the minimum inhibitory concentration (MIC) of meropenem from 0.03 to 32 mg/L. Adding our inhibitors at a concentration of 500 μM resulted in a 32-64-fold reduction in the MIC of meropenem demonstrating that compounds **5αF** and **5αE** were potent synergists (Table 2). For comparison, L- and D-captopril displayed a 32-fold reduction in the MIC of

Table 1
Structures and inhibitory activities of trifluoromethyl mercaptopropionamide derivatives **5α(A-G)** and **5β(A-H)** against NDM-1.

Entry	Compound	Structure	IC$_{50}$ (μM)[a]
1	L-captopril		7 ± 2 (157[d])
2	*rac*-**5αA**		20 ± 2
3	(+)-**5αA**[b]		10 ± 3 (1.5[e])
4	(−)-**5αA**[b]		75 ± 15 (5[e])
5	**5βA**		>300
6	**5αB**		65 ± 14
7	**5βB**		>300
8	(2R,2′S)-**5αC**		4.5 ± 1.5 (64[d])
9	(2R,2′R)-**5αC**		0.3 ± 0.1 (20[d]/8[e]/22[f])
10	**5βC**		>300
11	mix-**5αD**[c]		37 ± 18
12	(2S,2′S)-**5αD**		60 ± 20 (>500[d])
13	(2S,2′R)-**5αD**		6.1 ± 1.6
14	**5βD**		>300
15	**5αE**		3.2 ± 0.7 (6.9[f])
16	**5βE**		145 ± 20
17	**5αF**		2.2 ± 0.5 (4.9[f])

Table 1 (*continued*)

Entry	Compound	Structure	IC$_{50}$ (μM)[a]
18	**5βF**		>300
19	**5αG**		3.4 ± 0.5
20	**5βG**		22 ± 6
21	**5βH**		5.6 ± 1.4

[a] The experiments were run in at least two parallel replicates, and the inhibitory activities are given as the mean value along with the standard error of the mean.
[b] Stereochemistry assigned based on docking and NMR results in accordance with [13b].
[c] Mixture of diastereomers (approximately 3:1 of (2S,2′S)-**5αD** to (2S,2′R)-**5αD**).
[d] Reported IC$_{50}$ values of non-fluorinated analogue in reference [14a].
[e] Reported IC$_{50}$ values of non-fluorinated analogue in reference [13b].
[f] Reported IC$_{50}$ value of non-fluorinated analogue in reference [13c].
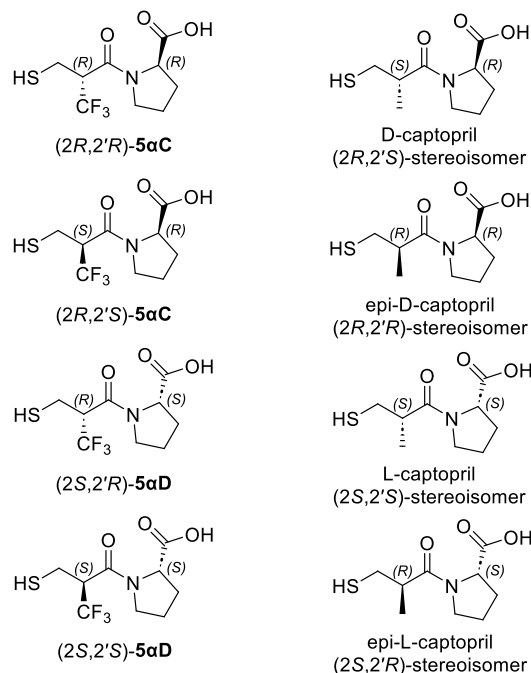
Fig. 2. Captopril stereoisomers and their trifluoromethyl-containing analogues.

meropenem. The tested inhibitors in themselves did not affect bacterial growth at the used concentration (500 μM).

The most potent synergists against NDM-1 were further evaluated for their synergistic effect against the B1 MBLs VIM-2 and IMP-26 (Table 2) at a fixed concentration of 500 μM. The minimum inhibitory concentration of meropenem alone was 0.5 and 2 mg/L for VIM-2 and IMP-26, respectively. The most potent synergist (2S,2′R)-**5αD** showed an 8-fold reduction in the MIC of meropenem for both VIM-2 and IMP-26. L-captopril and its fluorinated analogue (2S,2′R)-**5αD** displayed the same synergistic activity against VIM-2 and IMP-26, while D-captopril showed stronger synergy than its fluorinated analogue (2R,2′R)-**5αC**.

Table 2

MIC of meropenem (MEM) in combination with selected inhibitors. Susceptibility was determined using *E. coli* E. cloni™ producing NDM-1, VIM-2 or IMP-26 from a low copy number plasmid [27].

Inhibitor	MIC meropenem (mg/L)[a,b]		
	MP30-63 *bla*NDM-1	MP30-57 *bla*VIM-2	MP30-58 *bla*IMP-26
No inhibitor control	32	0.5	2
D-captopril	1	0.06	0.5
L-captopril	1	0.06	0.25
(2*R*,2'*R*)-**5αC**	4	0.25	4
(2*S*,2'*R*)-**5αD**	4	0.06	0.25
5αF	1	0.125	2
5αE	0.5	0.125	0.5

[a] Minimal inhibitory concentration was tested in the presence of 500 μM of the inhibitor in duplicates.

[b] Meropenem MIC of *E. coli* E.cloni™ (MP21-05) without *bla* genes = 0.03 mg/L.

2.3. NMR determination of the binding pose

We isolated the enantiomers of rac-**5αA** using preparative chiral HPLC (for details see the Supporting Information) and characterized their binding to NDM-1 using solution-state NMR. A solution of uniformly ^{15}N-enriched NDM-1, expressed and purified as described previously [20b] and dissolved in 2.5 % DMSO in an aqueous KH$_2$PO$_4$ buffer, was titrated with (+)-**5αA** and (−)-**5αA** and the weighted chemical shift changes, $\Delta\delta_{1H,15N}$, of the backbone amide functionalities were recorded. ^{1}H,^{15}N HSQC spectra were acquired after addition of 0, 0.5, 1, 1.5, 3, 6, 10, and 15 equivalents of the two ligands. The last titration step was omitted for the quantification of the binding of (−)-**5αA** because of sample precipitation. Both enantiomers showed binding in the slow exchange regime, with the resonances of the free and the ligand-bound forms of the protein being simultaneously detectable, with varying intensities, throughout the titration. In accordance with literature [20b], we classified chemical shift perturbations (CSP, eq. (1), where R$_{scale}$ = 6.5 [28]) as significant (SSP) when the observed $\Delta\delta_{1H,15N}$ was greater than the population mean plus the standard deviation (μ+1σ).

$$\text{CSP} = \Delta\delta_{(1H,15N)} = \sqrt{\left(\Delta\delta_{1H}^2 + \left(1/R_{scale} \times \Delta\delta_{15N}^2\right)\right)} \quad (1)$$

Significant chemical shift perturbations were observed for Thr119, His122, Asp124, Gly188, His189, Ser191, Lys211, Asp212, Ser213 Gly222, Thr226, Glu227, His228, Ser255, Lys268, Leu269, and Arg270 (Fig. 3), indicating that these amino acids either are involved in ligand binding or undergo larger binding induced conformational changes. These chemical shift perturbations were quantified (Table S3, Supporting Information), providing the dissociation constant K_d 149.2 ± 21.8 μM for enantiomer (+)-**5αA** by fitting the binding induced signal intensity changes to eq. (2) [29].

$$I_{obs} = I_{max} \frac{([P] + [L] + K_d) - \sqrt{([P] + [L] + K_d)^2 - 4[P][L]}}{2[P]} \quad (2)$$

where K_d is the dissociation constant, I_{obs} are the normalized integrals of the protein-ligand complex, I_{max} is the normalized integral for the last titration step, and [P] and [L] are protein and ligand concentrations, respectively. The K_d was the average of the K_d values separately obtained for the amino acids showing SSP. Due to the weaker binding of enantiomer (−)-**5αA**, its K_d could not be estimated.

We obtained additional information on the binding pose of (+)-**5αA** by detection of ^{19}F,[1]H heteronuclear Overhauser effects (HOEs) between its trifluoromethyl functionality and the protons of NDM-1. Amino acids Met67, His122 and Trp93 showed HOEs (Fig. 4), which corroborates the
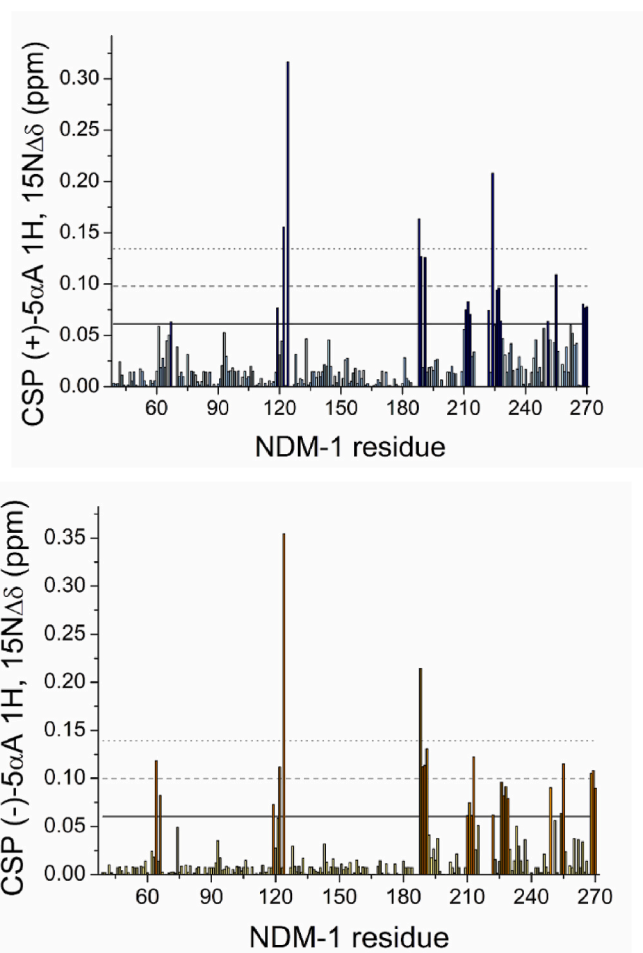
Fig. 3. The chemical shift perturbation (CSP) of the backbone amides of ^{15}N-labelled NDM-1 upon addition of 15 equivalents of (+)-**5αA** (upper) and (−)-**5αA** (lower). CSPs of residues above the first horizontal cut-off (solid line) are greater than the population mean plus standard deviation (μ+1σ), and are therefore considered to be significantly influenced by ligand binding. The solid and dashed lines represent the population mean (μ) plus one, two, and three standard deviations (σ), respectively.

large chemical shift perturbations observed for these amino acids during the titration experiment, indicating them to be directly involved in ligand binding.

2.4. Identification of the binding pose by molecular docking

Flexible docking of both enantiomers of **5αA** and of its previously known non-fluorinated analogue *N*-benzyl-3-mercapto-2-methylpropanamide [13b] was performed using the software Glide followed by Prime (Schrödinger Inc.), starting from the NDM-1 crystal structure PDB:5ZIO [13c] and using the MM-GBSA rescoring protocol. The docking poses were filtered, removing those incompatible with the binding induced NMR chemical shifts shown in Fig. 3, and with the HOEs shown in Fig. 4. The predicted binding mode of (*R*)-*N*-benzyl-3-mercapto-2-methylpropanamide was in agreement with the X-ray structure 5ZIO [13c]. Conceivable binding poses were then ranked based on their binding energies, with the best ranked poses shown in Fig. 5. The binding poses of (*R*)-*N*-benzyl-3-mercapto-2-methylpropanamide and of (+)-**5αA** possessed comparable binding energies, ΔG$_{bind}$ = −58.68 kcal/mol and −58.45 kcal/mol, respectively, whereas the (−)-**5αA** enantiomer is predicted to bind significantly weaker to NDM-1 (ΔG$_{bind}$ = −50.35 kcal/mol). This is in line with the experimentally determined IC$_{50}$ values of these compounds (1.5 μM for

Fig. 4. Selective ^{19}F,^{1}H HOESY spectrum observed for the (+)-**5αA** - NDM-1 complex. Upon irradiation of the trifluoromethyl functionality, HOE was observed on the ^{1}H NMR signals of Met67 (8.26 ppm), His122 (7.01 ppm) and Trp93 (6.85 ppm). The interaction of NDM-1 (0.25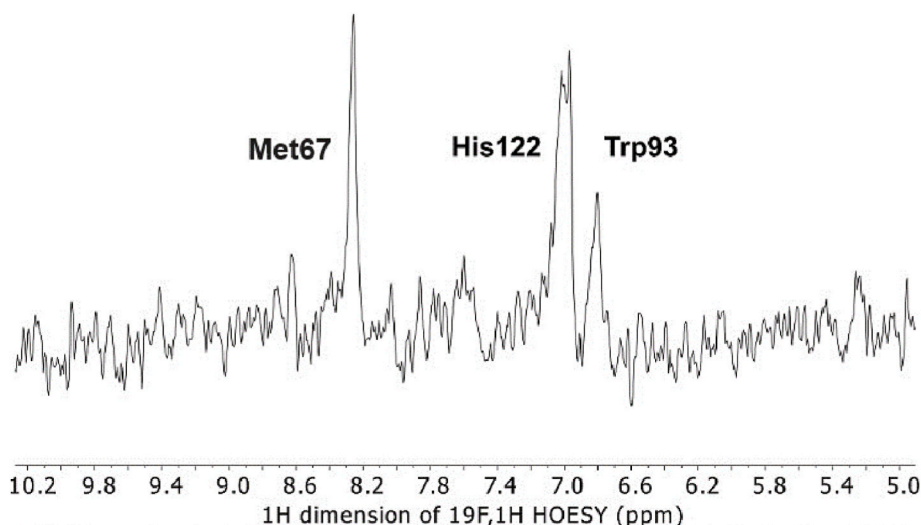 mM) and (+)-**5αA** (2.5 mM) was studied in a 20 mM KH_2PO_4 and 0.1 mM $ZnCl_2$ aqueous solutions (pH 7) on a 700 MHz NMR spectrometer, with irradiation at – 68.18 ppm (^{19}F NMR, CF_3).
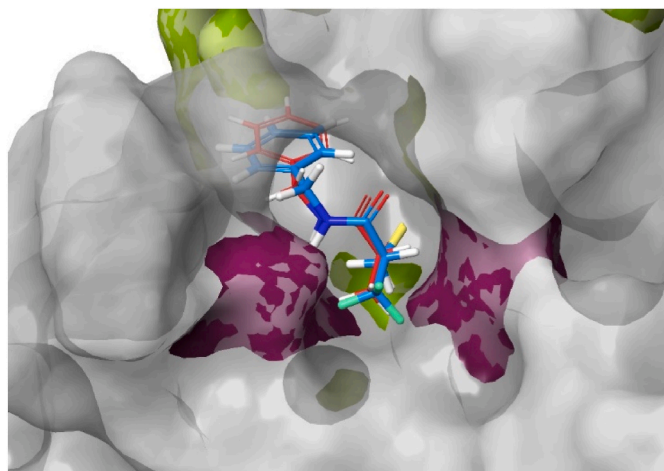

Fig. 5. The superimposed structures of (R)-N-benzyl-3-mercapto-2-methyl-propanamide (red) and (+)-**5αA** (blue) in complex with NDM-1, predicted by NMR-guided docking. Amino acids showing significant chemical shift perturbation upon ligand binding (SSP) are highlighted in green, and those showing HOE to the trifluoromethyl group of (+)-**5αA** in purple.

(R)-N-benzyl-3-mercapto-2-methylpropan–amide [13b], 10 μM (+)-**5αA** and 75 μM for (−)-**5αA**). Not just the binding energies, but even the binding modes of (R)-N-benzyl-3-mercapto-2-methylpropana-mide and (+)-**5αA** are highly similar. This suggests that fluorination did not considerably influence the binding pose of (R)-N-benzyl-3-mercap-to-2-methylpropanamide. Hence, both the native and the tri-fluoromethyl substituted inhibitors bind both zinc ions of the NDM-1 binding site via their thiol functionality (2.3 Å), and their carbonyl group forms a hydrogen bond with the side chain amide of Asn220 (1.6–1.7 Å). An N–H⋯F–C hydrogen bond (2.2 Å) was predicted be-tween the Gln123 amide proton of NDM-1 and the trifluoromethyl group of (+)-**5αA** that, however, is neither supported by an HOE correlation (NMR) nor by the inhibitory activity of (+)-**5αA** as compared to N-benzyl-3-mercapto-2-methylpropanamide. It should here be noted that our NMR data and energetic ranking based selection of theoretically feasible binding poses successfully identified the more active enan-tiomer, (+)-**5αA**, and allowed the determination of its binding pose, which well complements the data provided by Li et al. on the non-fluorinated analogue, N-benzyl-3-mercapto-2-methylpropanamide

[13b]. Due to the structural similarity of **5α(B–H)** and **5β(A-H)** to (+)-**5αA**, it is reasonable to presume that the compounds studied herein have comparable binding modes to NDM-1.

3. Conclusion

A series of novel trifluoromethylated captopril analogues was syn-thesized with several compounds demonstrating low-micromolar inhibitory activity against the B1 MBL NDM-1. The most active inhibi-tor was the CF_3-analogue of D-captopril with an IC_{50} value of 0.3 μM. Derivatives with an α-CF_3 group proved to be by far more active against NDM-1 than β-CF_3–containing compounds, while exhibiting consider-ably lower stability towards oxidation. Substitution of the α-CH_3 group with an α-CF_3 group did not seem to significantly influence the inhibi-tory activity. Several of the α-CF_3–containing inhibitors were potent synergists, on the same level as L-captopril, and were able to repoten-tiate meropenem in NDM-1 (up to 64-fold), VIM-2 (up to 8-fold) and IMP-26 (up tp 8-fold) harbouring *E. coli*. Direct comparison of an α-CF_3–containing and non-fluorinated D- and L-captopril indicates that the fluorinated inhibitors are only slightly less potent synergists.

Using NMR spectroscopy and molecular docking the binding pose of one representative molecule with NDM-1 was identified. The binding pose of the fluorine-labelled inhibitor resembled the binding pose determined for the crystal structure of L-captopril with NDM-1, demonstrating that fluorine-labelled analogues of inhibitors are valu-able probes for the determination of binding poses.

In conclusion, trifluoromethylated captopril analogues are potent MBL inhibitors and, thus, can become promising tools for structural studies of MBL-binding poses.

4. Experimental section

Description of the experimental procedures can be found in the Supporting information. Biological activity raw data will be made available through the DataverseNO repository before publication. The backbone resonance assignment [20b] of NDM-1 was deposited to the BMRBI with code 50945.

CRediT authorship contribution statement

Alexandra Kondratieva: Conceptualization, Data curation, Formal analysis, Investigation, Methodology, Software, Validation,

Visualization, Writing – original draft, Writing – review & editing. **Katarzyna Palica:** Formal analysis, Investigation, Methodology, Software, Validation, Visualization, Writing – original draft. **Christopher Frøhlich:** Investigation, Methodology, Supervision, Visualization, Writing – original draft, Writing – review & editing. **Rebekka Rolfsnes Hovd:** Methodology, Writing – review & editing. **Hanna-Kirsti S. Leiros:** Funding acquisition, Supervision, Writing – original draft, Writing – review & editing. **Mate Erdelyi:** Conceptualization, Funding acquisition, Methodology, Resources, Supervision, Writing – original draft, Writing – review & editing. **Annette Bayer:** Conceptualization, Funding acquisition, Methodology, Project administration, Resources, Supervision, Writing – original draft, Writing – review & editing.

Declaration of competing interest

The authors declare that they have no known competing financial interests or personal relationships that could have appeared to influence the work reported in this paper.

Data availability

Supporting information for compound identity and purity are attached as Supporting information. Biological data will be made available on request.

Acknowledgements

Appendix A. Supplementary data

Supplementary data to this article can be found online at https://doi.org/10.1016/j.ejmech.2024.116140.

References

[1] WHO in *Global action plan on Antimicrobial resistance*, Vol. Geneva, 2015.
[2] a) T. Palzkill, Ann. N. Y. Acad. Sci. 1277 (2013) 91–104;
    b) J.D. Docquier, S. Mangani, Drug Resist. Updates 36 (2018) 13–29.
[3] K. Bush, G.A. Jacoby, Antimicrob. Agents Chemother. 54 (2010) 969–976.
[4] T. Naas, S. Oueslati, R.A. Bonnin, M.L. Dabos, A. Zavala, L. Dortet, P. Retailleau, B. I. Iorga, J. Enzym. Inhib. Med. Chem. 32 (2017) 917–919.
[5] a) N. Farhat, A.U. Khan, Infect. Genet. Evol. 86 (2020) 104588;
    b) G. Bahr, L.J. González, A.J. Vila, Chem. Rev. 121 (2021) 7957–8094.
[6] D. Yahav, C.G. Giske, A. Grãmatniece, H. Abodakpi, V.H. Tam, L. Leibovici, Clin. Microbiol. Rev. 34 (2020), https://doi.org/10.1128/cmr.00115-20 e00115-00120.
[7] a) M.F. Mojica, M.A. Rossi, A.J. Vila, R.A. Bonomo, Lancet Infect. Dis. 22 (2022) e28–e34;
    b) E. Denakpo, T. Naas, B.I. Iorga, Expert Opin. Ther. Pat. (2023) 1–16;
    c) X. Gu, M. Zheng, L. Chen, H. Li, Microbiol. Res. 261 (2022) 127079.
[8] a) P. Linciano, L. Cendron, E. Gianquinto, F. Spyrakis, D. Tondi, ACS Infect. Dis. 5 (2019) 9–34;
    b) Y. Yang, Y.-H. Yan, C.J. Schofield, A. McNally, Z. Zong, G.-B. Li, Trends Microbiol. 31 (2023) 735–748.
[9] a) K. Bush, P.A. Bradford, Nat. Rev. Microbiol. 17 (2019) 295–306;
    b) K.H.M.E. Tehrani, N.I. Martin, Med. Chem. Commun. 9 (2018) 1439–1456.

[10] a) Y.L. Wang, S. Liu, Z.J. Yu, Y. Lei, M.Y. Huang, Y.H. Yan, Q. Ma, Y. Zheng, H. Deng, Y. Sun, C. Wu, Y. Yu, Q. Chen, Z. Wang, Y. Wu, G.B. Li, J. Med. Chem. 62 (2019) 7160–7184;
    b) S. Yahiaoui, K. Voos, J. Haupenthal, T.A. Wichelhaus, D. Frank, L. Weizel, M. Rotter, S. Brunst, J.S. Kramer, E. Proschak, C. Ducho, A.K.H. Hirsch, RSC Med. Chem. 12 (2021) 1698–1708;
    c) Y.H. Yan, J. Chen, Z. Zhan, Z.J. Yu, G. Li, L. Guo, G.B. Li, Y. Wu, Y. Zheng, RSC Adv. 10 (2020) 31377–31384;
    d) Z. Meng, M.L. Tang, L. Yu, Y. Liang, J. Han, C. Zhang, F. Hu, J.M. Yu, X. Sun, ACS Infect. Dis. 5 (2019) 903–916;
    e) F.M. Klingler, T.A. Wichelhaus, D. Frank, J. Cuesta-Bernal, J. El-Delik, H. F. Muller, H. Sjuts, S. Gottig, A. Koenigs, K.M. Pos, D. Pogoryelov, E. Proschak, J. Med. Chem. 58 (2015) 3626–3630.
[11] D.W. Cushman, M.A. Ondetti, Nat. Med. 5 (1999) 1110–1112.
[12] a) Y. Yusof, D.T.C. Tan, O.K. Arjomandi, G. Schenk, R.P. McGeary, Bioorg. Med. Chem. Lett. 26 (2016) 1589–1593;
    b) B.M. Lienard, G. Garau, L. Horsfall, A.I. Karsisiotis, C. Damblon, P. Lassaux, C. Papamicael, G.C. Roberts, M. Galleni, O. Dideberg, J.M. Frere, C.J. Schofield, Org. Biomol. Chem. 6 (2008) 2282–2294;
    c) U. Heinz, R. Bauer, S. Wommer, W. Meyer-Klaucke, C. Papamichaels, J. Bateson, H.W. Adolph, J. Biol. Chem. 278 (2003) 20659–20666.
[13] a) C. Kaya, J. Konstantinović, A.M. Kany, A. Andreas, J.S. Kramer, S. Brunst, L. Weizel, M.J. Rotter, D. Frank, S. Yahiaoui, R. Müller, R.W. Hartmann, J. Haupenthal, E. Proschak, T.A. Wichelhaus, A.K.H. Hirsch, J. Med. Chem. 65 (2022) 3913–3922;
    b) N. Li, Y. Xu, Q. Xia, C. Bai, T. Wang, L. Wang, D. He, N. Xie, L. Li, J. Wang, H. G. Zhou, F. Xu, C. Yang, Q. Zhang, Z. Yin, Y. Guo, Y. Chen, Bioorg. Med. Chem. Lett. 24 (2014) 386–389;
    c) G. Ma, S. Wang, K. Wu, W. Zhang, A. Ahmad, Q. Hao, X. Lei, H. Zhang, Bioorg. Med. Chem. 29 (2021) 115902.
[14] a) J. Brem, S.S. van Berkel, D. Zollman, S.Y. Lee, O. Gileadi, P.J. McHugh, T. R. Walsh, M.A. McDonough, C.J. Schofield, Antimicrob. Agents Chemother. 60 (2016) 142–150;
    b) Y. Guo, J. Wang, G. Niu, W. Shui, Y. Sun, H. Zhou, Y. Zhang, C. Yang, Z. Lou, Z. Rao, Protein Cell 2 (2011) 384–394.
[15] a) A.M. Rydzik, J. Brem, S.S. van Berkel, I. Pfeffer, A. Makena, T.D.W. Claridge, C. J. Schofield, Angew. Chem. Int. Ed. 53 (2014) 3129–3133;
    b) S.S. van Berkel, J. Brem, A.M. Rydzik, R. Salimraj, R. Cain, A. Verma, R. J. Owens, C.W.G. Fishwick, J. Spencer, C.J. Schofield, J. Med. Chem. 56 (2013) 6945–6953.
[16] a) C. Mollard, C. Moali, C. Papamicael, C. Damblon, S. Vessilier, G. Amicosante, C. J. Schofield, M. Galleni, J.M. Frère, G.C.K. Roberts, J. Biol. Chem. 276 (2001) 45015–45023;
    b) K.H.M.E. Tehrani, N.I. Martin, ACS Infect. Dis. 3 (2017) 711–717.
[17] K.H.M.E. Tehrani, N. Wade, V. Mashayekhi, N.C. Bruchle, W. Jespers, K. Voskuil, D. Pesce, M.J. van Haren, G.J.P. van Westen, N.I. Martin, J. Med. Chem. 64 (2021) 9141–9151.
[18] a) A. Abula, Z. Xu, Z. Zhu, C. Peng, Z. Chen, W. Zhu, H.A. Aisa, J. Chem. Inf. Model. 60 (2020) 6242–6250;
    b) B.M. Johnson, Y.-Z. Shu, X. Zhuo, N.A. Meanwell, J. Med. Chem. 63 (2020) 6315–6386;
    c) N.A. Meanwell, J. Med. Chem. 61 (2018) 5822–5880.
[19] a) I. Ojima, F.A. Jameison, B. Pete, H. Radunz, C. Schittenhelm, H.J. Linder, A. E. Emith, Drug Des. Discov. 11 (1994) 91–113;
    b) I. Ojima, F.A. Jameison, Bioorg. Med. Chem. Lett. 1 (1991) 581–584.
[20] a) G. Rivière, S. Oueslati, M. Gayral, J.B. Créchet, N. Nhiri, E. Jacquet, J. C. Cintrat, F. Giraud, C. van Heijenoort, E. Lescop, S. Pethe, B.I. Iorga, T. Naas, E. Guittet, N. Morellet, ACS Omega 5 (2020) 10466–10480;
    b) K. Palica, M. Vorácová, S. Skagseth, A. Andersson Rasmussen, L. Allander, M. Hubert, L. Sandegren, H.-K.S. Leiros, H. Andersson, M. Erdélyi, ACS Omega 7 (2022) 4550–4562;
    c) K. Cheng, Q. Wu, C. Yao, Z. Chai, L. Jiang, M. Liu, C. Li, JACS Au 3 (2023) 849–859;
    d) L.H.E. Wieske, J. Bogaerts, A.A.M. Leding, S. Wilcox, A. Andersson Rasmussen, K. Leszczak, L. Turunen, W.A. Herrebout, M. Hubert, A. Bayer, M. Erdélyi, ACS Med. Chem. Lett. 13 (2022) 257–261.
[21] Y. Hu, K. Cheng, L. He, X. Zhang, L. Jiang, L. Jiang, C. Li, G. Wang, Y. Yang, M. Liu, Anal. Chem. 93 (2021) 1866–1879.
[22] R.S. Norton, E.W.W. Leung, I.R. Chandrashekaran, C.A. MacRaild, Molecules 21 (2016) 860–873.
[23] E. van Groesen, C.T. Lohans, J. Brem, K.M.J. Aertker, T.D.W. Claridge, C. J. Schofield, Chem. Eur. J. 25 (2019) 11837–11841.
[24] T.P. Vasileva, A.F. Kolomiets, E.I. Mysov, A.V. Fokin, Russ. Chem. Bull. 46 (1997) 1230–1232.
[25] S. Skagseth, S. Akhter, M.H. Paulsen, Z. Muhammad, S. Lauksund, Ø. Samuelsen, H.-K.S. Leiros, A. Bayer, Eur. J. Med. Chem. 135 (2017) 159–173.
[26] D. Buttner, J.S. Kramer, F.M. Klingler, S.K. Wittmann, M.R. Hartmann, C.G. Kurz, D. Kohnhauser, L. Weizel, A. Bruggerhoff, D. Frank, D. Steinhilber, T. A. Wichelhaus, D. Pogoryelov, E. Proschak, ACS Infect. Dis. 4 (2018) 360–372.
[27] a) C. Fröhlich, V. Sørum, N. Tokuriki, P.J. Johnsen, Ø. Samuelsen, J. Antimicrob. Chemother. 77 (2022) 2429–2436;
    b) Ø.M. Lorentzen, A.S.B. Haukefer, P.J. Johnsen, C. Frøhlich, bioRxiv (2023), 2023.2010.2002.560492.
[28] M.P. Williamson, Prog. Nucl. Magn. Reson. Spectrosc. 73 (2013) 1–16.
[29] L. Fielding, Curr. Top. Med. Chem. 3 (2003) 39–53.

Supporting information

for

Fluorinated Captopril Analogues as Metallo-β-Lactamase Inhibitors – Fluorination Facilitates Structure Determination of NDM-1 Binding Pose

Alexandra Kondratieva[a], Katarzyna Palica[b], Christopher Frøhlich[c], Rebekka Rolfsnes Hovd[d], Hanna-Kirsti S. Leiros[a], Mate Erdelyi[b], Annette Bayer[a]*

[a] *Department of Chemistry, UiT The Arctic University of Norway, NO-9037 Tromsø, Norway.*
[b] *Department of Chemistry – BMC, Organic Chemistry, Uppsala University, 752 37 Uppsala, Sweden.*
[c] *Department of Pharmacy, UiT The Arctic University of Norway, NO-9037 Tromsø, Norway.*
[d] *Department of Pharmacy, University of Oslo, NO-0371 Oslo, Norway.*

Table of Contents

Chemistry

General methods

All reagents were purchased from commercial sources and used as supplied without further purification unless otherwise stated. *Tert*-butyl 4-(aminomethyl)benzoate[1], *tert*-butyl (*R*)-piperidine-2-carboxylate[2] and compounds 2α, 2β[3] were synthesized as described in literature and their analytical data were found to be in accordance with those reported. Solvents were dried according to standard procedures over appropriately sized molecular sieves.

For thin layer chromatography (TLC) analysis, aluminium plates pre-coated with silica gel (Merck silica gel 60 F_{254}) were used and visualized using either ultraviolet light or by treatment with an appropriate stain. Normal phase chromatography was carried out using Redisep Gold® silica gel columns on a CombiFlash® EZ Prep system. Final compounds were purified via preparative HPLC performed on a CombiFlash® EZ Prep system with a YMC-Actus Triart C18 column, eluting with mixtures of acetonitrile and H_2O (both containing 0.1% TFA). Enantiomers were separated with preparative chiral HPLC using single wavelength detection at 254 nm and a Lux i-Amylose-1 column (5 μm, 1000 Å, Ø 4.6 mm, L 100 mm) with isocratic Hex/IPA (8:2) as mobile phase at 10 ml/min flow rate.

^1H and ^{13}C NMR spectra for assignment were obtained on a 400 MHZ Bruker Advance III HD spectrometer equipped with a 5 mm SmartProbe BB/1H (BB = 19F, 31P-15N) at 20 ˚C. NMR spectra for the chemical shift perturbation experiments were recorded on a Bruker Avance III HD 600 MHz spectrometer equipped with a TCI cryogenic probe. 1D 19F-1H HOESY was acquired on a Bruker Avance III 700 MHz spectrometer, equipped with a 5mm QCI cryogenic probe. Chemical shifts are reported in ppm relative to the solvent residual peak (CDCl$_3$: δH 7.26 and δC 77.16; Acetone-*d6*: δH 2.05 and δC 206.26; Methanol-*d4*: δH 3.31 and δC 49.00). Coupling constants *J* are reported in Hertz (Hz). The ^{13}C NMR spectra were ^1H decoupled. The following abbreviations were used to indicate the multiplicities: s = singlet, d = doublet, t = triplet, q = quartet, qnt = quintet, dd = doublet of doublets, dq = doublet of quartets, dqd = doublet of quartet of doublets, tt = triplet of triplets, qntd = quintet of doublets, m = multiplet, app = appearing and br = broad. When possible, for compounds obtained as rotameric mixtures, chemical shifts of minor rotamers are reported separately, enclosed in square brackets.

High-resolution mass spectrometry (HRMS) was conducted from methanol or acetonitrile solutions on a ThermoScientific Vanquish UHPLC system coupled to a ThermoScientific Orbitrap Exploris 120 with electrospray ionization (ESI). The following solvent system, at a flow rate of 0.3 mL/min, was used: solvent A – MiliQ water/0.1% formic acid; solvent B – 90% acetonitrile/10% MiliQ water/0.1% formic acid. Gradient elution was as follows: 95:5 to 30:70 (A:B) over 3.5 min, 0:100 (A:B) for 1 min, then reversion back to 95:5 (A:B) for 1.5 min.

Infra-red (IR) spectra of the pure compounds were recorded on an Agilent Technologies Cary 630 FTIR. Selected absorption maxima (v_{max}) are reported in wavenumbers (cm^{-1}).

Melting points were measured on a Stuart SMP50 automatic melting point detector and are reported uncorrected in degree Celsius (˚C).

Optical rotations were determined on an Optical Activity LTD AA-10R Automatic Polarimeter at 20 ˚C in a cuvette with a length of 100 mm and the sodium D-line (589 nm). The concentrations and solvents (HPLC grade) were adjusted for each compound individually. The polarimeter was calibrated against the pure solvent. Concentrations are provided in g/(100 mL).

All final compounds were analyzed using the described above UHPLC-HRMS system and the purity is specified for each compound below.

General procedures

General Procedure A: Amide formation I

A solution of 2-(trifluoromethyl)acrylic acid or (*E*)-4,4,4-trifluorobut-2-enoic acid in DCM was treated with the respective coupling reagent (HBTU or T3P). The resulting mixture was cooled down to 0 ˚C and the respective base (DIPEA or Et$_3$N) and amine were sequentially added. After removal of the ice bath, the reaction was stirred at ambient temperature until TLC indicated full conversion. The solvent was removed under reduced pressure and the crude product was purified on an automated flash system equipped with a silica column, using heptane/EtOAc as the eluent. Alternatively, after completion of the reaction, water was added and the reaction mixture was extracted three times with DCM. The combined organic layers were washed with brine, dried over Na$_2$SO$_4$, filtered and the solvent was removed under reduced pressure. The resulting residue was purified on an automated flash system equipped with a silica column, using heptane/EtOAc as the eluent.

General Procedure B: Amide formation II

A mixture of 2-(trifluoromethyl)acrylic acid or (*E*)-4,4,4-trifluorobut-2-enoic acid and the respective amine in EtOAc was cooled down to 0 ˚C. DIPEA was added and the resulting mixture was stirred for 30 min at 0 ˚C. T3P in EtOAc (50% w/w) was added at 0 ˚C and the reaction was stirred at ambient temperature, after removal of the ice bath, until TLC indicated full conversion. Water was added and the reaction mixture was extracted three times with EtOAc. The combined organic layers were washed with brine, dried over Na$_2$SO$_4$, filtered and the solvent was removed under reduced pressure. The resulting residue was purified on an automated flash system equipped with a silica column, using heptane/EtOAc as the eluent.

General Procedure C: Michael addition of thioacetic acid

The respective acrylic amide was dissolved in THF. Thioacetic acid was added and the reaction mixture was stirred at ambient or elevated temperatures until TLC indicated full conversion. After the mixture cooled down to ambient temperature, the solvent was removed with a nitrogen stream. The crude product

was purified on an automated flash system equipped with a silica column, using heptane/EtOAc as the eluent.

General Procedure D: Thiol deprotection

The respective thioacetate was dissolved in methanol. The solution was cooled down to -20 ˚C and sodium thiomethoxide (1 M solution in MeOH) was added. The resulting mixture was stirred at -20 ˚C for 30 min, before an aqueous HCl solution (0.1 M) was added. The product precipitated and was collected via filtration to yield a white solid. If no precipitation was observed, the reaction mixture was extracted three times with DCM. The combined organic layers were washed with brine, dried over $MgSO_4$, filtered and the solvent was removed under reduced pressure. The crude product was purified by preparative HPLC.

General Procedure E: Acid and subsequent thiol deprotection

The respective thioacetate was dissolved in DCM. After the addition of TFA, the solution was heated to 50 ˚C and stirred under reflux overnight. Solvent and TFA residues were removed with a nitrogen stream. The crude was taken up in degassed water (10 mL). The mixture was cooled using an ice bath and treated with aqueous ammonia (32%). After removal of the ice bath, the reaction mixture was stirred for 3 h. The mixture was adjusted to pH 1 with 2 M HCl and extracted three times with EtOAc. The combined organic layers were washed with brine and dried over $MgSO_4$, filtered and the solvent was removed under reduced pressure. The crude product was purified by preparative HPLC.
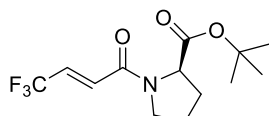
Spectroscopic data
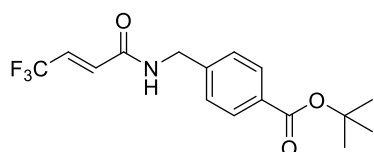
Tert-butyl (E)-4-((4,4,4-trifluorobut-2-enamido)methyl)benzoate (**3βB**).

Synthesized according to *General Procedure A* using (*E*)-4,4,4-trifluorobut-2-enoic acid (90 mg, 0.64 mmol, 1.2 eq), *tert*-butyl 4-(aminomethyl)benzoate (111 mg, 0.54 mmol, 1.0 eq), T3P (478 μl, 0.80 mmol, 1.5 eq), Et₃N (149 μl, 1.07 mmol, 2.0 eq) and DCM (4 mL). The reaction was stirred at ambient temperature for 4 h. The crude was purified using heptane/EtOAc to yield **3βB** (150 mg, 0.46 mmol, 85%) as a white solid. **¹H NMR** (400 MHz, CDCl₃) δ 7.98 – 7.88 (m, 2H), 7.30 (d, *J* = 8.0 Hz, 2H), 6.79 (dq, *J* = 15.3, 6.6 Hz, 1H), 6.53 (dq, *J* = 15.3, 1.9 Hz, 1H), 6.32 (br s, 1H), 4.57 (d, *J* = 5.8 Hz, 2H), 1.58 (s, 9H). **¹³C NMR** (101 MHz, CDCl₃) δ 165.6, 162.6, 141.8, 131.8, 130.5 (q, *J* = 5.9 Hz), 130.1 (2C), 129.3 (q, *J* = 35.2 Hz), 127.7 (2C), 122.5 (q, *J* = 270.0 Hz), 81.5, 43.9, 28.3 (3C). **HRMS** (ESI): calcd for $C_{16}H_{18}F_3NO_3Na^+$ [M+Na]⁺ 352.1131, found: 352.1131.
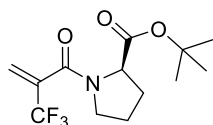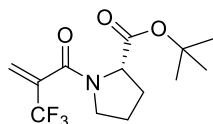
Tert-butyl (2-(trifluoromethyl)acryloyl)-D-prolinate (**3αC**).

Synthesized according to *General Procedure B* using 2-(trifluoromethyl)acrylic acid (140 mg, 1.00 mmol, 1.2 eq), (*R*)-*tert*-butyl pyrrolidine-2-carboxylate hydrochloride (172 mg, 1.00 mmol, 1.0 eq), DIPEA (477 μl, 3.30 mmol, 3.3 eq), T3P (692 μl, 1.40 mmol, 1.4 eq) and EtOAc (4 mL). The reaction was stirred at ambient temperature overnight. The crude was purified using heptane/EtOAc to yield **3αC** (160 mg, 0.55 mmol, 66%) as a colourless oil. **¹H NMR** (400 MHz, CDCl₃) (a 3:1 mixture of rotamers*) δ 6.10 (s, 1H) [5.99], 5.82 (s, 1H) [5.71], 4.41 (dd, *J* = 8.4, 4.8 Hz, 1H) [4.29 (*J* = 8.4, 2.3 Hz)], 3.68 – 3.49 (m, 2H), 2.33 – 1.83 (m, 4H), 1.44 (s, 9H) [1.43]. **¹³C NMR** (101 MHz, CDCl₃) δ 170.7 [171.2], 162.5 [162.7], 135.6 [135.8] (q, *J* = 31.9 Hz), 123.6 [123.2] (q, *J* = 5.5 Hz), 121.6 (q, *J* = 273.7 Hz), 81.8 [82.5], 59.7 [61.5], 49.3 [46.4], 29.5 [31.3], 28.0 [27.9] (3C), 25.0 [22.4]. **HRMS** (ESI): calcd for C₁₃H₁₈F₃NO₃Na⁺ [M+Na]⁺ 316.1131, found: 316.1128.

(E)-(4,4,4-trifluorobut-2-enoyl)-D-prolinate (**3βC**).

Synthesized according to *General Procedure A* using (*E*)-4,4,4-trifluorobut-2-enoic acid (150 mg, 1.07 mmol, 1.0 eq), (*R*)-*tert*-butyl pyrrolidine-2-carboxylate hydrochloride (267 mg, 1.29 mmol, 1.2 eq), HBTU (609 mg, 1.61 mmol, 1.5 eq), DIPEA (278 μl, 1.61 mmol, 1.5 eq) and DCM (7 mL). The reaction was stirred at ambient temperature for 3 h. The crude was purified using heptane/EtOAc to yield **3βC** (273 mg, 0.93 mmol, 87%) as a yellow solid. **¹H NMR** (400 MHz, CDCl₃) (a 2:1 mixture of rotamers*) δ 6.86 – 6.61 (m, 2H), 4.45 (dd, *J* = 8.5, 4.0 Hz, 1H) [4.37 (*J* = 8.2, 3.2 Hz)], 3.80 – 3.56 (m, 2H), 2.32 – 1.88 (m, 4H), 1.45 (s, 9H) [1.43]. **¹³C NMR** (101 MHz, CDCl₃) δ 170.8, 161.6 [162.2], 129.5 [129.1] (q, *J* = 34.9 Hz), 128.6 [128.8] (q, *J* = 5.9 Hz), 122.7 (q, *J* = 270.0 Hz), 81.8 [83.0], 60.1 [60.3], 47.3 [47.1], 29.2 [31.3], 28.1 [27.9] (3C), 24.7 [22.7]. **HRMS** (ESI): calcd for C₁₃H₁₈F₃NO₃Na⁺ [M+Na]⁺ 316.1131, found: 316.1127.

Tert-butyl (2-(trifluoromethyl)acryloyl)-L-prolinate (**3αD**).

Synthesized according to *General Procedure A* using 2-(trifluoromethyl)acrylic acid (98 mg, 0.70 mmol, 1.2 eq), *tert*-butyl L-prolinate (100 mg, 0.58 mmol, 1.0 eq), T3P (904 μl, 1.52 mmol, 2.6 eq), Et₃N (122 μl, 0.88 mmol, 1.5 eq) and DCM (4 mL). The reaction was stirred at ambient temperature for 1 h. The crude was purified using heptane/EtOAc to yield **3αD** (82 mg, 0.28 mmol, 48%) as a colourless oil. **¹H NMR** (400 MHz, CDCl₃) (a 3:1 mixture of rotamers*) δ 6.08 (s, 1H) [5.97], 5.80 (s, 1H) [5.69], 4.38 (dd, *J* = 8.6, 4.7 Hz, 1H) [4.27 (*J* = 8.4, 2.3 Hz)], 3.66 – 3.47 (m, 2H), 2.31 – 1.81 (m, 4H), 1.41 (s, 9H) [1.40]. **¹³C NMR** (101 MHz, CDCl₃) δ 170.6 [171.2],

---

* Chemical shifts of minor rotamer are enclosed in square brackets.

162.5 [162.7], 135.5 [135.7] (q, J = 32.2 Hz), 123.5 [123.2] (q, J = 5.6 Hz), 121.6 (q, J = 273.7 Hz), 81.7 [82.4], 59.6 [61.4], 49.3 [46.4], 29.4 [31.2], 27.9 [27.8] (3C), 24.9 [22.3]. **HRMS** (ESI): calcd for $C_{13}H_{18}F_3NO_3Na^+$ [M+Na]$^+$ 316.1131, found: 316.1131.
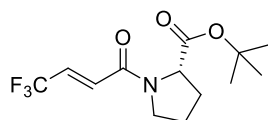
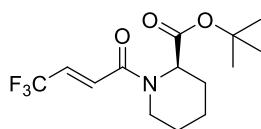*(E)-(4,4,4-trifluorobut-2-enoyl)-L-prolinate* (**3βD**).

Synthesized according to *General Procedure A* using (*E*)-4,4,4-trifluorobut-2-enoic acid (150 mg, 1.07 mmol, 1.0 eq), *tert*-butyl L-prolinate (220 mg, 1.29 mmol, 1.2 eq), HBTU (609 mg, 1.61 mmol, 1.5 eq), DIPEA (278 μl, 1.61 mmol, 1.5 eq) and DCM (7 mL). The reaction was stirred at ambient temperature for 3 h. The crude was purified using heptane/EtOAc to yield **3βD** (266 mg, 0.91 mmol, 85%) as a yellow solid. **¹H NMR** (400 MHz, CDCl₃) (a 2:1 mixture of rotamers*) δ 6.87 – 6.62 (m, 2H), 4.46 (dd, J = 8.5, 3.8 Hz, 1H) [4.38 (*J* = 8.3, 3.2 Hz)], 3.81 – 3.57 (m, 2H), 2.32 – 1.90 (m, 4H), 1.46 (s, 9H) [1.44]. **¹³C NMR** (101 MHz, CDCl₃) δ 170.8, 161.6 [162.2], 129.6 [129.1] (q, J = 34.9 Hz), 128.6 [128.8] (q, J = 5.9 Hz), 122.7 (q, J = 269.7 Hz), 81.9 [83.1], 60.1 [60.3], 47.4 [47.1], 29.3 [31.3], 28.1 [27.9] (3C), 24.7 [22.8]. **HRMS** (ESI): calcd for $C_{13}H_{18}F_3NO_3Na^+$ [M+Na]$^+$ 316.1131, found: 316.1130. **IR** (v_{max}/cm^{-1}, neat): 2980, 2885, 1737, 1685, 1639, 1432, 1371, 1305. 1255, 1225, 1154, 1132, 967.
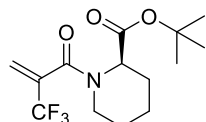
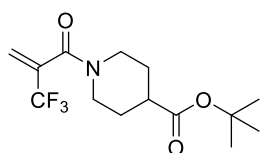*Tert-butyl (R)-1-(2-(trifluoromethyl)acryloyl)piperidine-2-carboxylate* (**3αE**).

Synthesized according to *General Procedure B* using 2-(trifluoromethyl)acrylic acid (210 mg, 1.50 mmol, 1.0 eq), *tert*-butyl (*R*)-piperidine-2-carboxylate (278 mg, 1.50 mmol, 1.0 eq), DIPEA (862 μl, 4.95 mmol, 3.3 eq), T3P (1.25 mL, 2.10 mmol, 1.4 eq) and EtOAc (5 mL). The reaction was stirred at ambient temperature overnight. The crude was purified using heptane/EtOAc to yield **3αE** (353 mg, 1.15 mmol, 77%) as a colourless oil. **¹H NMR** (400 MHz, CDCl₃) (a 2.3:1 mixture of rotamers*) δ 5.85 (s, 1H) [5.90], 5.61 (s, 1H), 5.16 (app d, J = 5.7 Hz, 1H) [4.37 (*J* = 5.5 Hz)], 3.74 – 3.61 (m, 1H) [4.39 – 4.32], 3.24 – 3.05 (m, 1H) [2.81 – 2.64], 2.25 – 2.10 (m, 1H), 1.72 – 1.45 (m, 3H), 1.42 – 1.17 (m, 11H). **¹³C NMR** (101 MHz, CDCl₃) δ 169.5 [169.4], 164.0, 134.9 (q, J = 32.4 Hz), 122.6 (q, J = 5.7 Hz), 121.6 (q, J = 273.6 Hz), 82.8 [82.2], 52.7 [58.6], 45.6 [39.8], 28.1 [28.0] (3C), 26.7 [27.5], 25.4 [24.6], 21.1 [21.0]. **HRMS** (ESI): calcd for $C_{14}H_{20}F_3NO_3Na^+$ [M+Na]$^+$ 330.1288, found: 330.1288.

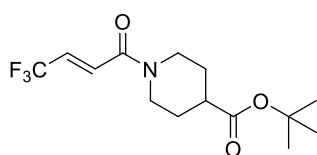* Chemical shifts of minor rotamer are enclosed in square brackets.

Tert-butyl (R,E)-1-(4,4,4-trifluorobut-2-enoyl)piperidine-2-carboxylate (**3βE**).

Synthesized according to *General Procedure B* using (*E*)-4,4,4-trifluorobut-2-enoic acid (280 mg, 2.00 mmol, 1.0 eq), *tert*-butyl (*R*)-piperidine-2-carboxylate (371 mg, 2.00 mmol, 1.0 eq), DIPEA (1.15 mL, 6.60 mmol, 3.3 eq), T3P (1.67 mL, 2.80 mmol, 1.4 eq) and EtOAc (7 mL). The reaction was stirred at ambient temperature overnight. The crude was purified using heptane/EtOAc to yield **3βE** (429 mg, 1.40 mmol, 70%) as a colourless oil. **^{1}H NMR** (400 MHz, CDCl$_3$) (a 2.6:1 mixture of rotamers*) δ 6.98 – 6.85 (m, 1H) [6.83 – 6.73], 6.61 – 6.40 (m, 1H), 5.21 – 5.05 (m, 1H) [4.44 – 4.38], 3.74 – 3.62 (m, 1H) [4.38 – 4.31], 3.33 – 3.17 (m, 1H) [2.70 – 2.54], 2.25 – 2.06 (m, 1H), 1.69 – 1.45 (m, 3H), 1.42 – 1.11 (m, 11H). **^{13}C NMR** (101 MHz, CDCl$_3$) δ 169.5 [169.0], 163.7 [164.4], 128.5 [129.0] (q, *J* = 6.3 Hz), 128.6 [128.1] (q, *J* = 34.5 Hz), 122.5 [122.4] (q, *J* = 269.9 Hz), 81.7 [82.6], 53.0 [56.9], 43.8 [40.0], 27.8 [27.7] (3C), 26.6 [26.8], 25.2 [24.2], 20.6 [20.4]. **HRMS** (ESI): calcd for C$_{14}$H$_{20}$F$_3$NO$_3$Na$^+$ [M+Na]$^+$ 330.1288, found: 330.1288.

Tert-butyl 1-(2-(trifluoromethyl)acryloyl)piperidine-4-carboxylate (**3αF**).

Synthesized according to *General Procedure A* using 2-(trifluoromethyl)acrylic acid (98 mg, 0.70 mmol, 1.0 eq), *tert*-butyl piperidine-4-carboxylate hydrochloride (155 mg, 0.70 mmol, 1.0 eq), T3P (1.67 mL, 2.80 mmol, 4.0 eq), Et$_3$N (782 μl, 5.61 mmol, 8.0 eq) and DCM (5 mL). The reaction was stirred at ambient temperature for 4 h. The crude was purified using heptane/EtOAc to yield **3αF** (64 mg, 0.21 mmol, 30%) as a colourless oil. **^{1}H NMR** (400 MHz, CDCl$_3$) δ 6.00 (q, *J* = 1.6 Hz, 1H), 5.64 (br s, 1H), 4.41 – 4.23 (m, 1H), 3.88 – 3.67 (m, 1H), 3.22 – 2.87 (m, 2H), 2.45 (app tt, *J* = 10.5, 4.0 Hz, 1H), 2.00 – 1.79 (m, 2H), 1.71 – 1.52 (m, 2H), 1.42 (s, 9H). **^{13}C NMR** (101 MHz, CDCl$_3$) δ 173.2, 162.7, 134.9 (q, *J* = 32.2 Hz), 122.3 (q, *J* = 5.5 Hz), 121.5 (q, *J* = 273.9 Hz), 80.9, 46.6, 41.6, 41.2, 28.4, 28.1 (3C), 27.8. **HRMS** (ESI): calcd for C$_{14}$H$_{20}$F$_3$NO$_3$Na$^+$ [M+Na]$^+$ 330.1288, found: 330.1287.

Tert-butyl (E)-1-(4,4,4-trifluorobut-2-enoyl)piperidine-4-carboxylate (**3βF**).

Synthesized according to *General Procedure A* using (*E*)-4,4,4-trifluorobut-2-enoic acid (145 mg, 1.04 mmol, 1.0 eq), *tert*-butyl piperidine-4-carboxylate hydrochloride (276 mg, 1.24 mmol, 1.2 eq), HBTU (589 mg, 1.55 mmol, 1.5 eq), DIPEA (448 μl, 2.59 mmol, 2.5 eq) and DCM (7 mL). The reaction was stirred at ambient temperature for 3 h. The crude was purified using heptane/EtOAc to yield **3βF** (318 mg, 0.47 mmol, 45%) as a colourless oil. **^{1}H NMR** (400 MHz, CDCl$_3$) δ 6.94 (dq, *J* = 15.4, 2.0 Hz, 1H), 6.65 (dq, *J* =

---

* Chemical shifts of minor rotamer are enclosed in square brackets.

15.4, 6.6 Hz, 1H), 4.40 – 4.29 (m, 1H), 3.88 – 3.76 (m, 1H), 3.25 – 3.13 (m, 1H), 3.01 – 2.88 (m, 1H), 2.46 (app tt, J = 10.4, 4.1 Hz, 1H), 1.97 – 1.87 (m, 2H), 1.72 – 1.56 (m, 2H), 1.41 (s, 9H). ^{13}**C NMR** (101 MHz, CDCl$_3$) δ 173.2, 162.3, 129.1 (q, J = 34.8 Hz), 128.2 (q, J = 5.9 Hz), 122.7 (q, J = 269.9 Hz), 80.9, 45.5, 41.8, 41.6, 28.7, 28.1 (3C), 27.8. **HRMS** (ESI): calcd for C$_{14}$H$_{20}$F$_3$NO$_3$Na$^+$ [M+Na]$^+$ 330.1288, found: 330.1287.
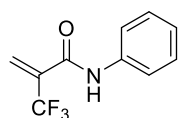
N-phenyl-2-(trifluoromethyl)acrylamide (**3αG**).

Synthesized according to *General Procedure A* using 2-(trifluoromethyl)acrylic acid (99 mg, 0.71 mmol, 1.2 eq), aniline (55 mg, 0.59 mmol, 1.0 eq), T3P (879 μl, 1.48 mmol, 2.5 eq), Et$_3$N (165 μl, 1.18 mmol, 2.0 eq) and DCM (3 mL). The reaction was stirred at ambient temperature for 4 h. The crude was purified using H$_2$O/MeCN (0.1% TFA) to yield **3αG** (76 mg, 0.35 mmol, 60%) as a white solid. ^{1}**H NMR** (400 MHz, CDCl$_3$) δ 7.65 (br s, 1H), 7.58 – 7.51 (m, 2H), 7.41 – 7.31 (m, 2H), 7.22 – 7.14 (m, 1H), 6.62 (q, J = 1.7 Hz, 1H), 6.33 (q, J = 1.4 Hz, 1H). ^{13}**C NMR** (101 MHz, CDCl$_3$) δ 159.1, 136.9, 134.5 (q, J = 30.9 Hz), 129.9 (q, J = 5.5 Hz), 129.3 (2C), 125.6, 122.3 (q, J = 272.9 Hz), 120.8 (2C). **HRMS** (ESI): calcd for C$_{10}$H$_8$F$_3$NONa$^+$ [M+Na]$^+$ 238.0450, found: 238.0449.

(E)-4,4,4-trifluoro-N-phenylbut-2-enamide (**3βG**).

Synthesized according to *General Procedure A* using (*E*)-4,4,4-trifluorobut-2-enoic acid (280 mg, 2.00 mmol, 1.0 eq), aniline (224 mg, 2.40 mmol, 1.2 eq), HBTU (1.14 g, 3.00 mmol, 1.5 eq), DIPEA (519 μl, 3.00 mmol, 1.5 eq) and DCM (7 mL). The reaction was stirred at ambient temperature for 3 h. The crude was purified using heptane/EtOAc to yield **3βG** (393 mg, 1.83 mmol, 91%) as a white solid. ^{1}**H NMR** (400 MHz, CDCl$_3$) δ 7.62 – 7.53 (m, 3H), 7.35 (t, J = 7.9 Hz, 2H), 7.18 (t, J = 7.4 Hz, 1H), 6.88 (dq, J = 15.3, 6.6 Hz, 1H), 6.65 (dq, J = 15.2, 1.9 Hz, 1H). ^{13}**C NMR** (101 MHz, CDCl$_3$) δ 160.6, 137.0, 131.2 (q, J = 5.8 Hz), 129.7 (q, J = 35.1 Hz), 129.5 (2C), 125.6, 122.5 (q, J = 269.9 Hz), 120.4 (2C). **HRMS** (ESI): calcd for C$_{10}$H$_8$F$_3$NONa$^+$ [M+Na]$^+$ 238.0450, found: 238.0447.
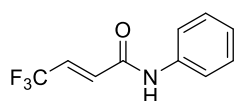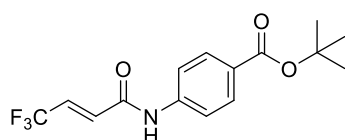
Tert-butyl (E)-4-(4,4,4-trifluorobut-2-enamido)benzoate (**3βH**).

Synthesized according to *General Procedure A* using (*E*)-4,4,4-trifluorobut-2-enoic acid (98 mg, 0.70 mmol, 1.2 eq), *tert*-butyl 4-aminobenzoate (113 mg, 0.59 mmol, 1.0 eq), T3P (870 μl, 1.46 mmol, 2.5 eq), Et$_3$N (163 μl, 1.17 mmol, 2.0 eq) and DCM (3 mL). The reaction was stirred at ambient temperature for 4 h. The crude was purified using heptane/EtOAc to yield **3βH** (118 mg, 0.37 mmol, 64%) as a white solid. ^{1}**H NMR** (400 MHz, CDCl$_3$) δ 8.06 (br s, 1H), 7.99 – 7.93 (m, 2H), 7.64 (d, J = 8.3 Hz, 2H), 6.89 (dq, J = 15.3, 6.5 Hz, 1H),

6.69 (dq, J = 15.3, 1.9 Hz, 1H), 1.59 (s, 9H). **^{13}C NMR** (101 MHz, CDCl$_3$) δ 165.5, 160.8, 140.9, 131.0 (q, J = 5.9 Hz), 130.9 (2C), 130.2 (q, J = 35.3 Hz), 128.6, 122.4 (q, J = 270.0 Hz), 119.4 (2C), 81.5, 28.3 (3C). **HRMS** (ESI): calcd for C$_{15}$H$_{15}$F$_3$NO$_3^-$ [M-H]$^-$ 314.1010, found: 314.1008.
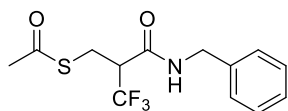
S-(2-(benzylcarbamoyl)-3,3,3-trifluoropropyl) ethanethioate (**4αA**).

Compound 2α (216 mg, 1.00 mmol, 1.0 eq), EDCl (383 mg, 2.00 mmol, 2.0 eq), HOBt (162 mg, 1.20 mmol, 1.2 eq) and *N*-methylmorpholine (121 μl, 1.10 mmol, 1.1 eq) were taken up in DCM (20 mL). The mixture was cooled down to 0 ˚C and benzylamine (120 μl, 1.10 mmol, 1.1 eq) was added. The reaction mixture was stirred at 0 ˚C for 30 min and overnight at ambient temperature. The reaction was quenched with a saturated NaCl$_{(aq)}$ solution and the aqueous layer was extracted three times with EtOAc. The combined organic layers were washed three times with a 5% citric acid$_{(aq)}$ solution, dried over MgSO$_4$, filtered and the solvent was removed under reduced pressure. The crude was purified on an automated flash system equipped with a silica column, using heptane/EtOAc as the eluent, to yield **4αA** (214 mg, 0.70 mmol, 70%) as a white solid. **^{1}H NMR** (400 MHz, CDCl$_3$) δ 7.34 – 7.21 (m, 5H), 6.36 (br s, 1H), 4.44 (d, J = 5.7 Hz, 2H), 3.38 – 3.29 (m, 1H), 3.26 – 3.15 (m, 2H), 2.27 (s, 3H). **^{13}C NMR** (101 MHz, CDCl$_3$) δ 195.8, 164.5 (q, J = 2.4 Hz), 137.4, 128.9 (2C), 127.9, 127.8 (2C), 124.3 (q, J = 281.4 Hz), 51.1 (q, J = 26.4 Hz), 44.2, 30.5, 25.2 (q, J = 2.6 Hz). **HRMS** (ESI): calcd for C$_{13}$H$_{14}$F$_3$NO$_2$SNa$^+$ [M+Na]$^+$ 328.0590, found: 328.0590.
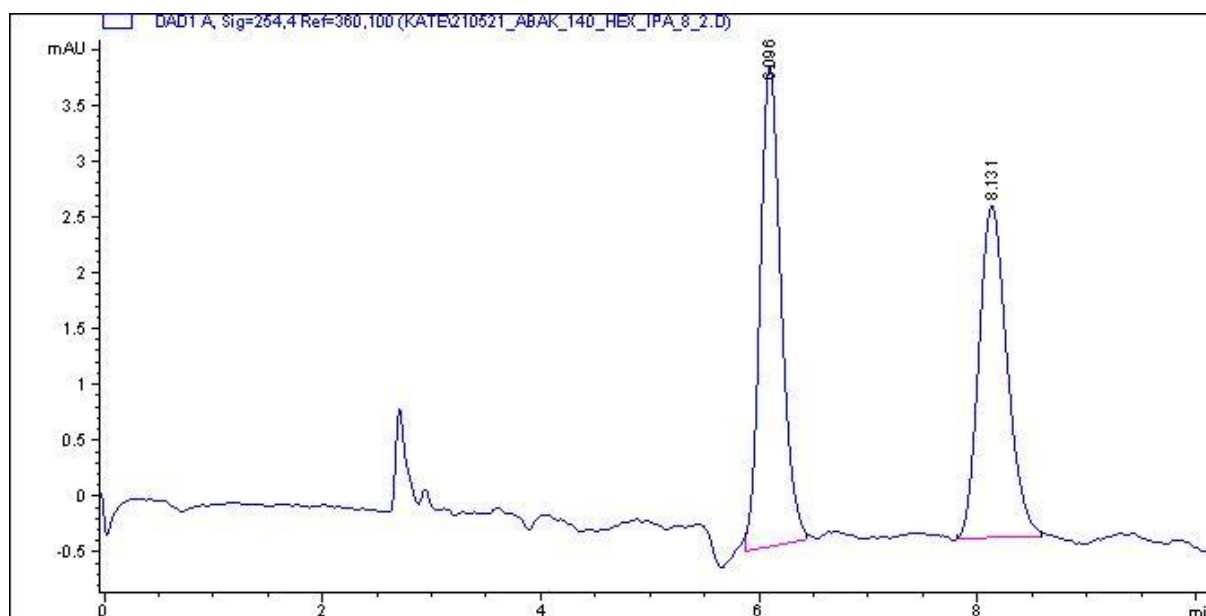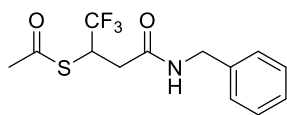
Enantiomer separation

Figure S1. Enantiomers of S-(2-(benzylcarbamoyl)-3,3,3-trifluoropropyl) ethanethioate (**4αA**) were separated using chiral HPLC on a Lux i-Amylose-1 column (5 μm, 1000 Å, ∅ 4.6 mm, L 100 mm) with isocratic Hex/IPA (8:2) as mobile phase at 10 ml/min flow rate and detection at 254 nm wavelength.

S-(4-(benzylamino)-1,1,1-trifluoro-4-oxobutan-2-yl) ethanethioate (**4βA**).

Compound 2β (331 mg, 1.53 mmol, 1.0 eq), EDCl (587 mg, 3.06 mmol, 2.0 eq), HOBt (247 mg, 1.84 mmol, 1.2 eq) and *N*-methylmorpholine (185 μl, 1.69 mmol, 1.1 eq) were taken up in DCM (15 mL). The mixture was cooled down to 0 ˚C and benzylamine (184 μl, 1.68 mmol, 1.1 eq) was added. The reaction mixture was stirred at 0 ˚C for 30 min and overnight at ambient temperature. The reaction was quenched with a saturated $NaCl_{(aq)}$ solution and the aqueous layer was extracted three times with EtOAc. The combined organic layers were washed three times with a 5% citric acid$_{(aq)}$ solution, dried over $MgSO_4$, filtered and the solvent was removed under reduced pressure. The crude was purified on an automated flash system equipped with a silica column, using heptane/EtOAc as the eluent, to yield **4βA** (190 mg, 0.62 mmol, 41%) as a white solid. **¹H NMR** (400 MHz, CDCl$_3$) δ 7.37 – 7.22 (m, 5H), 5.87 (br s, 1H), 4.71 (dqd, *J* = 10.1, 8.7, 4.4 Hz, 1H), 4.44 (d, *J* = 5.7 Hz, 2H), 2.90 (dd, *J* = 15.4, 4.5 Hz, 1H), 2.51 (dd, *J* = 15.4, 10.0 Hz, 1H), 2.36 (s, 3H). **¹³C NMR** (101 MHz, CDCl$_3$) δ 191.2, 167.3, 137.8, 128.9 (2C), 128.0 (2C), 127.9, 125.8 (q, *J* = 278.3 Hz), 44.1, 42.0 (q, *J* = 31.1 Hz), 35.4 (d, *J* = 1.7 Hz), 30.3. **HRMS** (ESI): calcd for $C_{13}H_{14}F_3NO_2SNa^+$ [M+Na]$^+$ 328.0590, found: 328.0589.
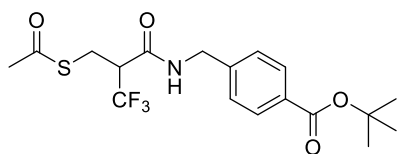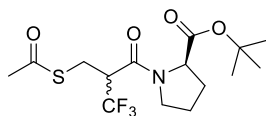
Tert-butyl 4-((2-((acetylthio)methyl)-3,3,3-trifluoropropanamido)methyl)benzoate (**4αB**).

Compound 2α (120 mg, 0.56 mmol, 1.0 eq), EDCl (213 mg, 1.11 mmol, 2.0 eq), HOBt (90 mg, 0.67 mmol, 1.2 eq) and *N*-methylmorpholine (67 μl, 0.61 mmol, 1.1 eq) were taken up in DCM (10 mL). The mixture was cooled down to 0 ˚C and *tert*-butyl 4-(aminomethyl)benzoate (127 mg, 0.61 mmol, 1.1 eq) was added. The reaction mixture was stirred at 0 ˚C for 30 min and overnight at ambient temperature. The reaction was quenched with a saturated $NaCl_{(aq)}$ solution and the aqueous layer was extracted three times with EtOAc. The combined organic layers were washed three times with a 5% citric acid$_{(aq)}$ solution, dried over $MgSO_4$, filtered and the solvent was removed under reduced pressure. The crude was purified on an automated flash system equipped with a silica column, using heptane/EtOAc as the eluent, to yield **4αB** (70 mg, 0.17 mmol, 31%) as a white solid. **¹H NMR** (400 MHz, CDCl$_3$) δ 7.94 – 7.81 (m, 2H), 7.31 – 7.20 (m, 2H), 6.79 (t, *J* = 5.9 Hz, 1H), 4.47 (d, *J* = 5.8 Hz, 2H), 3.35 (dd, *J* = 12.5, 3.5 Hz, 1H), 3.32 – 3.24 (m, 1H), 3.20 (dd, *J* = 12.5, 9.7 Hz, 1H), 2.28 (s, 3H), 1.57 (s, 9H). **¹³C NMR** (101 MHz, CDCl$_3$) δ 195.6, 165.7, 164.9 (q, *J* = 2.4 Hz), 142.1, 131.4, 129.9 (2C), 127.4 (2C), 124.3 (q, *J* = 281.4 Hz), 81.4, 51.1 (q, *J* = 26.4 Hz), 43.7, 30.5, 28.3 (3C), 25.2 (q, *J* = 2.8 Hz). **HRMS** (ESI): calcd for $C_{18}H_{22}F_3NO_4SNa^+$ [M+Na]$^+$ 428.1114, found: 428.1114.
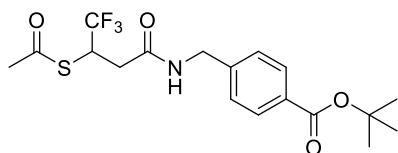
Tert-butyl 4-((3-(acetylthio)-4,4,4-trifluorobutanamido)methyl)benzoate (**4βB**).

Synthesized according to *General Procedure C* using **3βB** (130 mg, 0.40 mmol, 1.0 eq), thioacetic acid (56 µl, 0.79 mmol, 2.0 eq) and THF (4 mL). The reaction was stirred at 60 ˚C for 60 h. The crude was purified using heptane/EtOAc to yield **4βB** (133 mg, 0.33 mmol, 83%) as a white solid. **^{1}H NMR** (400 MHz, CDCl$_3$) δ 7.96 – 7.75 (m, 2H), 7.27 – 7.21 (m, 2H), 6.67 – 6.56 (m, 1H), 4.76 – 4.58 (m, 1H), 4.51 – 4.31 (m, 2H), 2.88 (dd, *J* = 15.4, 4.6 Hz, 1H), 2.61 – 2.47 (m, 1H), 2.33 (s, 3H), 1.56 (s, 9H). **^{13}C NMR** (101 MHz, CDCl$_3$) δ 191.2, 167.8, 165.7, 142.6, 131.3, 129.8 (2C), 127.4 (2C), 125.7 (q, *J* = 278.4 Hz), 81.3, 43.5, 41.9 (q, *J* = 31.0 Hz), 35.2, 30.2, 28.2 (3C). **HRMS** (ESI): calcd for C$_{18}$H$_{22}$F$_3$NO$_4$SNa$^+$ [M+Na]$^+$ 428.1114, found: 428.1114.

Tert-butyl ((R)/(S)-2-((acetylthio)methyl)-3,3,3-trifluoropropanoyl)-D-prolinate (**4αC**).[4]**
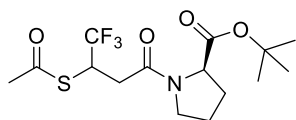
Synthesized according to *General Procedure C* using **3αC** (210 mg, 0.72 mmol, 1.0 eq), thioacetic acid (101 µl, 1.43 mmol, 2.0 eq) and THF (5 mL). The reaction was stirred at ambient temperature overnight. The crude was purified using heptane/EtOAc to give the corresponding diastereomers (2*R*,2`*R*)-**4αC** (163 mg, 0.44 mmol, 62%) and (2*R*,2`*S*)-**4αC** (50 mg, 0.14 mmol, 19%) in 81% total yield.

(2*R*,2`*R*)-**4αC**: White solid; [α]$_D^{20}$ –51.4º (*c* 1.05, CHCl$_3$); **^{1}H NMR** (400 MHz, CDCl$_3$) (a 7:1 mixture of rotamers*) δ 4.41 – 4.33 (m, 1H), 3.69 – 3.50 (m, 3H), 3.41 – 3.20 (m, 2H), 2.34 (s, 3H) [2.35], 2.22 – 1.91 (m, 4H), 1.45 (s, 9H) [1.43]. **^{13}C NMR** (101 MHz, CDCl$_3$) δ 195.7 [195.1], 170.7 [170.4], 163.7 [164.5] (q, *J* = 2.3 Hz), 124.4 (q, *J* = 281.7 Hz), 81.5 [82.9], 60.3 [60.7], 47.8 (q, *J* = 26.2 Hz), 47.8 [47.0], 30.7 [30.6], 29.3 [31.4], 28.1 [27.8] (3C), 25.8 [26.5] (q, *J* = 2.6 Hz), 24.6 [22.5]. **HRMS** (ESI): calcd for C$_{15}$H$_{22}$F$_3$NO$_4$SNa$^+$ [M+Na]$^+$ 392.1114, found: 392.1111.

(2*R*,2`*S*)-**4αC**: Colourless oil; [α]$_D^{20}$ +192.8º (*c* 1.11, CHCl$_3$); **^{1}H NMR** (400 MHz, CDCl$_3$) (a 4:1 mixture of rotamers*) δ 4.39 (dd, *J* = 8.3, 3.8 Hz, 1H), 3.73 – 3.64 (m, 1H), 3.63 – 3.53 (m, 1H), 3.52 – 3.20 (m, 3H), 2.33 (s, 3H) [2.31], 2.25 – 1.81 (m, 4H), 1.41 (s, 9H) [1.45]. **^{13}C NMR** (101 MHz, CDCl$_3$) δ 195.7, 170.5 [170.6], 163.5 [163.6] (q, *J* = 2.5 Hz), 124.4 (q, *J* = 282.0 Hz), 81.7 [82.7], 60.5 [60.0], 47.9 (q, *J* = 26.3 Hz), 47.8 [47.1], 30.7 [30.5], 29.3 [31.6], 27.9 [28.1] (3C), 25.8 [25.6] (q, *J* = 2.8 Hz), 24.9 [22.2]. **HRMS** (ESI): calcd for C$_{15}$H$_{22}$F$_3$NO$_4$SNa$^+$ [M+Na]$^+$ 392.1114, found: 392.1110.

** Stereochemistry determined based on the X-ray crystal structure and analytical data published in [4].

* Chemical shifts of minor rotamer are enclosed in square brackets.

Tert-butyl (3-(acetylthio)-4,4,4-trifluorobutanoyl)-D-prolinate (**4βC**).

Synthesized according to *General Procedure C* using **3βC** (190 mg, 0.65 mmol, 1.0 eq), thioacetic acid (91 µl, 1.30 mmol, 2.0 eq) and THF (5 mL). The reaction was stirred at 60 ˚C for 60 h. The crude was purified using heptane/EtOAc to yield **4βC** (160 mg, 0.43 mmol, 67%) as a colourless oil. The title compound was obtained as a diastereomeric mixture, with each diastereomer being present as two rotamers.

NMR data is reported for the mixture of four isomers and, where possible, chemical shifts are reported separately for the diastereomers, of which the shifts of the minor rotamers can be found in square brackets. In the case of ^{13}C NMR semicolons are used to indicate chemical shifts belonging to the same carbon in the different isomers. **^{1}H NMR** (400 MHz, CDCl$_3$) (a 2:1 mixture of rotamers of each diastereomer) δ 4.86 – 4.68 (m, 1H), 4.40, 4.35 (dd, *J* = 8.4, 3.5 Hz, 1H) [4.23 – 4.15 (m)], 3.68 – 3.39 (m, 2H), 2.94 – 2.45 (m, 2H), 2.35 (s, 3H) [2.36, 2.35], 2.28 – 1.82 (m, 4H), 1.42 (s, 9H) [1.47, 1.44]. **^{13}C NMR** (101 MHz, CDCl$_3$) δ 191.0, 190.9 [191.1, 190.85]; 171.2, 171.1 [171.05, 170.9]; 166.1 [166.5, 166.3]; 126.0 (q, *J* = 278.3 Hz); 81.6, 81.4 [82.8, 82.7]; 59.9, 59.7 [60.3, 60.1]; 47.2, 47.1 [46.9, 46.8]; 41.5, 41.2 [41.4, 41.2] (q, *J* = 30.8 Hz); 33.4, 32.9 [33.0, 32.9]; 30.2 [30.15]; 29.2 [31.5, 31.45]; 28.05, 28.0 [27.9] (3C); 24.7, 24.5 [22.65, 22.6]. **HRMS** (ESI): calcd for C$_{15}$H$_{22}$F$_3$NO$_4$SNa$^+$ [M+Na]$^+$ 392.1114, found: 392.1111.
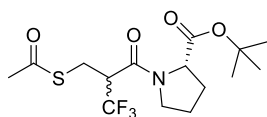
Tert-butyl ((S)/(R)-2-((acetylthio)methyl)-3,3,3-trifluoropropanoyl)-L-prolinate (**4αD**).[4]**

Synthesized according to *General Procedure C* using **3αD** (170 mg, 0.58 mmol, 1.0 eq), thioacetic acid (82 µl, 1.16 mmol, 2.0 eq) and THF (4 mL). The reaction was stirred at ambient temperature overnight. The crude was purified using heptane/EtOAc to give the corresponding diastereomers (2*S*,2`*S*)-**4αD** (121 mg, 0.33 mmol, 57%) and (2*S*,2`*R*)-**4αD** (44 mg, 0.12 mmol, 20%) in 77% total yield.

(2*S*,2`*S*)-**4αD**: White solid; [α]$_D^{20}$ +59.4° (*c* 1.15, CHCl$_3$); **^{1}H NMR** (400 MHz, CDCl$_3$) (a 7:1 mixture of rotamers*) δ 4.41 – 4.34 (m, 1H), 3.70 – 3.51 (m, 3H), 3.41 – 3.20 (m, 2H), 2.35 (s, 3H), 2.22 – 1.91 (m, 4H), 1.45 (s, 9H) [1.43]. **^{13}C NMR** (101 MHz, CDCl$_3$) δ 195.7 [195.2], 170.7 [170.4], 163.7 [164.5] (q, *J* = 2.5 Hz), 124.4 (q, *J* = 281.8 Hz), 81.5 [82.9], 60.3 [60.8], 47.8 (q, *J* = 26.1 Hz), 47.8 [47.0], 30.7 [30.6], 29.3 [31.4], 28.1 [27.8] (3C), 25.8 [26.5] (q, *J* = 2.6 Hz), 24.6 [22.5]. **HRMS** (ESI): calcd for C$_{15}$H$_{22}$F$_3$NO$_4$SNa$^+$ [M+Na]$^+$ 392.1114, found: 392.1113.

(2*S*,2`*R*)-**4αD**: Colourless oil; [α]$_D^{20}$ –270° (*c* 1.00, CHCl$_3$); **^{1}H NMR** (400 MHz, CDCl$_3$) (a 4:1 mixture of rotamers*) δ 4.40 (dd, *J* = 8.3, 3.8 Hz, 1H), 3.74 – 3.65 (m, 1H), 3.64 – 3.53 (m, 1H), 3.52 – 3.20 (m,

---

** Stereochemistry determined based on the X-ray crystal structure and analytical data published in [4].

* Chemical shifts of minor rotamer are enclosed in square brackets.

3H), 2.34 (s, 3H) [2.31], 2.25 – 1.80 (m, 4H), 1.42 (s, 9H) [1.45]. **^{13}C NMR** (101 MHz, CDCl$_3$) δ 195.8, 170.5 [170.6], 163.5 [163.7] (q, J = 2.3 Hz), 124.4 (q, J = 282.0 Hz), 81.7 [82.7], 60.5 [60.0], 47.9 (q, J = 26.3 Hz), 47.8 [47.2], 30.7 [30.5], 29.3 [31.6], 27.9 [28.1] (3C), 25.8 [25.6] (q, J = 2.8 Hz), 24.9 [22.2]. **HRMS** (ESI): calcd for C$_{15}$H$_{22}$F$_3$NO$_4$SNa$^+$ [M+Na]$^+$ 392.1114, found: 392.1113.
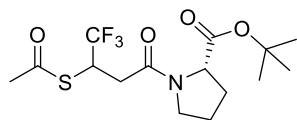

Tert-butyl (3-(acetylthio)-4,4,4-trifluorobutanoyl)-L-prolinate (**4βD**).

Synthesized according to *General Procedure C* using **3βD** (135 mg, 0.46 mmol, 1.0 eq), thioacetic acid (65 μl, 0.92 mmol, 2.0 eq) and THF (5 mL). The reaction was stirred at 60 °C for 60 h. The crude was purified using heptane/EtOAc to yield **4βD** (131 mg, 0.36 mmol, 77%) as a colourless oil. The title compound was obtained as a diastereomeric mixture, with each diastereomer being present as two rotamers.

NMR data is reported for the mixture of four isomers and, where possible, chemical shifts are reported separately for the diastereomers, of which the shifts of the minor rotamers can be found in square brackets. In the case of ^{13}C NMR the semicolons are used to indicate chemical shifts belonging to the same carbon in the different isomers. **^{1}H NMR** (400 MHz, CDCl$_3$) (a 2.5:1 mixture of rotamers of each diastereomer) δ 4.86 – 4.70 (m, 1H), 4.41, 4.37 (dd, J = 8.5, 3.6 Hz, 1H) [4.24 – 4.17 (m)], 3.68 – 3.42 (m, 2H), 2.95 – 2.46 (m, 2H), 2.37, 2.36 (s, 3H) [2.38, 2.37], 2.30 – 1.85 (m, 4H), 1.43 (s, 9H) [1.48, 1.45]. **^{13}C NMR** (101 MHz, CDCl$_3$) δ 191.0, 190.95 [191.2, 190.9]; 171.2, 171.15 [171.1, 171.0]; 166.2, 166.1 [166.5, 166.4]; 126.0 (q, J = 278.0 Hz); 81.6, 81.4 [82.85, 82.8]; 60.0, 59.7 [60.4, 60.1]; 47.2, 47.15 [46.9, 46.8]; 41.5, 41.3 [41.4, 41.3] (q, J = 30.8 Hz); 33.4, 33.0 [33.1, 33.0]; 30.3 [30.2]; 29.3, 29.25 [31.6, 31.5]; 28.1, 28.0 [28.0] (3C); 24.7, 24.6 [22.7, 22.6]. **HRMS** (ESI): calcd for C$_{15}$H$_{22}$F$_3$NO$_4$SNa$^+$ [M+Na]$^+$ 392.1114, found: 392.1110.
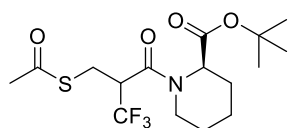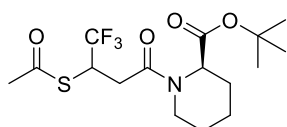

Tert-butyl (2R)-1-(2-((acetylthio)methyl)-3,3,3-trifluoropropanoyl)piperidine-2-carboxylate (**4αE**).

Synthesized according to *General Procedure C* using **3αE** (350 mg, 1.14 mmol, 1.0 eq), thioacetic acid (161 μl, 2.28 mmol, 2.0 eq) and THF (5 mL). The reaction was stirred at ambient temperature overnight. The crude was purified using heptane/EtOAc to yield **4αE** (383 mg, 1.00 mmol, 88%) as a colourless oil. The title compound was obtained as a diastereomeric mixture, with each diastereomer being present as two rotamers.

NMR data is reported for the mixture of four isomers and, where possible, chemical shifts are reported separately for the diastereomers, of which the shifts of the minor rotamers can be found in square brackets. In the case of ^{13}C NMR the semicolons are used to indicate chemical shifts belonging to the same carbon in the different isomers. **^{1}H NMR** (400 MHz, CDCl$_3$) (a 3.5:1 mixture of rotamers of each diastereomer) δ 5.27 – 5.15 (m, 1H) [4.44 – 4.36], 3.87 – 3.73 (m, 1H), 3.72 – 3.61 (m, 1H) [4.55 –

4.45], 3.38 – 2.58 (m, 3H), 2.29 – 2.12 (m, 4H), 1.72 – 1.56 (m, 2H), 1.55 – 1.20 (m, 12H). **^{13}C NMR** (101 MHz, CDCl$_3$) δ 195.5, 195.4 [195.8, 195.5]; 169.4, 169.3 [168.9, 168.7]; 164.6, 164.5 [164.7, 164.4] (q, J = 2.4 Hz); 124.2, 124.15 [124.1] (q, J = 281.9 Hz); 81.8, 81.7 [82.5, 82.45]; 53.1 [57.2, 57.0]; 44.9 [44.8] (q, J = 26.3 Hz); 44.4, 44.2 [40.1, 40.0]; 30.3 [30.4, 30.3]; 28.0, 27.8 [27.8] (3C); 26.65, 26.6 [27.7, 27.3]; 26.0, 25.9 (q, J = 2.6 Hz); 25.6, 25.1 [24.8, 24.5]; 20.7, 20.6 [20.7, 20.55]. **HRMS** (ESI): calcd for C$_{16}$H$_{24}$F$_3$NO$_4$SNa$^+$ [M+Na]$^+$ 406.1270, found: 406.1270.

Tert-butyl (2R)-1-(3-(acetylthio)-4,4,4-trifluorobutanoyl)piperidine-2-carboxylate (**4βE**).

Synthesized according to *General Procedure C* using **3βE** (420 mg, 1.37 mmol, 1.0 eq), thioacetic acid (193 μl, 2.73 mmol, 2.0 eq) and THF (5 mL). The reaction was stirred at 60 ˚C for 60 h. The crude was purified using heptane/EtOAc to yield **4βE** (443 mg, 1.16 mmol, 85%) as a colourless oil. The title compound was obtained as a diastereomeric mixture, with each diastereomer being present as two rotamers.

NMR data is reported for the mixture of four isomers and, where possible, chemical shifts are reported separately for the diastereomers, of which the shifts of the minor rotamers can be found in square brackets. In the case of ^{13}C NMR the semicolons are used to indicate chemical shifts belonging to the same carbon in the different isomers. **^{1}H NMR** (400 MHz, CDCl$_3$) (a 3:1 mixture of rotamers of each diastereomer) δ 5.27 – 5.15 (m, 1H) [4.35 – 4.27], 4.88 – 4.71 (m, 1H), 3.69 – 3.56 (m, 1H) [4.55 – 4.45], 3.36 – 2.51 (m, 3H), 2.38, 2.37 (s, 3H) [2.38], 2.31 – 2.16 (m, 1H), 1.78 – 1.65 (m, 2H), 1.64 – 1.23 (m, 12H). **^{13}C NMR** (101 MHz, CDCl$_3$) δ 191.4, 191.15 [191.3, 191.1]; 170.2, 170.1 [169.5, 169.4]; 167.7, 167.5 [167.8, 167.4]; 126.1 (q, J = 277.8 Hz); 81.8, 81.75 [82.9, 82.8]; 53.1, 53.0 [56.6, 56.5]; 43.5, 43.3 [40.2, 40.0]; 41.7, 41.5 [41.5] (q, J = 30.6 Hz); 32.1, 32.0 [31.95, 31.8]; 30.3 [30.25]; 28.2 [28.15, 28.1] (3C); 26.9 [27.2, 27.0]; 25.5, 25.3 [24.6]; 20.9, 20.85 [20.75, 20.7]. **HRMS** (ESI): calcd for C$_{16}$H$_{24}$F$_3$NO$_4$SNa$^+$ [M+Na]$^+$ 406.1270, found: 406.1271. **IR** (v_{max}/cm^{-1}, neat): 2974, 2942, 2865, 1717, 1655, 1447, 1370, 1249, 1154, 1104, 1020, 962.
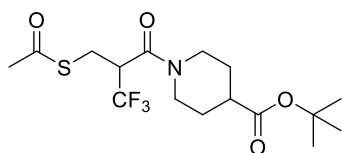
*Tert-butyl 1-(2-((acetylthio)methyl)-3,3,3-trifluoropropanoyl)piperidine-4-carboxylate* (**4αF**).

Synthesized according to *General Procedure C* using **3αF** (120 mg, 0.39 mmol, 1.0 eq), thioacetic acid (55 μl, 0.78 mmol, 2.0 eq) and THF (2 mL). The reaction was stirred at ambient temperature overnight. The crude was purified using heptane/EtOAc to yield **4αF** (96 mg, 0.25 mmol, 64%) as a colourless oil. **^{1}H NMR** (400 MHz, CDCl$_3$)

(a 1.2:1 mixture of rotamers*) δ 4.41 – 4.27 (m, 1H), 3.85 – 3.67 (m, 2H), 3.39 – 3.31 (m, 1H), 3.27 – 3.07 (m, 2H), 2.98 – 2.82 (m, 1H), 2.49 – 2.36 (m, 1H), 2.30 (s, 3H) [2.28], 1.93 – 1.79 (m, 2H), 1.68 – 1.47 (m, 2H), 1.39 (s, 9H). ^{13}C NMR (101 MHz, CDCl$_3$) δ 195.8 [195.6], 173.3 [173.1], 163.3 (app qnt, two quartets of rotamers overlapping), 124.2 (q, J = 281.7 Hz), 80.75 [80.8], 45.8 [45.7], 44.9 [45.0] (q, J = 26.3 Hz), 42.1 [42.0], 41.55 [41.5], 30.55 [30.5], 28.6 [28.4], 28.2 [27.9], 28.0 (3C), 26.2 – 26.1 (app m, two quartets of rotamers overlapping). **HRMS** (ESI): calcd for C$_{16}$H$_{24}$F$_3$NO$_4$SNa$^+$ [M+Na]$^+$ 406.1270, found: 406.1270.
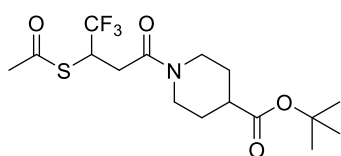
*Tert-butyl 1-(3-(acetylthio)-4,4,4-trifluorobutanoyl)piperidine-4-carboxylate* (**4βF**).

Synthesized according to *General Procedure C* using **3βF** (140 mg, 0.46 mmol, 1.0 eq), thioacetic acid (64 μl, 0.91 mmol, 2.0 eq) and THF (3 mL). The reaction was stirred at 60 ˚C for 60 h. The crude was purified using heptane/EtOAc to yield **4βF** (120 mg, 0.31 mmol, 69%) as a colourless oil. ^{1}H NMR (400 MHz, CDCl$_3$) (a 1.1:1 mixture of rotamers*) δ 4.75 (qntd, J = 9.2, 3.8 Hz, 1H), 4.36 – 4.25 (m, 1H), 3.75 – 3.64 (m, 1H), 3.16 – 3.03 (m, 1H), 2.89 – 2.77 (m, 2H), 2.76 – 2.66 (m, 1H), 2.46 – 2.37 (m, 1H), 2.35 (s, 3H) [2.34], 1.93 – 1.81 (m, 2H), 1.68 – 1.50 (m, 2H), 1.40 (s, 9H) [1.41]. ^{13}C NMR (101 MHz, CDCl$_3$) δ 191.1 [191.05], 173.4 [173.3], 165.8 [165.75], 126.0 (q, J = 278.1 Hz), 80.8, 44.9, 41.65 [41.7], 41.6 (q, J = 30.6 Hz), 41.5 [41.6], 31.75 [31.7], 30.2, 28.45 [28.4], 28.1 (3C), 27.9 [27.85]. **HRMS** (ESI): calcd for C$_{16}$H$_{24}$F$_3$NO$_4$SNa$^+$ [M+Na]$^+$ 406.1270, found: 406.1269.
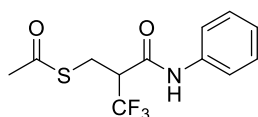
*S-(3,3,3-trifluoro-2-(phenylcarbamoyl)propyl) ethanethioate* (**4αG**).

Synthesized according to *General Procedure C* using **3αG** (145 mg, 0.67 mmol, 1.0 eq), thioacetic acid (95 μl, 1.35 mmol, 2.0 eq) and THF (3 mL). The reaction was stirred at ambient temperature overnight. The crude was purified using heptane/EtOAc to yield **4αG** (174 mg, 0.60 mmol, 89%) as a white solid. ^{1}H NMR (400 MHz, CDCl$_3$) δ 7.79 (br s, 1H), 7.56 – 7.50 (m, 2H), 7.37 – 7.30 (m, 2H), 7.20 – 7.13 (m, 1H), 3.48 – 3.29 (m, 3H), 2.36 (s, 3H). ^{13}C NMR (101 MHz, CDCl$_3$) δ 196.5, 162.7 (q, J = 2.7 Hz), 137.1, 129.3 (2C), 125.4, 124.3 (q, J = 281.6 Hz), 120.3 (2C), 52.1 (q, J = 26.4 Hz), 30.7, 25.5 (q, J = 2.8 Hz). **HRMS** (ESI): calcd for C$_{12}$H$_{13}$F$_3$NO$_2$S$^+$ [M+H]$^+$ 292.0614, found: 292.0612.

* Chemical shifts of minor rotamer are enclosed in square brackets.
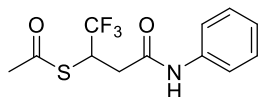
S-(1,1,1-trifluoro-4-oxo-4-(phenylamino)butan-2-yl) ethanethioate (**4βG**).

Synthesized according to *General Procedure C* using **3βG** (80 mg, 0.37 mmol, 1.0 eq), thioacetic acid (52 μl, 0.74 mmol, 2.0 eq) and THF (2 mL). The reaction was stirred at 60 °C for 60 h. The crude was purified using heptane/EtOAc to yield **4βG** (93 mg, 0.32 mmol, 86%) as a white solid. **^{1}H NMR** (400 MHz, CDCl$_3$) δ 8.03 (br s, 1H), 7.51 – 7.42 (m, 2H), 7.33 – 7.23 (m, 2H), 7.14 – 7.07 (m, 1H), 4.77 (dqd, *J* = 10.0, 8.8, 4.4 Hz, 1H), 3.02 (dd, *J* = 15.8, 4.4 Hz, 1H), 2.76 – 2.65 (m, 1H), 2.34 (s, 3H). **^{13}C NMR** (101 MHz, CDCl$_3$) δ 191.5, 166.2, 137.4, 129.1 (2C), 125.8 (q, *J* = 278.3 Hz), 125.0, 120.5 (2C), 41.8 (q, *J* = 31.0 Hz), 36.0, 30.2. **HRMS** (ESI): calcd for C$_{12}$H$_{12}$F$_3$NO$_2$SNa$^+$ [M+Na]$^+$ 314.0433, found: 314.0431.
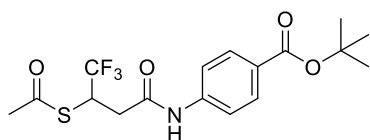
*Tert-butyl 4-(3-(acetylthio)-4,4,4-trifluorobutanamido)benzoate* (**4βH**).

Synthesized according to *General Procedure C* using **3βH** (195 mg, 0.62 mmol, 1.0 eq), thioacetic acid (87 μl, 1.24 mmol, 2.0 eq) and THF (5 mL). The reaction was stirred at 60 °C for 60 h. The crude was purified using heptane/EtOAc to yield **4βH** (176 mg, 0.45 mmol, 73%) as a white solid. **^{1}H NMR** (400 MHz, CDCl$_3$) δ 7.97 – 7.88 (m, 2H), 7.81 (br s, 1H), 7.55 (d, *J* = 8.6 Hz, 2H), 4.84 – 4.69 (m, 1H), 3.08 (dd, *J* = 15.9, 4.4 Hz, 1H), 2.72 (dd, *J* = 15.9, 9.9 Hz, 1H), 2.38 (s, 3H), 1.58 (s, 9H). **^{13}C NMR** (101 MHz, CDCl$_3$) δ 191.4, 166.0, 165.5, 141.2, 130.8 (2C), 128.1, 125.7 (q, *J* = 278.3 Hz), 119.1 (2C), 81.3, 41.7 (q, *J* = 31.2 Hz), 36.5, 30.3, 28.3 (3C). **HRMS** (ESI): calcd for C$_{17}$H$_{20}$F$_3$NO$_4$SNa$^+$ [M+Na]$^+$ 414.0957, found: 414.0957.
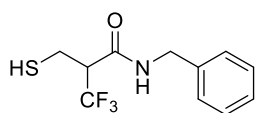
N-benzyl-3,3,3-trifluoro-2-(mercaptomethyl)propanamide (**5αA**).

Synthesized according to *General Procedure D* using **4αA** (135 mg, 0.44 mmol, 1.0 eq), sodium thiomethoxide (62 mg, 0.88 mmol, 2.0 eq) and MeOH (4 mL). The crude was purified using H$_2$O/MeCN (0.1% TFA) to yield **5αA** (56 mg, 0.21 mmol, 48%) as a white solid. **^{1}H NMR** (400 MHz, Acetone-*d6*) δ 8.12 (br s, 1H), 7.38 – 7.22 (m, 5H), 4.53, 4.49 (ABdq, *J* = 15.0, 5.9 Hz, 2H), 3.55 – 3.41 (m, 1H), 3.15 – 3.02 (m, 1H), 2.92 – 2.84 (m, 1H). **^{13}C NMR** (101 MHz, Acetone-*d6*) δ 165.2 (q, *J* = 2.7 Hz), 139.7, 129.9 (2C), 128.5 (2C), 128.1, 125.7 (q, *J* = 280.8 Hz), 55.1 (q, *J* = 25.1 Hz), 44.1, 20.9 (q, *J* = 2.9 Hz). **HRMS** (ESI): calcd for C$_{11}$H$_{11}$F$_3$NOS$^-$ [M-H]$^-$ 262.0519, found: 262.0517. **M.p.:** 130 – 133 °C. Purity: >99% (UV 214 nm). (+)-**5αA**: [α]$_D^{20}$ +24.1° (*c* 0.3, CHCl$_3$); (−)-**5αA**: [α]$_D^{20}$ –21.0° (*c* 0.28, CHCl$_3$).

N-benzyl-4,4,4-trifluoro-3-mercaptobutanamide (**5βA**).
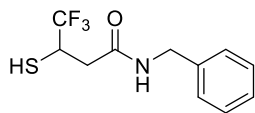
Synthesized according to *General Procedure D* using **4βA** (190 mg, 0.62 mmol, 1.0 eq), sodium thiomethoxide (87 mg, 1.25 mmol, 2.0 eq) and MeOH (5 mL). The crude was purified using H_2O/MeCN (0.1% TFA) to yield **5βA** (116 mg, 0.44 mmol, 71%) as a white solid. **^{1}H NMR** (400 MHz, Acetone-*d6*) δ 7.75 (br s, 1H), 7.36 – 7.20 (m, 5H), 4.47, 4.42 (ABdq, J = 15.1, 5.9 Hz, 2H), 4.07 – 3.93 (m, 1H), 2.93 (dd, J = 15.2, 4.0 Hz, 1H), 2.74 (d, J = 8.9 Hz, 1H), 2.59 (dd, J = 15.2, 9.9 Hz, 1H). **^{13}C NMR** (101 MHz, Acetone-*d6*) δ 168.5, 140.1, 129.3 (2C), 128.4 (2C), 127.9, 127.6 (q, J = 275.5 Hz), 43.8, 39.1 (q, J = 31.1 Hz), 38.9 (d, J = 1.9 Hz). **HRMS** (ESI): calcd for $C_{11}H_{11}F_3NOS^-$ [M-H]$^-$ 262.0519, found: 262.0518. **M.p.:** 103 – 105 ˚C. Purity: >99% (UV 214 nm).

4-((3,3,3-trifluoro-2-(mercaptomethyl)propanamido)methyl)benzoic acid (**5αB**).
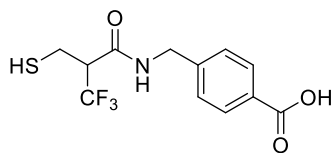
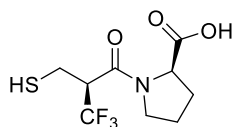Synthesized according to *General Procedure E* using **4αB** (54 mg, 0.13 mmol, 1.0 eq), TFA (102 μl, 1.33 mmol, 10 eq) and NH_4OH (806 μl, 13.32 mmol, 100 eq). Upon addition of 2 M HCl, the title compound precipitated and was collected via filtration to yield **5αB** (8 mg, 0.03 mmol, 20%) as a white solid. **^{1}H NMR** (400 MHz, Methanol-*d4*) δ 8.10 – 7.99 (m, 2H), 7.48 – 7.33 (m, 2H), 4.58, 4.48 (ABq, J = 15.7 Hz, 2H), 4.28 – 4.15 (m, 1H), 3.51 (t, J = 6.0 Hz, 1H), 3.34 (dd, J = 6.4, 2.6 Hz, 1H). **^{13}C NMR** (101 MHz, Methanol-*d4*) δ 169.3, 162.5 (q, J = 4.4 Hz), 141.6, 131.7, 131.4 (2C), 129.1 (2C), 125.6 (q, J = 275.3 Hz), 53.2 (q, J = 30.8 Hz), 46.8, 41.1 (q, J = 3.4 Hz). **HRMS** (ESI): calcd for $C_{12}H_{11}F_3NO_3S^-$ [M-H]$^-$ 306.0417, found: 306.0416. **M.p.:** 161 – 163 ˚C. Purity: >99% (UV 214 nm).

4-((4,4,4-trifluoro-3-mercaptobutanamido)methyl)benzoic acid (**5βB**).
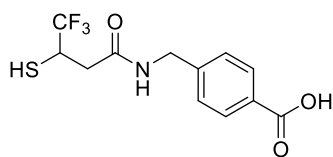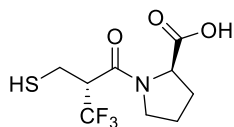
Synthesized according to *General Procedure E* using **4βB** (130 mg, 0.32 mmol, 1.0 eq), TFA (246 μl, 3.21 mmol, 10 eq), DCM (5 mL) and NH_4OH (1.94 mL, 32.1 mmol, 100 eq). Upon addition of a 2 M aqueous HCl solution, the title compound precipitated and was collected via filtration to yield **5βB** (93 mg, 0.30 mmol, 95%) as a white solid. **^{1}H NMR** (400 MHz, Methanol-*d4*) δ 8.09 – 7.87 (m, 2H), 7.48 – 7.34 (m, 2H), 4.52, 4.43 (ABq, J = 15.5 Hz, 2H), 3.98 – 3.78 (m, 1H), 2.92 (dd, J = 14.9, 4.2 Hz, 1H), 2.53 (dd, J = 14.9, 10.3 Hz, 1H). **^{13}C NMR** (101 MHz, Methanol-*d4*) δ 170.9, 169.6, 145.0, 131.0 (2C), 130.8, 128.5 (2C), 127.6 (q, J = 276.2 Hz), 44.0, 39.4 (q, J = 31.5 Hz), 39.2. **HRMS** (ESI): calcd for $C_{12}H_{11}F_3NO_3S^-$ [M-H]$^-$ 306.0417, found: 306.0414. **M.p.:** 204 – 206 ˚C. Purity: >96% (UV 214 nm).

((S)-3,3,3-trifluoro-2-(mercaptomethyl)propanoyl)-D-proline ((2R,2`S)-**5αC**).

Synthesized according to *General Procedure E* using (2R,2`S)-**4αC** (50 mg, 0.14 mmol, 1.0 eq), TFA (104 μl, 1.35 mmol, 10 eq), DCM (5 mL) and NH₄OH (819 μl, 13.5 mmol, 100 eq). The crude was purified using $H_2O$/MeCN (0.1% TFA) to yield (2R,2`S)-**5αC** (30 mg, 0.11 mmol, 82%) as a colourless oil that solidified after standing for several days. **¹H NMR** (400 MHz, Methanol-*d4*) (an 8:1 mixture of rotamers*) δ 4.51 (dd, *J* = 8.5, 3.4 Hz, 1H) [4.67 (dd, *J* = 6.6, 3.8 Hz)], 3.95 – 3.49 (m, 3H), 3.09 – 2.93 (m, 1H), 2.92 – 2.82 (m, 1H), 2.37 – 1.88 (m, 4H). **¹³C NMR** (101 MHz, Methanol-*d4*) δ 174.7 [174.6], 166.2 (q, *J* = 2.5 Hz), 125.6 (q, *J* = 281.3 Hz), 60.7 [61.3], 52.5 [52.9] (q, *J* = 25.7 Hz), 49.2 [48.1], 30.4 [31.9], 25.6 [23.3], 21.3 (q, *J* = 2.8 Hz). **HRMS** (ESI): calcd for $C_9H_{13}F_3NO_3S^+$ [M+H]⁺ 272.0563, found: 272.0561. **M.p.:** 122 – 124 ˚C. Purity: >99% (UV 214 nm). **[α]$_D^{20}$**: +133.7° (*c* 1.0, CHCl₃).

((R)-3,3,3-trifluoro-2-(mercaptomethyl)propanoyl)-D-proline ((2R,2`R)-**5αC**).

Synthesized according to *General Procedure E* using (2R,2`R)-**4αC** (162 mg, 0.44 mmol, 1.0 eq), TFA (337 μl, 4.39 mmol, 10 eq), DCM (5 mL) and NH₄OH (2.65 mL, 43.9 mmol, 100 eq). The crude was purified using $H_2O$/MeCN (0.1% TFA) to yield (2R,2`R)-**5αC** (101 mg, 0.37 mmol, 85%) as a colourless oil. **¹H NMR** (400 MHz, Methanol-*d4*) (a 10:1 mixture of rotamers*) δ 4.49 (dd, *J* = 8.6, 3.6 Hz, 1H) [4.91 (dd, *J* = 6.9, 3.6 Hz)], 4.02 – 3.57 (m, 3H), 3.20 – 2.68 (m, 2H), 2.40 – 1.94 (m, 4H). **¹³C NMR** (101 MHz, Methanol-*d4*) δ 174.6 [174.5], 166.4 [167.1] (q, *J* = 2.5 Hz), 125.6 (q, *J* = 281.0 Hz), 60.8 [61.5], 52.7 [52.2] (q, *J* = 25.7 Hz), 49.3 [48.0], 30.4 [31.8], 25.5 [23.5], 22.0 [22.3] (q, *J* = 2.8 Hz). **HRMS** (ESI): calcd for $C_9H_{13}F_3NO_3S^+$ [M+H]⁺ 272.0563, found: 272.0562. Purity: 98% (UV 214 nm). **[α]$_D^{20}$**: +37.9° (*c* 1.0, CHCl₃).
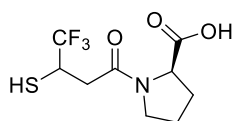

(4,4,4-trifluoro-3-mercaptobutanoyl)-D-proline (**5βC**).

Synthesized according to *General Procedure E* using **4βC** (160 mg, 0.43 mmol, 1.0 eq), TFA (333 μl, 4.33 mmol, 10 eq), DCM (5 mL) and NH₄OH (2.62 mL, 43.3 mmol, 100 eq). The crude was purified using H_2O/MeCN (0.1% TFA) to yield **5βC** (96 mg, 0.35 mmol, 82%) as a colourless oil. The title compound was obtained as a diastereomeric mixture, with each diastereomer being present as two rotamers.

NMR data is reported for the mixture of four isomers and, where possible, chemical shifts are reported separately for the diastereomers, of which the shifts of the minor rotamers can be found in square brackets. In the case of ¹³C NMR semicolons are used to indicate chemical shifts belonging to the same carbon in the different isomers. **¹H NMR** (400 MHz, Methanol-*d4*) (a 3:1 mixture of rotamers of each

---

* Chemical shifts of minor rotamer are enclosed in square brackets.

diastereomer) δ 4.47, 4.44 (dd, *J* = 8.6, 2.8 Hz, 1H) [4.68, 4.54], 4.02 – 3.79 (m, 1H), 3.77 – 3.47 (m, 2H), 3.08 – 2.47 (m, 2H), 2.42 – 1.82 (m, 4H). **13C NMR** (101 MHz, Methanol-*d4*) δ 175.45, 175.4 [175.0, 174.9]; 169.3 [169.7, 169.4]; 127.8 (q, *J* = 276.4 Hz); 60.5, 60.4 [60.9, 60.7]; 48.4 [47.9, 47.8]; 38.9, 38.8 [39.2, 38.7] (q, *J* = 31.4 Hz); 38.1, 37.9 [38.0]; 30.4, 30.3 [32.1, 32.0]; 25.6, 25.5 [23.5, 23.45]. **HRMS** (ESI): calcd for $C_9H_{11}F_3NO_3S^-$ [M-H]⁻ 270.0417, found: 270.0416. Purity: 97% (UV 214 nm).
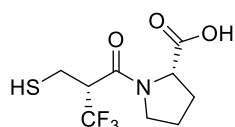
*((R)-3,3,3-trifluoro-2-(mercaptomethyl)propanoyl)-L-proline ((2S,2`R)-**5αD**).*

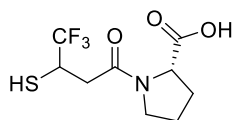Synthesized according to *General Procedure E* using (2*S*,2`*R*)-**4αD** (60 mg, 0.16 mmol, 1.0 eq), TFA (125 μl, 1.62 mmol, 10 eq), DCM (5 mL) and NH₄OH (982 μl, 16.2 mmol, 100 eq). The crude was purified using H₂O/MeCN (0.1% TFA) to yield (2*S*,2`*R*)-**5αD** (37 mg, 0.14 mmol, 84%) as a colourless oil that solidified after standing for several days. **1H NMR** (400 MHz, Methanol-*d4*) (an 8:1 mixture of rotamers*) δ 4.51 (dd, *J* = 8.6, 3.6 Hz, 1H) [4.67 (dd, *J* = 6.5, 3.8 Hz)], 3.96 – 3.50 (m, 3H), 3.10 – 2.93 (m, 1H), 2.92 – 2.82 (m, 1H), 2.37 – 1.90 (m, 4H). **13C NMR** (101 MHz, Methanol-*d4*) δ 174.7 [174.5], 166.2 (q, *J* = 2.5 Hz), 125.6 (q, *J* = 281.3 Hz), 60.7 [61.3], 52.5 [52.9] (q, *J* = 25.7 Hz), 49.2 [48.1], 30.4 [31.9], 25.6 [23.3], 21.3 (q, *J* = 2.8 Hz). **HRMS** (ESI): calcd for $C_9H_{11}F_3NO_3S^-$ [M-H]⁻ 270.0417, found: 270.0416. **M.p.:** 122 – 124 ˚C. Purity: >99% (UV 214 nm). **[α]$_D^{20}$**: –133.7° (*c* 1.0, CHCl₃).
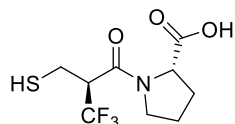
*((S)-3,3,3-trifluoro-2-(mercaptomethyl)propanoyl)-L-proline ((2S,2`S)-**5αD**).*

Synthesized according to *General Procedure E* using (2*S*,2`*S*)-**4αD** (225 mg, 0.61 mmol, 1.0 eq), TFA (468 μl, 6.09 mmol, 10 eq), DCM (5 mL) and NH₄OH (3.68 mL, 60.9 mmol, 100 eq). The crude was purified using H₂O/MeCN (0.1% TFA) to yield (2*S*,2`*S*)-**5αD** (141 mg, 0.52 mmol, 85%) as a colourless oil. **1H NMR** (400 MHz, Methanol-*d4*) (a 10:1 mixture of rotamers*) δ 4.49 (dd, *J* = 8.6, 3.6 Hz, 1H) [4.91 (dd, *J* = 6.9, 3.6 Hz)], 4.03 – 3.58 (m, 3H), 3.19 – 2.68 (m, 2H), 2.40 – 1.96 (m, 4H). **13C NMR** (101 MHz, Methanol-*d4*) δ 174.6 [174.5], 166.4 [167.2] (q, *J* = 2.2 Hz), 125.6 (q, *J* = 280.8 Hz), 60.8 [61.6], 52.7 [52.3] (q, *J* = 25.7 Hz), 49.3 [48.0], 30.4 [31.8], 25.5 [23.5], 22.0 [22.3] (q, *J* = 2.9 Hz). **HRMS** (ESI): calcd for $C_9H_{11}F_3NO_3S^-$ [M-H]⁻ 270.0417, found: 270.0416. Purity: 98% (UV 214 nm). **[α]$_D^{20}$**: –26.9° (*c* 1.0, CHCl₃).

---

* Chemical shifts of minor rotamer are enclosed in square brackets.

(4,4,4-trifluoro-3-mercaptobutanoyl)-L-proline (**5βD**).

Synthesized according to *General Procedure E* using **4βD** (128 mg, 0.35 mmol, 1.0 eq), TFA (266 μl, 3.47 mmol, 10 eq), DCM (5 mL) and NH₄OH (2.10 mL, 34.7 mmol, 100 eq). The crude was purified using H_2O/MeCN (0.1% TFA) to yield **5βD** (69 mg, 0.25 mmol, 73%) as a colourless oil. The title compound was obtained as a diastereomeric mixture, with each diastereomer being present as two rotamers.
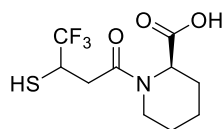
NMR data is reported for the mixture of four isomers and, where possible, chemical shifts are reported separately for the diastereomers, of which the shifts of the minor rotamers can be found in square brackets. In the case of ^{13}C NMR semicolons are used to indicate chemical shifts belonging to the same carbon in the different isomers. **^{1}H NMR** (400 MHz, Methanol-*d4*) (a 3:1 mixture of rotamers of each diastereomer) δ 4.47, 4.44 (dd, *J* = 8.6, 2.8 Hz, 1H) [4.68, 4.54], 4.02 – 3.79 (m, 1H), 3.77 – 3.46 (m, 2H), 3.06 – 2.47 (m, 2H), 2.41 – 1.82 (m, 4H). **^{13}C NMR** (101 MHz, Methanol-*d4*) δ 175.5, 175.4 [175.0, 174.9]; 169.3 [169.7, 169.4]; 127.8 (q, *J* = 276.6 Hz); 60.5, 60.4 [60.9, 60.7]; 48.4 [47.9, 47.8]; 38.9, 38.8 [39.2, 38.7] (q, *J* = 31.3 Hz); 38.1, 37.9 [38.0]; 30.4, 30.3 [32.1, 32.05]; 25.6, 25.5 [23.5, 23.45]. **HRMS** (ESI): calcd for $C_9H_{11}F_3NO_3S^-$ [M-H]⁻ 270.0417, found: 270.0415. Purity: >99% (UV 214 nm).
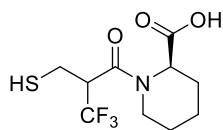
(2R)-1-(3,3,3-trifluoro-2-(mercaptomethyl)propanoyl)piperidine-2-carboxylic acid (**5αE**).

Synthesized according to *General Procedure E* using **4αE** (250 mg, 0.65 mmol, 1.0 eq), TFA (501 μl, 6.52 mmol, 10 eq), DCM (5 mL) and NH₄OH (3.94 mL, 65.2 mmol, 100 eq). The crude was purified using H_2O/MeCN (0.1% TFA) to yield **5αE** (77 mg, 0.27 mmol, 41%) as a colourless oil. The title compound was obtained as a diastereomeric mixture, with each diastereomer being present as two rotamers.

NMR data is reported for the mixture of four isomers and, where possible, chemical shifts are reported separately for the diastereomers, of which the shifts of the minor rotamers can be found in square brackets. In the case of ^{13}C NMR semicolons are used to indicate chemical shifts belonging to the same carbon in the different isomers. **^{1}H NMR** (400 MHz, Methanol-*d4*) (a 4.5:1 mixture of rotamers of each diastereomer) δ 5.40 – 4.98 (m, 1H), 4.63 – 4.02 (m, 2H), 3.42 – 2.74 (m, 3H), 2.43 – 2.25 (m, 1H), 1.85 – 1.35 (m, 5H). **^{13}C NMR** (101 MHz, Methanol-*d4*) δ 173.5, 173.4 [173.2, 173.15]; 167.7, 167.3 (q, *J* = 2.5 Hz) [167.0]; 125.7 (q, *J* = 281.2 Hz); 54.15, 54.1 [58.1, 58.0]; 49.9 [50.1] (q, *J* = 25.7 Hz); 45.7, 45.5 [41.6, 41.5]; 27.9, 27.6 [29.0, 28.4]; 26.6, 26.3 [26.1, 25.8]; 21.9, 21.8 [22.0]; 21.6 [21.5] (q, *J* = 2.9 Hz). **HRMS** (ESI): calcd for $C_{10}H_{13}F_3NO_3S^-$ [M-H]⁻ 284.0574, found: 284.0573. Purity: >99% (UV 214 nm).

(2R)-1-(4,4,4-trifluoro-3-mercaptobutanoyl)piperidine-2-carboxylic acid (**5βE**).
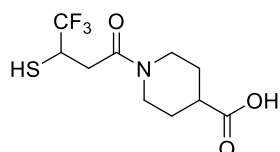
Synthesized according to *General Procedure E* using **4βE** (365 mg, 0.95 mmol, 1.0 eq), TFA (731 μl, 9.52 mmol, 10 eq), DCM (5 mL) and NH$_4$OH (5.76 mL, 95.2 mmol, 100 eq). The crude was purified using H$_2$O/MeCN (0.1% TFA) to yield **5βE** (222 mg, 0.78 mmol, 82%) as a colourless oil. The title compound was obtained as a diastereomeric mixture, with each diastereomer being present as two rotamers.

NMR data is reported for the mixture of four isomers and, where possible, chemical shifts are reported separately for the diastereomers, of which the shifts of the minor rotamers can be found in square brackets. In the case of ^{13}C NMR semicolons are used to indicate chemical shifts belonging to the same carbon in the different isomers. **^{1}H NMR** (400 MHz, Methanol-*d4*) (a 2.5:1 mixture of rotamers of each diastereomer) δ 5.30 – 4.71 (m, 1H), 4.51 – 3.80 (m, 2H), 3.35 – 2.59 (m, 3H), 2.39 – 2.23 (m, 1H), 1.82 – 1.31 (m, 5H). **^{13}C NMR** (101 MHz, Methanol-*d4*) δ 172.8, 172.7 [172.3, 172.2]; 169.3 [169.7, 169.4]; 126.5 (q, *J* = 276.7 Hz); 52.5, 52.4 [55.9, 55.8]; 43.3, 43.2 [40.0, 39.8]; 37.8, 37.7 [37.9, 37.6] (q, *J* = 30.8 Hz); 35.6, 35.4 [35.5, 35.1]; 26.3, 26.25 [26.7, 26.6]; 24.9, 24.8 [24.3, 24.25]; 20.5 [20.55]. **HRMS** (ESI): calcd for C$_{10}$H$_{13}$F$_3$NO$_3$S$^-$ [M-H]$^-$ 284.0574, found: 284.0573. Purity: 94% (UV 214 nm).
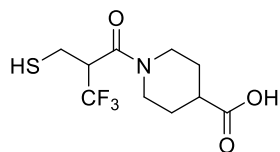
1-(3,3,3-trifluoro-2-(mercaptomethyl)propanoyl)piperidine-4-carboxylic acid (**5αF**).

Synthesized according to *General Procedure E* using **4αF** (87 mg, 0.23 mmol, 1.0 eq), TFA (174 μl, 2.27 mmol, 10 eq), DCM (5 mL) and NH$_4$OH (1.37 mL, 22.7 mmol, 100 eq). The crude was purified using H$_2$O/MeCN (0.1% TFA) to yield **5αF** (44 mg, 0.15 mmol, 68%) as a colourless oil that solidified after standing for several days. **^{1}H NMR** (400 MHz, Methanol-*d4*) (a 1.2:1 mixture of rotamers*) δ 4.53 – 4.44 (m, 1H) [4.40 – 4.31], 4.21 – 4.03 (m, 2H), 3.43 – 3.25 (m, 1H), 3.13 – 2.80 (m, 3H), 2.72 – 2.59 (m, 1H), 2.08 – 1.92 (m, 2H), 1.85 – 1.52 (m, 2H). **^{13}C NMR** (101 MHz, Methanol-*d4*) δ 177.8 [177.7], 165.75 [165.7], 125.7 (q, *J* = 281.1 Hz), 49.7 (q, *J* = 25.3 Hz), 47.1 [46.9], 43.4 [43.1], 41.8 [41.5], 30.1 [29.8], 29.4 [29.1], 21.5 [21.7] (q, *J* = 2.7 Hz). **HRMS** (ESI): calcd for C$_{10}$H$_{13}$F$_3$NO$_3$S$^-$ [M-H]$^-$ 284.0574, found: 284.0572. **M.p.**: 96 – 98 ˚C. Purity: >99% (UV 214 nm).


1-(4,4,4-trifluoro-3-mercaptobutanoyl)piperidine-4-carboxylic acid (**5βF**).

Synthesized according to *General Procedure E* using **4βF** (280 mg, 0.73 mmol, 1.0 eq), TFA (561 μl, 7.30 mmol, 10 eq), DCM (5 mL) and NH$_4$OH (4.42 mL, 73.0 mmol, 100 eq). The crude was purified using H$_2$O/MeCN

* Chemical shifts of minor rotamer are enclosed in square brackets.

(0.1% TFA) to yield **5βF** (139 mg, 0.49 mmol, 67%) as a colourless oil. **^{1}H NMR** (400 MHz, Methanol-*d4*) (a 1.1:1 mixture of rotamers[*]) δ 4.42 – 4.28 (m, 1H), 4.00 – 3.82 (m, 2H), 3.29 – 3.15 (m, 1H), 3.01 – 2.78 (m, 3H), 2.67 – 2.50 (m, 1H), 2.02 – 1.89 (m, 2H), 1.76 – 1.49 (m, 2H). **^{13}C NMR** (101 MHz, Methanol-*d4*) δ 177.85 [177.8], 168.8 [168.7], 127.8 (q, *J* = 276.6 Hz), 46.2, 42.8 [42.7], 41.8 [41.7], 39.4 (q, *J* = 31.1 Hz), 36.4, 29.75 [29.7], 29.1 [29.0]. **HRMS** (ESI): calcd for $C_{10}H_{13}F_3NO_3S^-$ [M-H]$^-$ 284.0574, found: 284.0573. Purity: >99% (UV 214 nm). **IR** (v_{max}/cm^{-1}, neat): 2954, 2868, 1725, 1607, 1453, 1363, 1310, 1254, 1158, 1105, 1032.
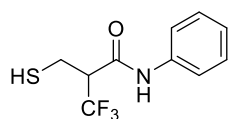
3,3,3-trifluoro-2-(mercaptomethyl)-N-phenylpropanamide (**5αG**).

Synthesized according to *General Procedure D* using **4αG** (170 mg, 0.58 mmol, 1.0 eq), sodium thiomethoxide (82 mg, 1.17 mmol, 2.0 eq) and MeOH (5 mL). Upon addition of a 0.1 M aqueous HCl solution, the title compound precipitated and was collected via filtration to yield **5αG** (135 mg, 0.54 mmol, 93%) as a white solid. **^{1}H NMR** (400 MHz, Methanol-*d4*) δ 7.64 – 7.53 (m, 2H), 7.40 – 7.29 (m, 2H), 7.20 – 7.09 (m, 1H), 3.58 – 3.45 (m, 1H), 3.14 – 3.02 (m, 1H), 2.95 – 2.85 (m, 1H). **^{13}C NMR** (101 MHz, Methanol-*d4*) δ 165.3 (q, *J* = 2.6 Hz), 139.1, 129.9 (2C), 125.9, 125.8 (q, *J* = 280.5 Hz), 121.5 (2C), 56.1 (q, *J* = 25.6 Hz), 20.8 (q, *J* = 2.8 Hz). **HRMS** (ESI): calcd for $C_{10}H_{11}F_3NOS^+$ [M+H]$^+$ 250.0508, found: 250.0505. **M.p.**: 135 – 137 ˚C. Purity: 97% (UV 214 nm).
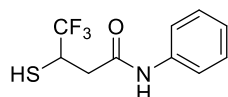
4,4,4-trifluoro-3-mercapto-N-phenylbutanamide (**5βG**).

Synthesized according to *General Procedure D* using **4βG** (90 mg, 0.31 mmol, 1.0 eq), sodium thiomethoxide (43 mg, 0.62 mmol, 2.0 eq) and MeOH (4 mL). Upon addition of a 0.1 M aqueous HCl solution, the title compound precipitated and was collected via filtration to yield **5βG** (50 mg, 0.20 mmol, 65%) as a white solid. **^{1}H NMR** (400 MHz, Methanol-*d4*) δ 7.62 – 7.49 (m, 2H), 7.37 – 7.26 (m, 2H), 7.16 – 7.06 (m, 1H), 4.02 – 3.87 (m, 1H), 3.03 (dd, *J* = 15.1, 4.3 Hz, 1H), 2.66 (dd, *J* = 15.2, 10.1 Hz, 1H). **^{13}C NMR** (101 MHz, Methanol-*d4*) δ 169.0, 139.6, 129.8 (2C), 127.8 (q, *J* = 276.5 Hz), 125.5, 121.3 (2C), 40.0 (q, *J* = 1.9 Hz), 39.3 (q, *J* = 31.4 Hz). **HRMS** (ESI): calcd for $C_{10}H_9F_3NOS^-$ [M-H]$^-$ 248.0362, found: 248.0361. **M.p.**: 102 – 104 ˚C. Purity: >99% (UV 214 nm).
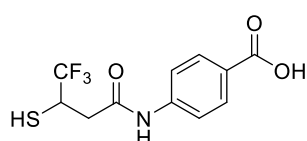
4-(4,4,4-trifluoro-3-mercaptobutanamido)benzoic acid (**5βH**).

Synthesized according to *General Procedure E* using **4βH** (170 mg, 0.43 mmol, 1.0 eq), TFA (334 μl, 4.34 mmol, 10 eq), DCM (5 mL) and NH$_4$OH

---

[*] Chemical shifts of minor rotamer are enclosed in square brackets.

(2.63 mL, 43.4 mmol, 100 eq). Upon addition of a 2 M aqueous HCl solution, the title compound precipitated and was collected via filtration to yield **5βH** (125 mg, 0.43 mmol, 98%) as a white solid. **^{1}H NMR** (400 MHz, Methanol-*d4*) δ 8.03 – 7.95 (m, 2H), 7.73 – 7.65 (m, 2H), 3.96 (dqd, J = 10.1, 8.3, 4.2 Hz, 1H), 3.07 (dd, J = 15.3, 4.2 Hz, 1H), 2.69 (dd, J = 15.4, 10.1 Hz, 1H). **^{13}C NMR** (101 MHz, Methanol-*d4*) δ 169.4, 169.2, 144.0, 131.8 (2C), 127.7 (q, J = 275.9 Hz), 127.2, 120.2 (2C), 40.2, 39.1 (q, J = 31.4 Hz). **HRMS** (ESI): calcd for $C_{11}H_9F_3NO_3S^-$ [M-H]$^-$ 292.0261, found: 292.0258. **M.p.**: decomposition 267 ˚C. Purity: >99% (UV 214 nm).

Enzyme inhibition assay

For the determination of the inhibitor concentration 50% (IC_{50}), histidine and TEV tagged NDM-1 without signal peptide was expressed as described previously.[5] The TEV cleavage side was removed resulting in a truncated version of NDM-1 with G36. Purified NDM-1 was preincubated (final concentration of 10 nM) at various inhibitor concentrations ranging from 0 to 1000 μM. The incubation was carried out for 5 min in 50 mM HEPES buffer pH 7.5 containing 1 μM $ZnSO_4$ (Sigma-Aldrich) at 25°C. The changes in the initial reaction velocity were determined for meropenem (Sigma Aldrich, 30 μM) as a reporter substrate. The kinetics were recorded at 360 nm under stable temperature conditions (25°C) using a BioTek Epoch plate reader (Agilent). Data evaluation as well as the IC_{50} calculation of at least two independent measurements was done using GraphPad Prism® (v. 9). All reported concentrations are final values for 100 μL assay volume.

Biological activity

The ability of the inhibitors to potentiate the antimicrobial effect of meropenem was determined by using a previously constructed *Escherichia coli* (E. cloni™) expressing *bla*NDM-1, *bla*VIM-2 or *bla*IMP-26 from a low copy (p15A origin, ca. 10 copies per cell) number plasmid (Table S1).[6, 7] The gene encoding for IMP-26 was sub-cloned as described previously.[7] In brief, *bla*IMP-26 was amplified from the *E. coli* strain 50857972 using the forward (5`- TTTTTCATT<u>CCATGG</u>GAAGCAAGTTAT -3`) and reverse primers (5`- TTTTT<u>CTCGAG</u>TTAGTTGCTTAGTTTTGA -3`) and Phusion polymerase (NEB). PCR products were digested using DpnI, XhoI, and NcoI (Thermo Scientific) and ligated with backbone using T4 Ligase (Thermo Scientific). The vector backbone was amplified using the forward

(5`-GCTTTCCCATGGATGTTTTTCCTCCTTATGTTAAGCTTACTCAG-3`) and reverse (5`-GCTTCTCGAGAAGTGGTTAGCGCGTATTTGTG -3`) primers previously described and digested similarly to the insert.[6] Ligated vectors were transformed into the *E. coli* E. cloni (MP-21-5).

A broth microdilution (LB medium, Sigma Aldrich) was set up with increasing concentrations of meropenem (0 to 32 mg/L) in the presence and absence of 500 μM inhibitor. The 96 well plates (Corning) with and without inhibitor were inoculated with 5×10^5 CFU/ mL and supplemented with 25 mg/L chloramphenicol. Plates were incubated statically for 20 h at 37°C and the optical density at 600 nm was read using a BioTek Epoch plate reader (Agilent). Inhibition was visualised using GraphPad Prism (v. 9).

Table S1. Strains constructed and used in this study.

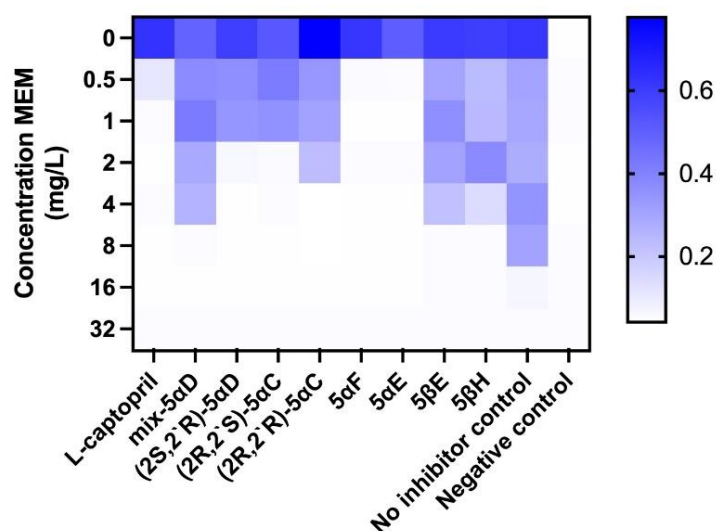| Strain no.	Strain background	Vector number	Insert	Reference
21-05	*E. coli* E. cloni® 10G	None	None	Lucigen
30-63	*E. coli* E. cloni® 10G	pUNS-157	bla_{NDM-1} (NG_049326.1)	[6]
30-57	*E. coli* E. cloni® 10G	pUNS-236	bla_{VIM-2} (NG_050347.1)	[7]
30-58	*E. coli* E. cloni® 10G	pUNS-237	bla_{IMP-26} (NG_049190)	This study
		Clinical isolates for strain constructions:		
50857972	*E. coli*	-	Carrier bla_{IMP-26}	[8]

Figure S2. Heatmap of bacterial growth using increasing meropenem (MEM) concentrations and a fixed concentration of 500 μM of selected inhibitors. Susceptibility was determined using *E. coli* E. cloni™ producing NDM-1 from a low copy number plasmid.[6] Blue scale represents the determined optical density at 600 nm.

NMR

^{1}H,^{15}N HSQC titration experiments. For the titrations, two ^{15}N-labelled NDM-1 (0.25 mM) batches were prepared. Ligands **(+)-5αA** and **(–)-5αA** were prepared in the same buffer as the protein (20 mM KPO$_4$, 0.1 mM ZnCl$_2$, and 2.5% d_6-DMSO pH 7.0). ^{1}H,^{15}N HSQC spectra were acquired at 310 K with 128 × 1024 complex points (F$_1$ × F$_2$) and spectral width of 9090 × 2740 Hz on ^{15}N-labeled NDM-1 and with every titration step up to 1:15 eq ratio between protein: ligand. The NMR data were processed using the MestReNova software, with the Mnova Binding plugin.

^{19}F,^{1}H 1D HOESY. A mixture of NDM-1 (0.25 mM) and **(+)-5αA** in a 1:10 eq ratio was prepared in the buffer of 20 mM KPO$_4$, 0.1 mM ZnCl$_2$ and 2.5% d_6-DMSO at pH 7.0. Selective 1D ^{19}F-^{1}H 1D HOESY spectra (-68.176 ppm) were acquired with 18432 complex points and spectral widths of 9803.8 Hz with a mixing time of 0.8s. Spectra were recorded at 310 K, and the data was processed using the software MestReNova.

Table S2. Chemical shift perturbations for each amino acid for enantiomers of **5αA**: (+)-**5αA**(E1) and (–)-**5Aα**(E2).

AA	SSP (E1)	noSSP(E1)	SSP (E2)	noSSP(E2)
039M		0.00369	--	0.00177
040E		0.00259	--	0.00179
041T		0.00319	--	2.99E-04
042G		0.02435	--	0.01
043D		0.01133	--	0.00162
044Q		0.00162	--	3.34E-04
045R		2.99E-04	--	5.70E-04
046F		0.00169	--	0.00721
047G		0.01417	--	0.00772
048D		0.00557	--	0.00384
049L		0.01441	--	6.26E-04
050V		0.0015	--	0.00818
051F		4.43E-04	--	0.00177
052R		0.01728	--	1.26E-04
053Q		0.01497	--	0.00777
054L		0.00568	--	0.00709
055A		0.00161	--	0.00701
--		--	--	--
057N		0.0061	--	0.00849
058V		0.0034	--	0.00738
059W		0.00566	--	0.01403
060Q		0.01541	--	0.00161
061H		0.05901	--	2.36E-05

062T		0.01847	--	0.02412
063S		0.02783	--	0.01812
064Y		0.01878	0.11827	--
065L		0.04459	--	0.01404
066D		0.05032	0.08217	--
067M	0.06323	--	--	0.00218
--	--	--	--	--
--	--	--	--	--
070F	--	0.03886	--	0.00139
071G	--	0.01006	--	0.00208
072A	--	0.01399	--	0.00262
073V	--	0.00991	--	0.001
074A	--	8.37E-04	--	0.04903
075S	--	0.03147	--	0.00241
076N	--	0.00101	--	0.00853
077G	--	0.01517	--	5.09E-04
078L	--	0.01445	--	0.00973
079I	--	0.01138	--	0.00212
080V	--	0.00467	--	0.00869
081R	--	0.0018	--	2.56E-05
082D	--	0.00503	--	0.00137
083G	--	0.01476	--	0.00623
084G	--	0.01417	--	0.00772
085R	--	0.00196	--	4.96E-04
086V	--	0.01402	--	3.01E-04
087L	--	3.32E-05	--	0.00731
088V	--	0.00223	--	8.70E-04
089V	--	3.27E-04	--	0.00702
090D	--	0.00266	--	0.00711
091T	--	0.00763	--	0.00703
092A	--	0.02072	--	0.01247
093W	--	0.05289	--	0.03513
094T	--	0.0297	--	0.01751
095D	--	0.01474	--	0.00464
096D	--	0.01565	--	0.00541
097Q	--	0.01822	--	0.00831
098T	--	0.01514	--	0.00707
099A	--	2.99E-04	--	5.70E-04
100Q	--	0.01557	--	0.00526
101I	--	9.94E-04	--	0.00199
102L	--	0.00941	--	0.00821
103N	--	0.0152	--	0.00751
104W	--	0.00815	--	0.00363
105I	--	0.00986	--	0.00731
106K	--	0.01993	--	0.01475
107Q	--	0.0154	--	0.00712
108E	--	8.55E-04	--	1.56E-04
109I	--	0.00159	--	0.00778

110N	--	0.00358	--	5.08E-04
111L	--	0.00806	--	8.14E-04
--	--	--	--	--
113V	--	0.00369	--	0.00177
114A	--	4.85E-04	--	0.00956
115L	--	0.00565	--	0.00234
116A	--	0.00313	--	0.00221
117V	--	0.00472	--	0.00701
118V	--	0.01402	--	0.00702
119T	0.07673	--	0.07293	--
120H	--	0.03098	--	0.02765
121A	--	0.0442	--	0.0586
122H	0.15563	--	0.11201	--
123Q	--	0.00104	--	0.00701
124D	0.31642	--	0.35433	--
--	--	--	--	--
--	--	--	--	--
127G	--	0.00213	--	0.00704
128G	--	0.0315	--	0.0296
129M	--	0.00357	--	0.00831
130D	--	0.00789	--	0.00279
131A	--	0.00675	--	0.00835
132L	--	0.00302	--	0.00233
133H	--	0.04677	--	0.01678
134A	--	0.00189	--	6.17E-04
135A	--	0.00409	--	3.68E-04
136G	--	0.01477	--	0.0075
137I	--	0.01462	--	0.0075
138A	--	0.00896	--	0.00523
139T	--	0.0145	--	0.00317
140Y	--	0.00994	--	0.00235
141A	--	0.01457	--	0.00702
142N	--	0.02164	--	0.00202
143A	--	0.01996	--	0.0318
144L	--	0.04571	--	0.013
145S	--	0.01961	--	0.00268
146N	--	0.00159	--	0.00778
147Q	--	0.01053	--	0.01609
148L	--	0.00425	--	0.0073
149A	--	0.01413	--	0.00711
--	--	--	--	--
151Q	--	0.00816	--	0.01083
152E	--	0.02586	--	0.00526
153G	--	0.0278	--	0.00784
154M	--	0.00372	--	0.00613
155V	--	0.00528	--	0.01266
156A	--	0.01338	--	4.47E-04
157A	--	0.01778	--	0.00144

158Q	--	0.00355	--	0.01513
159H	--	0.01566	--	0.00805
160S	--	0.00803	--	0.00126
161L	--	0.01612	--	0.00764
162T	--	0.00176	--	0.00723
163F	--	0.00305	--	0.00702
164A	--	2.99E-04	--	5.70E-04
--	--	--	--	--
166N	--	9.61E-04	--	5.58E-04
167G	--	0.00218	--	6.36E-05
168W	--	0.00675	--	0.00835
169V	--	0.00416	--	0.01446
170E	--	0.01539	--	0.00129
--	--	--	--	--
172A	--	0.01405	--	0.01117
173T	--	9.48E-04	--	7.72E-04
174A	--	0.00122	--	1.64E-04
--	--	--	--	--
176N	--	0.00748	--	0.01085
177F	--	0.00223	--	8.70E-04
178G	--	5.48E-04	--	5.39E-04
--	--	--	--	--
180L	--	0.00331	--	0.01405
181K	--	0.02833	--	0.00704
182V	--	0.00819	--	0.00726
183F	--	0.00568	--	0.00709
184Y	--	0.00434	--	0.00705
--	--	--	--	--
--	--	--	--	--
--	--	--	--	--
188G	0.16351	--	0.21437	--
189H	0.12701	--	0.11222	--
190T	--	0.01872	0.11337	--
191S	0.1259	--	0.1307	--
192D	--	0.01431	--	0.04103
193N	--	0.0185	--	0.01742
194I	--	0.01915	--	0.02666
195T	--	0.01598	--	0.01494
196V	--	0.02553	--	0.03752
197G	--	0.02672	--	0.00309
198I	--	1.17E-04	--	4.07E-04
199D	--	0.00647	--	4.31E-04
--	--	--	--	--
201T	--	2.39E-04	--	6.06E-04
202D	--	0.01432	--	0.01298
203I	--	0.01402	--	0.00708
204A	--	0.0199	--	0.00144
205F	--	0.01307	--	0.02132

206G	--	0.01249	--	0.00717
--	--	--	--	--
--	--	--	--	--
209L	--	0.01465	--	0.00703
210I	--	0.05576	0.06102	--
211K	0.07481	--	0.07471	--
212D	0.08302	--	0.06127	--
213S	0.07067	--	0.12219	--
214K	--	0.02939	--	0.02589
215A	--	0.03388	--	0.05095
--	--	--	--	--
217S	--	1.47E-04	--	6.22E-05
--	--	--	--	--
--	--	--	--	--
--	--	--	--	--
--	--	--	--	--
222G	0.07433	--	0.06168	--
223D	--	0.01402	--	0.0156
224A	0.20805	--	--	0.00121
225D	--	0.05988	--	0.01384
226T	0.09411	--	0.09586	--
227E	0.0962	--	0.08175	--
228H	0.06409	--	0.09144	--
229Y	--	0.04705	0.07916	--
230A	--	0.0308	--	0.02626
231A	--	0.01416	--	0.00398
232S	--	0.03269	--	0.01432
233A	--	0.04176	--	0.05029
234R	--	0.01587	--	0.02968
235A	--	3.72E-04	--	0.01447
236F	--	0.01708	--	0.00255
237G	--	0.02917	--	0.03616
238A	--	0.01993	--	0.01475
239A	--	0.00234	--	2.17E-04
240F	--	0.01676	--	0.00142
--	--	--	--	--
242K	--	0.00304	--	0.00707
243A	--	0.01403	--	0.00715
244S	--	0.02813	--	0.00175
245M	--	0.04587	--	0.00174
246I	--	0.01432	--	0.02117
247V	--	0.01867	--	0.00754
248M	--	0.00446	--	0.00208
249S	--	0.05692	0.09029	--
--	--	--	--	--
251S	0.06373	--	--	0.05614
252A	--	0.04587	--	0.00174
--	--	--	--	--

AA				
254D	--	0.04294	0.06352	--
255S	0.10919	--	0.11489	--
256R	--	0.03457	--	0.0236
--	--	--	--	--
258A	--	0.02194	--	0.00884
259I	--	0.01474	--	0.00704
260T	--	0.03866	--	0.03744
261H	--	0.0141	--	0.00204
262T	--	0.06064	--	0.03625
263A	--	0.05225	--	0.00722
264R	--	0.04047	--	0.03392
265M	--	0.04209	--	0.00255
266A	--	0.00164	--	0.01405
267D	--	0.00103	--	6.87E-04
268K	0.08036	--	0.10523	--
269L	0.07659	--	0.10782	--
270R	0.07793	--	0.08967	--

Table S3. Estimated K_d values (with standard error) for each amino acid showing SSP for (+)-**5αA**.

AA	(+)-**5αA** K_d (μM)
Met67	249.4
Thr119	125.4
His122	123.2
Asp124	104.0
Gly188	134.3
His189	111.3
Lys211	15.2
Asp212	26.8
Ser213	184.7
Gly222	263.5
Ala224	143.3
Thr226	99.5
Glu227	445.7
His228	122.7
Ser251	130.6
Ser255	185.5
Lys268	152.0
Leu269	65.4
Arg270	152.7

Average K_d = 149.2 ± 21.8 μM

Molecular docking

Schrödinger software (Schrödinger, LLC, New York, NY, 2019) was used and unless otherwise stated, default settings were used in the computations. The crystal structure of NDM-1 (pdb 6NY7) was prepared using the Protein Preparation Wizard;[9] involving Prime[10] to fill in missing side chains and

loops, Epik[11, 12] to generate heteroatom states (pH 7.0 ± 2.0), PropKa (pH 7) to optimize the hydrogen bond network (sampling of water orientations when appropriate), and the OPLS3e force field[13] in the restrained minimization (hydrogens only). The Receptor Grid Generation module in Glide[14-16] was used to define the active site by creating a rectangular box centered on the native ligand (crystal structure) and extending in all directions to encompass ligands of similar size (i.e. 16.5 Å) or ligands < 22 Å. Grids with no water molecules in the active site were generated and validated. The ligands were converted to 3D all atom structures using LigPrep. Epik was used to generate possible ionization states at target pH 7 ± 2, including metal binding states. Tautomers were selected to be generated. The molecular docking was performed using Glide. The inhibitors were docked using the flexible docking mode, with sampling of nitrogen inversions and ring conformations, and with extra precision (XP) rescoring. Biased sampling of torsions was selected for amides by penalizing non-planar conformations. Epik state penalties was selected to be added to the docking score. A maximum of 40 poses were selected to be generated for each ligand. Post-docking minimization was used, and per-residue interaction scores were written for residues within 10 Å from the grid center. Prime MM-GBSA rescoring of docking poses (VSGB 2.0 solvation model and OPLS3e force field) were performed providing poses ranked based on free energy of binding (ΔG_{bind} in kcal mol^{-1}). For these calculations, flexibility was allowed for residues within 10 Å from the ligands, and minimization was selected as sampling method. Structural interaction fingerprints (SIFts) in Canvas were used for representation and analysis of the docking poses. Side chain, zinc ion, and hydrogen bonding interactions were used to generate the SIFts. The similarity between the SIFts were evaluated using the Tanimoto similarity metric, and clustering was performed using the Flexible Beta linkage method. Epik (Schrödinger, LLC, New York, NY, 2020) was used for empirical predictions of aqueous pKa values.

¹H and ¹³C NMR spectra of final compounds

N-benzyl-3,3,3-trifluoro-2-(mercaptomethyl)propanamide (**5αA**)
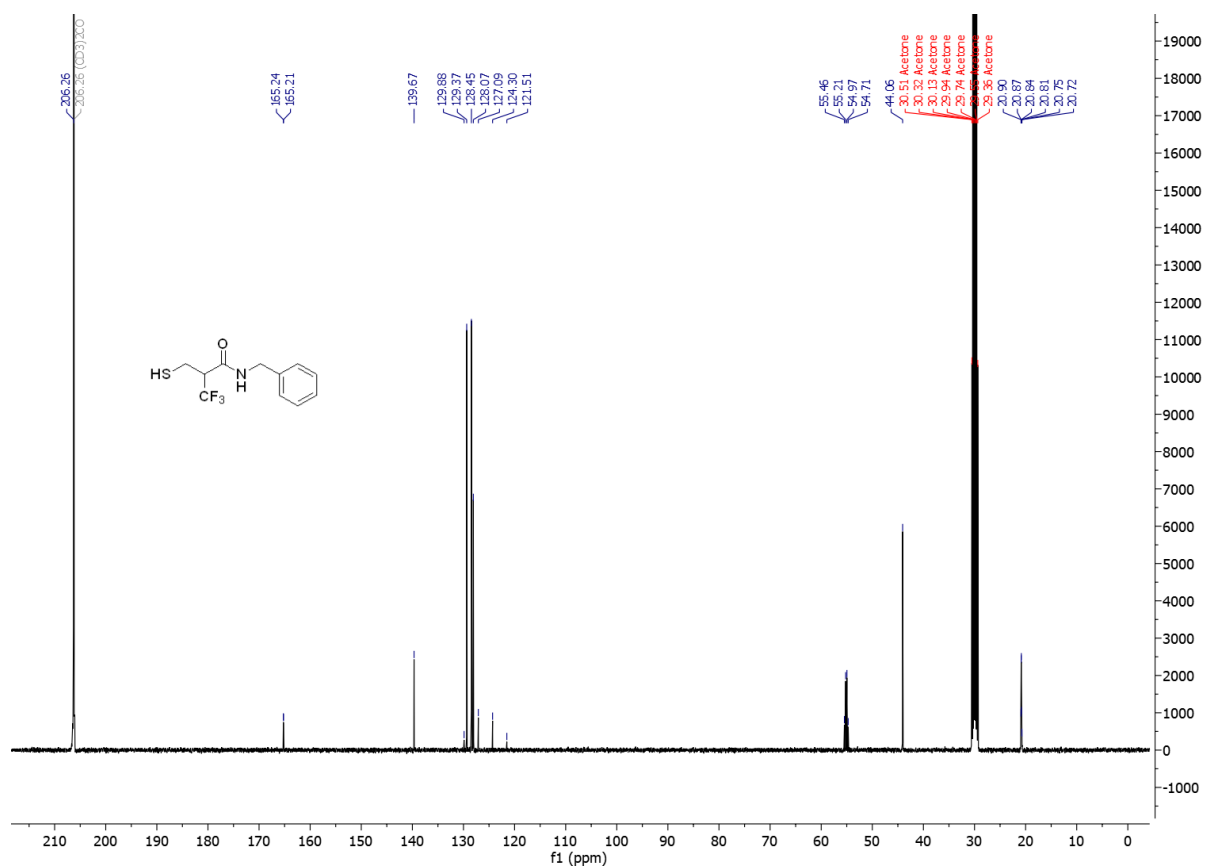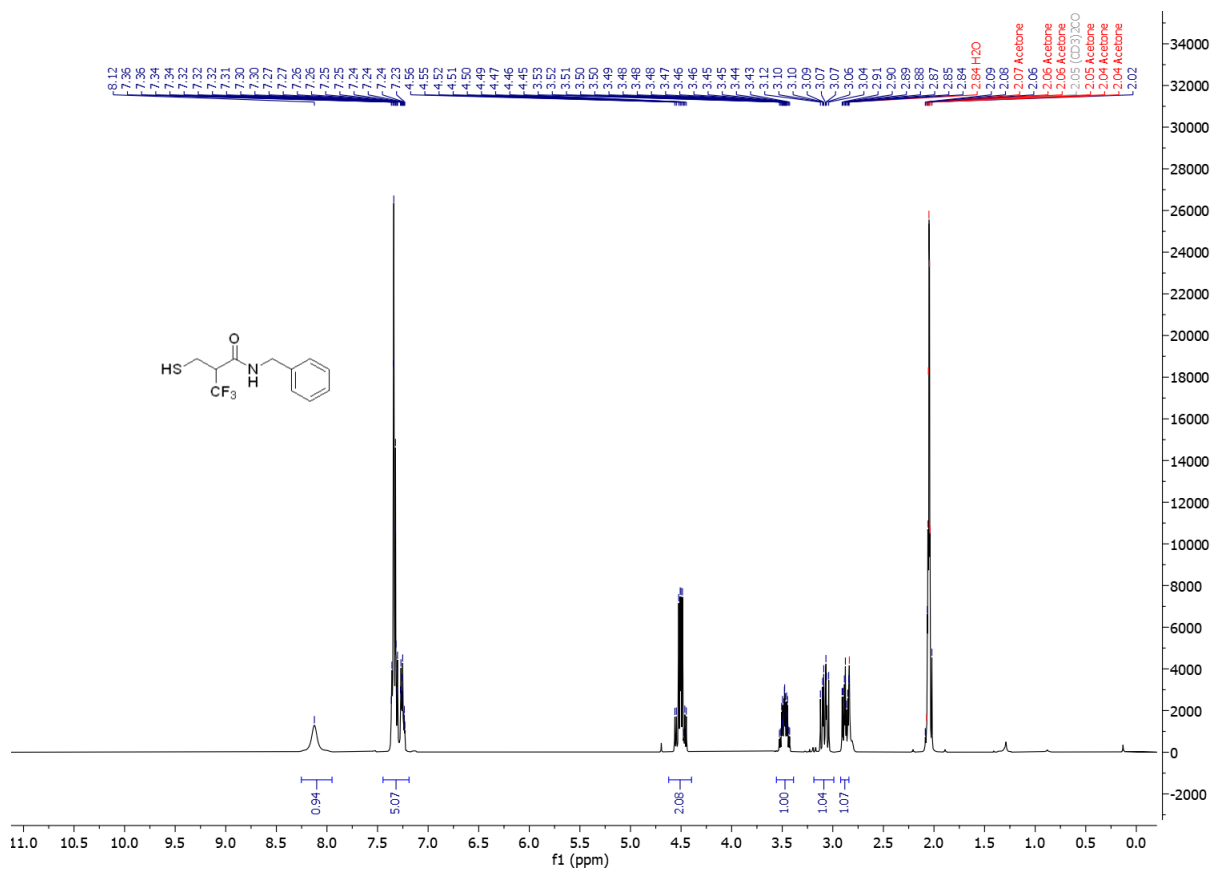
N-benzyl-4,4,4-trifluoro-3-mercaptobutanamide (**5βA**)
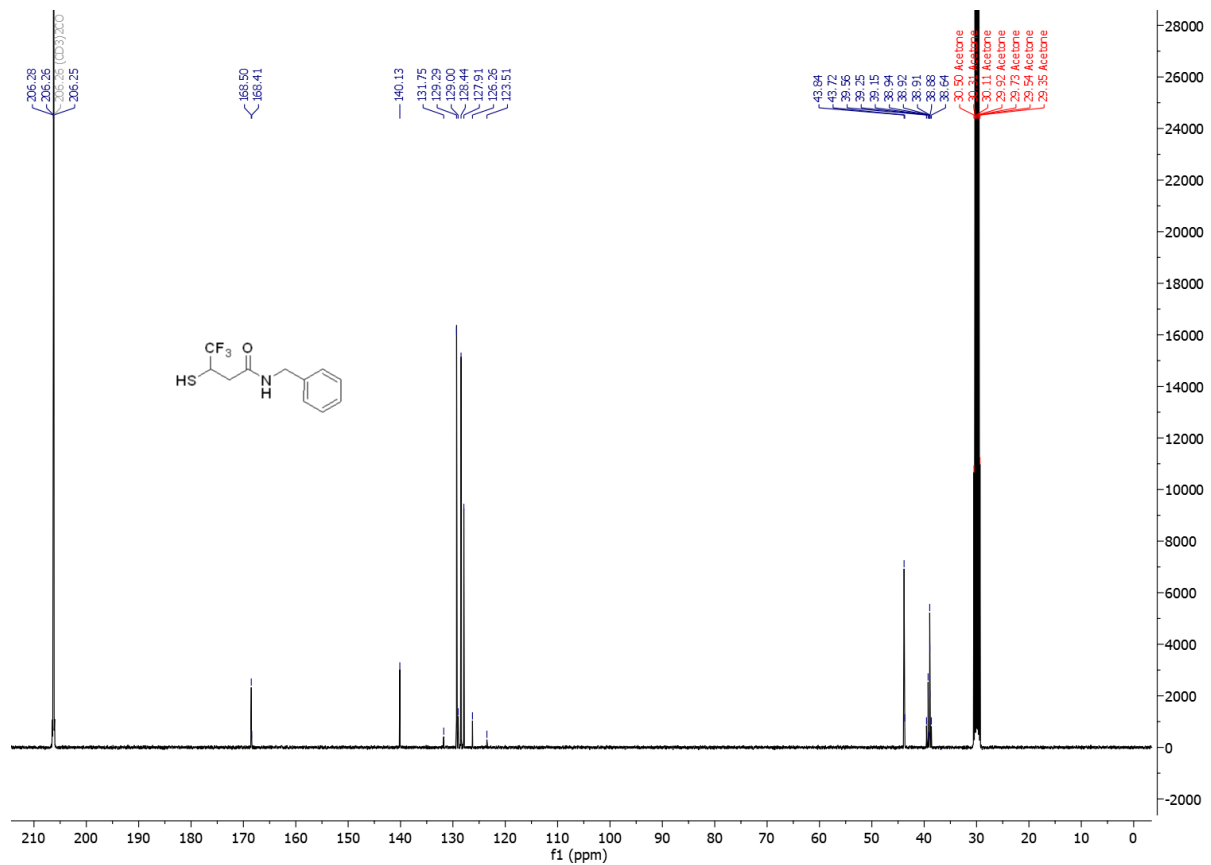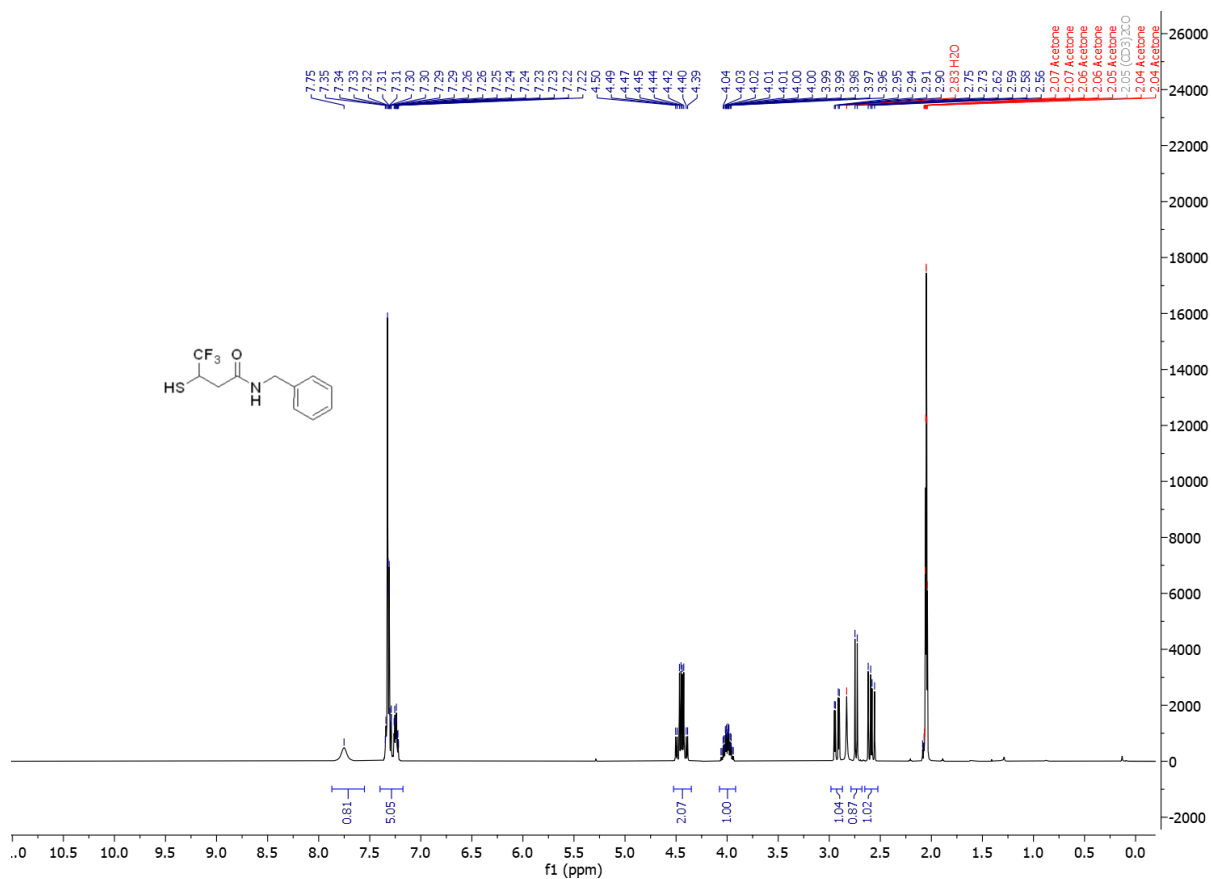
4-((3,3,3-trifluoro-2-(mercaptomethyl)propanamido)methyl)benzoic acid (**5αB**)
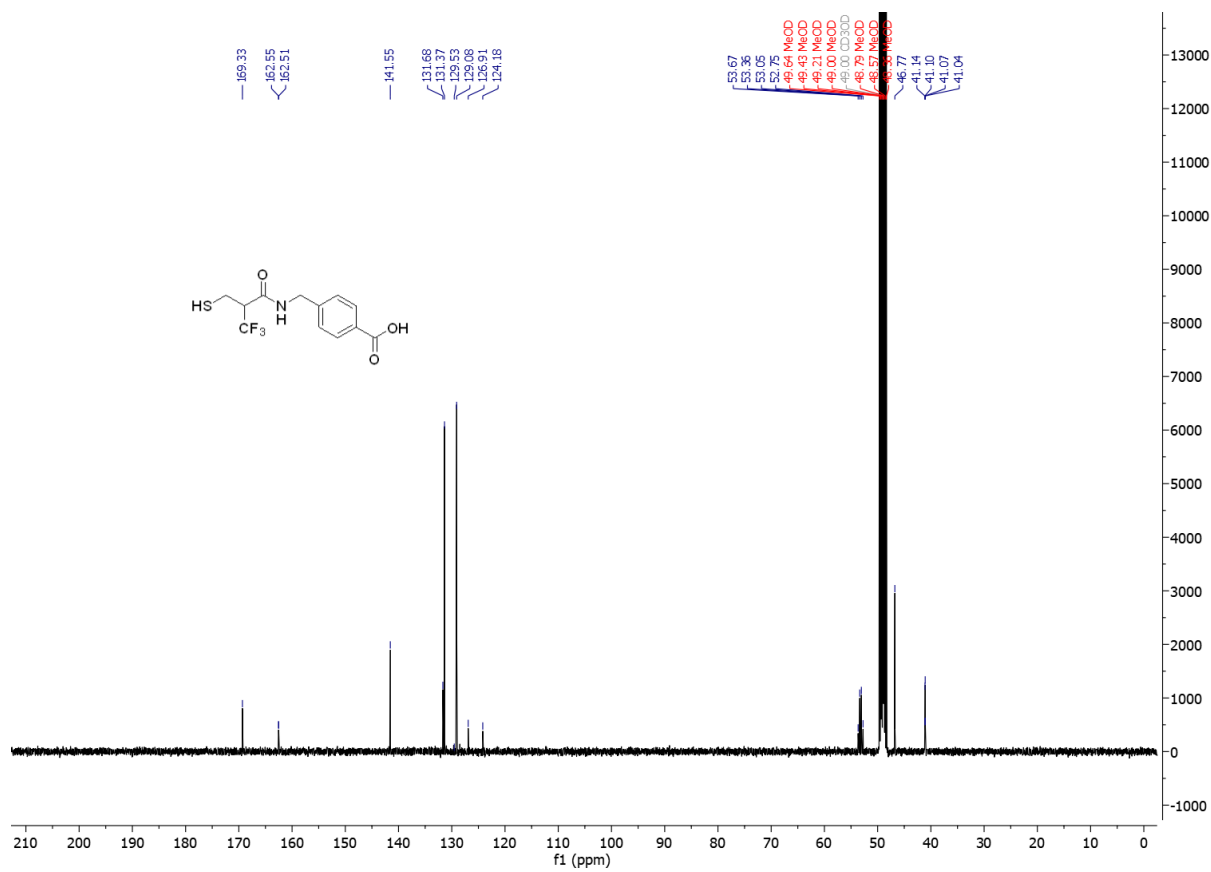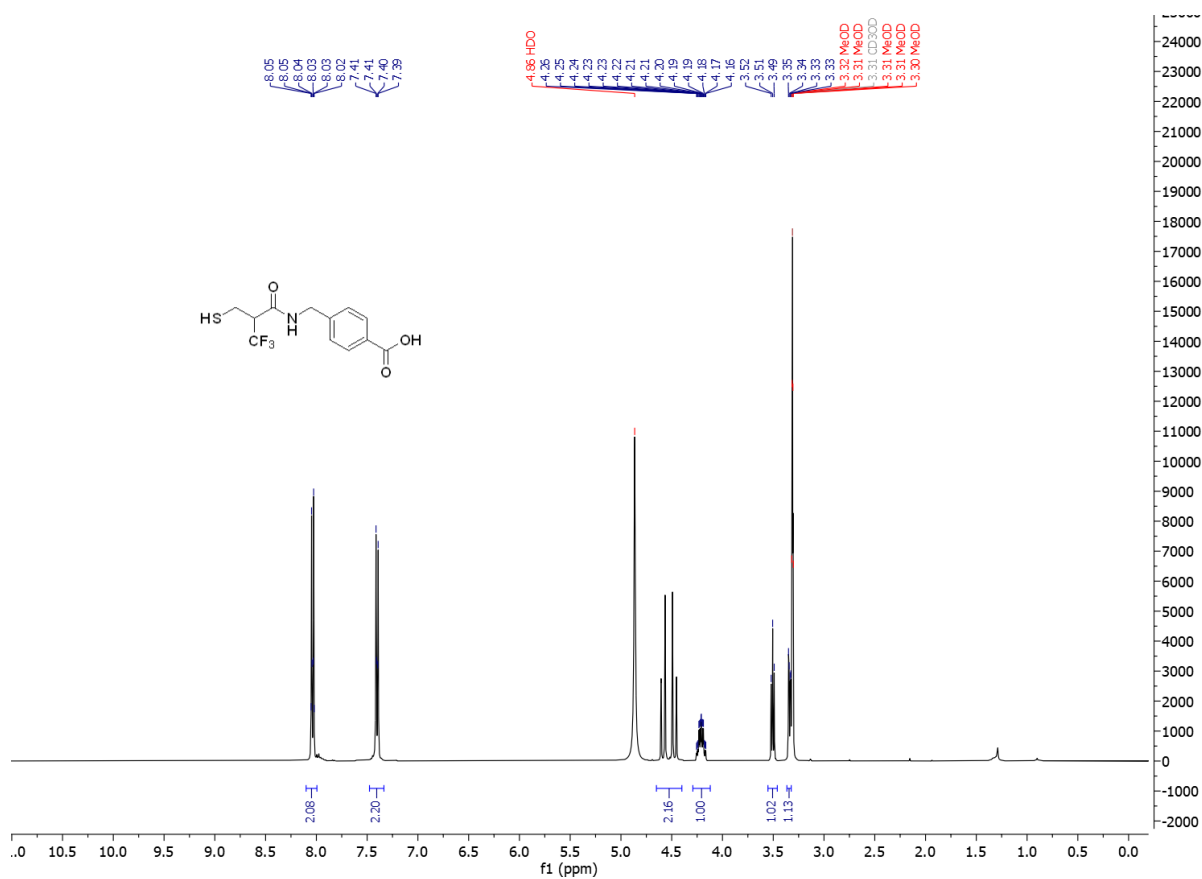
4-((4,4,4-trifluoro-3-mercaptobutanamido)methyl)benzoic acid (5βB)
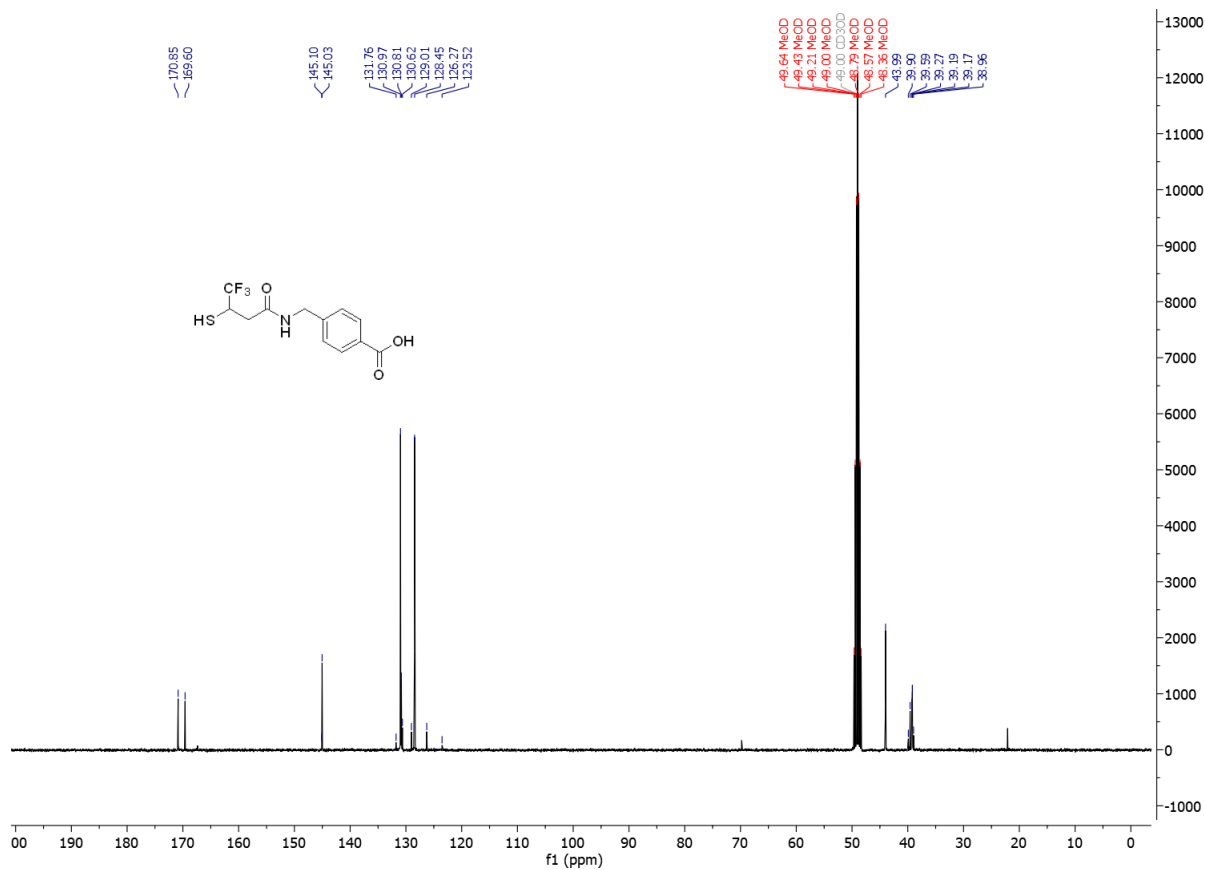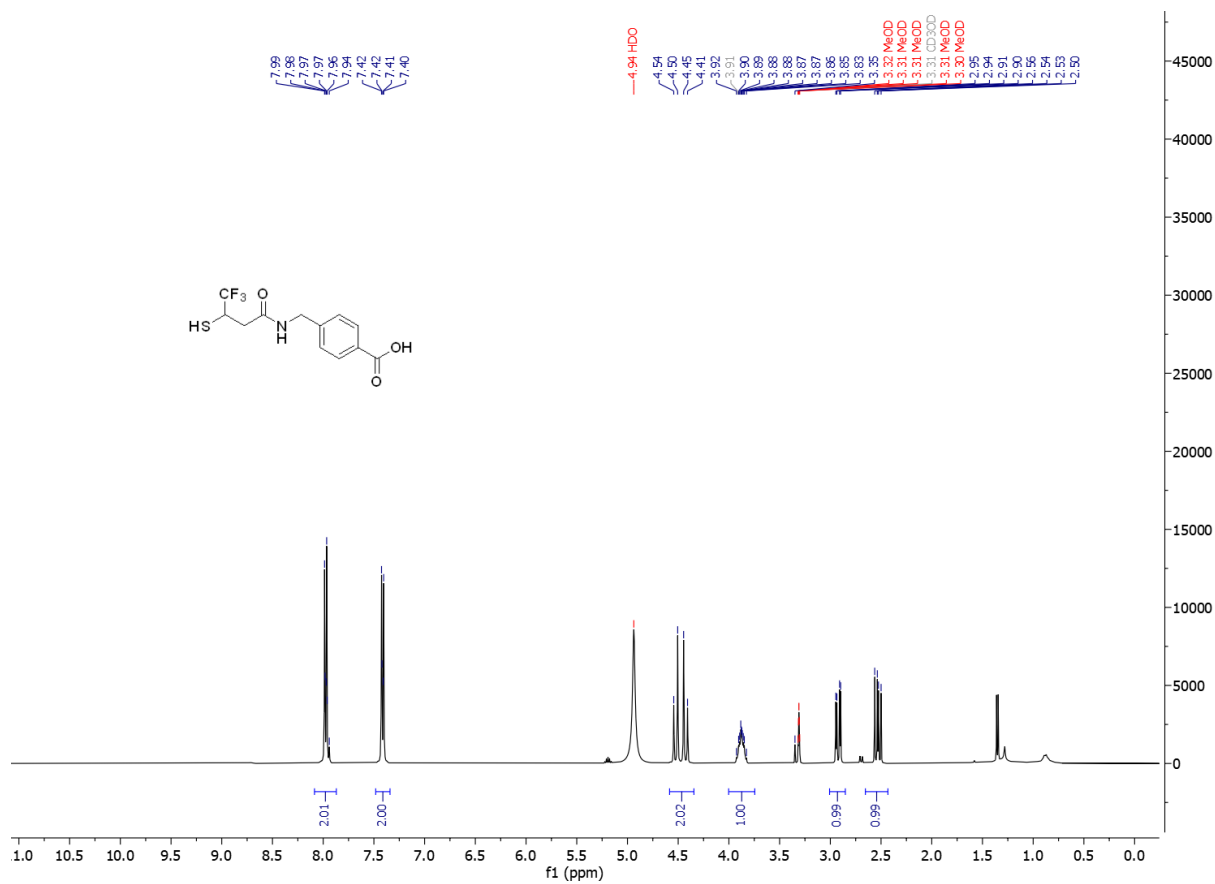
((*S*)-3,3,3-trifluoro-2-(mercaptomethyl)propanoyl)-*D*-proline ((2*R*,2`*S*)-**5αC**)
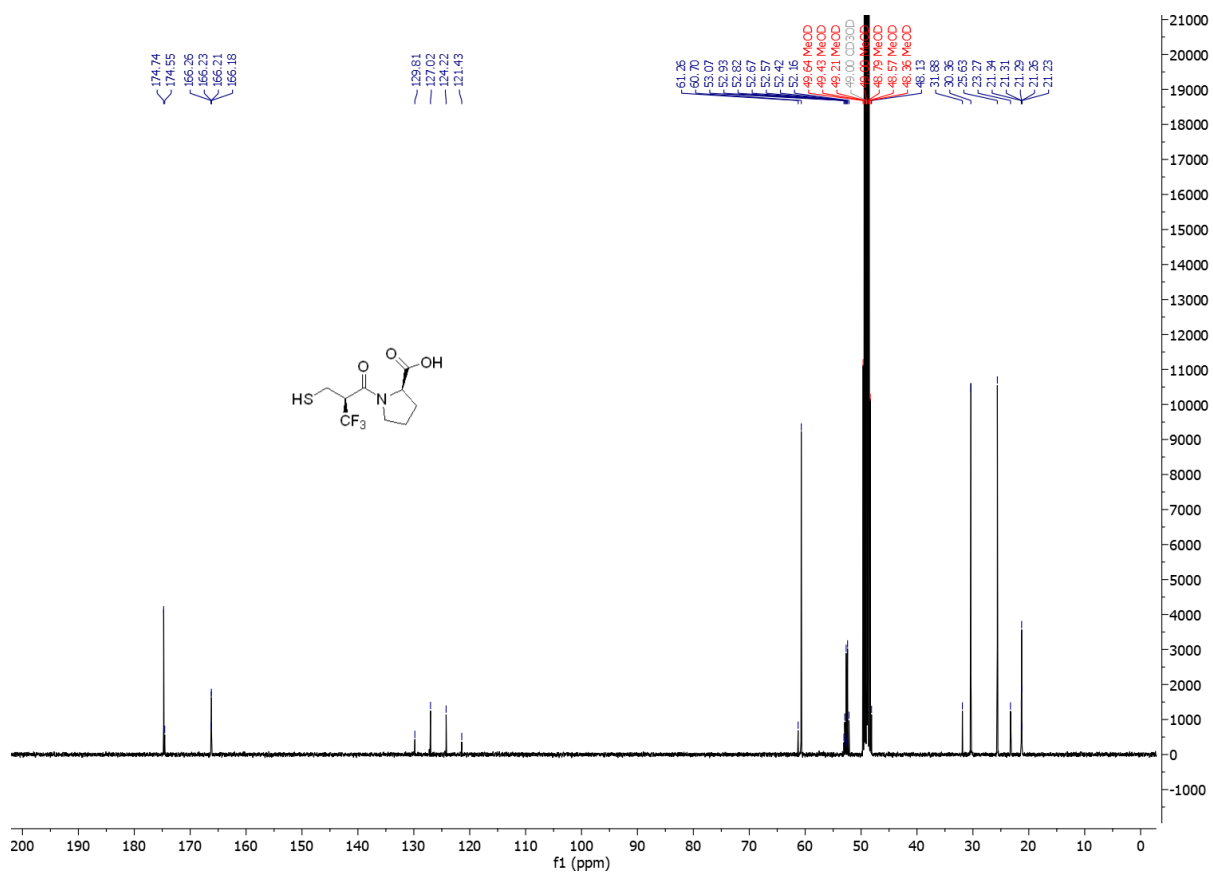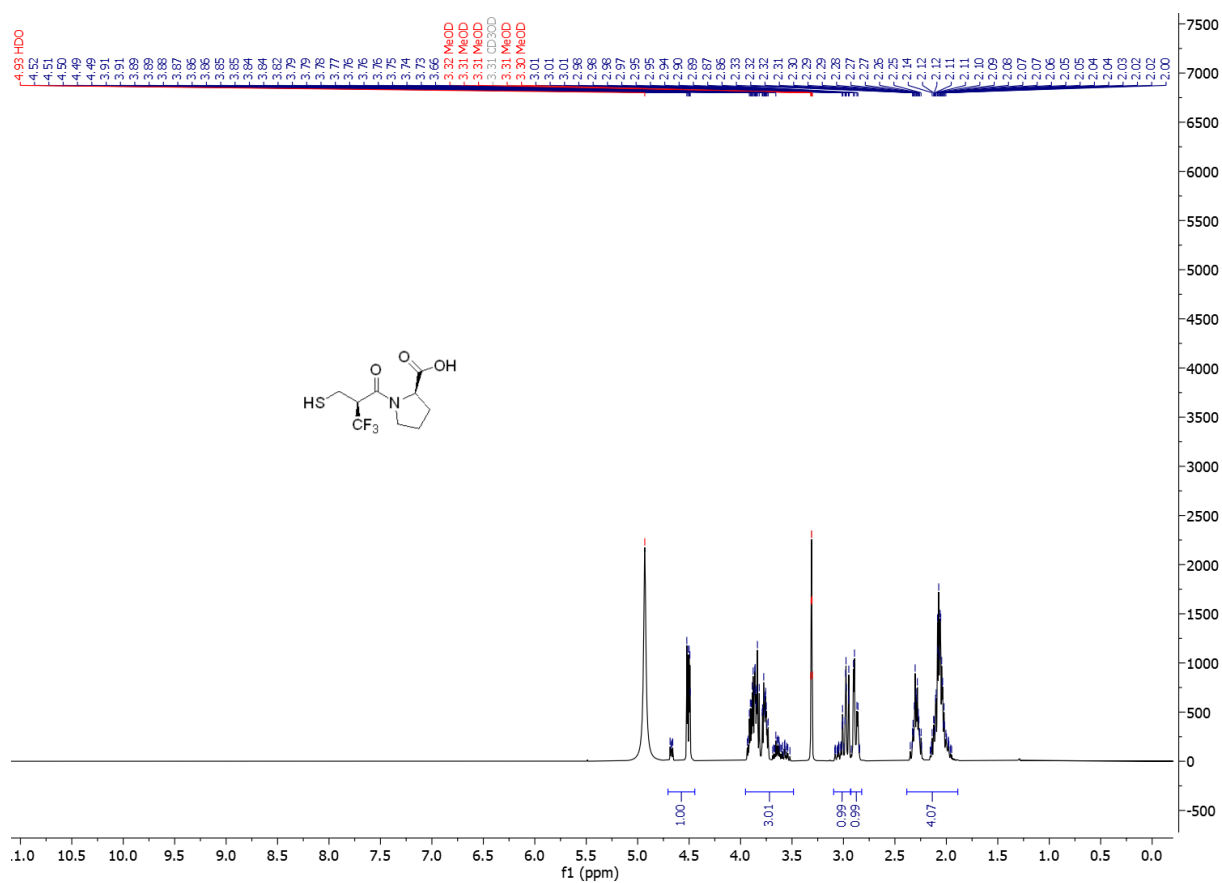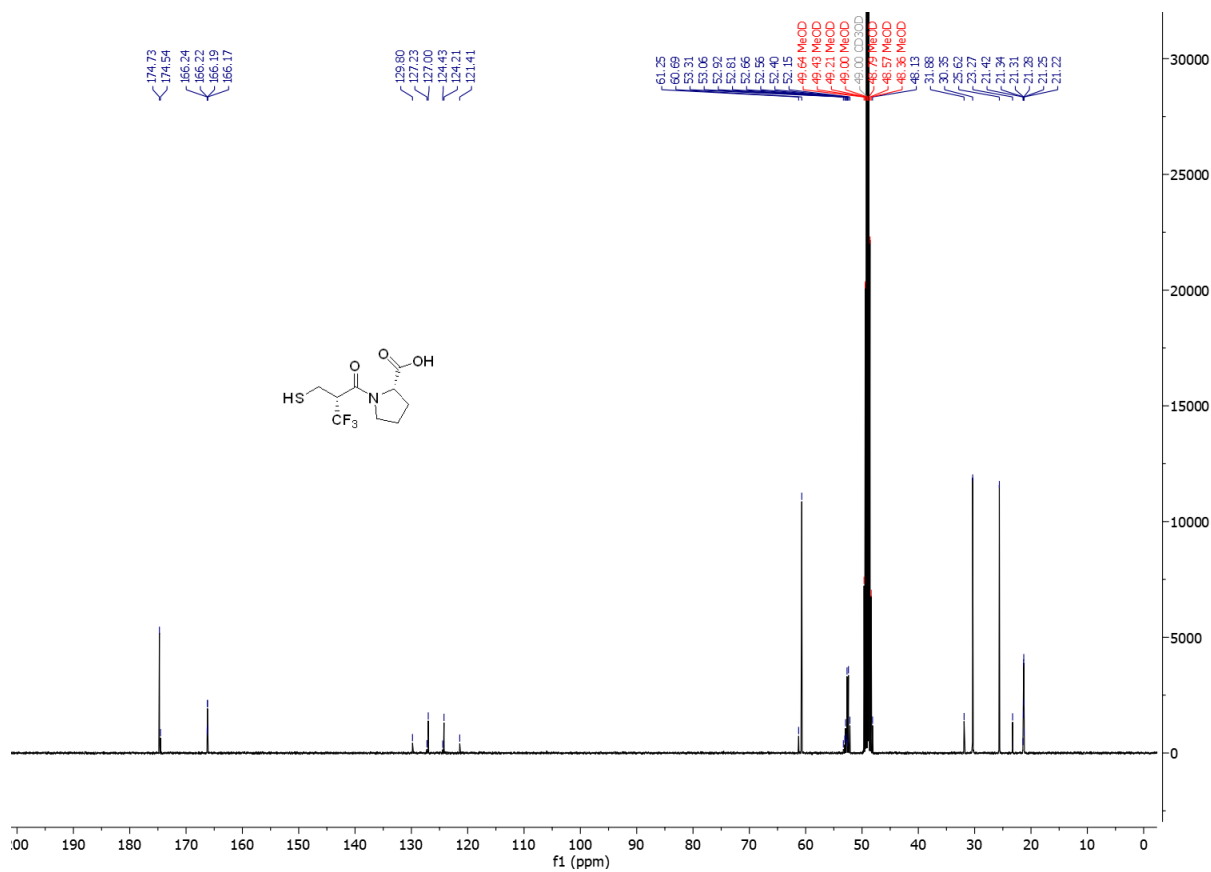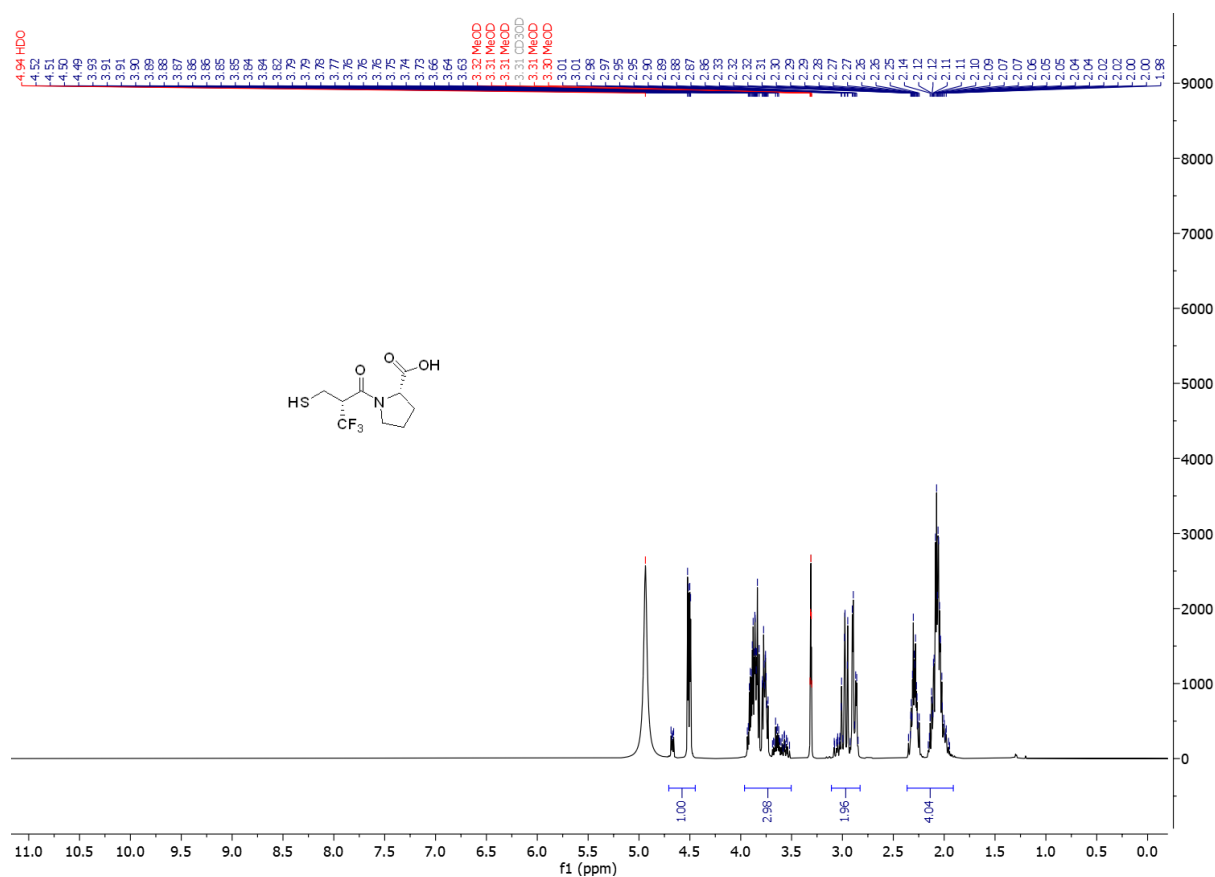
((*R*)-3,3,3-trifluoro-2-(mercaptomethyl)propanoyl)-*D*-proline ((2*R*,2`*R*)-**5αC**)
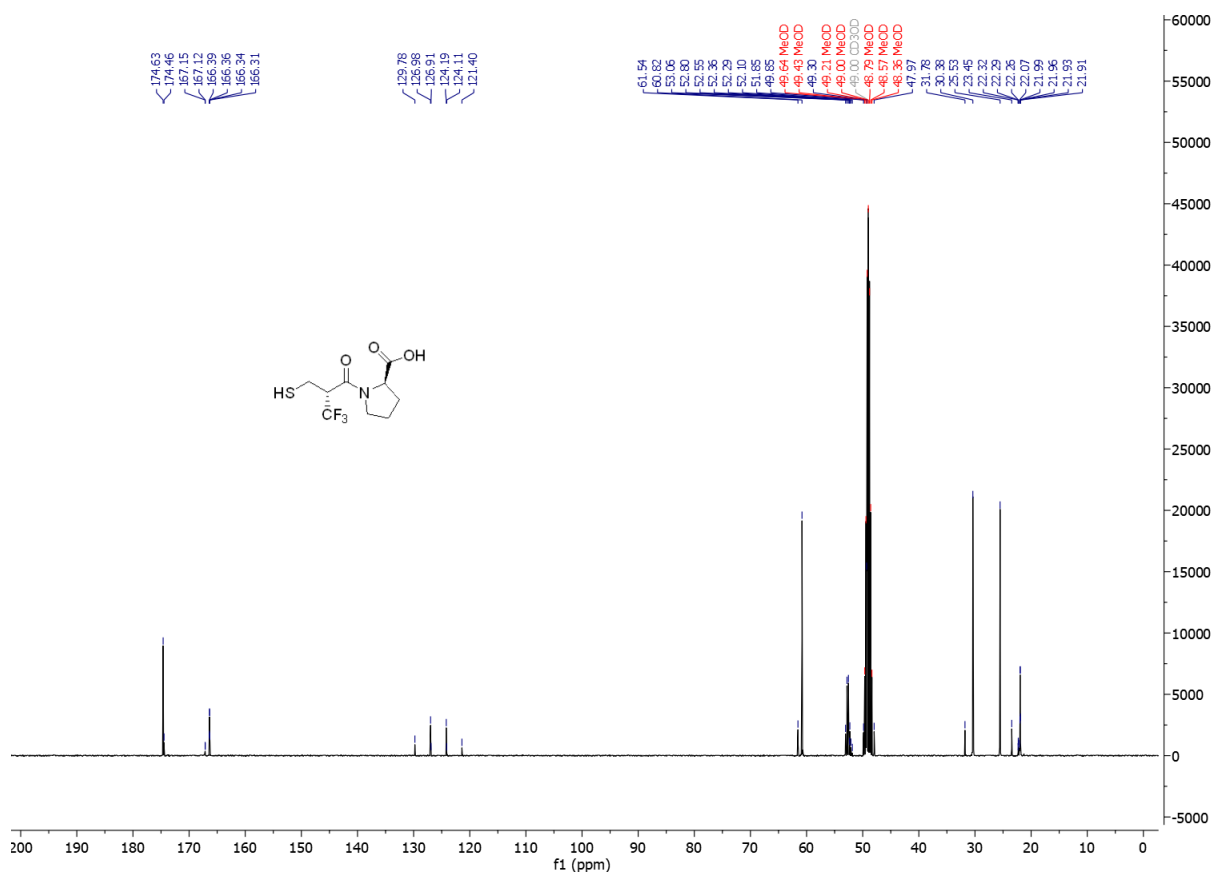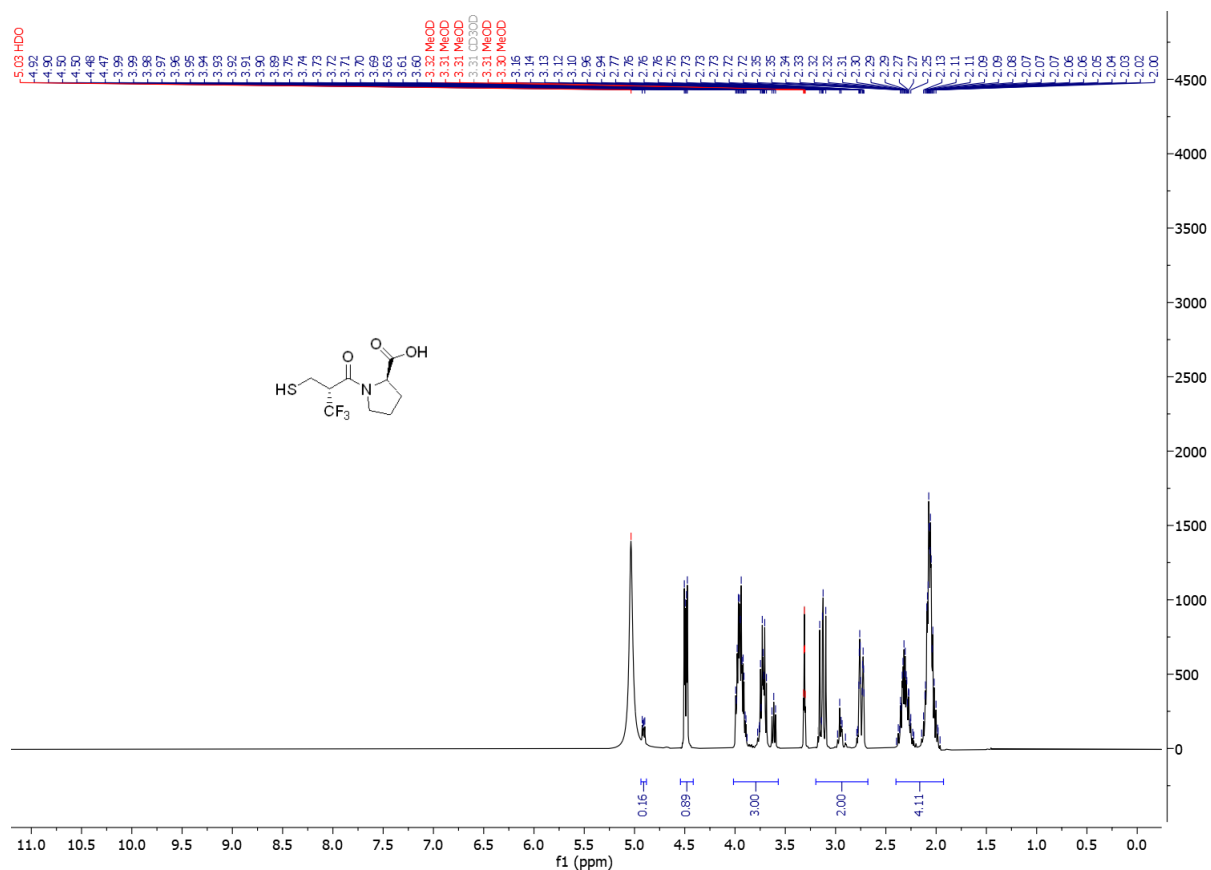
(4,4,4-trifluoro-3-mercaptobutanoyl)-*D*-proline (**5βC**)
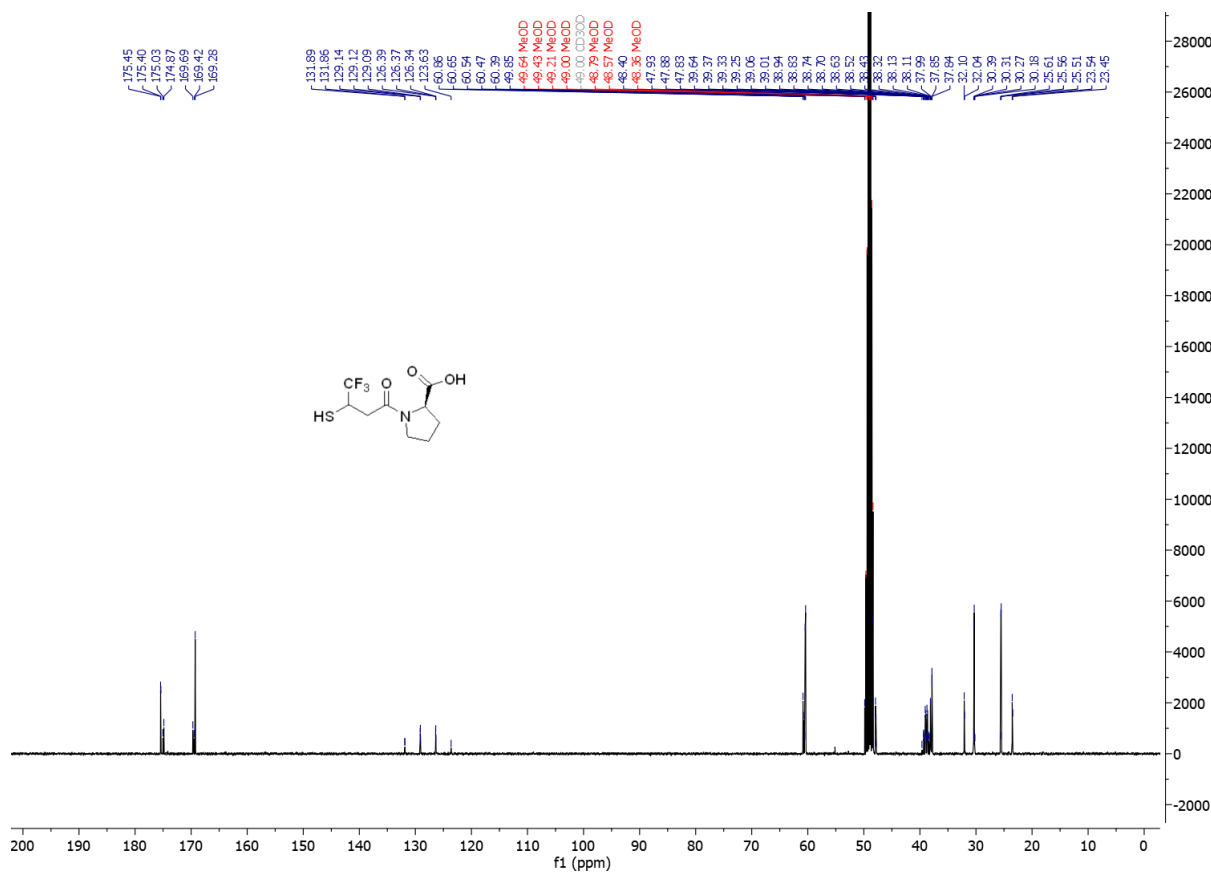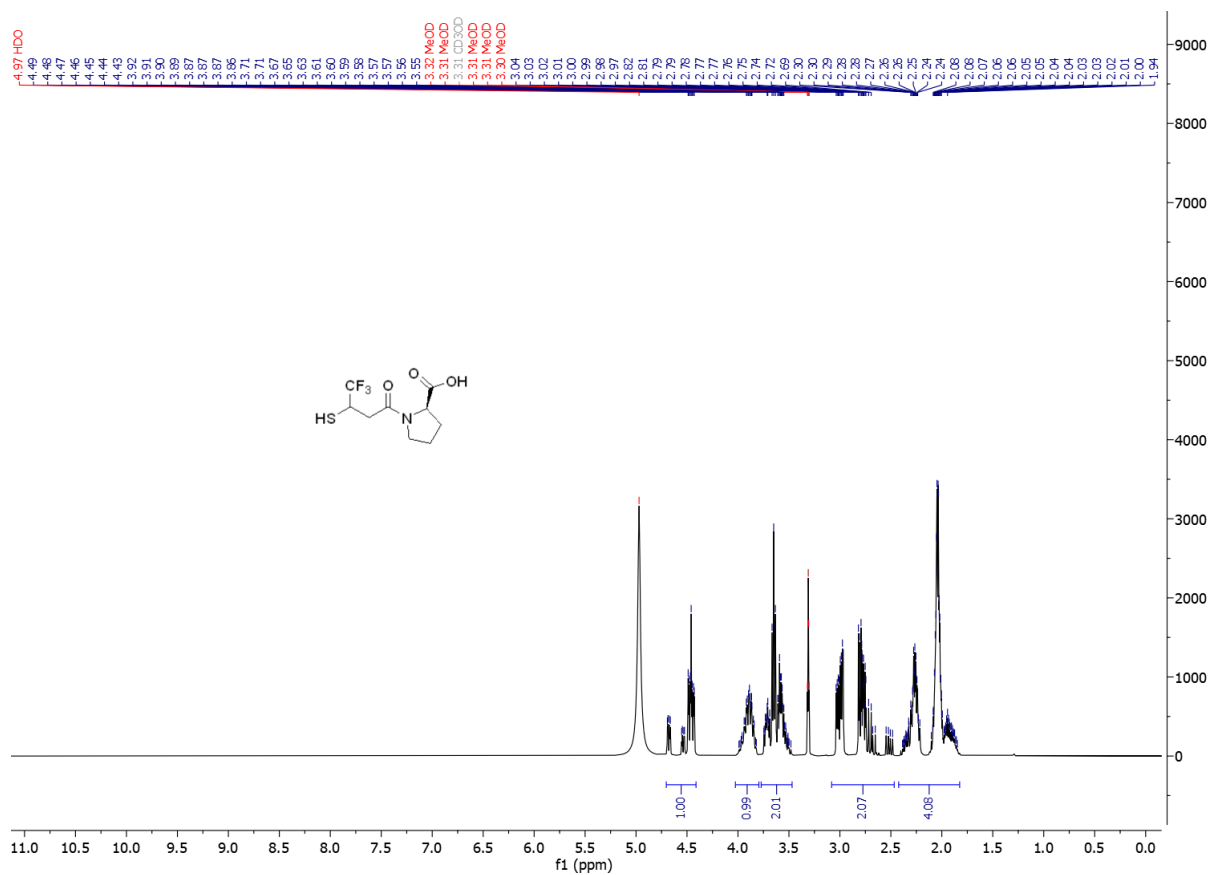
((*S*)-3,3,3-trifluoro-2-(mercaptomethyl)propanoyl)-*L*-proline ((2*S*,2`*S*)-**5αD**)
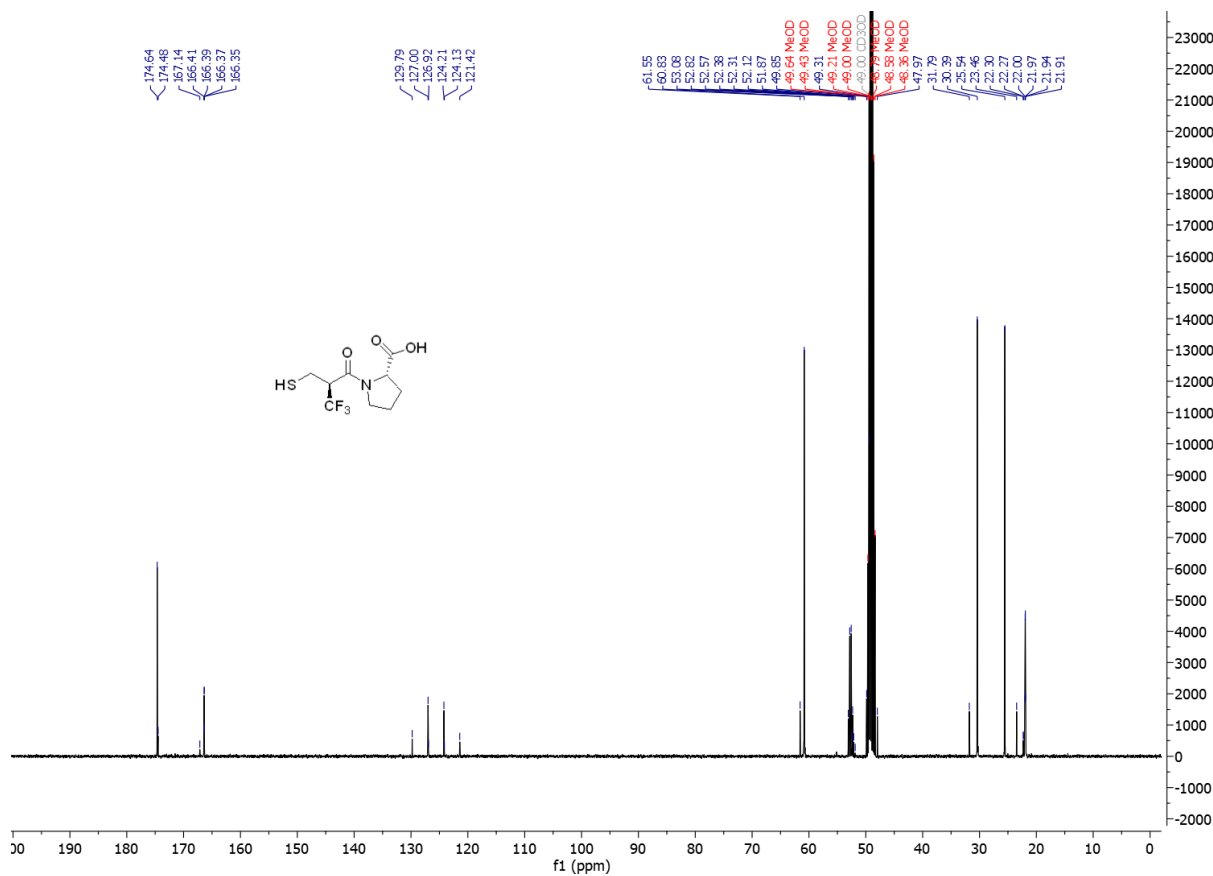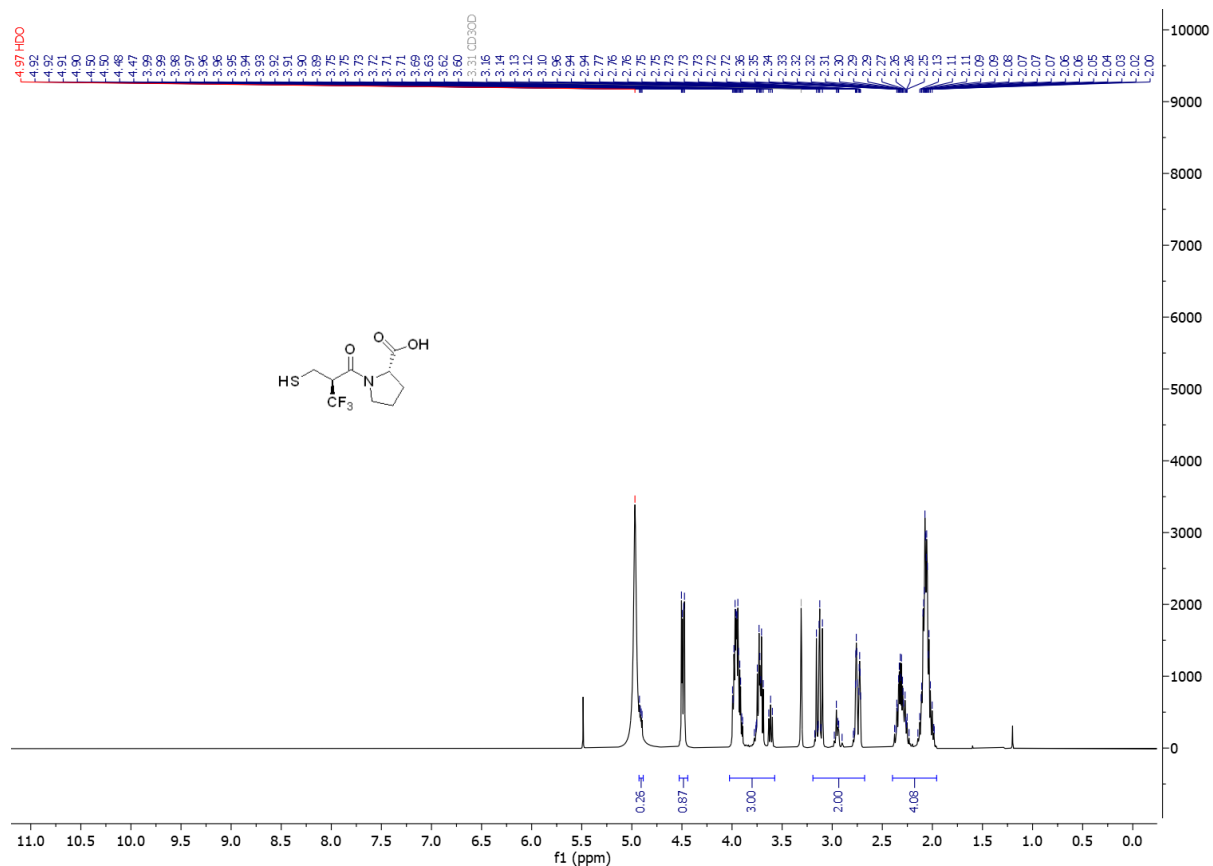
((R)-3,3,3-trifluoro-2-(mercaptomethyl)propanoyl)-L-proline ((2S,2`R)-**5αD**)

(4,4,4-trifluoro-3-mercaptobutanoyl)-*L*-proline (**5βD**)
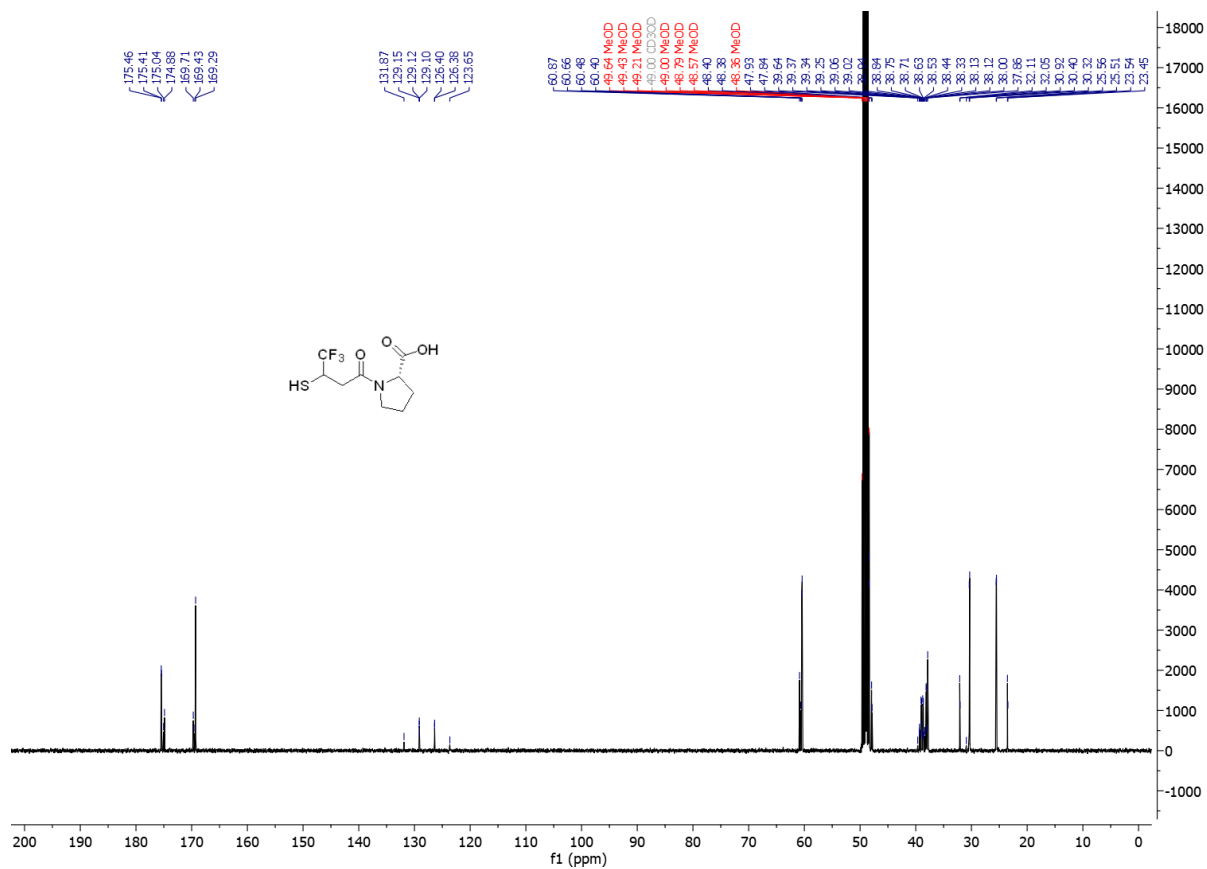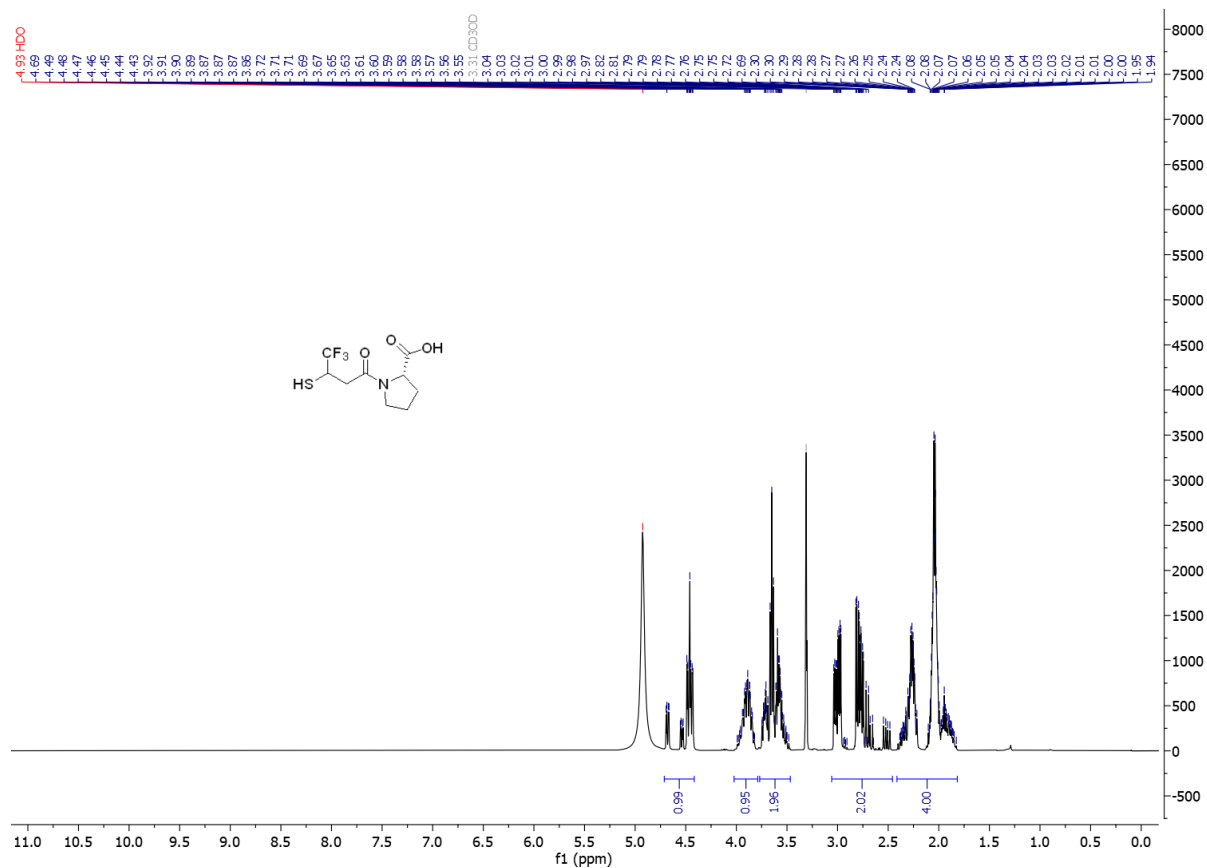
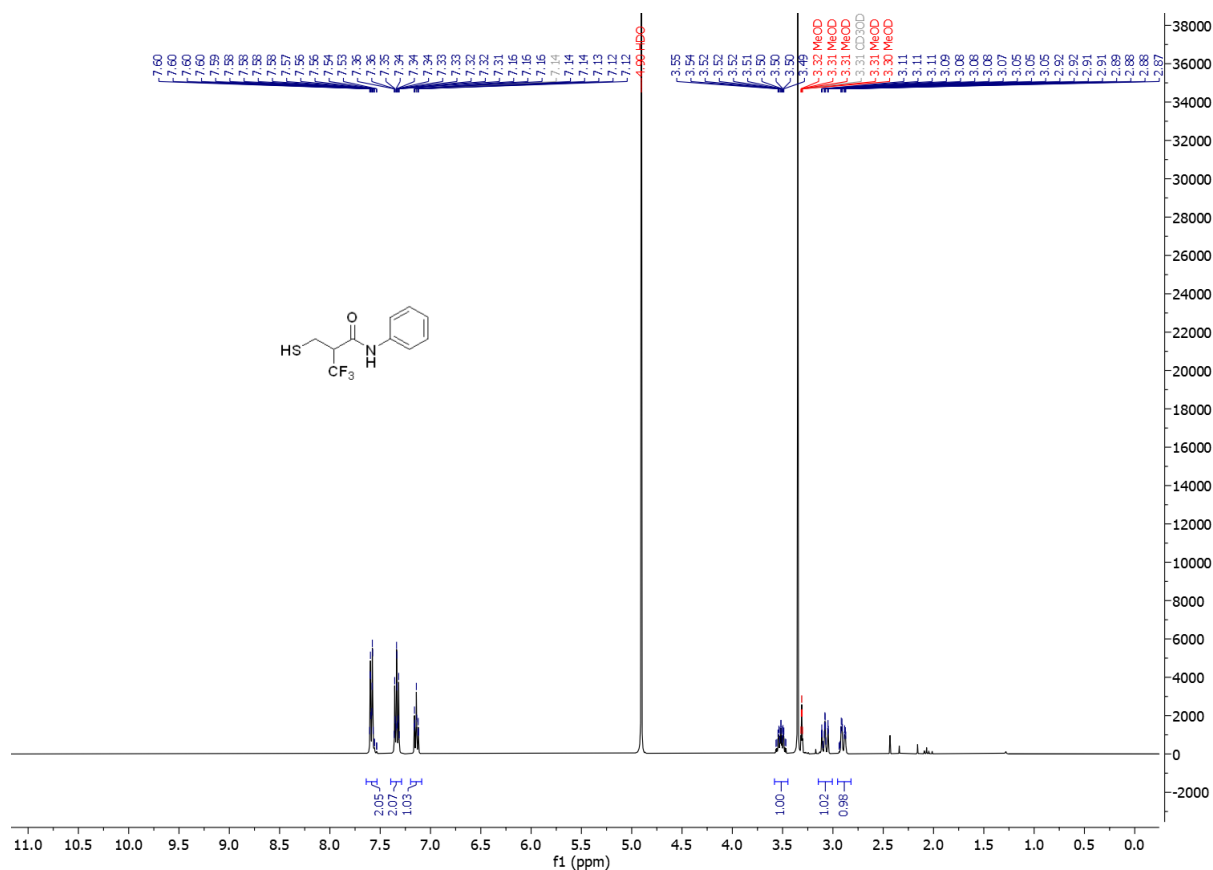(2*R*)-1-(4,4,4-trifluoro-3-mercaptobutanoyl)piperidine-2-carboxylic acid (**5αE**)
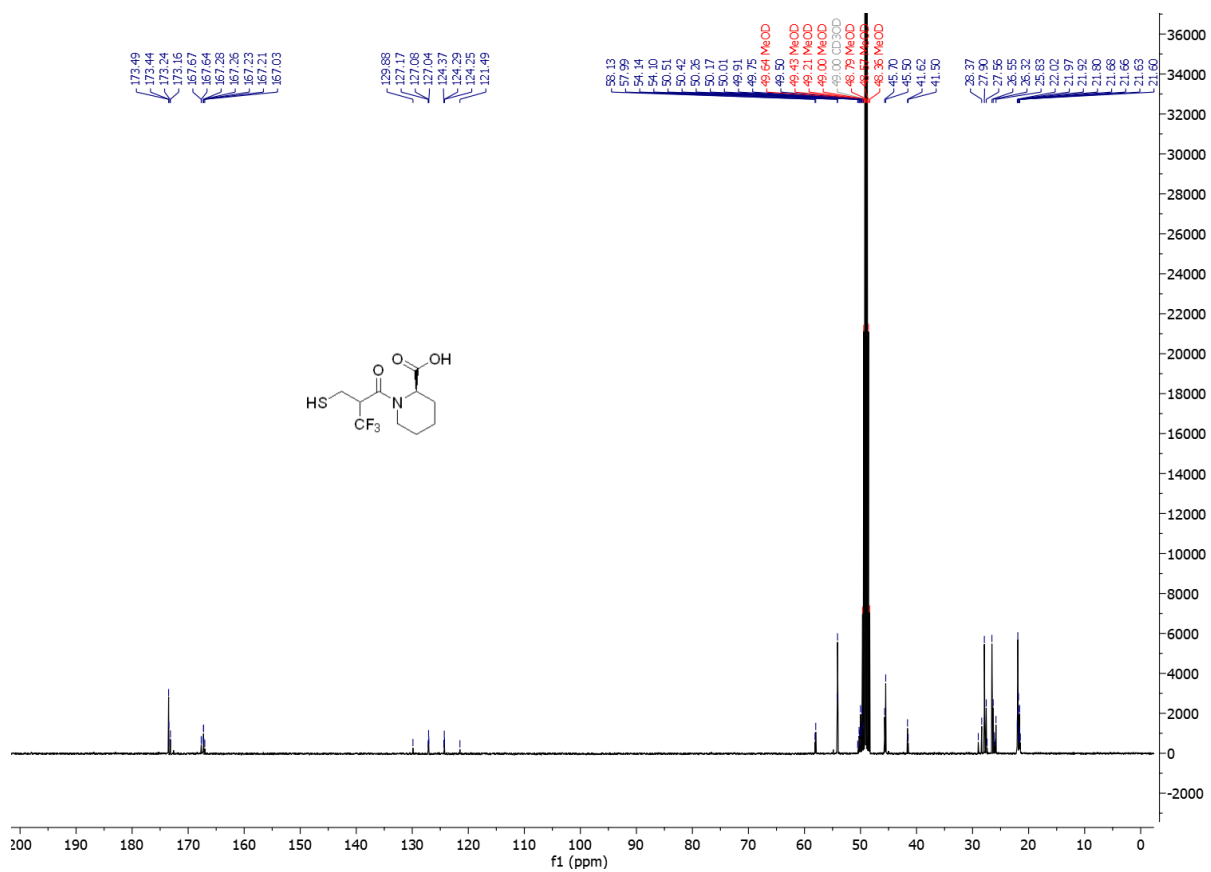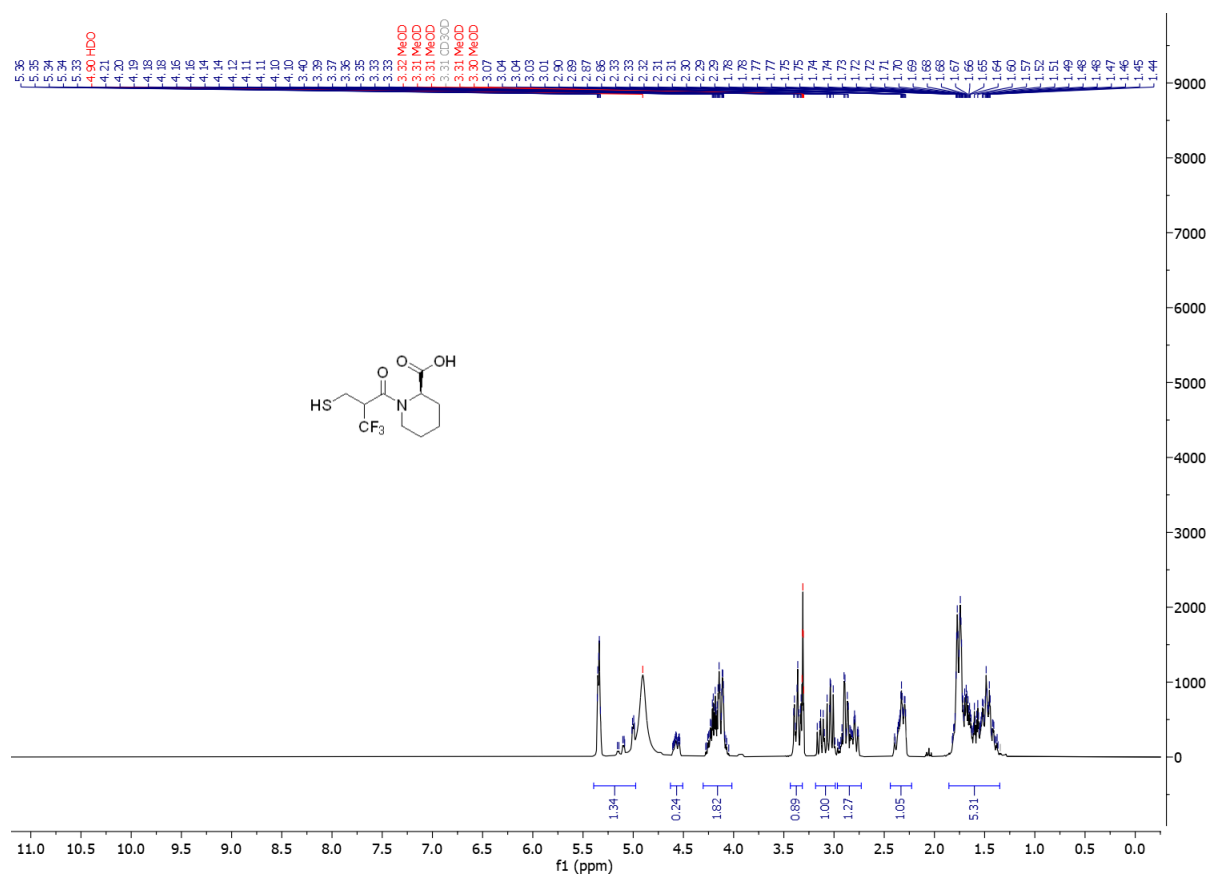
(2*R*)-1-(4,4,4-trifluoro-3-mercaptobutanoyl)piperidine-2-carboxylic acid (**5βE**)
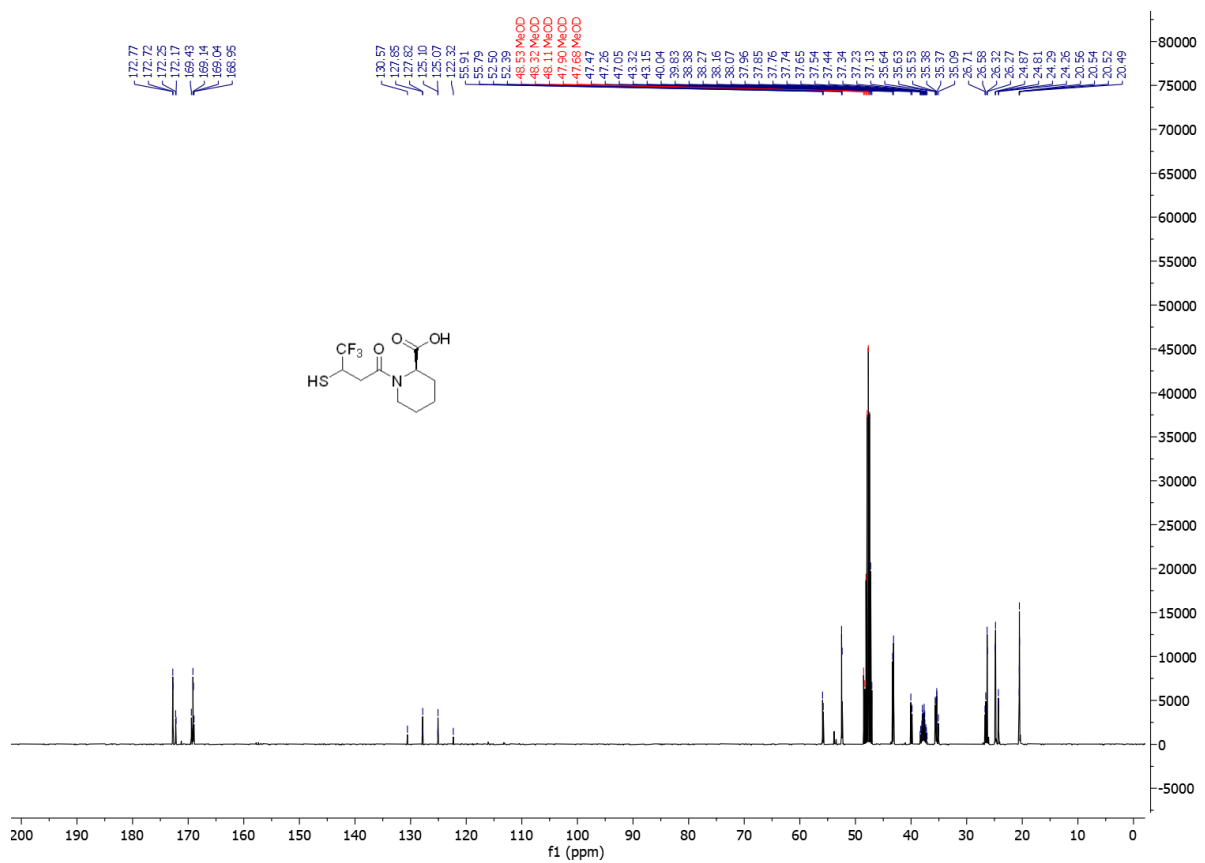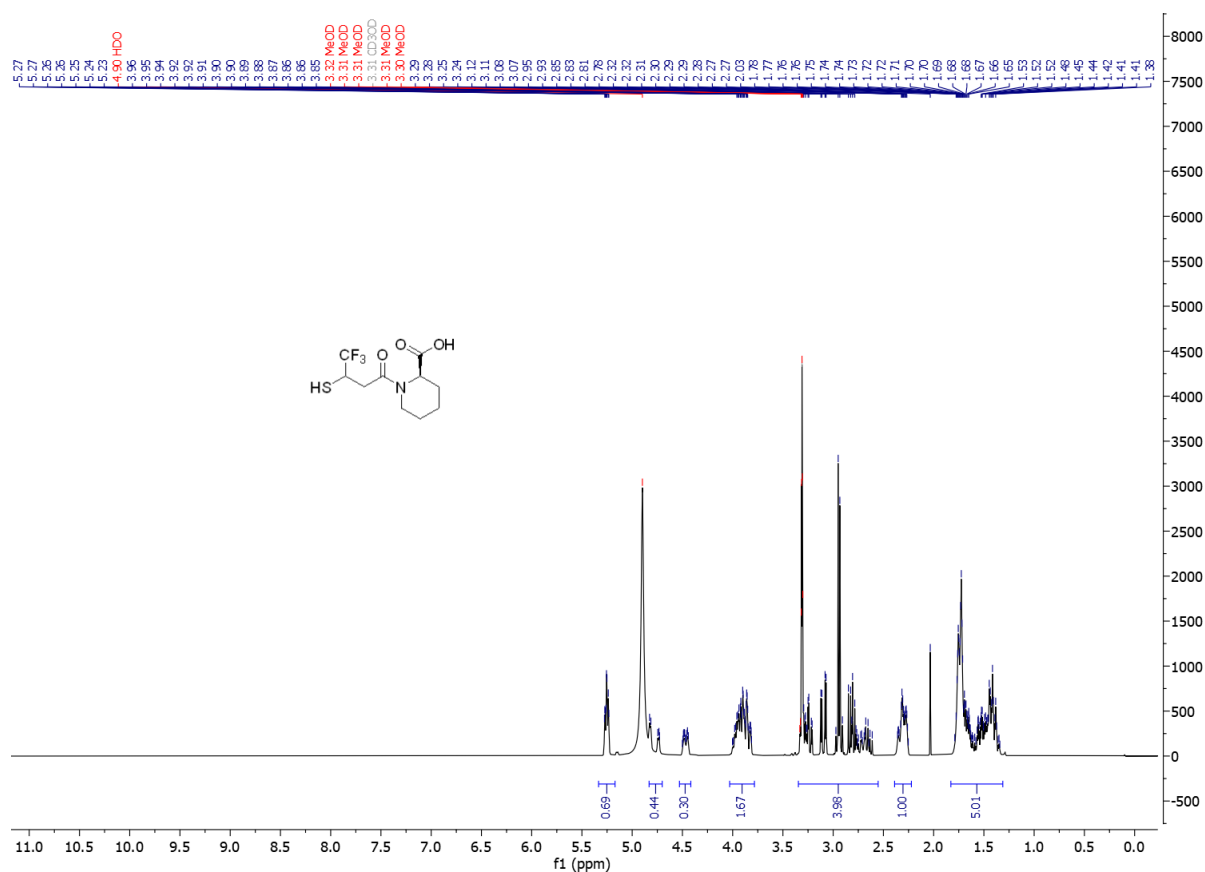
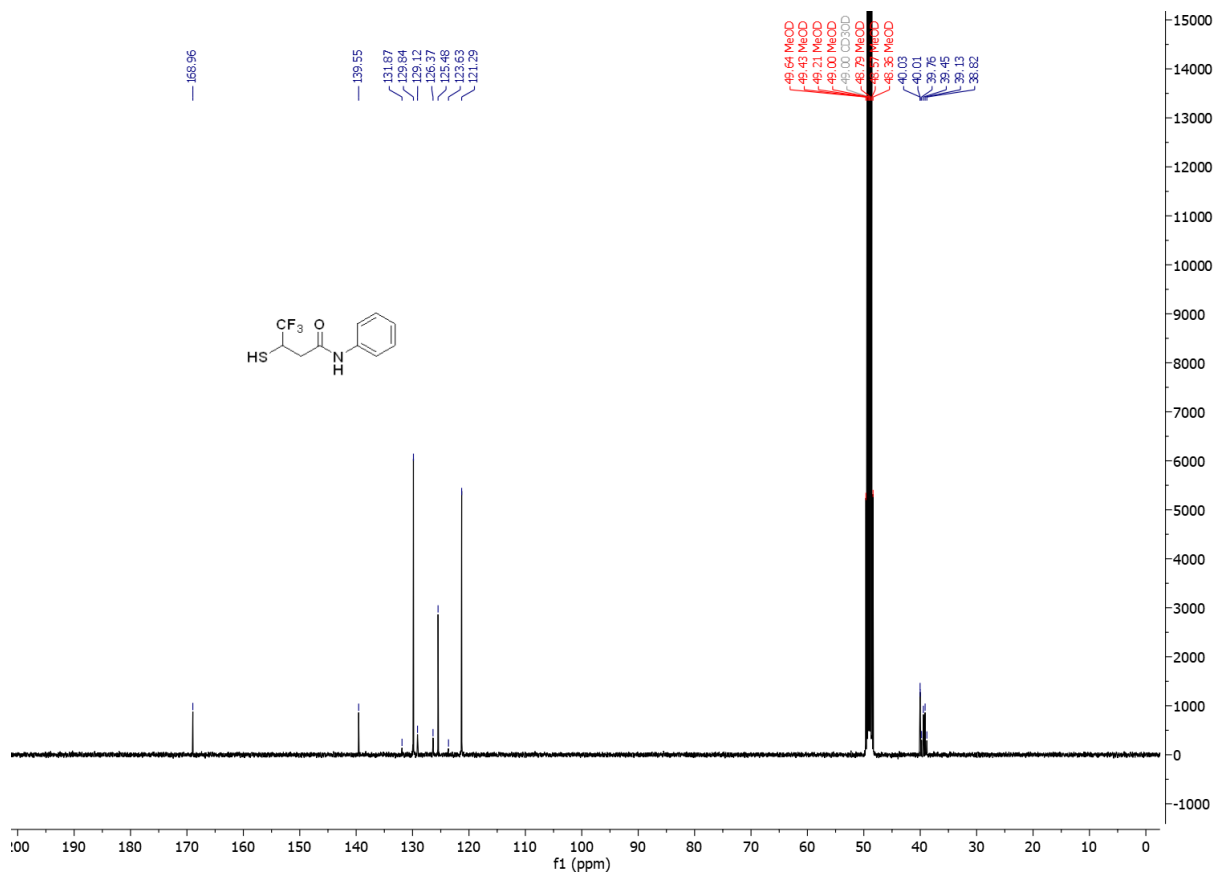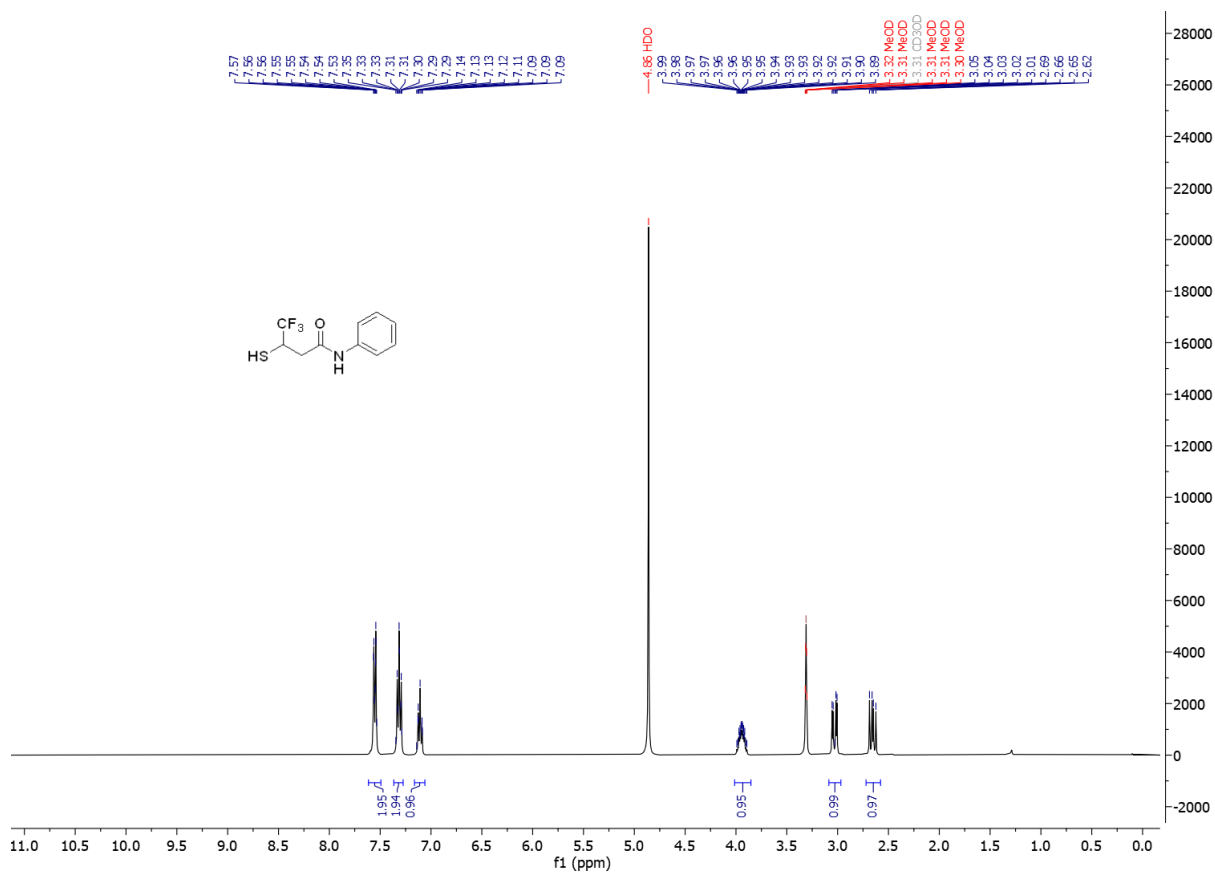# 1-(3,3,3-trifluoro-2-(mercaptomethyl)propanoyl)piperidine-4-carboxylic acid (**5αF**)
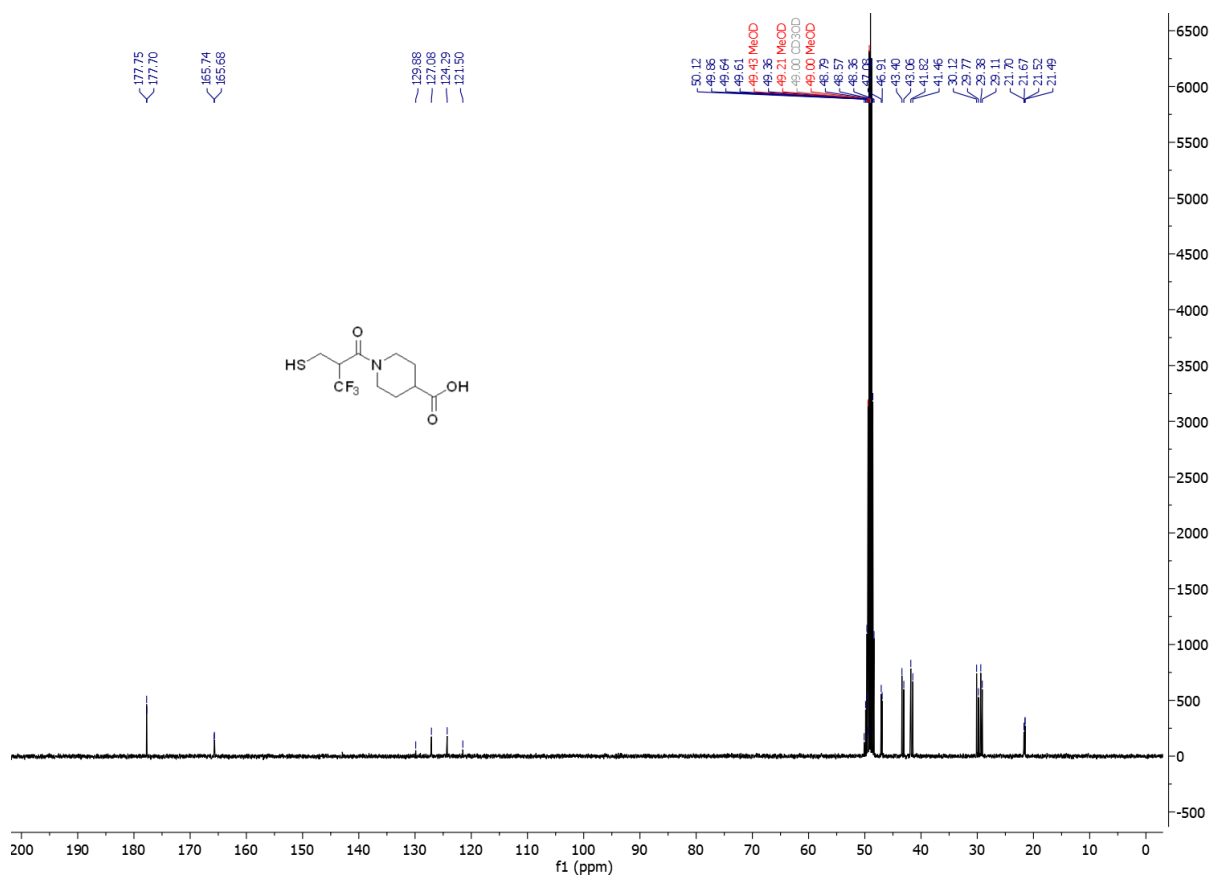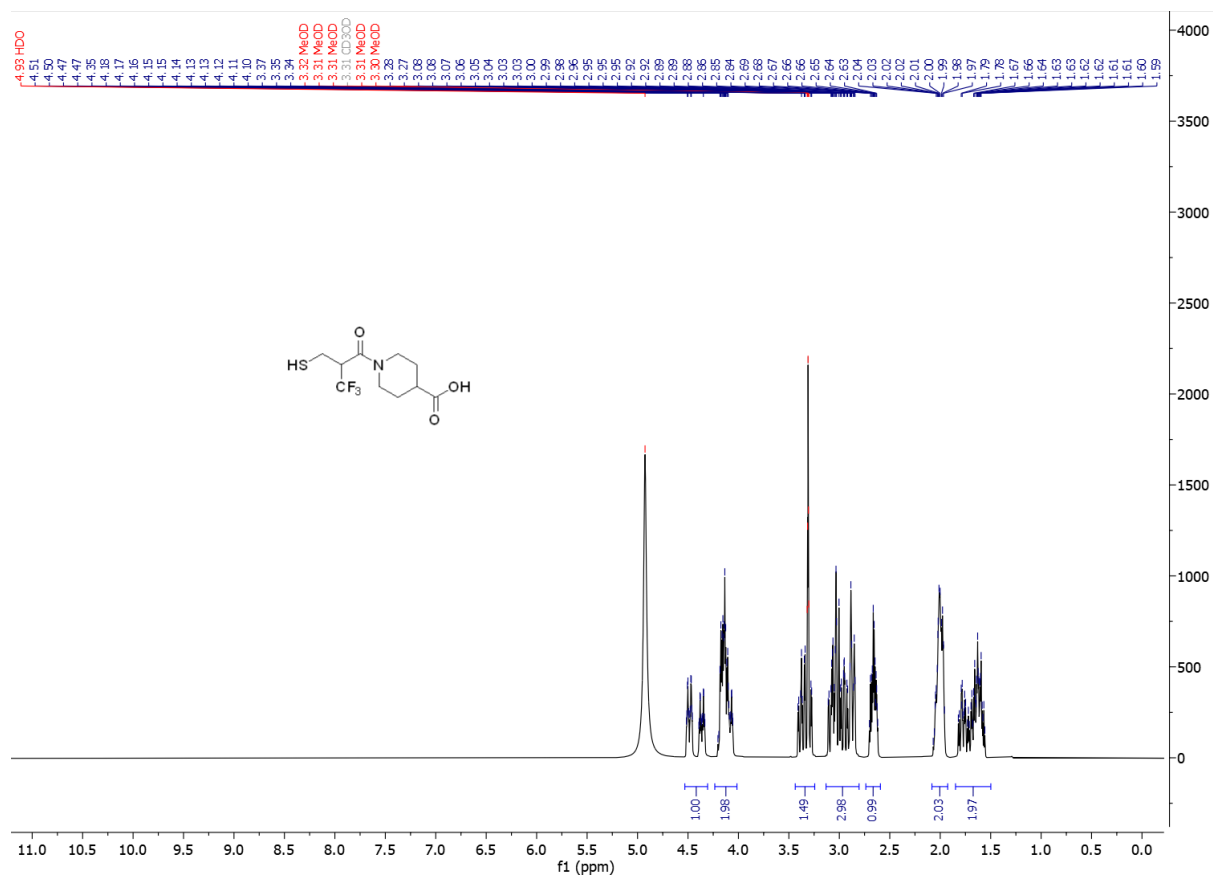
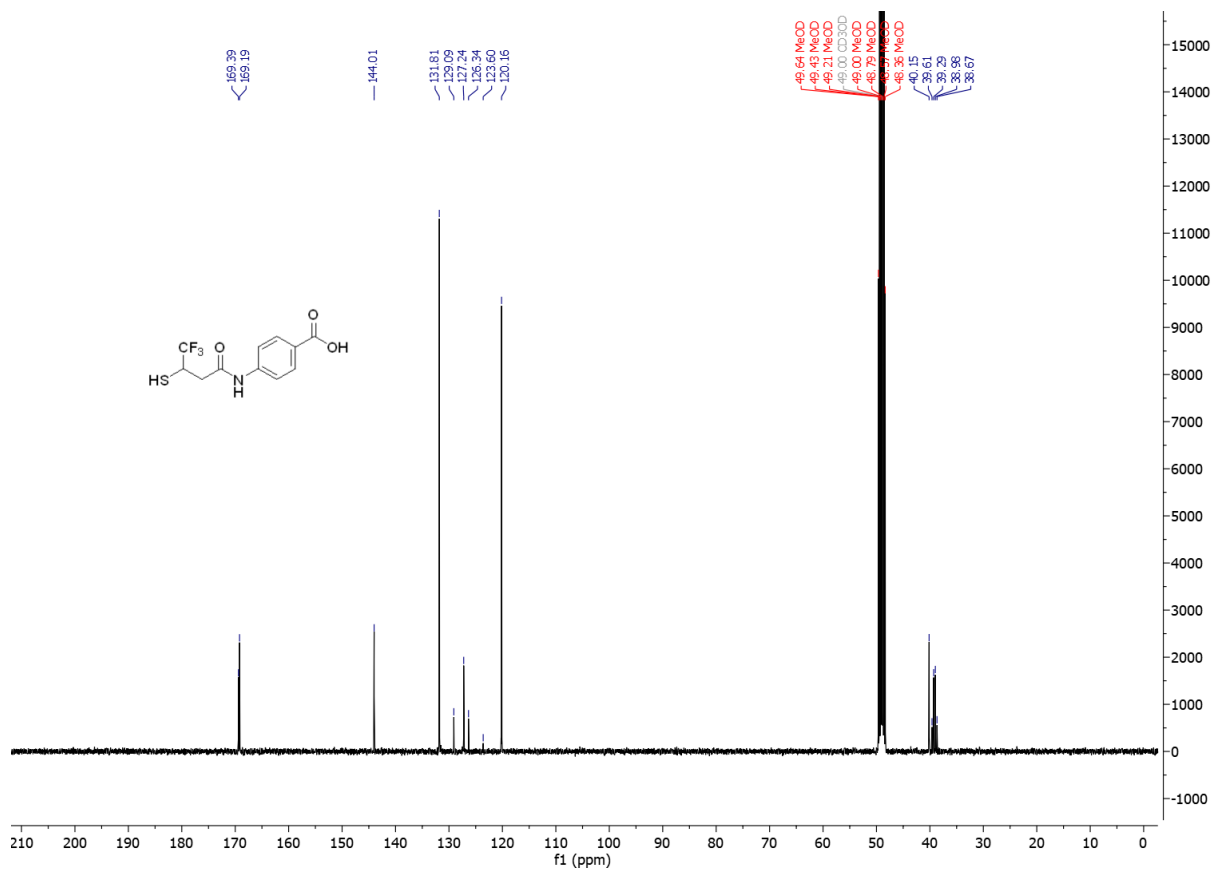# 1-(4,4,4-trifluoro-3-mercaptobutanoyl)piperidine-4-carboxylic acid (**5βF**)
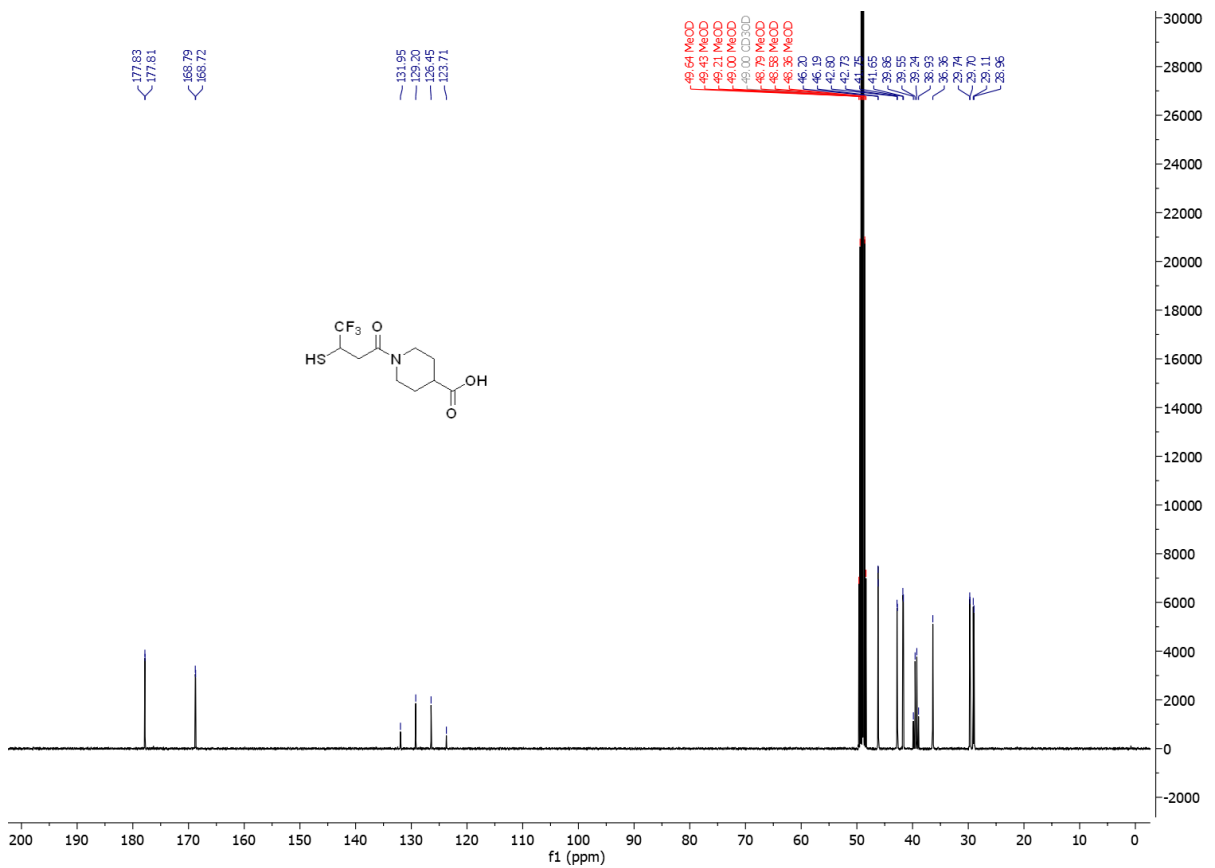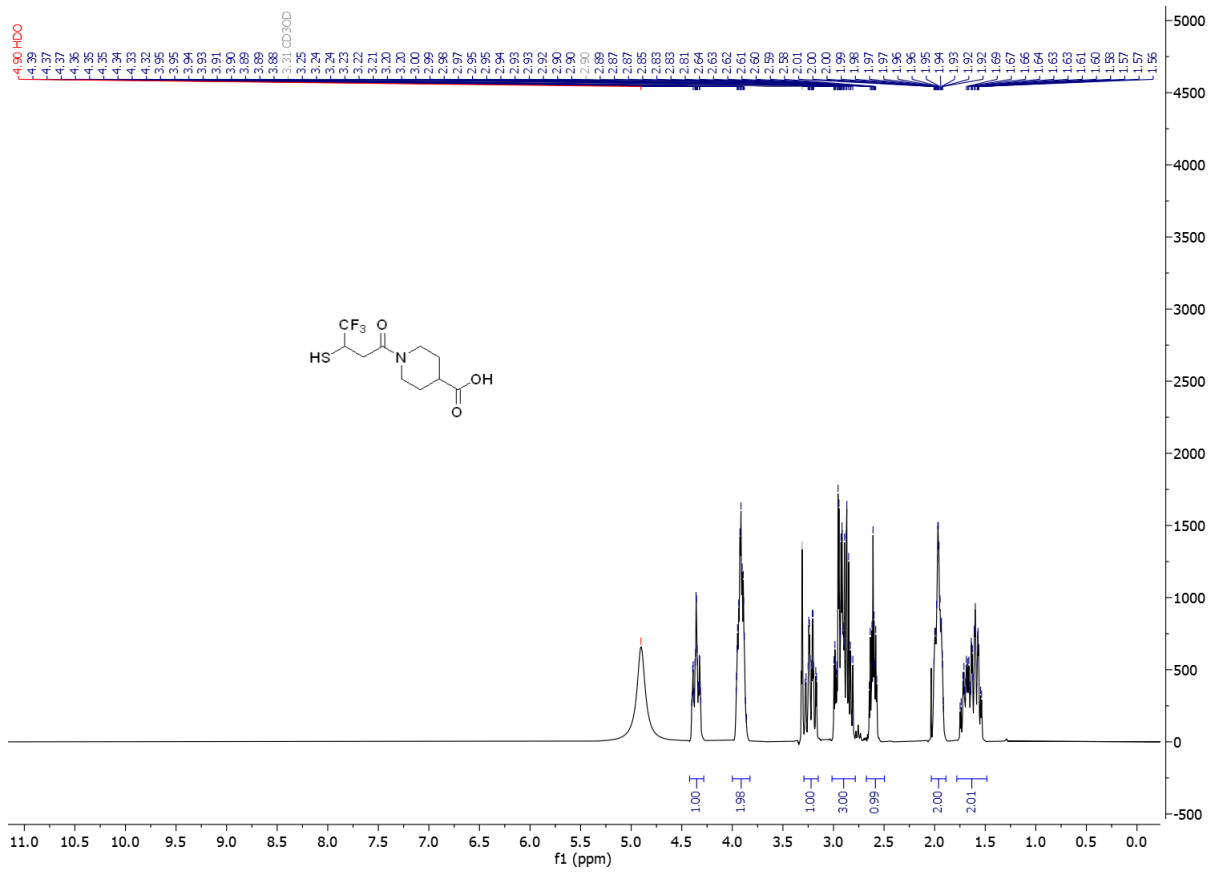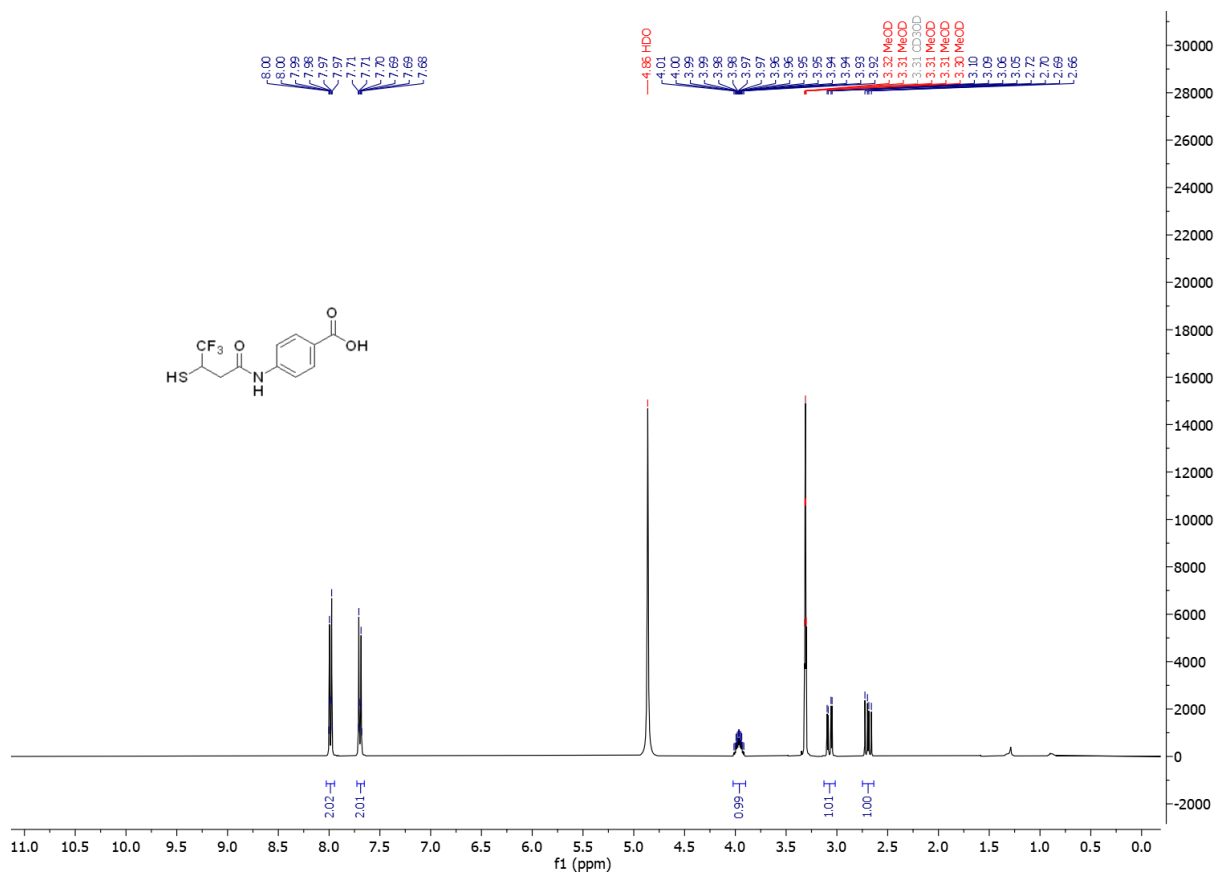
3,3,3-trifluoro-2-(mercaptomethyl)-N-phenylpropanamide (**5αG**)
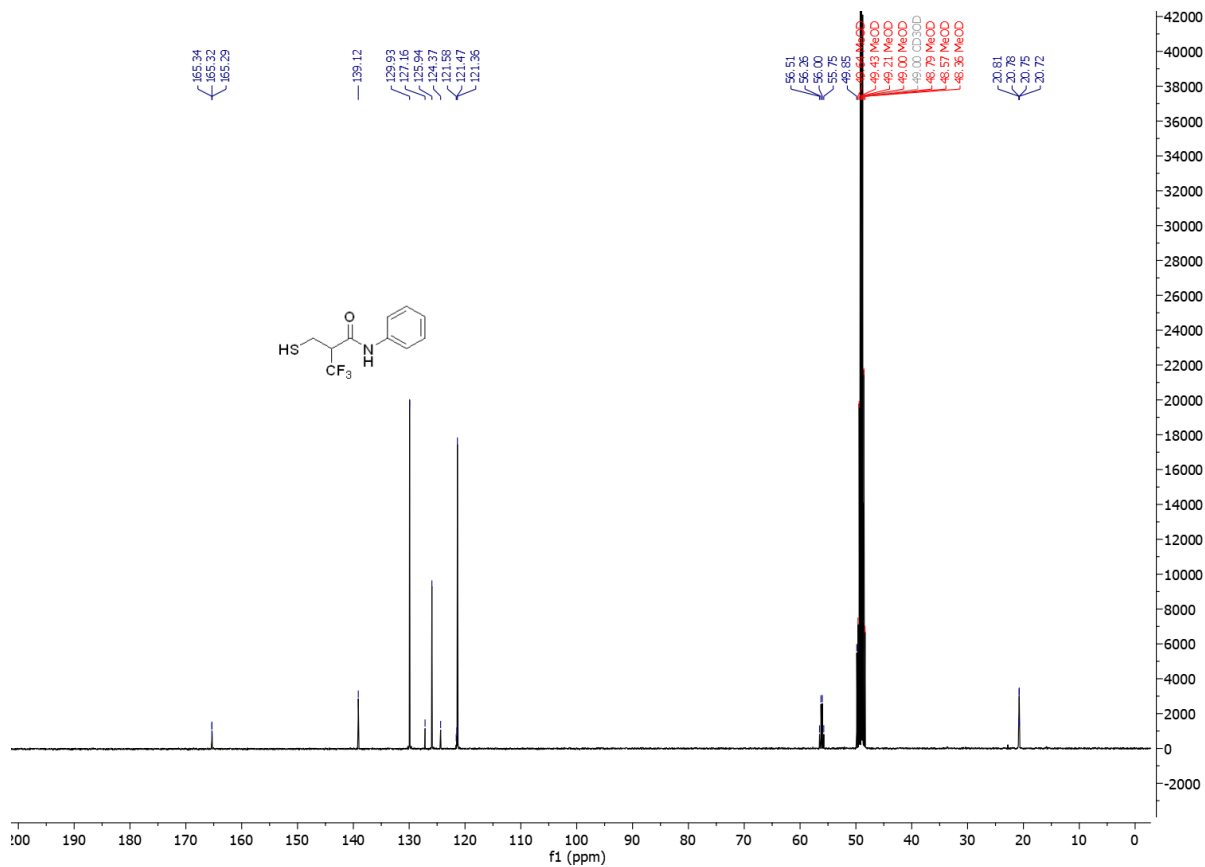
4,4,4-trifluoro-3-mercapto-N-phenylbutanamide (**5βG**)

4-(4,4,4-trifluoro-3-mercaptobutanamido)benzoic acid (**5βH**)

References

[1] M.D. Bartolowits, et al., ACS Omega, 4 (2019) 15181-15196.
[2] D. Buttner, et al., ACS Infect. Dis., 4 (2018) 360-372.
[3] T.P. Vasileva, et al., Russ. Chem. Bull., 46 (1997) 1230-1232.
[4] I. Ojima, et al., Drug Des. Discov., 11 (1994) 91-113.
[5] T. Christopeit, H.-K.S. Leiros, Bioorg. Med. Chem. Lett., 26 (2016) 1973-1977.
[6] C. Fröhlich, et al., J. Antimicrob. Chemother., 77 (2022) 2429-2436.
[7] Ø.M. Lorentzen, et al., bioRxiv, (2023) 2023.2010.2002.560492.
[8] Ø. Samuelsen, et al., PloS one, 12 (2017) e0187832.
[9] G.M. Sastry, et al., Journal of computer-aided molecular design, 27 (2013) 221-234.
[10] M.P. Jacobson, et al., Proteins, 55 (2004) 351-367.
[11] J.R. Greenwood, et al., Journal of computer-aided molecular design, 24 (2010) 591-604.
[12] J.C. Shelley, et al., J. Comput. Aid. Mol. Des., 21 (2007) 681-691.
[13] E. Harder, et al., Journal of chemical theory and computation, 12 (2016) 281-296.
[14] R.A. Friesner, et al., J. Med. Chem., 47 (2004) 1739-1749.
[15] T.A. Halgren, et al., J. Med. Chem., 47 (2004) 1750-1759.
[16] R.A. Friesner, et al., J. Med. Chem., 49 (2006) 6177-6196.

Paper II

The Use of Fluorinated Aliphatic Thiols in the Design of Cephalosporin Conjugates

Alexandra Kondratieva, Philip Rainsford, Perwez Bakht, Hanna-Kirsti S. Leiros, Ranjana Pathania, Annette Bayer

Manuscript

The Use of Fluorinated Aliphatic Thiols in the Design of Cephalosporin Conjugates

Alexandra Kondratieva[a], Philip Rainsford[a], Perwez Bakht[b], Hanna-Kirsti S. Leiros[a], Ranjana Pathania[b], Annette Bayer[a]*

[a] *Department of Chemistry, UiT The Arctic University of Norway, NO-9037 Tromsø, Norway.*
[b] *Department of Biosciences and Bioengineering, Indian Institute of Technology, Roorkee, Uttarakhand-247667, India.*
Corresponding author.

MANUSCRIPT INFO

ABSTRACT

Antimicrobial resistance is considered a global health challenge, with the dissemination of metallo-β-lactamase (MBL)-expressing bacteria presenting a major clinical threat. In this study, we synthesized and investigated a series of novel cephalosporin conjugates envisioned to release MBL inhibitors upon MBL-mediated hydrolysis. The designed compounds consist of a cephalosporin core linked to trifluoromethylated aliphatic thiol MBL inhibitors. In the presence of the New Delhi Metallo-β-lactamase-1 (NDM-1), the conjugates are hydrolyzed and release the corresponding thiol as confirmed by spectroscopic assays. The conjugates exhibited potent inhibitory activity against several B1 MBLs. In addition, the application of ^{19}F NMR as an alternative method for hydrolysis monitoring was exemplified. These findings demonstrate the potential of altering the leaving group ability of aliphatic thiol-based inhibitors to exploit antibiotic resistance for selective release of inhibitors targeting MBL-producing bacteria.

1. Introduction

The use of β-lactams (BLs), the most important class of antibiotics, is continuously compromised by the development of resistance mechanisms in bacteria.[1] Expression of β-lactamases (BLases), enzymes capable of destroying the β-lactam ring, is of particular concern. Metallo-β-lactamases (MBLs) possess the ability to inactivate the majority of β-lactams and there are currently no approved drugs targeting these enzymes.[2-4] Hydrolysis of the β-lactam ring, mediated by MBLs, occurs through a water molecule activated by one or two zinc ions present in the active site.[5]

To exploit β-lactamase activity compounds were designed based on the principal that BLase-mediated cleavage of the β-lactam ring, followed by spontaneous fragmentation, leads to the release of a reporter molecule or a bioactive species. The compounds reported in literature predominantly consist of a cephalosporin core linked to an antibiotic, siderophore, membrane permeabilizer or inhibitor. Various BL probes have been designed to be applied in diagnostics, imaging and as co- and pro-drugs.[6]

A promising strategy to combat resistance caused by MBLs is the development of β-lactamase inhibitors. These inhibitors majorly act via coordination to or removal of the zinc ions from the active site. Many structurally diverse compound classes, such as sulfones, carboxylates, diazabicyclooctanones, boronates and thiols, have been described.[7-8] Thiols or, more specifically aliphatic thiols, being among the most investigated MBL inhibiting compound classes, have gained attention due to their broad-spectrum inhibition of all three MBL subclasses.[9-10]

A major limitation of thiol-based MBL inhibitors is their tendency to form disulfides, resulting in the loss of zinc binding ability.[11] Due to this stability issue, protecting the thiol moiety with a scaffold that is removable under certain conditions is of great interest. Furthermore, using zinc-binding molecules in a more complex biological surrounding, could inevitably lead to selectivity issues, as metalloproteins are estimated to constitute a substantial part of the human proteome.[12] Controllable release of an inhibitor, only in the presence of the target MBL, would limit off-target effects, while the BL-like structure of the conjugate could help overcome permeability issues. Thus, a selection of cephalosporin-based conjugates designed to release thiol inhibitors have been described in literature.[13-17]

Hydrolysis of BLs has been thoroughly investigated and it has been established that hydrolysis of the β-lactam ring, in the presence of a suitable leaving group, leads to release of the attached moiety and formation of a vinylic elimination product **V** (Fig. 1, top). While aromatic thiols have proven to be successfully released upon enzymatic hydrolysis, aliphatic thiol release remains a problem. Liberation of the inhibitor, in this case, has been shown to happen slowly or not at all due to the poor leaving group ability of the aliphatic thiols.

In a recent study[16], even though the conjugates demonstrated MBL inhibition, the thiols were established to be unreleased after enzymatic hydrolysis, resulting in compounds with the general structure **H** (Fig. 1, top), based on NMR and MS analysis. Intermediates possessing both the cleaved β-lactam ring and the leaving group were also
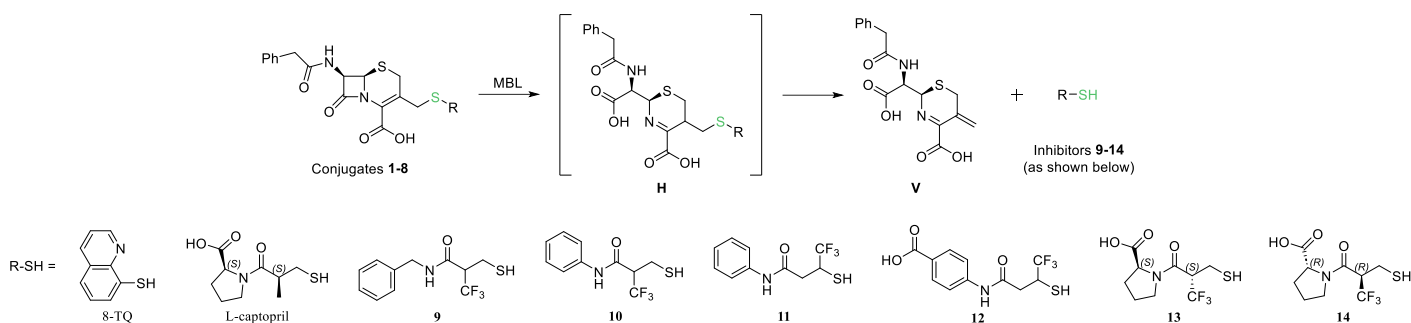
Figure 1. Cephalosporin conjugates of thiols previously reported as MBL inhibitors: **9-14**, 8-TQ and L-captopril.

obtained in a study of alkaline degradation of oxacephem derivatives.[18] Depending on the leaving group, alkaline hydrolysis led to mixtures of various content, with or without the production of the vinylic elimination product. These examples demonstrate that β-lactam ring cleavage and thiol release are not necessarily simultaneous processes and that, in order to design a conjugate releasing an aliphatic thiol inhibitor, alteration of the leaving group ability is necessary.

We hypothesized that introduction of electron-withdrawing groups in the vicinity of the thiol could lead to the release of the inhibitor. Thus, we envisioned attaching trifluoromethylated aliphatic thiol MBL inhibitors to a cephalosporin scaffold. To investigate this strategy, conjugates **2-8** were designed (Fig. 1), combining a cephalosporin core with previously reported thiol MBL inhibitors, including L-captopril and compounds **9-14**.[19] The hydrolysis of the conjugates under basic and enzymatic conditions was studied using LC-MS and NMR techniques. Furthermore, the inhibitory activity of the conjugates against different B1 MBLs was investigated.

2. Results and Discussion

The cephalosporin-thiol conjugates were synthesized following a slightly adapted literature procedure[16] (Scheme 1). The corresponding thiols were linked to 7-aminocephalosporanic acid (7-ACA) by Lewis acid catalysis, followed by acylation to yield compounds **1-8**. Compounds **3-6** were obtained as diastereomeric mixtures, given that the used thiols were a mixture of enantiomers. Conjugate **1** was synthesized as a reference compound, which has been shown to release 8-thioquinoline (8-TQ) upon enzymatic hydrolysis.[13]

The hydrolysis of cephalosporin-based compounds has been extensively studied, with conditions varying from buffer systems to enzyme-catalyzed assays.[20-22] To gain a better understanding of the leaving group ability of the thiols for the synthesized compounds we decided to test both base- and enzyme-mediated hydrolyses. To assess release of the thiol inhibitors we used HPLC-MS and NMR to determine the presence of the released thiol **9-14** and elimination product **V**, respectively.

Previously, cephalosporin hydrolysis has been studied utilizing MS techniques.[13, 16-17] In a similar manner, we

tested the hydrolysis of compounds **2-8** in an aqueous 1 M Na_2CO_3 solution. Namely, the respective compound was incubated in the basic solution and aliquots were taken out at different time points (0.5, 1 and 4 h) and analyzed using HPLC-MS. In all cases, the formation of the vinylic elimination product (**V**) was observed through its relative abundance in the sample, determined by MS, due to the lack of UV-activity of the aforementioned compound. For thiols **10-12** monitoring of the release was based on the detection of the free thiol, as an aromatic ring present in the structure enables UV-activity of the compounds. The results (see Supporting Information, Fig. S1-S8) demonstrated that the compounds could be divided into three groups based on the contents of the mixtures obtained after hydrolysis. Compounds **5** and **6** seemed to be the most promising conjugates in terms of inhibitor release, while compound **2** mostly resulted in hydrolysis of the BL ring without the release of L-captopril (compound **2H**). For compounds **3**, **4**, **7** and **8** the vinylic elimination product was detected, however majorly the product with the hydrolyzed β-lactam ring (**H**) without the thiol being released was observed.

Next, we switched to a weaker base – ammonium carbonate, thus testing conditions closer to those of enzymatic hydrolysis. We used the 7-phenylacetamide derivative of the commercially available 7-ACA (compound **15**, Fig. 2, A) as a positive control. After incubation in 3 M $(NH_4)_2CO_3$ for 2 h, the peak of the conjugate **15** (m/z = 391.09) had disappeared, indicating that full consumption of compound **15** had occurred. The two emerged peaks with m/z = 348.10 corresponded to the mass of the vinylic elimination product (**V_N**), implying cleavage of the β-lactam ring by ammonia and release of the allylic leaving group (OAc). In contrast, under the same conditions, the conjugate prepared from L-captopril (compound **2**, Fig. 2, B) did not produce the elimination product, according to MS. While the conjugate peak (m/z = 548.15) was no longer present after 2 h, showing full consumption of the conjugate, a new peak with m/z = 563.17 was observed. This corresponded to the formation of intermediate **2H_N**, in which the β-lactam ring has been opened, but L-captopril is still attached to the compound. This result is in line with previous reports using aliphatic thiols as leaving groups[16], and is attributed to their poor leaving group ability. Next, compound **5** was subjected to the
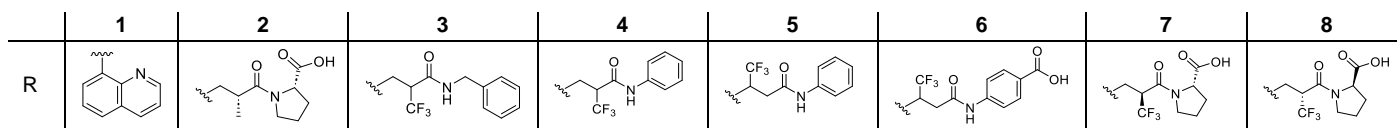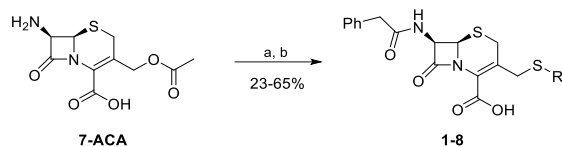
Scheme 1. Synthesis of conjugates 1-8. Reaction conditions: (a) BF$_3$·Et$_2$O, acetonitrile, 50 ºC, 2 h; (b) phenylacetyl chloride, acetone, saturated NaHCO$_{3(aq)}$ solution, r.t., overnight.

same conditions (Fig. 2, C), demonstrating a slower rate of ring cleavage than 15 and 2, as conjugate 5 (m/z = 580.12) was still detectable by MS after 2 h of incubation in 3 M (NH$_4$)$_2$CO$_3$. However, the emergence of a new peak with m/z = 248.04 corresponding to the thiol 11 confirmed that degradation of compound 5 resulted in the release of the thiol.

With these results in hand, we moved on to test enzyme-catalyzed hydrolysis of conjugates 4, 5 and 6. The conjugates were incubated with New Delhi Metallo-β-lactamase-1 (NDM-1) (for details see Supporting Information), aliquots were taken out at different time points (0, 20, 40, 60 and 90 min) and analyzed using HPLC-MS. For compound 4 (m/z = 580.12), after 20 min incubation, two new peaks with m/z =
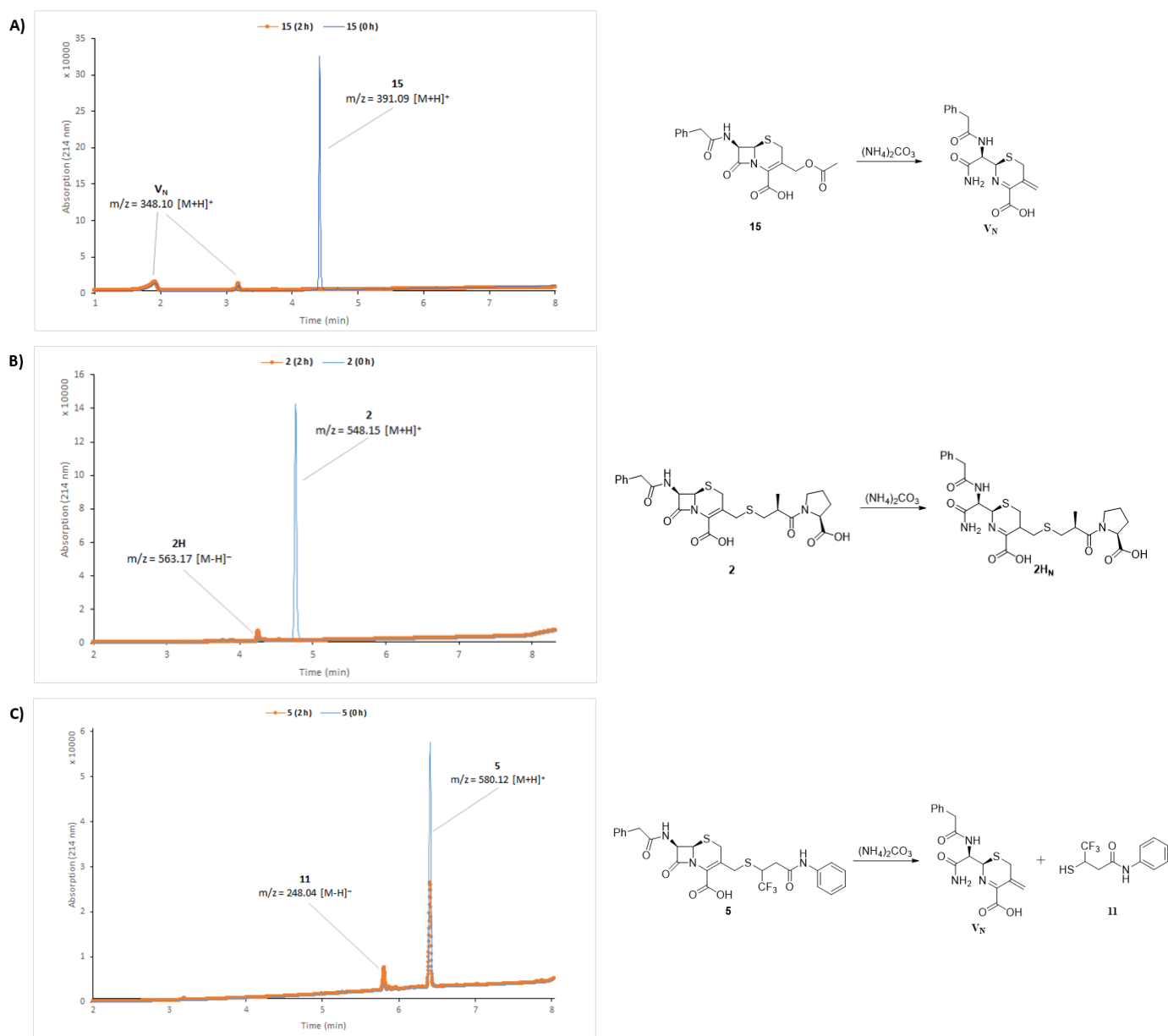

Figure 2. LC-MS analysis of (NH$_4$)$_2$CO$_3$-mediated degradation of 15(A), 2(B) and 5(C).

596.11 and m/z = 248.04 were observed, corresponding to **4H** and **10**, respectively (Fig. 3). In the following measurements, the conjugate peak was found to be decreasing and the peak of **4H** increasing, with no increase being observed for the thiol peak. Furthermore, the released thiol **10** was shown to degrade under the assay conditions, presumably forming the corresponding disulfide. Compounds **5** and **6** demonstrated similar hydrolysis patterns (Fig. 4 and S9, respectively). In the case of conjugate **5**, the initial measurement after 20 min incubation showed peaks with m/z = 248.05 (thiol **11**) and m/z = 596.10 (**5H**). In the following measurements a slight increase of both the peaks could be observed.

In all three cases, the appearance of the thiol peak after the initial 20 min of incubation was observed, confirming the release of the inhibitor. However, only minimal changes occurred to the peak in subsequent measurements, indicating no further substantial release or alteration of the inhibitor. Nevertheless, the intermediates with the cleaved β-lactam ring and the intact thioethers (of the general structure **H**) were also detected, complicating any quantitative analysis of the spectra.

To confirm our findings, we further examined MBL-mediated hydrolysis of conjugates **2-8** using an *in-situ* NMR assay (for details see Supporting Information). We utilized conjugate **1** as a positive control since it has been reported to form the vinylic elimination product (**V**) based on NMR monitoring of the hydrolysis. The ^{1}H NMR data (Fig. 3, 4 and S10-S13) demonstrate the appearance of vinylic proton signals at ca. 5.70 ppm corresponding to the vinylic

elimination product (**V**). However, the intensity of these peaks remains weak throughout the measurements and does not change greatly, while the proton signals of the conjugates disappear with time. As can be seen from Figures 3 and 4, full consumption of conjugate **5** occurs faster than that of conjugate **4**, indicating that the rate of hydrolysis is dependent on the position of the CF_3-group. No hydrolysis was detected in control experiments in the absence of NDM-1 in the solution. It is also worth noting that addition of excess zinc ions during the course of hydrolysis (data not shown), did not influence the chemical shift of the conjugate proton signals, indicating minimal zinc binding affinity of the conjugates. However, excess zinc caused clear shifts in the other peaks and led to increased, more pronounced vinylic proton peak signals. This could be an indication that the vinylic compound (**V**) is involved in some kind of binding in the active site, this being the reason behind the broad peaks of the vinylic protons in the NMR.

Both LC-MS and NMR analysis confirm thiol release and formation of the vinylic elimination product. All of the fluorinated conjugates appear to be superior to the non-fluorinated conjugate, demonstrating thiol release to varying extents. Compounds **5** and **6**, while showing the most promising results, do not exhibit the same properties as a conjugate with an aromatic thiol. The discrepancy in the proton signal appearance of compound **V** and disappearance for the respective conjugate indicates that there are several processes occurring simultaneously, making it difficult to explain and quantify the results. The formation of intermediates of the general structure **H** further complicates
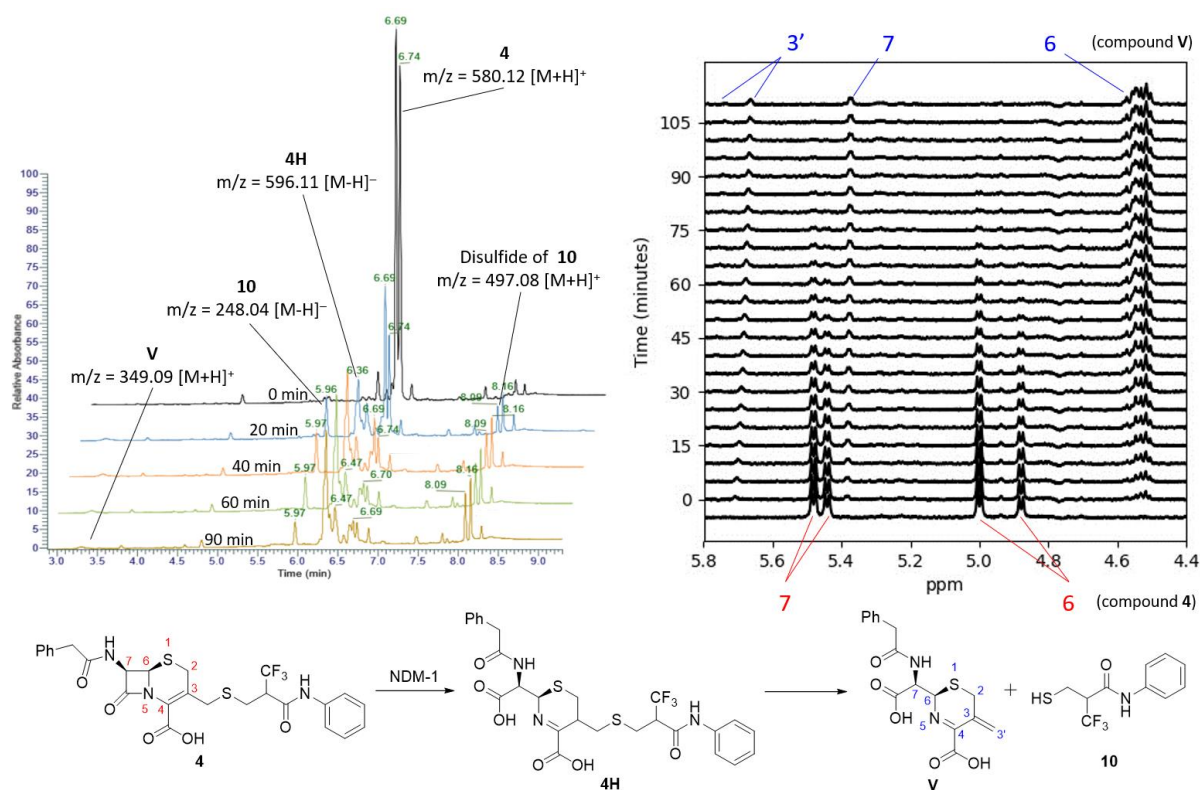

Figure 3. LC-MS (left) and NMR (right) analysis of NDM-1-mediated degradation of **4**.
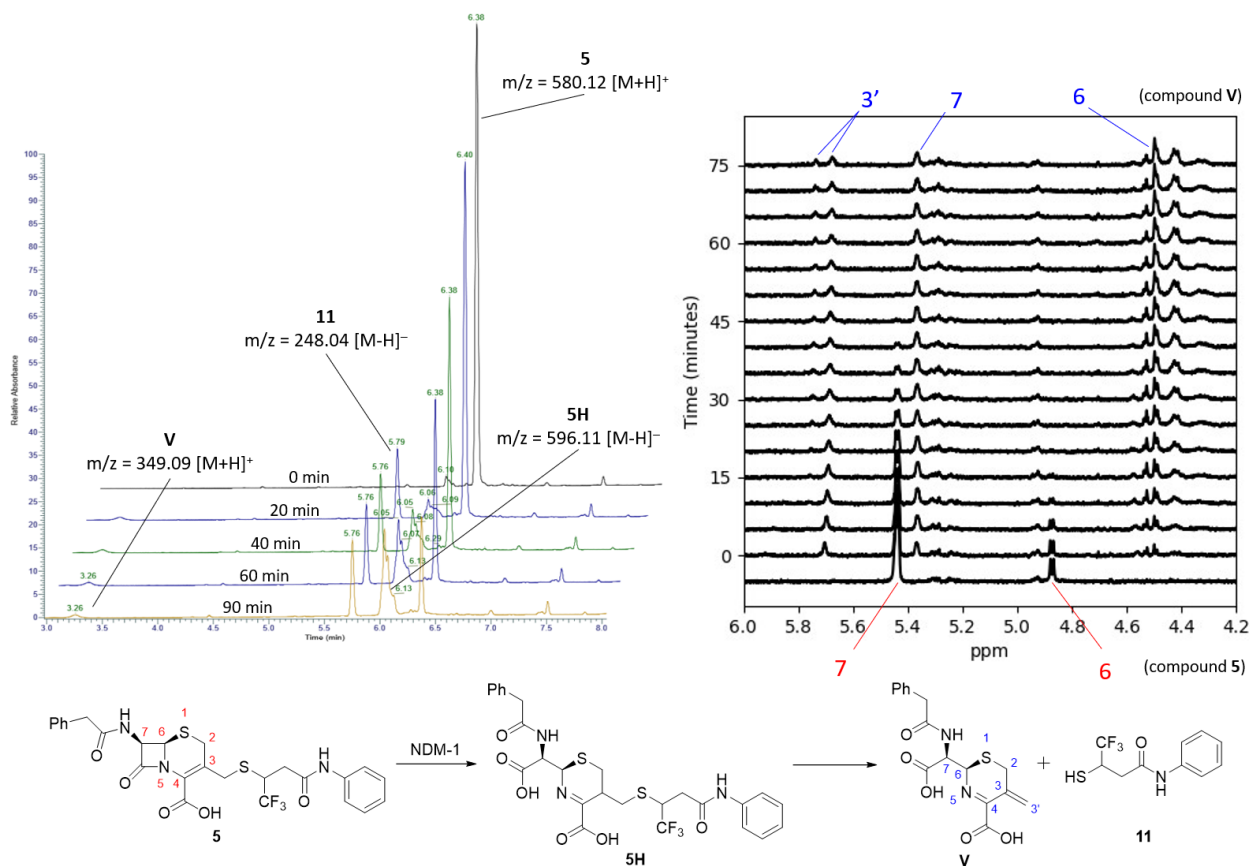
Figure 4. LC-MS (left) and NMR (right) analysis of NDM-1-mediated degradation of **5**.

the analysis of conjugate hydrolysis. The results, acquired from basic and enzymatic hydrolysis experiments, indicate that the position of the CF$_3$-group is of significance for the release of the inhibitor as well as for the stability of the released thiol. Comparison of the hydrolysis of conjugates **4** and **5** demonstrate that the β-CF$_3$-derivative (**5**) is hydrolyzed faster than the α-CF$_3$-derivative (**4**).

Fluorinated compounds have been used as probes for the investigation of structures and mechanisms in chemical biology.[23-24] ^{19}F NMR lacks background interference and has a broader chemical shift range than ^{1}H NMR, making it

a sensitive and convenient tool for solution-state NMR studies. Hence, we set out to demonstrate that the aforementioned *in-situ* NMR assay can be extended to ^{19}F NMR. For that, the course of NDM-1-mediated hydrolyses of conjugates **4** and **5** was analyzed using ^{19}F NMR (Fig. 5 and 6, respectively). The obtained spectra show the disappearance of the two starting peaks, corresponding to the two diastereomers of the conjugates, and the appearance of several new peaks. The data obtained from LC-MS experiments indicates that the emerging peaks correspond to the two diastereomers of **4H** or **5H**, the thiol (**10** or **11**) and
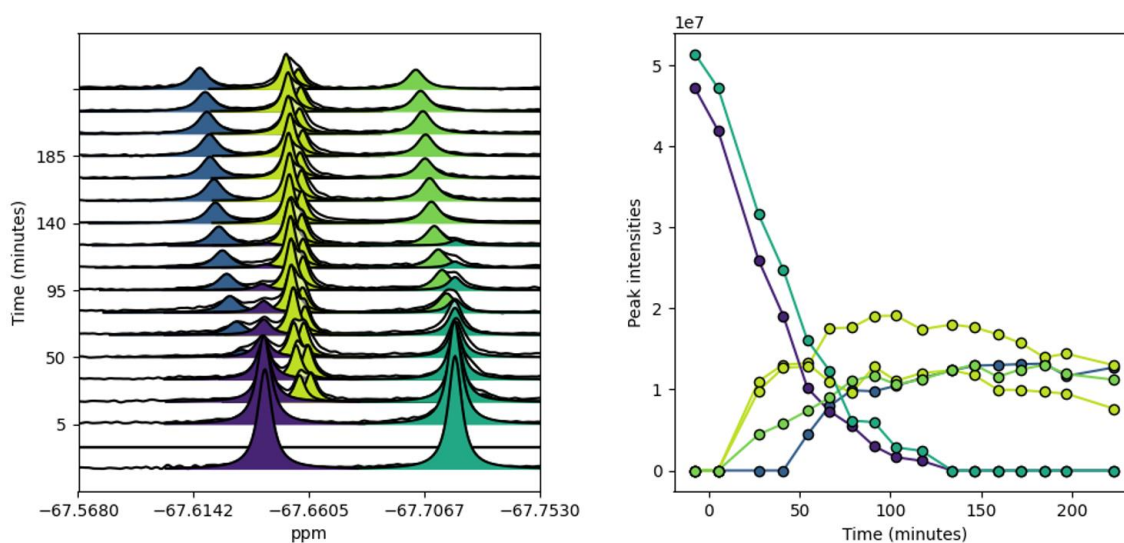

Figure 5. ^{19}F NMR-based monitoring of NDM-1-mediated degradation of **4**.
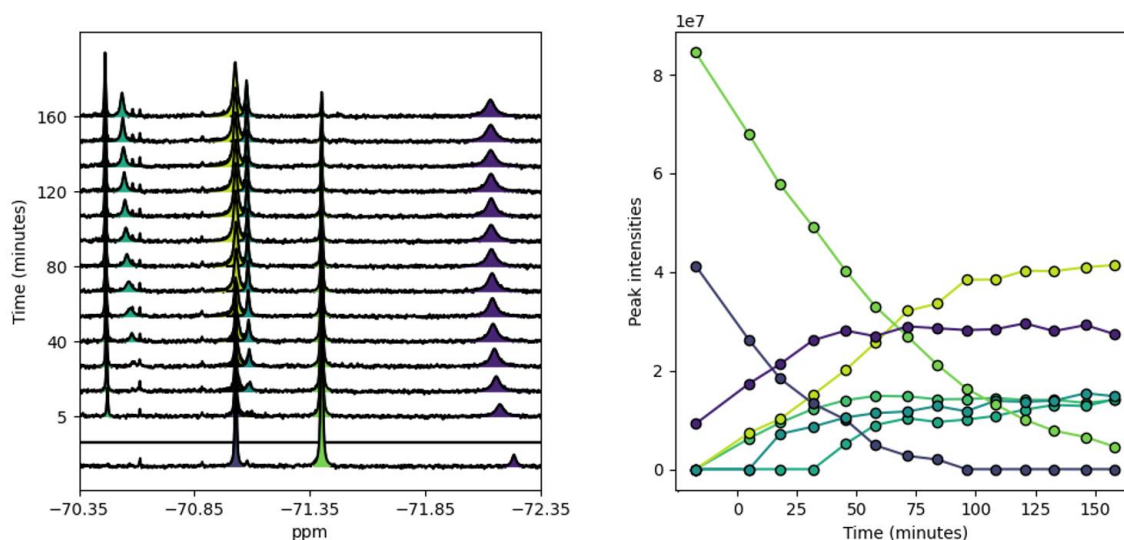
Figure 6. ^{19}F NMR-based monitoring of NDM-1-mediated degradation of **5**.

its corresponding disulfide. However, assigning the peaks to the respective products was challenging as the chemical shifts of isolated compounds in the buffer could only be determined for thiol **11**. Guided by the LC-MS experiments with conjugate **4** (Fig. 3, left), we assigned the two fast-emerging peaks (grass green) to the diastereomeric intermediates **4H** (Fig. 5). Based on the time-dependence of the fluorine peak intensities, we suggest that the broad upfield peak (lime green) corresponds to thiol **10**, while the downfield broad peak (dark blue), appearing slower than the rest, should be the disulfide. For conjugate **5**, the broad upfield peak (ca -72.1 ppm, purple) was identified as the thiol (**11**), whereas the broad peak around -70.5 ppm (mint green), emerging later than the other peaks, was presumed to be the disulfide (Fig. 6). Surprisingly, three additional peaks were observed, two of which should account for the two diastereomers of **5H**, which is in agreement with LC-MS analysis and time-dependence of the fluorine peak intensities. We hypothesize that the additional peak may be a C-6 epimer of **5H** as previously observed in the hydrolysis of cephalosporin-based β-lactam antibiotics.[25]

The inhibitory activity of conjugates **1**-**8** was evaluated against a selection of representative B1 MBLs (Table 1) with nitrocefin used as the reporter substrate. Following pre-incubation of the enzyme with the conjugate (10 min), the initial rates of the reactions with various concentrations of the inhibitors in a 2-fold dilution series were measured. The half maximal inhibitory concentration (IC$_{50}$) values were derived from the fitted dose-response curves. L-captopril was used as reference compound as well as conjugate **1**, for which inhibitory activity data has been published previously.[13] Compound **16** (for structure see Table S1) was included in the testing library to verify that the cephalosporin core of the conjugates is not responsible for the inhibition of MBLs.

The tested conjugates demonstrated inhibition to various extents with IC$_{50}$ values ranging from 0.61 to 91.72 μM. Conjugate **8** displayed activity against all of the tested MBLs with IC$_{50}$ values of 2.02, 4.28, 1.98 and 3.19 μM against

NDM-1, VIM-2, IMP-2 and IMP-7, respectively. Comparing the inhibitory activity of conjugates **4** and **5**, the β-CF$_3$-derivative (**5**) is slightly more potent than the α-CF$_3$-derivative (**4**) against IMP-type MBLs, while conjugate **4** is more active against NDM-1 and VIM-2. Notably, the IC$_{50}$ values obtained for the conjugates are in a similar range to those reported for the corresponding thiol inhibitors (see Table S1 for comparison).[19]

Table 1. Inhibitory activity of conjugates **1**-**8**, L-captopril and **16** against selected B1 MBLs.

| Compound | IC$_{50}$ (μM)^a | | | |
	NDM-1	VIM-2	IMP-2	IMP-7
1	1.92 ± 0.06	1.99 ± 0.07	1.4 ± 0.09	2.4 ± 0.17
2	31.81 ± 4.93	10.37 ± 1.64	22.44 ± 3.11	6.91 ± 0.49
3	27.76 ± 8.4	4.58 ± 0.22	19.24 ± 0.73	18.61 ± 1.32
4	3.76 ± 0.35	**0.61 ± 0.05**	11.28 ± 2.17	13.47 ± 1.75
5	8.22 ± 0.34	7.11 ± 0.37	6.07 ± 0.83	8.61 ± 0.45
6	4.5 ± 0.38	33.64 ± 4.49	2.79 ± 0.93	4.12 ± 0.11
7	91.72 ± 5.08	15.34 ± 1.22	82.33 ± 26.17	21.84 ± 0.84
8	**2.02 ± 0.55**	4.28 ± 0.86	**1.98 ± 0.52**	**3.19 ± 0.11**
16	>300	49.94 ± 5.18	>300	60.05 ± 6.94
L-captopril	13.12 ± 3.23	4.487 ± 0.19	6.16 ± 0.31	10.15 ± 0.76

^{a} The half-maximal inhibitory concentrations of the compounds are provided as the mean value along with the standard error of the mean. The reported values are based on triplicate experiments.

3. Conclusion

A series of novel conjugates, designed to release trifluoromethylated thiol-based inhibitors upon enzymatic hydrolysis, was synthesized. Thiol release, as determined using LC-MS and ^{1}H NMR assays, confirmed improved leaving group properties of aliphatic thiols upon fluorination. Furthermore, the course of hydrolysis was monitored using ^{19}F NMR, demonstrating its potential use for the analysis of enzyme-catalyzed reactions. The conjugates exhibited inhibitory activity against B1 MBLs such as NDM-1, VIM-2, IMP-2 and IMP-7.

Neither the stalling of the release, nor the formation of intermediates with the cleaved β-lactam ring and the intact thioethers have been reported for conjugates with aromatic

thiols. Subsequently, these findings provide new insights for further development of cephalosporin-based MBL-inhibitor conjugates.

4. Experimental section

Description of the experimental procedures, analytical data and IC_{50} curves can be found in the Supporting information.

5. Acknowledgements

6. References

[1] Mora-Ochomogo, M.; Lohans, C. T., β-Lactam Antibiotic Targets and Resistance Mechanisms: from Covalent Inhibitors to Substrates. *RSC Med. Chem.* **2021**, *12*, 1623-1639.

[2] Yang, Y.; Yan, Y.-H.; Schofield, C. J.; McNally, A.; Zong, Z.; Li, G.-B., Metallo-β-Lactamase-Mediated Antimicrobial Resistance and Progress in Inhibitor Discovery. *Trends Microbiol.* **2023**, *31*, 735-748.

[3] Bahr, G.; González, L. J.; Vila, A. J., Metallo-β-Lactamases in the Age of Multidrug Resistance: From Structure and Mechanism to Evolution, Dissemination, and Inhibitor Design. *Chem. Rev.* **2021**, *121*, 7957-8094.

[4] Denakpo, E.; Naas, T.; Iorga, B. I., An Updated Patent Review of Metallo-β-Lactamase Inhibitors (2020–2023). *Expert Opin. Ther. Pat.* **2023**, 1-16.

[5] Palzkill, T., Metallo-β-Lactamase Structure and Function. *Ann. N. Y. Acad. Sci.* **2013**, *1277*, 91-104.

[6] Cole, M. S.; Hegde, P. V.; Aldrich, C. C., β-Lactamase-Mediated Fragmentation: Historical Perspectives and Recent Advances in Diagnostics, Imaging, and Antibacterial Design. *ACS Infect. Dis.* **2022**, *8*, 1992-2018.

[7] Bush, K.; Bradford, P. A., Interplay Between β-Lactamases and New β-Lactamase Inhibitors. *Nat. Rev. Microbiol.* **2019**, *17*, 295-306.

[8] Shi, C.; Chen, J.; Kang, X.; Shen, X.; Lao, X.; Zheng, H., Approaches for the Discovery of Metallo-β-Lactamase Inhibitors: A Review. *Chem. Biol. Drug Des.* **2019**, *94*, 1427-1440.

[9] Lienard, B. M.; Garau, G.; Horsfall, L.; Karsisiotis, A. I.; Damblon, C.; Lassaux, P.; Papamicael, C.; Roberts, G. C.; Galleni, M.; Dideberg, O.; Frere, J. M.; Schofield, C. J., Structural Basis for the Broad-Spectrum Inhibition of Metallo-β-Lactamases by Thiols. *Org. Biomol. Chem.* **2008**, *6*, 2282-2294.

[10] Chen, C.; Wang, D.; Yang, K.-W. (2023). Chapter 14 - Thiols as a Privileged Scaffold Against Metallo-β-Lactamases. In: Yu, B.; Li, N.; Fu, C. (eds.) Privileged Scaffolds in Drug Discovery, Academic Press, 301-318.

[11] Tehrani, K. H. M. E.; Martin, N. I., Thiol-Containing Metallo-β-Lactamase Inhibitors Resensitize Resistant Gram-Negative Bacteria to Meropenem. *ACS Infect. Dis.* **2017**, *3*, 711-717.

[12] Lothian, A.; Hare, D.; Masters, C.; Ryan, T.; Grimm, R. R., Blaine, Metalloproteomics: Principles, Challenges and Applications to Neurodegeneration. *Front. Aging Neurosci.* **2013**, *5*, 35.

[13] van Haren, M. J.; Tehrani, K. H. M. E.; Kotsogianni, I.; Wade, N.; Bruchle, N. C.; Mashayekhi, V.; Martin, N. I., Cephalosporin Prodrug Inhibitors Overcome Metallo-β-Lactamase Driven Antibiotic Resistance. *Chemistry* **2021**, *27*, 3806-3811.

[14] Jackson, A. C.; Zaengle-Barone, J. M.; Puccio, E. A.; Franz, K. J., A Cephalosporin Prochelator Inhibits New Delhi Metallo-β-lactamase 1 without Removing Zinc. *ACS Infect. Dis.* **2020**, *6*, 1264-1272.

[15] Zaengle-Barone, J. M.; Jackson, A. C.; Besse, D. M.; Becken, B.; Arshad, M.; Seed, P. C.; Franz, K. J., Copper Influences the Antibacterial Outcomes of a β-Lactamase-Activated Prochelator against Drug-Resistant Bacteria. *ACS Infect. Dis.* **2018**, *4*, 1019-1029.

[16] Tehrani, K. H. M. E.; Wade, N.; Mashayekhi, V.; Bruchle, N. C.; Jespers, W.; Voskuil, K.; Pesce, D.; van Haren, M. J.; van Westen, G. J. P.; Martin, N. I., Novel Cephalosporin Conjugates Display Potent and Selective Inhibition of Imipenemase-Type Metallo-β-Lactamases. *J. Med. Chem.* **2021**, *64*, 9141-9151.

[17] Tian, H.; Wang, Y.; Dai, Y.; Mao, A.; Zhou, W.; Cao, X.; Deng, H.; Lu, H.; Ding, L.; Shen, H.; Wang, X., A Cephalosporin-Tripodalamine Conjugate Inhibits Metallo-β-Lactamase with High Efficacy and Low Toxicity. *Antimicrob. Agents Chemother.* **2022**, *66*, e00352-00322.

[18] Nishikawa, J.; Watanabe, F.; Shudou, M.; Terui, Y.; Narisada, M., Proton NMR Study of Degradation Mechanisms of Oxacephem Derivatives with Various 3'-Substituents in Alkaline Solution. *J. Med. Chem.* **1987**, *30*, 523-527.

[19] Kondratieva, A.; Palica, K.; Frøhlich, C.; Hovd, R. R.; Leiros, H.-K. S.; Erdelyi, M.; Bayer, A., Fluorinated Captopril Analogues Inhibit Metallo-β-Lactamases and Facilitate Structure Determination of NDM-1 Binding Pose. *Eur. J. Med. Chem.* **2024**, *266*, 116140.

[20] Yamana, T.; Tsuji, A., Comparative Stability of Cephalosporins in Aqueous Solution: Kinetics and Mechanisms of Degradation. *J. Pharm. Sci.* **1976**, *65*, 1563-1574.

[21] Hanessian, S.; Wang, J., Design and Synthesis of a Cephalosporin–Carboplatinum Prodrug Activatable by a β-Lactamase. *Can. J. Chem.* **1993**, *71*, 896-906.

[22] Feng, H.; Ding, J.; Zhu, D.; Liu, X.; Xu, X.; Zhang, Y.; Zang, S.; Wang, D.-C.; Liu, W., Structural and Mechanistic Insights into NDM-1 Catalyzed Hydrolysis of Cephalosporins. *J. Am. Chem. Soc.* **2014**, *136*, 14694-14697.

[23] Gimenez, D.; Phelan, A.; Murphy, C. D.; Cobb, S. L., ^{19}F NMR as a Tool in Chemical Biology. *Beilstein J. Org. Chem.* **2021**, *17*, 293-318.

[24] Cobb, S. L.; Murphy, C. D., ^{19}F NMR Applications in Chemical Biology. *J. Fluor. Chem.* **2009**, *130*, 132-143.

[25] Badarau, A.; Llinás, A.; Laws, A. P.; Damblon, C.; Page, M. I., Inhibitors of Metallo-β-Lactamase Generated from β-Lactam Antibiotics. *Biochemistry* **2005**, *44*, 8578-8589.

Supporting information

for

The Use of Fluorinated Aliphatic Thiols in the Design of Cephalosporin Conjugates

Alexandra Kondratieva[a], Philip Rainsford[a], Perwez Bakht[b], Hanna-Kirsti S. Leiros[a], Ranjana Pathania[b], Annette Bayer[a]*

[a] *Department of Chemistry, UiT The Arctic University of Norway, NO-9037 Tromsø, Norway.*
[b] *Department of Biosciences and Bioengineering, Indian Institute of Technology, Roorkee, Uttarakhand-247667, India.*
Corresponding author.

Table of Contents

Chemistry

General methods

All reagents were purchased from commercial sources and used as supplied without further purification unless otherwise stated. Thiols **9-14** were prepared according to previously published procedures.[1] (6*R*,7*R*)-8-oxo-7-(2-phenylacetamido)-3-((quinolin-8-ylthio)methyl)-5-thia-1-azabicyclo[4.2.0]oct-2-ene-2-carboxylic acid (**1**)[2], (6*R*,7*R*)-3-(acetoxymethyl)-8-oxo-7-(2-phenylacetamido)-5-thia-1-azabicyclo[4.2.0]oct-2-ene-2-carboxylic acid (**15**)[3] and (6*R*,7*R*)-3-methyl-8-oxo-7-(2-phenylacetamido)-5-thia-1-azabicyclo[4.2.0]oct-2-ene-2-carboxylic acid (**16**)[4] were synthesized following previously reported procedures and their analytical data were found to be in accordance with those reported. Solvents were dried according to standard procedures over appropriately sized molecular sieves.

For thin layer chromatography (TLC) analysis, aluminium plates pre-coated with silica gel (Merck silica gel 60 F_{254}) were used and visualized using either ultraviolet light or by treatment with an appropriate stain. Compounds were purified via preparative HPLC performed on a CombiFlash® EZ Prep system with a YMC-Actus Triart C18 column, eluting with mixtures of acetonitrile and H_2O (both containing 0.1% TFA).

^{1}H and ^{13}C NMR spectra for assignment were obtained on a 400 MHZ Bruker Advance III HD spectrometer equipped with a 5 mm SmartProbe BB/1H (BB = 19F, 31P-15N) at 20 ˚C. Chemical shifts are reported in ppm relative to the solvent residual peak (CDCl$_3$: δH 7.26 and δC 77.16; Acetone-*d6*: δH 2.05 and δC 206.26; Methanol-*d4*: δH 3.31 and δC 49.00). Coupling constants J are reported in Hertz (Hz). The ^{13}C NMR spectra were ^{1}H decoupled. The following abbreviations were used to indicate the multiplicities: s = singlet, d = doublet, t = triplet, q = quartet, qnt = quintet, dd = doublet of doublets, dq = doublet of quartets, dqd = doublet of quartet of doublets, tt = triplet of triplets, qntd = quintet of doublets, m = multiplet, app = appearing and br = broad. When possible, for compounds obtained as rotameric mixtures, chemical shifts of minor rotamers are reported separately, enclosed in square brackets.

High-resolution mass spectrometry (HRMS) was conducted from methanol or acetonitrile solutions on a ThermoScientific Vanquish UHPLC system coupled to a ThermoScientific Orbitrap Exploris 120 with electrospray ionization (ESI). The following solvent system, at a flow rate of 0.3 mL/min, was used: solvent A – MiliQ water/0.1% formic acid; solvent B – 90% acetonitrile/10% MiliQ water/0.1% formic acid. Gradient elution was as follows: 95:5 to 30:70 (A:B) over 7 min, 0:100 (A:B) for 2 min, then reversion back to 95:5 (A:B) for 3 min.

Melting points were measured on a Stuart SMP50 automatic melting point detector and are reported uncorrected in degree Celsius (˚C).

All final compounds were analyzed using the described above UHPLC-HRMS system and the purity is specified for each compound below.
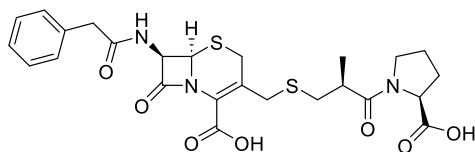
General procedure

In an oven-dried two-neck round-bottom flask BF$_3$·Et$_2$O (3.0 eq) was mixed with MeCN (2-4 mL) under an argon atmosphere, followed by the sequential addition of the respective thiol (1.5 eq) and 7-ACA (1.0 eq). The reaction mixture was stirred at 50 ºC for 2 h, after which water and an ammonium hydroxide solution (32%) were added, adjusting the pH to 4. The formed precipitate was collected, washed with water and the crude product was suspended in a mixture of a saturated bicarbonate solution and acetone (2:3). Next, phenylacetyl chloride (2.0 eq) was added dropwise and the resulting mixture was stirred overnight at ambient temperature. After that, the mixture was diluted with water and the pH was adjusted to 2 using 1 M HCl. If a precipitate formed, it was filtered and washed with a small amount of cold water. Alternatively, the volatiles were evaporated using a nitrogen stream. The obtained crude material was purified by reversed-phase prep-HPLC.

Spectroscopic data

Compounds **3-6** were obtained as diastereomeric mixtures and NMR data is reported for the mixture. For compounds **7-8**, obtained as rotameric mixtures, when possible, chemical shifts of the minor rotamers are reported separately, enclosed in square brackets. Carbon assignment for compounds **3-8** can be found on pages S7-S12.

(6R,7R)-3-((((S)-3-((S)-2-carboxypyrrolidin-1-yl)-2-methyl-3-oxopropyl)thio)methyl)-8-oxo-7-(2-phenylacetamido)-5-thia-1-azabicyclo[4.2.0]oct-2-ene-2-carboxylic acid (**2**).

Synthesized according to the *General Procedure* using 7-ACA (220 mg, 0.81 mmol, 1.0 eq), *L*-captopril (264 mg, 1.21 mmol, 1.5 eq), boron trifluoride ethyl etherate (305 μl, 2.42 mmol, 3.0 eq), MeCN (3 mL) and phenylacetyl chloride (194 μl, 1.47 mmol, 2.0 eq). The crude was purified using H$_2$O/MeCN (0.1% TFA) to yield **2** (151 mg, 0.28 mmol, 35%, over two steps) as a white solid. **^{1}H NMR** (400 MHz, DMSO-*d6*) δ 9.10 (app d, *J* = 8.2 Hz, 1H), 7.35 – 7.17 (m, 5H), 5.61 (dd, *J* = 8.2, 4.7 Hz, 1H), 5.15 – 5.07 (m, 1H), 4.23 (dd, *J* = 8.8, 3.9 Hz, 1H), 3.74 – 3.29 (m, 8H), 2.83 – 2.63 (m, 2H), 2.42 – 2.32 (m, 1H), 2.21 – 2.05 (m, 1H), 1.99 – 1.71 (m, 3H), 1.10 – 0.96 (m, 3H). **^{13}C NMR** (101 MHz, DMSO-*d6*) δ 173.4, 172.7, 171.0, 164.6, 163.2, 135.9, 129.0 (2C), 128.2 (2C), 128.1, 126.5, 124.7, 59.0, 58.3, 58.0, 46.5, 41.6, 37.6, 33.8, 32.8, 28.7, 26.9, 24.4, 16.9. **HRMS** (ESI): calcd for C$_{25}$H$_{30}$N$_3$O$_7$S$_2$$^+$ [M+H]$^+$ 548.1520, found: 548.1518. **M.p.**: 122 – 125 ˚C. Purity: >99% (UV 214 nm).

(6R,7R)-3-(((2-(benzylcarbamoyl)-3,3,3-trifluoropropyl)thio)methyl)-8-oxo-7-(2-phenylacetamido)-5-thia-1-azabicyclo[4.2.0]oct-2-ene-2-carboxylic acid (**3**).
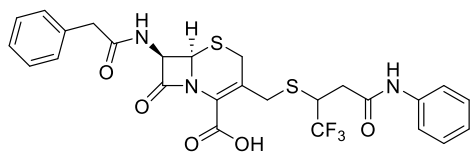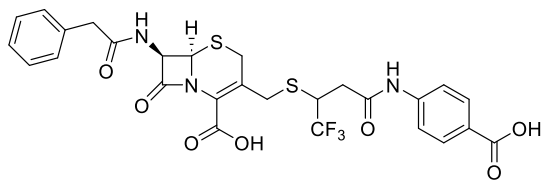

Synthesized according to the *General Procedure* using 7-ACA (85 mg, 0.31 mmol, 1.0 eq), *N*-benzyl-3,3,3-trifluoro-2-(mercaptomethyl)propanamide (123 mg, 0.47 mmol, 1.5 eq), boron trifluoride ethyl etherate (118 μl, 0.94 mmol, 3.0 eq), MeCN (2 mL) and phenylacetyl chloride (79 μl, 0.60 mmol, 2.0 eq). The crude was purified using H_2O/MeCN (0.1% TFA) to yield **3** (75 mg, 0.13 mmol, 36%, over two steps) as a white solid. **^{1}H NMR** (400 MHz, DMSO-*d6*) δ 9.16, 9.10 (d, *J* = 8.4 Hz, 1H), 9.03, 8.95 (d, *J* = 5.9 Hz, 1H), 7.43 – 7.16 (m, 10H), 5.71 – 5.58 (m, 1H), 5.17 – 5.05 (m, 1H), 4.46 – 4.31 (m, 2H), 3.98, 3.33 (app d, *J* = 13.6 Hz, 1H), 3.81 (app d, *J* = 13.5 Hz, 0.5H), 3.74 – 3.41 (m, 5.5H), 3.03 – 2.72 (m, 2H). **^{13}C NMR** (101 MHz, DMSO-*d6*) δ 171.0, 164.8, 164.6, 164.4, 163.1, 163.0, 138.6, 138.5, 135.9, 135.85, 129.1, 128.4, 128.35, 128.3, 127.9, 127.5, 127.2, 127.05, 127.0, 126.5, 125.2, 124.9, 124.8 (q, *J* = 281.9 Hz), 59.0, 58.95, 58.0, 49.8 (q, J = 24.6 Hz), 49.6 (q, J = 24.6 Hz), 42.5, 41.6, 33.1, 32.6, 27.1, 26.7, 26.1. **HRMS** (ESI): calcd for $C_{27}H_{27}F_3N_3O_5S_2^+$ [M+H]$^+$ 594.1339, found: 594.1337. **M.p.:** 113 – 115 ˚C. Purity: >99% (UV 214 nm).

(6R,7R)-8-oxo-7-(2-phenylacetamido)-3-(((3,3,3-trifluoro-2-(phenylcarbamoyl)propyl)thio)methyl)-5-thia-1-azabicyclo[4.2.0]oct-2-ene-2-carboxylic acid (**4**).

Synthesized according to the *General Procedure* using 7-ACA (95 mg, 0.35 mmol, 1.0 eq), 3,3,3-trifluoro-2-(mercaptomethyl)-*N*-phenylpropanamide (131 mg, 0.53 mmol, 1.5 eq), boron trifluoride ethyl etherate (132 μl, 1.05 mmol, 3.0 eq), MeCN (3 mL) and phenylacetyl chloride (178 μl, 1.34 mmol, 4.0 eq). The crude was purified using H_2O/MeCN (0.1% TFA) to yield **4** (131 mg, 0.23 mmol, 65%, over two steps) as a white solid. **^{1}H NMR** (400 MHz, DMSO-*d6*) δ 10.57, 10.51 (s, 1H), 9.16, 9.09 (d, *J* = 8.4 Hz, 1H), 7.64 – 7.57 (m, 2H), 7.39 – 7.31 (m, 2H), 7.31 – 7.19 (m, 5H), 7.16 – 7.09 (m, 1H), 5.70 – 5.63 (m, 1H), 5.13, 5.11 (d, *J* = 4.7 Hz, 1H), 4.05 (app d, *J* = 13.6 Hz, 0.5H), 3.89 – 3.80 (m, 1H), 3.71 – 3.44 (m, *overlapping water peak*, 5H), 3.30 (app d, *J* = 13.7 Hz, 0.5H), 3.09 – 2.74 (m, 2H). **^{13}C NMR** (101 MHz, DMSO-*d6*) δ 171.0, 170.95, 164.8, 164.7, 163.3, 163.1, 163.05, 163.0, 138.2, 138.1, 135.85, 135.8, 129.0, 128.95, 128.9, 128.2, 128.0, 127.4, 126.5, 125.1, 124.9, 124.7 (q, *J* = 281.5 Hz), 124.3, 124.2, 119.5, 119.4, 59.0, 58.0, 50.6 (q, *J* = 24.4 Hz), 50.4 (q, *J* = 24.4 Hz), 41.65, 41.6, 33.1, 32.4, 27.1, 26.7, 26.0. **HRMS** (ESI): calcd for $C_{26}H_{25}F_3N_3O_5S_2^+$ [M+H]$^+$ 580.1182, found: 580.1181. **M.p.:** 131 – 133 ˚C. Purity: >95% (UV 214 nm).

(6R,7R)-8-oxo-7-(2-phenylacetamido)-3-(((1,1,1-trifluoro-4-oxo-4-(phenylamino)butan-2-yl)thio)methyl)-5-thia-1-azabicyclo[4.2.0]oct-2-ene-2-carboxylic acid (**5**).
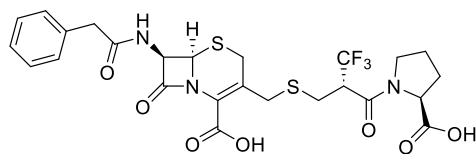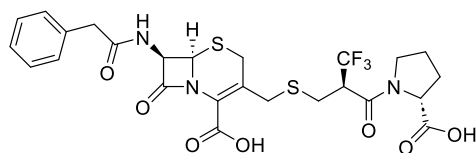

Synthesized according to the *General Procedure* using 7-ACA (172 mg, 0.63 mmol, 1.0 eq), 4,4,4-trifluoro-3-mercapto-*N*-phenylbutanamide (236 mg, 0.95 mmol, 1.5 eq), boron trifluoride ethyl etherate (238 μl, 1.90 mmol, 3.0 eq), MeCN (4 mL) and phenylacetyl chloride (321 μl, 2.43 mmol, 4.0 eq). The crude was purified using H_2O/MeCN (0.1% TFA) to yield **5** (134 mg, 0.23 mmol, 37%, over two steps) as a white solid. **^{1}H NMR** (400 MHz, CD_3CN) δ 8.50, 8.47 (s, 1H), 7.62 – 7.51 (m, 2H), 7.39 – 7.21 (m, 8H), 7.17 – 7.08 (m, 1H), 5.74, 5.68 (dd, *J* = 8.7, 4.8 Hz, 1H), 5.09, 4.96 (d, *J* = 4.8 Hz, 1H), 4.08 – 3.77 (m, 2H), 3.73 – 3.36 (m, 5H), 2.98 – 2.84 (m, 1H), 2.62 – 2.44 (m, 1H). **^{13}C NMR** (101 MHz, CD_3CN) δ 172.4, 172.35, 167.6, 167.5, 165.9, 165.7, 163.4, 163.3, 139.4, 139.3, 136.3, 130.1, 129.9, 129.85, 129.8, 129.4, 128.1 (q, *J* = 275.8 Hz), 127.8, 127.7, 125.9, 125.5, 125.2, 125.0, 120.6, 120.5, 60.25, 60.2, 58.5, 58.3, 44.9 (q, *J* = 29.7 Hz), 44.3 (q, *J* = 29.7 Hz), 43.0, 42.95, 37.5, 36.8, 36.0, 35.6, 28.2, 28.0. **HRMS** (ESI): calcd for $C_{26}H_{25}F_3N_3O_5S_2^+$ [M+H]$^+$ 580.1182, found: 580.1179. **M.p.**: 140 – 142 ˚C. Purity: >98% (UV 214 nm).

(6R,7R)-3-(((4-((4-carboxyphenyl)amino)-1,1,1-trifluoro-4-oxobutan-2-yl)thio)methyl)-8-oxo-7-(2-phenylacetamido)-5-thia-1-azabicyclo[4.2.0]oct-2-ene-2-carboxylic acid (**6**).

Synthesized according to the *General Procedure* using 7-ACA (150 mg, 0.55 mmol, 1.0 eq), 4-(4,4,4-trifluoro-3-mercaptobutanamido)benzoic acid (242 mg, 0.83 mmol, 1.5 eq), boron trifluoride ethyl etherate (208 μl, 1.65 mmol, 3.0 eq), MeCN (4 mL) and phenylacetyl chloride (283 μl, 2.14 mmol, 4.0 eq). The crude was purified using H_2O/MeCN (0.1% TFA) to yield **6** (118 mg, 0.19 mmol, 34%, over two steps) as a white solid. **^{1}H NMR** (400 MHz, DMSO-*d6*) δ 10.48, 10.44 (s, 1H), 9.19 – 9.03 (m, 1H), 7.96 – 7.87 (m, 2H), 7.76 – 7.64 (m, 2H), 7.38 – 7.16 (m, *overlapping water peak*, 5H), 5.71, 5.63 (dd, *J* = 8.3, 4.7 Hz, 1H), 5.13, 5.03 (d, *J* = 4.8 Hz, 1H), 4.11 – 3.77 (m, 2H), 3.72 – 3.42 (m, 5H), 3.08 – 2.90 (m, 1H), 2.77 – 2.57 (m, 1H). **^{13}C NMR** (101 MHz, DMSO-*d6*) δ 171.0, 167.0, 166.9, 166.85, 164.5, 163.05, 163.0, 142.75, 142.65, 135.9, 135.8, 130.6, 130.5, 129.1, 128.3, 127.1 (q, *J* = 277.6 Hz), 126.5, 126.2, 125.8, 125.6, 125.5, 125.4, 124.1, 118.6, 118.4, 59.05, 59.0, 57.7, 57.5, 43.8 (q, *J* = 29.1 Hz), 42.7 (q, *J* = 29.1 Hz), 41.6, 36.4, 35.6, 34.7, 26.8, 26.5. **HRMS** (ESI): calcd for $C_{27}H_{23}F_3N_3O_7S_2^-$ [M-H]$^-$ 622.0935, found: 622.0932. **M.p.**: 137 – 140 ˚C. Purity: 96% (UV 214 nm).

(6R,7R)-3-((((S)-2-((S)-2-carboxypyrrolidine-1-carbonyl)-3,3,3-trifluoropropyl)thio)methyl)-8-oxo-7-(2-phenylacetamido)-5-thia-1-azabicyclo[4.2.0]oct-2-ene-2-carboxylic acid (**7**).
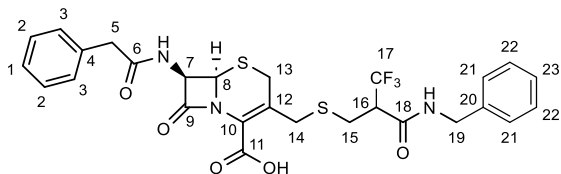

Synthesized according to the *General Procedure* using 7-ACA (100 mg, 0.37 mmol, 1.0 eq), ((*S*)-3,3,3-trifluoro-2-(mercaptomethyl)propanoyl)-L-proline (149 mg, 0.55 mmol, 1.5 eq), boron trifluoride ethyl etherate (138 µl, 1.10 mmol, 3.0 eq), MeCN (3 mL) and phenylacetyl chloride (175 µl, 1.32 mmol, 4.0 eq). The crude was purified using H_2O/MeCN (0.1% TFA) to yield **7** (47 mg, 0.08 mmol, 23%, over two steps) as a white solid. **^{1}H NMR** (400 MHz, DMSO-*d6*) (a 6:1 mixture of rotamers[*]) δ 9.20 – 9.07 (m, 1H), 7.35 – 7.18 (m, 5H), 5.65 (dd, *J* = 8.4, 4.7 Hz, 1H), 5.11 (d, *J* = 4.8 Hz, 1H), [4.75 – 4.69], 4.33 – 4.23 (m, 1H), 4.19 – 3.93 (m, 2H), 3.81 – 3.11 (m, *overlapping water peak*, 7H), 2.95 – 2.78 (m, 2H), 2.25 – 2.08 (m, 1H), 2.00 – 1.82 (m, 3H). **^{13}C NMR** (101 MHz, DMSO-*d6*) δ [173.2], 173.15, [171.85], 171.8, 165.1, [164.8], 164.0, 163.6, [163.5], 136.1, 129.4, 129.1, 128.7, [128.5], 127.0, 125.4, 125.0 (q, *J* = 282.4 Hz), [60.0], 59.5, 59.3, 58.3, 48.0, [47.7 (q, *J* = 24.8 Hz)], 47.6 (q, *J* = 24.8 Hz), [46.9], 42.0, [33.6], 33.0, [30.9], 29.3, [28.2], 27.0, 26.8, 24.6, [22.4]. **HRMS** (ESI calcd for $C_{25}H_{25}F_3N_3O_7S_2^-$ [M-H]$^-$ 600.1092, found: 600.1089. **M.p.:** 160 – 162 ˚C. Purity: >98% (UV 214 nm).

(6R,7R)-3-((((R)-2-((R)-2-carboxypyrrolidine-1-carbonyl)-3,3,3-trifluoropropyl)thio)methyl)-8-oxo-7-(2-phenylacetamido)-5-thia-1-azabicyclo[4.2.0]oct-2-ene-2-carboxylic acid (**8**).

Synthesized according to the *General Procedure* using 7-ACA (193 mg, 0.71 mmol, 1.0 eq), ((*R*)-3,3,3-trifluoro-2-(mercaptomethyl)propanoyl)-D-proline (289 mg, 1.07 mmol, 1.5 eq), boron trifluoride ethyl etherate (268 µl, 2.13 mmol, 3.0 eq), MeCN (4 mL) and phenylacetyl chloride (186 µl, 1.41 mmol, 2.0 eq). The crude was purified using H_2O/MeCN (0.1% TFA) to yield **8** (104 mg, 0.17 mmol, 24%, over two steps) as a white solid. **^{1}H NMR** (400 MHz, DMSO-*d6*) (a 6:1 mixture of rotamers[*]) δ 9.19 – 8.99 (m, 1H), 7.34 – 7.18 (m, 5H), 5.70 – 5.54 (m, 1H), 5.21 – 5.05 (m, 1H), [4.76 – 4.67], 4.34 – 4.23 (m, 1H), 4.15 – 3.81 (m, 1H), 3.78 – 3.10 (m, *overlapping water peak*, 8H), 3.03 – 2.81 (m, 2H), 2.23 – 2.11 (m, 1H), 2.01 – 1.82 (m, 3H). **^{13}C NMR** (101 MHz, DMSO-*d6*) δ [172.8], 172.7, 171.0, [170.95], [164.6], 164.5, [164.1 (q, *J* = 2.1 Hz)], 163.3 (q, *J* = 2.1 Hz), 163.2, [163.1], 135.9, 129.0, 128.4, 128.3, [127.4], 126.5, [125.1], 125.0, 124.6 (q, *J* = 281.8 Hz), [59.6], 59.1, 59.0, 57.9, 47.5, 47.3 (q, *J* = 24.5 Hz), [46.5], 41.6, [34.0], 33.3, [30.4], 28.9, 27.4, 26.9, 24.2, [22.1]. *TFA signals were observed but are not reported*. **HRMS** (ESI): calcd for $C_{25}H_{25}F_3N_3O_7S_2^-$ [M-H]$^-$ 600.1092, found: 600.1086. **M.p.:** 127 – 129 ˚C. Purity: >95% (UV 214 nm).

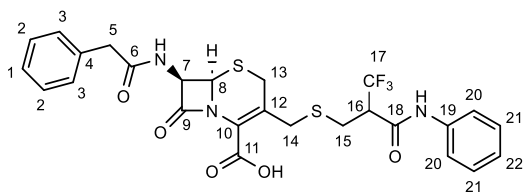[*] Chemical shifts of minor rotamer are enclosed in square brackets.

Carbon assignment

(6R,7R)-3-(((2-(benzylcarbamoyl)-3,3,3-trifluoropropyl)thio)methyl)-8-oxo-7-(2-phenylacetamido)-5-thia-1-azabicyclo[4.2.0]oct-2-ene-2-carboxylic acid **(3)**.
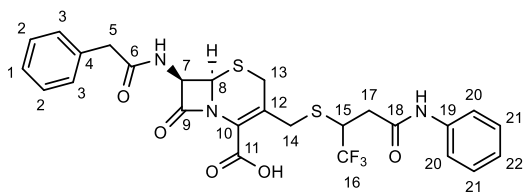

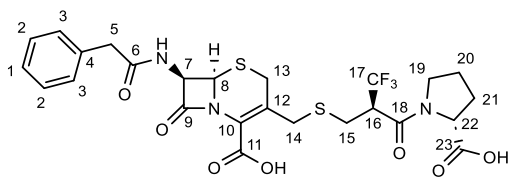| Carbon №	Shift (ppm)
1	126.5
2	128.3
3	129.1
4	135.9, 135.85
5	41.6
6	171.0
7	59.0, 58.95
8	58.0
9	164.8, 164.6
10	127.9, 127.5 or 125.2, 124.9
11	163.1, 163.0
12	127.9, 127.5 or 125.2, 124.9
13	27.1, 26.7
14	33.1, 32.6
15	26.7, 26.1
16	49.8, 49.6 (q, J = 24.6 Hz)
17	124.8 (q, J = 281.9 Hz)
18	164.6, 164.4
19	42.5
20	138.6, 138.5
21	127.2
22	128.4, 128.35
23	127.05, 127.0

(6R,7R)-8-oxo-7-(2-phenylacetamido)-3-(((3,3,3-trifluoro-2-(phenylcarbamoyl)propyl)thio)methyl)-5-thia-1-azabicyclo[4.2.0]oct-2-ene-2-carboxylic acid (**4**).

Carbon №	Shift (ppm)
1	126.5
2	128.2
3	129.0
4	135.85, 135.8
5	41.65, 41.6
6	171.0, 170.95
7	59.0
8	58.0
9	164.8, 164.7
10	128.0, 127.4 or 125.1, 124.9
11	163.05, 163.0
12	128.0, 127.4 or 125.1, 124.9
13	27.1, 26.7
14	33.1, 32.4
15	26.7, 26.0
16	50.6, 50.4 (q, *J* = 24.4 Hz)
17	124.7 (q, *J* = 281.5 Hz)
18	163.3, 163.1
19	138.2, 138.1
20	119.5, 119.4
21	128.95, 128.9
22	124.3, 124.2

(6R,7R)-8-oxo-7-(2-phenylacetamido)-3-(((1,1,1-trifluoro-4-oxo-4-(phenylamino)butan-2-yl)thio)methyl)-5-thia-1-azabicyclo[4.2.0]oct-2-ene-2-carboxylic acid (**5**).

Carbon №	Shift (ppm)
1	127.8, 127.7
2	129.4
3	130.1
4	136.3
5	43.0, 42.95
6	172.4, 172.35
7	60.25, 60.2
8	58.5, 58.3
9	165.9, 165.7
10	125.9, 125.5
11	163.4, 163.3
12	129.9, 129.8
13	28.2, 28.0
14	36.0, 35.6
15	44.9, 44.3(q, *J* = 29.7 Hz)
16	128.1 (q, *J* = 275.8 Hz)
17	37.5, 36.8
18	167.6, 167.5
19	139.4, 139.3
20	120.6, 120.5
21	129.9, 129.85
22	125.2, 125.0

(6R,7R)-3-(((4-((4-carboxyphenyl)amino)-1,1,1-trifluoro-4-oxobutan-2-yl)thio)methyl)-8-oxo-7-(2-phenylacetamido)-5-thia-1-azabicyclo[4.2.0]oct-2-ene-2-carboxylic acid **(6)**.

Carbon №	Shift (ppm)
1	126.5
2	128.3
3	129.1
4	135.9, 135.8
5	41.6
6	171.0
7	59.05, 59.0
8	57.7, 57.5
9	164.5
10	126.2, 125.8 or 125.5, 124.1
11	163.05, 163.0
12	126.2, 125.8 or 125.5, 124.1
13	26.8, 26.5
14	34.7
15	43.8, 42.7 (q, *J* = 29.1 Hz)
16	127.1 (q, *J* = 277.6 Hz)
17	36.4, 35.6
18	167.0 or 166.9, 166.85
19	125.6, 125.4
20	118.6, 118.4
21	130.6, 130.5
22	142.75, 142.65
23	167.0 or 166.9, 166.85

(6R,7R)-3-((((S)-2-((S)-2-carboxypyrrolidine-1-carbonyl)-3,3,3-trifluoropropyl)thio)methyl)-8-oxo-7-(2-phenylacetamido)-5-thia-1-azabicyclo[4.2.0]oct-2-ene-2-carboxylic acid (**7**).

Carbon №	Shift (ppm)
1	127.0
2	128.7
3	129.4
4	136.1
5	42.0
6	171.85, 171.8
7	59.3
8	58.3
9	165.1
10	129.1, 128.5 or 125.4
11	163.6, 163.5
12	129.1, 128.5 or 125.4
13	26.8
14	33.6, 33.0
15	28.2, 27.0
16	47.7, 47.6 (q, *J* = 24.8 Hz)
17	125.0 (q, *J* = 282.4 Hz)
18	164.8, 164.0
19	48.0, 46.9
20	24.6, 22.4
21	30.9, 29.3
22	60.0, 59.5
23	173.2, 173.15

(6R,7R)-3-((((R)-2-((R)-2-carboxypyrrolidine-1-carbonyl)-3,3,3-trifluoropropyl)thio)methyl)-8-oxo-7-(2-phenylacetamido)-5-thia-1-azabicyclo[4.2.0]oct-2-ene-2-carboxylic acid (**8**).

Carbon №	Shift (ppm)
1	126.5
2	128.3
3	129.0
4	135.9
5	41.6
6	171.0, 170.95
7	59.1
8	57.9
9	164.6, 164.5
10	128.4, 127.4 or 125.1, 125.0
11	163.2, 163.1
12	128.4, 127.4 or 125.1, 125.0
13	26.9
14	34.0, 33.3
15	27.4
16	47.3 (q, J = 24.5 Hz)
17	124.6 (q, J = 281.8 Hz)
18	164.1, 163.3 (q, J = 2.1 Hz)
19	47.5, 46.5
20	24.2, 22.1
21	30.4, 28.9
22	59.6, 59.0
23	172.8, 172.7

LC-MS-based hydrolysis experiments

Hydrolysis using basic conditions

The conjugates (6 µL, 0.174 M in DMSO) were added to 1 M $Na_2CO_{3(aq)}$ or 3 M $(NH_4)_2CO_{3(aq)}$. At the indicated time intervals, samples were taken from the reaction mixture and diluted in water or methanol (1:1 v/v) and analyzed following the general procedure for UHPLC-HRMS (Fig. S1–S8).

Figure S1. LC-MS analysis of Na_2CO_3 (left) and $(NH_4)_2CO_3$-mediated (right) degradation of **1**.

Figure S2. LC-MS analysis of Na_2CO_3 (left) and $(NH_4)_2CO_3$-mediated (right) degradation of **2**.

Figure S3. LC-MS analysis of Na₂CO₃-mediated degradation of **3**.

Figure S4. LC-MS analysis of Na₂CO₃ (left) and (NH₄)₂CO₃-mediated (right) degradation of **4**.

Figure S5. LC-MS analysis of Na$_2$CO$_3$ (left) and (NH$_4$)$_2$CO$_3$-mediated (right) degradation of **5**.

Figure S6. LC-MS analysis of Na$_2$CO$_3$ (left) and (NH$_4$)$_2$CO$_3$-mediated (right) degradation of **6**.

Figure S7. LC-MS analysis of Na$_2$CO$_3$ (left) and (NH$_4$)$_2$CO$_3$-mediated (right) degradation of **7**.

Figure S8. LC-MS analysis of Na$_2$CO$_3$ (left) and (NH$_4$)$_2$CO$_3$-mediated (right) degradation of **8**.

Enzymatic hydrolysis

Stock solutions of conjugates **10–12** in DMSO-*d6* were prepared (0.174 M). To a mixture of 586 μl 20 mM HEPES buffer (pH 7.4), 6 μl ZnSO$_4$ (50 mM in H$_2$O) and 6 μl compound **1–8** (stock solution: 0.174 M in DMSO-*d6*) 2 μl of NDM-1 (37.4 μM) were added. At various time-points after incubation at ambient temperature, samples were taken from the reaction mixture and diluted in acetonitrile (1:2 v/v).

After centrifugation for 5 minutes at 6000 rpm, the supernatant was analyzed following the general procedure for UHPLC-HRMS.

Figure S9. LC-MS analysis of NDM-1-mediated degradation of **6**.

NMR-based enzymatic hydrolysis experiments

1D ^{1}H NMR spectra were acquired with a fid size of 65k points over a 4 second acquisition time and a 4 second relaxation delay (D1) for 32 scans (4 dummy scans) for a total experiment time of 5 minutes per spectra. Excitation sculpting was utilized to remove the residual water peak at 4.7 ppm. 1D ^{19}F spectra were acquired with a fid size of 131k points with an acquisition time of 700 ms and a relaxation delay of 2 s for 64 scans with a total experiment time of 3 minutes.

Stock solutions of conjugates **1**–**8** in DMSO-*d6* were prepared (0.174 M). The NMR sample consisted of 582 µl HEPES buffer (20 mM in D$_2$O), 6 µl ZnSO$_4$ (50 mM in D$_2$O) and 6 µl compound **1**–**8** (stock solution: 0.174 M in DMSO-*d6*). An initial ^{1}H spectra was acquired before the addition of 2 µl NDM-1 (37.4 µM). After NDM-1 addition, ^{1}H spectra were acquired in a continuous manner over a period of 2 hours. Conjugate **1** was used as a reference compound to optimize the conditions of the hydrolysis experiment and the obtained data was found to be in accordance with literature reports.[2] Conjugate **3** displayed limited solubility in the conditions of the experiment, therefore, the results are not shown.

Figure S10. NMR analysis of NDM-1-mediated degradation of **2**.

Figure S11. NMR analysis of NDM-1-mediated degradation of **6**.

Figure S12. NMR analysis of NDM-1-mediated degradation of **7**.

Figure S13. NMR analysis of NDM-1-mediated degradation of **8**.

MBL inhibition assay and IC$_{50}$ curves

All the compounds were tested for their inhibitory activity against the purified enzymes of NDM-1, VIM-2, IMP-2 and IMP-7. The molecules at 2-fold dilution (88-0.085938 µg/ml) were tested in triplicates in a direct competition assay with nitrocefin in HEPES buffer 50 mM pH 7.2, supplemented with 0.01% triton X-100 at room temperature. Inhibitors were incubated for 10 minutes with the respective enzymes and the reaction was started by adding 20 µM nitrocefin and the hydrolysis was recorded every 2 s for 2 minutes at A$_{486}$. IC$_{50}$ values were calculated by plotting the *log[I] vs normalized response (variable slope)* program in GraphPad prism. The normalized response was obtained by taking the initial rate of hydrolysis at different concentrations of the inhibitor converted to the percentage of residual activity, compared to a reaction without inhibitor. The rate of the reaction without an inhibitor was considered as 100% activity.

$$\%RA = \frac{100}{1 + 10^{(\log IC_{50} - \log[I])*h}}$$
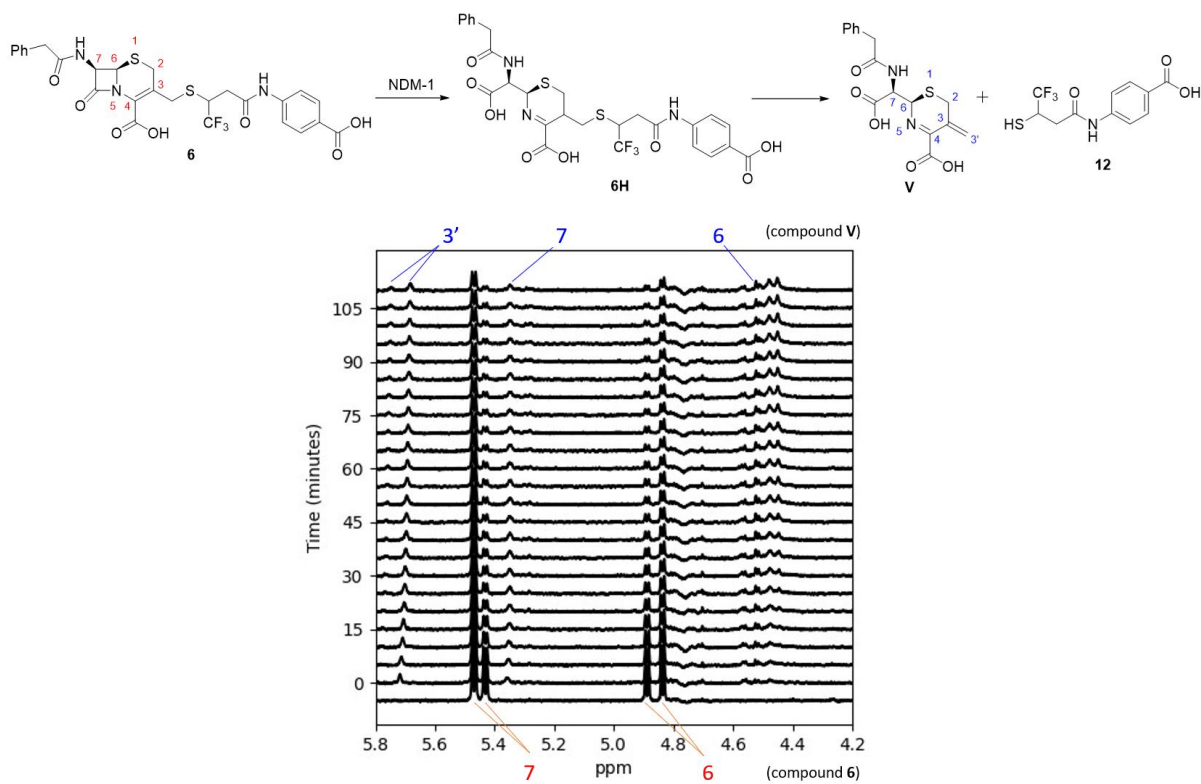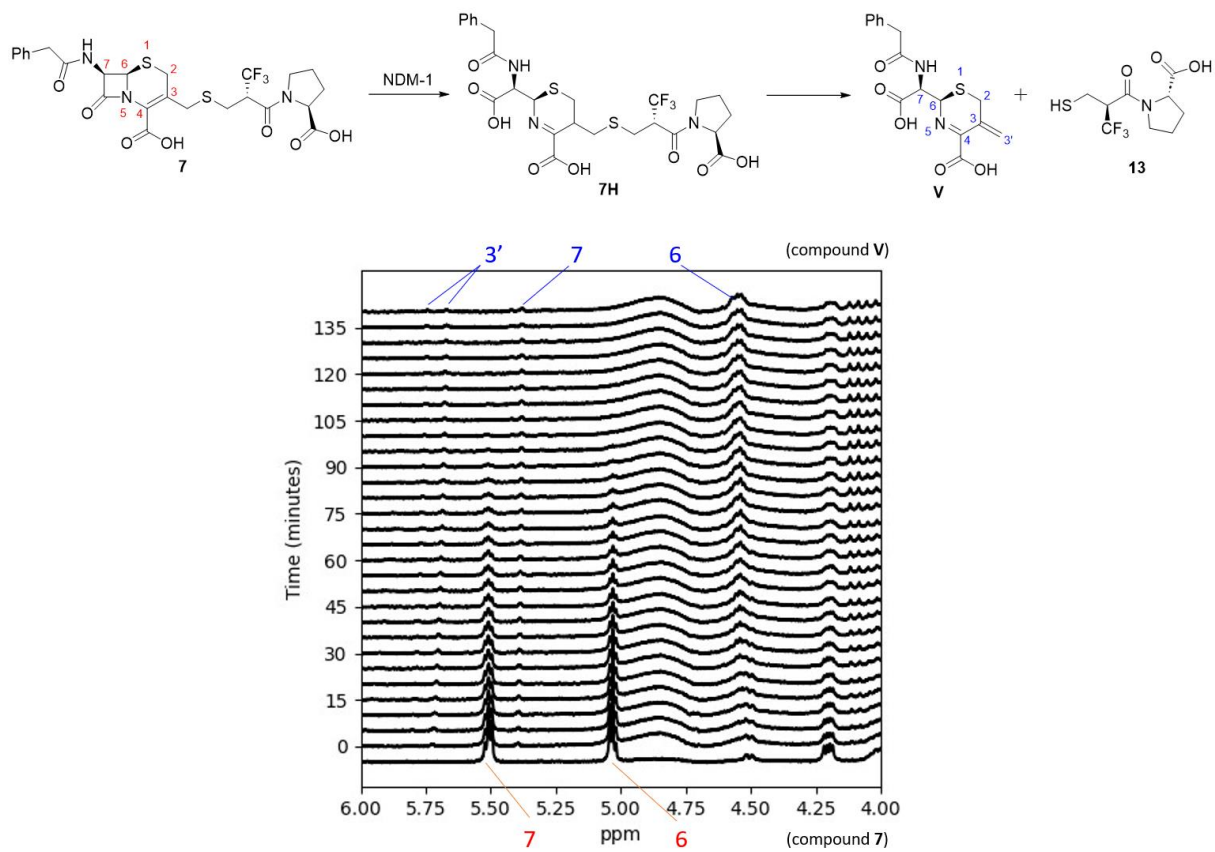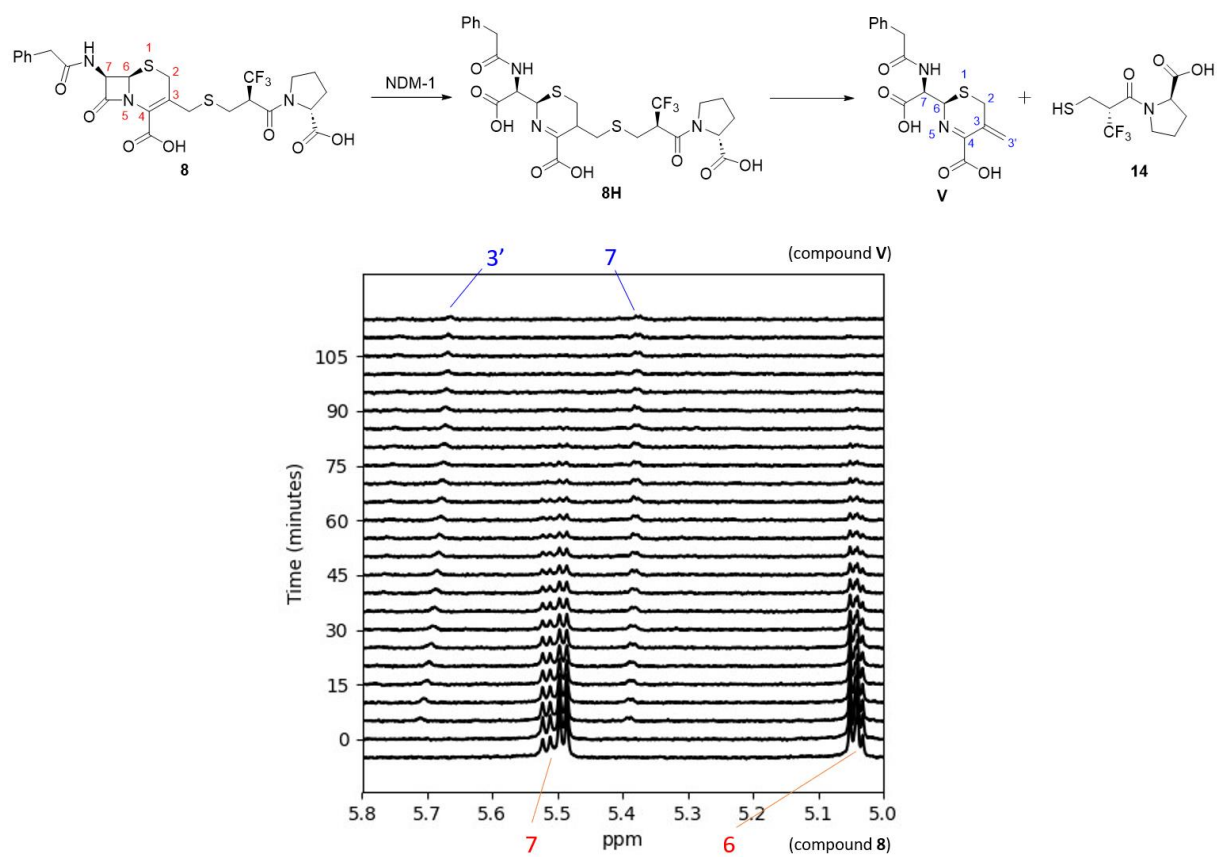
Where h is the Hill coefficient, IC$_{50}$ is the half-maximal inhibitory concentration and %RA is the percentage of residual activity.

Table S1. IC$_{50}$ values of conjugates and thiols against selected B1 MBLs.

Compound	Corresponding thiol	IC$_{50}$ (µM)			
		NDM-1	VIM-2	IMP-2	IMP-7
1	8-TQ	1.92 ± 0.06 (2.31 ± 0.25[a])	1.99 ± 0.07 (3.64 ± 0.27[a])	1.4 ± 0.09	2.4 ± 0.17
2	L-captopril	31.81 ± 4.93	10.37 ± 1.64	22.44 ± 3.11	6.91 ± 0.49
3	9	27.76 ± 8.4	4.58 ± 0.22	19.24 ± 0.73	18.61 ± 1.32
4	10	3.76 ± 0.35	0.61 ± 0.05	11.28 ± 2.17	13.47 ± 1.75
5	11	8.22 ± 0.34	7.11 ± 0.37	6.07 ± 0.83	8.61 ± 0.45
6	12	4.5 ± 0.38	33.64 ± 4.49	2.79 ± 0.93	4.12 ± 0.11
7	13	91.72 ± 5.08	15.34 ± 1.22	82.33 ± 26.17	21.84 ± 0.84
8	14	2.02 ± 0.55	4.28 ± 0.86	1.98 ± 0.52	3.19 ± 0.11
9	-	4.25 ± 0.08 (20 ± 2[b])	7.39 ± 0.54	6.18 ± 0.47	33.82 ± 2.58
10	-	4.28 ± 0.50 (3.4 ± 0.5[b])	5.95 ± 0.96	5.82 ± 0.16	17 ± 0.45
11	-	27.65 ± 0.95 (22 ± 6[b])	86.14 ± 7.76	43.53 ± 3.59	89.51 ± 0.46
12	-	(5.6 ± 1.4[b])	-	-	-
13	-	(60 ± 20[b])	-	-	-
14	-	(0.3 ± 0.1[b])	-	-	-
16[c]	-	>300	49.94 ± 5.18	>300	60.05 ± 6.94
L-captopril	-	13.12 ± 3.23 (7 ± 2[b])	4.487 ± 0.19	6.16 ± 0.31	10.15 ± 0.76

a-b Previously reported IC$_{50}$ values in a[2] and b[1]. *c* Structure **16** (right), synthesized as reported.[4]
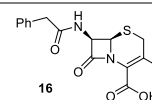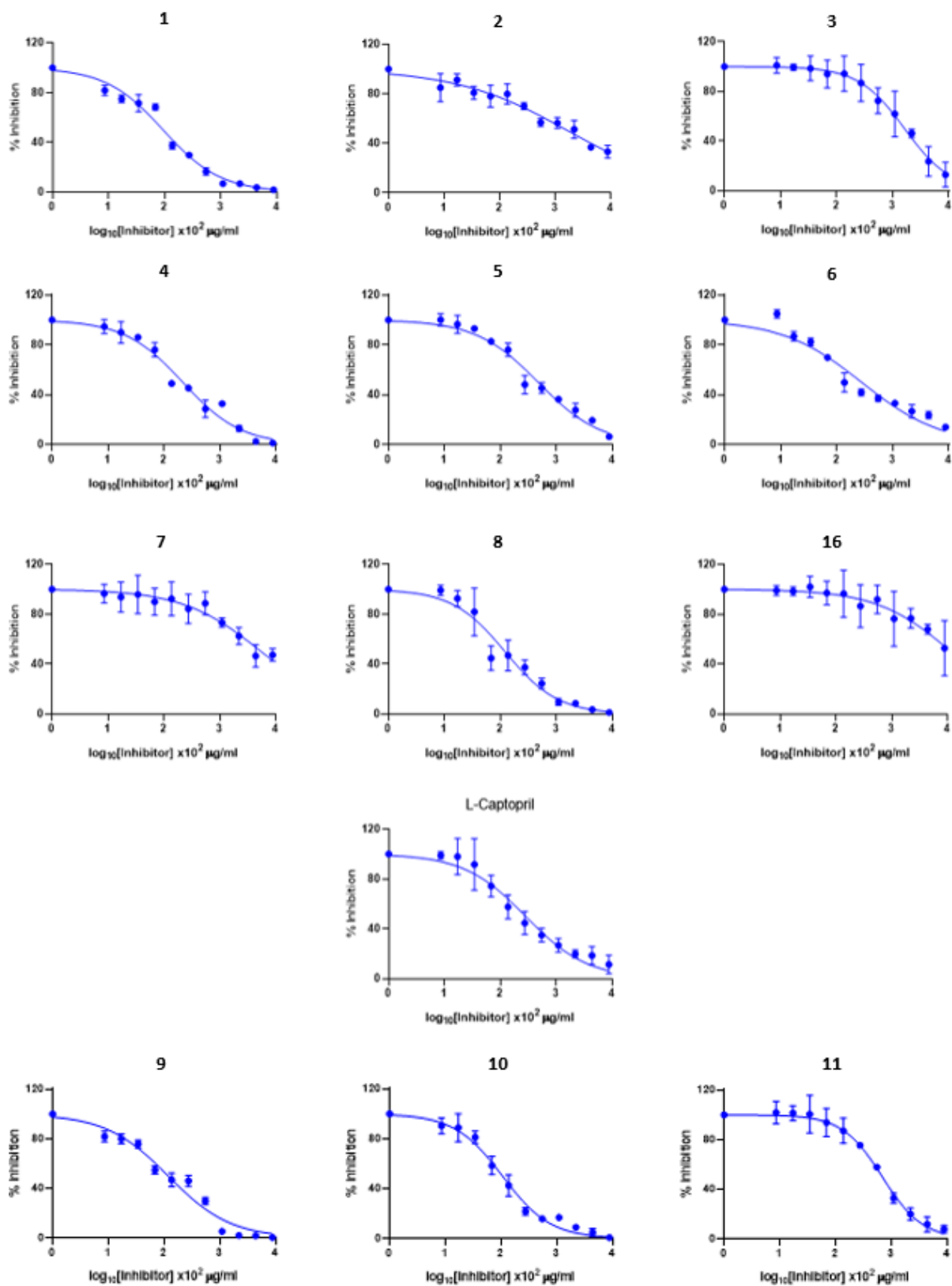
Figure S14. IC$_{50}$ curves for compounds **1**-**8**, **16** and L-captopril against NDM-1.
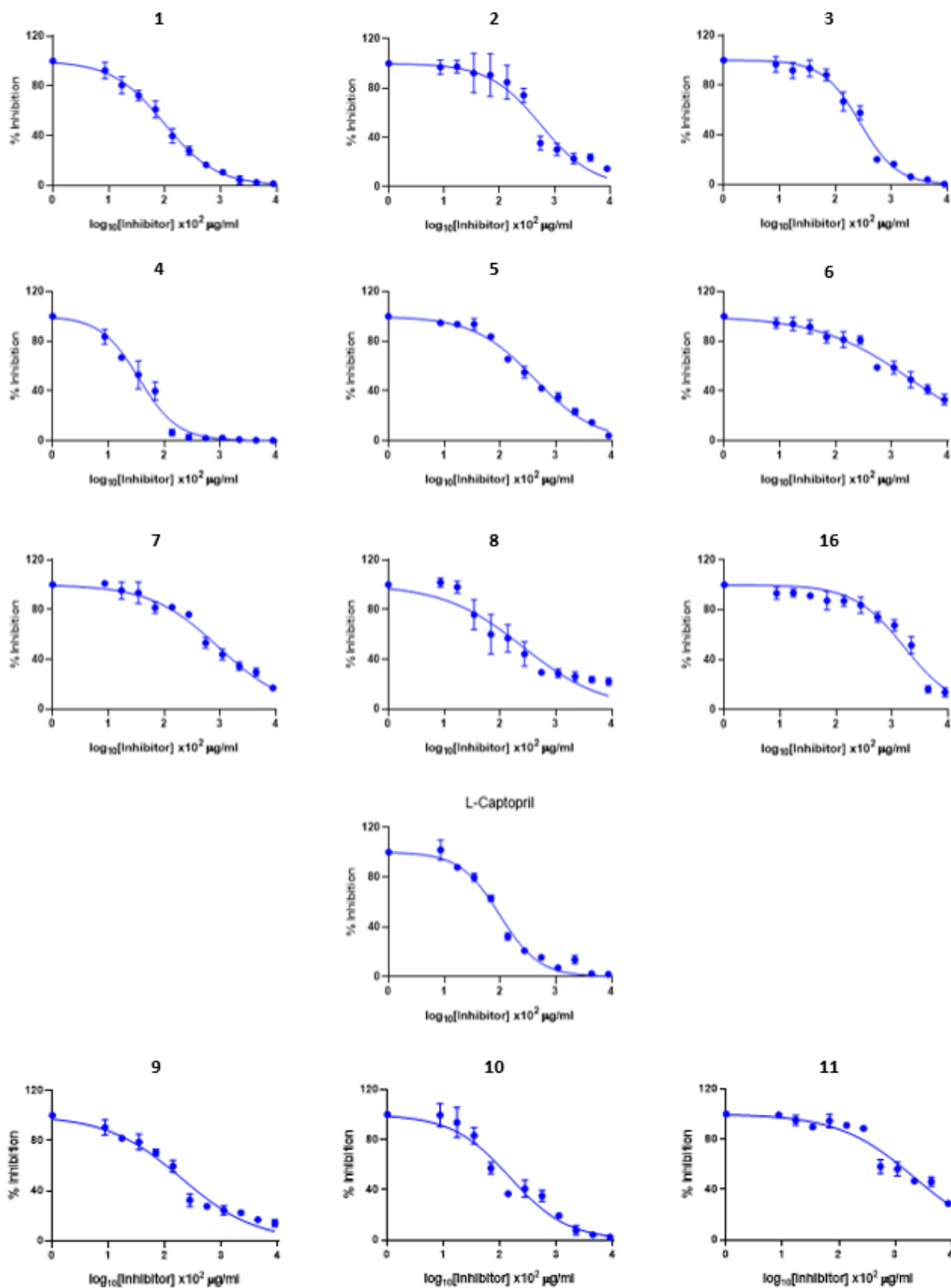
Figure S15. IC$_{50}$ curves for compounds **1-8**, **16** and L-captopril against VIM-2.
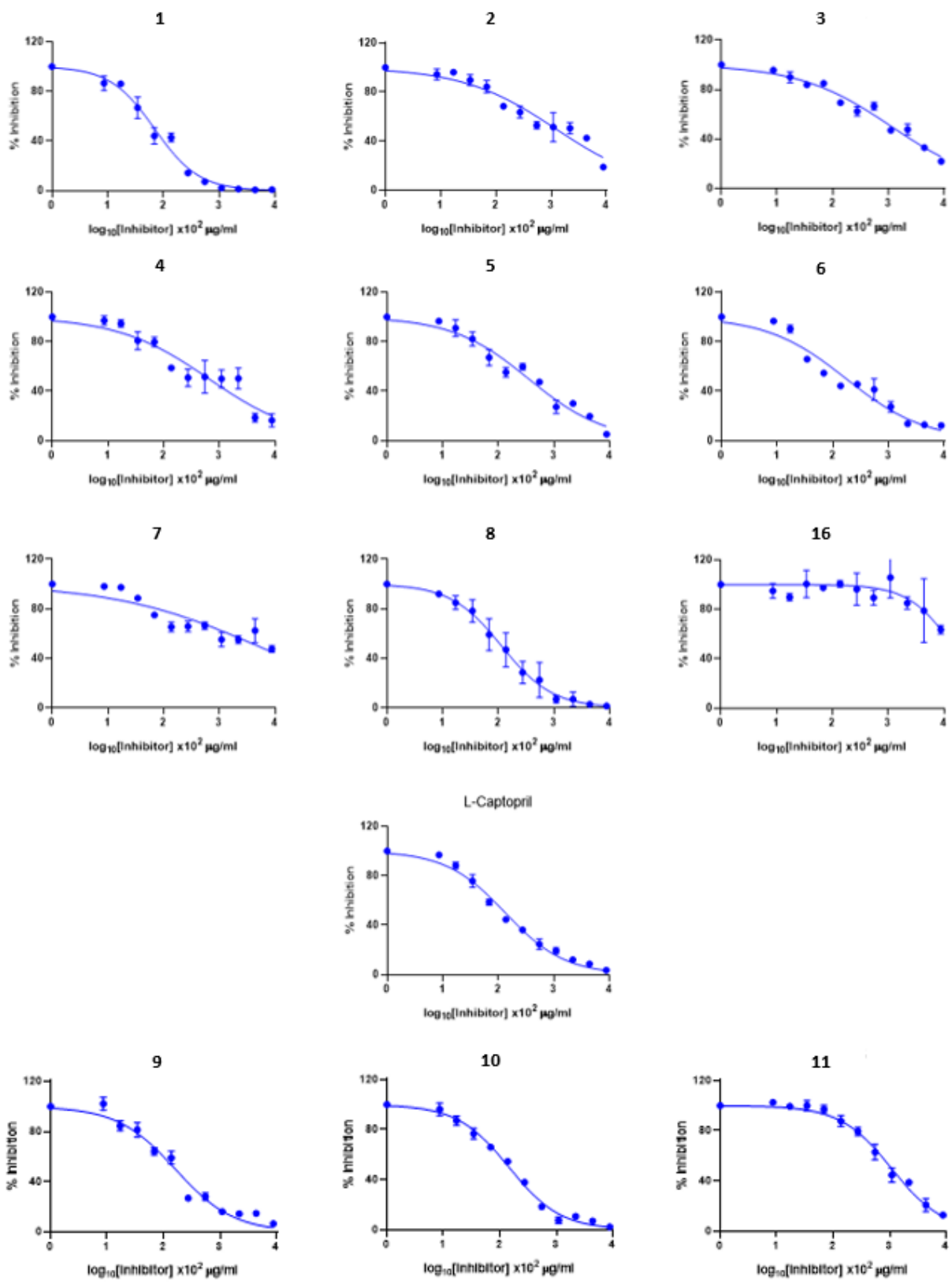
**Figure S16**. IC$_{50}$ curves for compounds **1-8**, **16** and L-captopril against IMP-2.
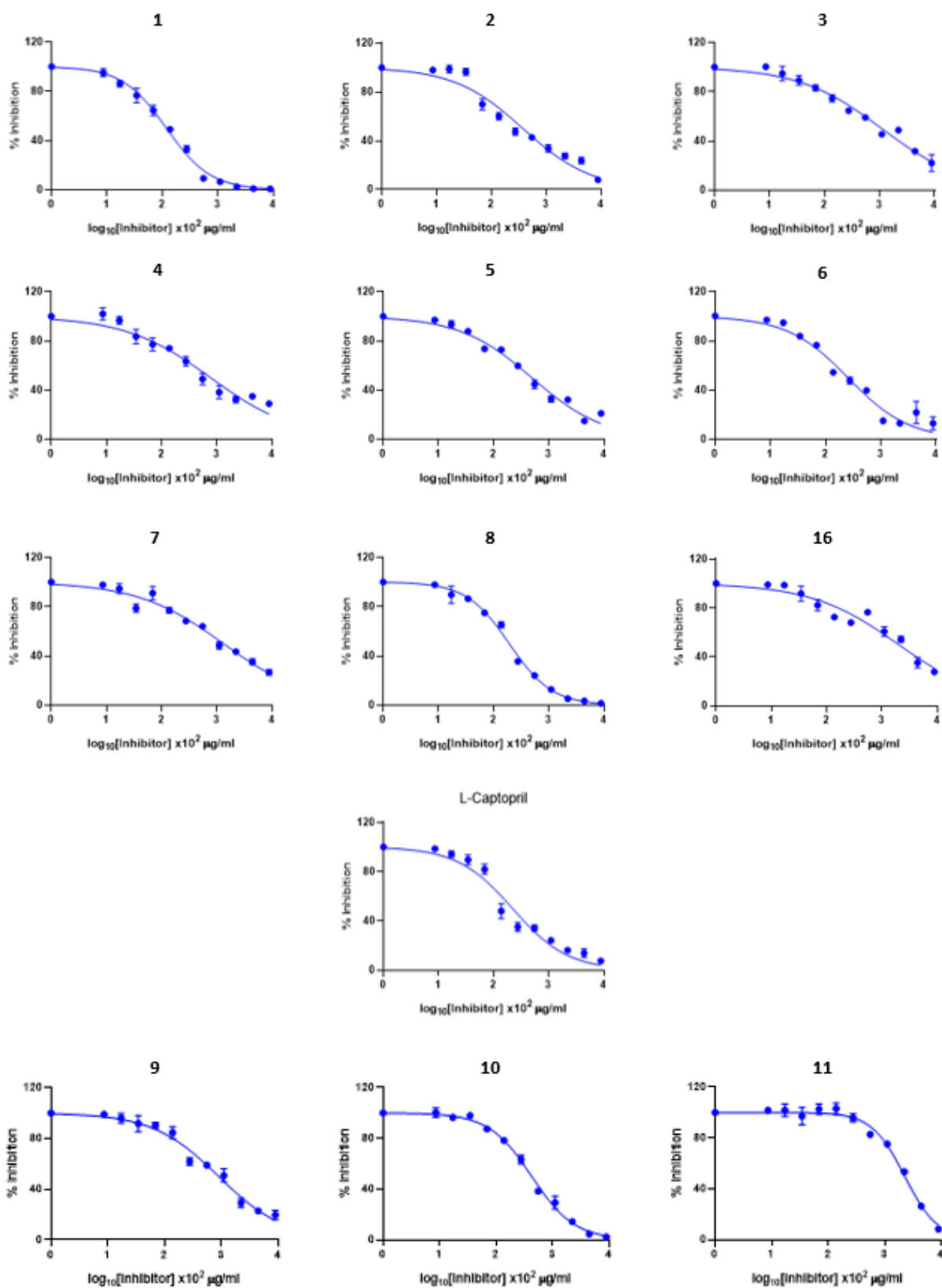
Figure S17. IC$_{50}$ curves for compounds **1**-**8**, **16** and L-captopril against IMP-7.

^{1}H and ^{13}C NMR spectra of final compounds

(6R,7R)-3-((((S)-3-((S)-2-carboxypyrrolidin-1-yl)-2-methyl-3-oxopropyl)thio)methyl)-8-oxo-7-(2-phenylacetamido)-5-thia-1-azabicyclo[4.2.0]oct-2-ene-2-carboxylic acid (**2**)
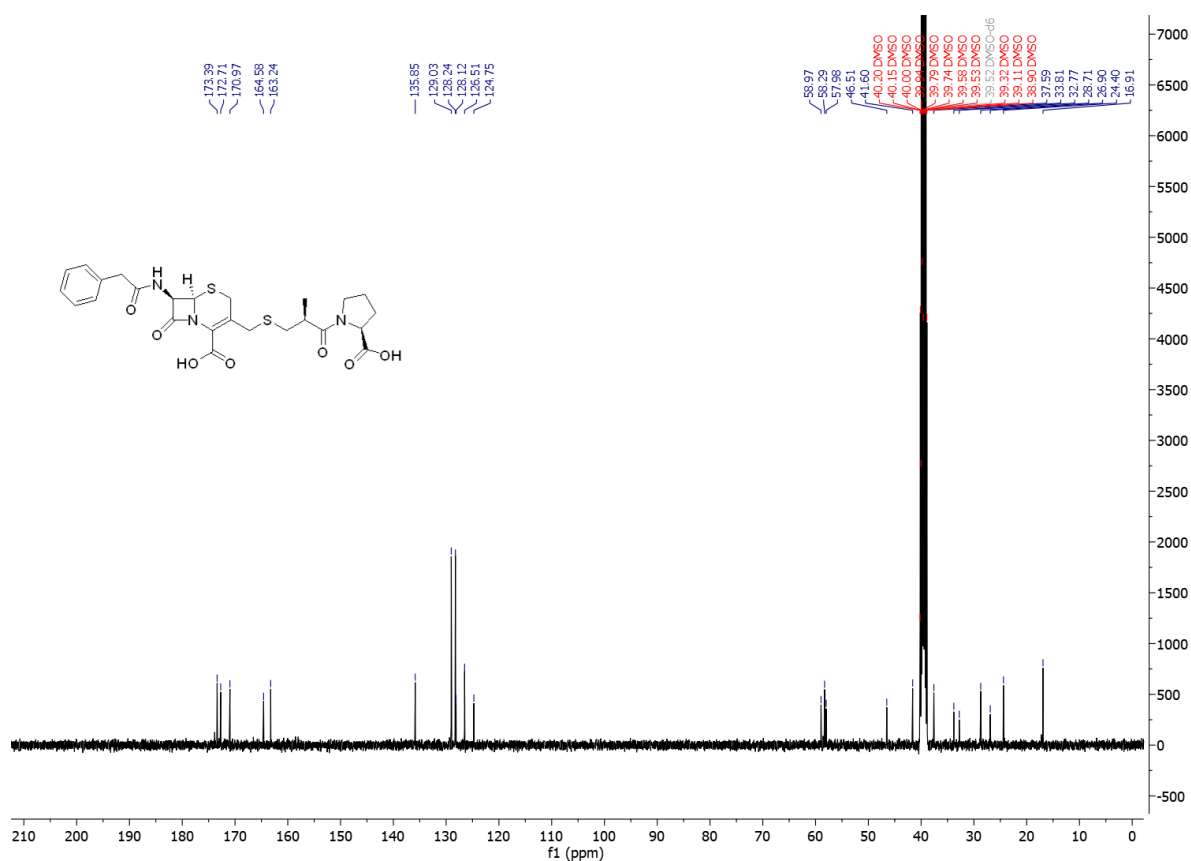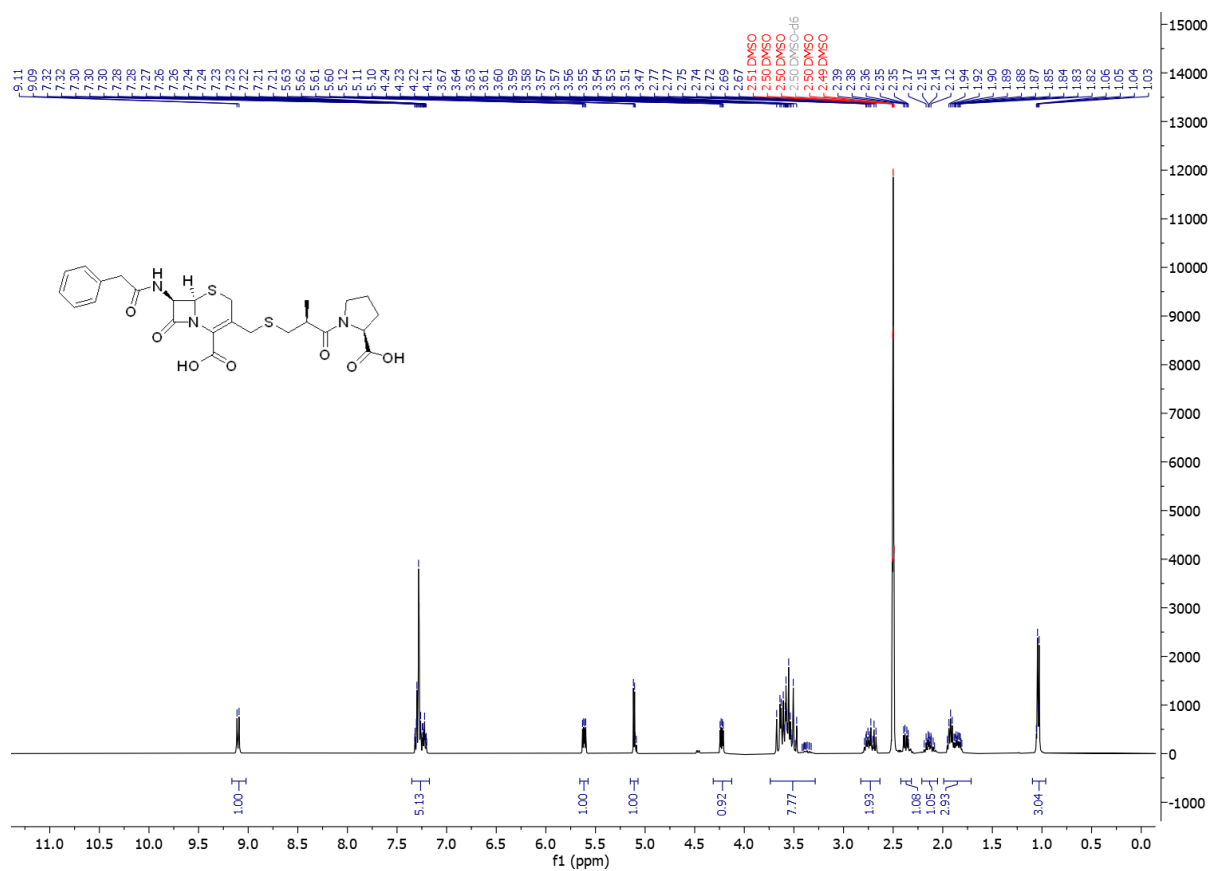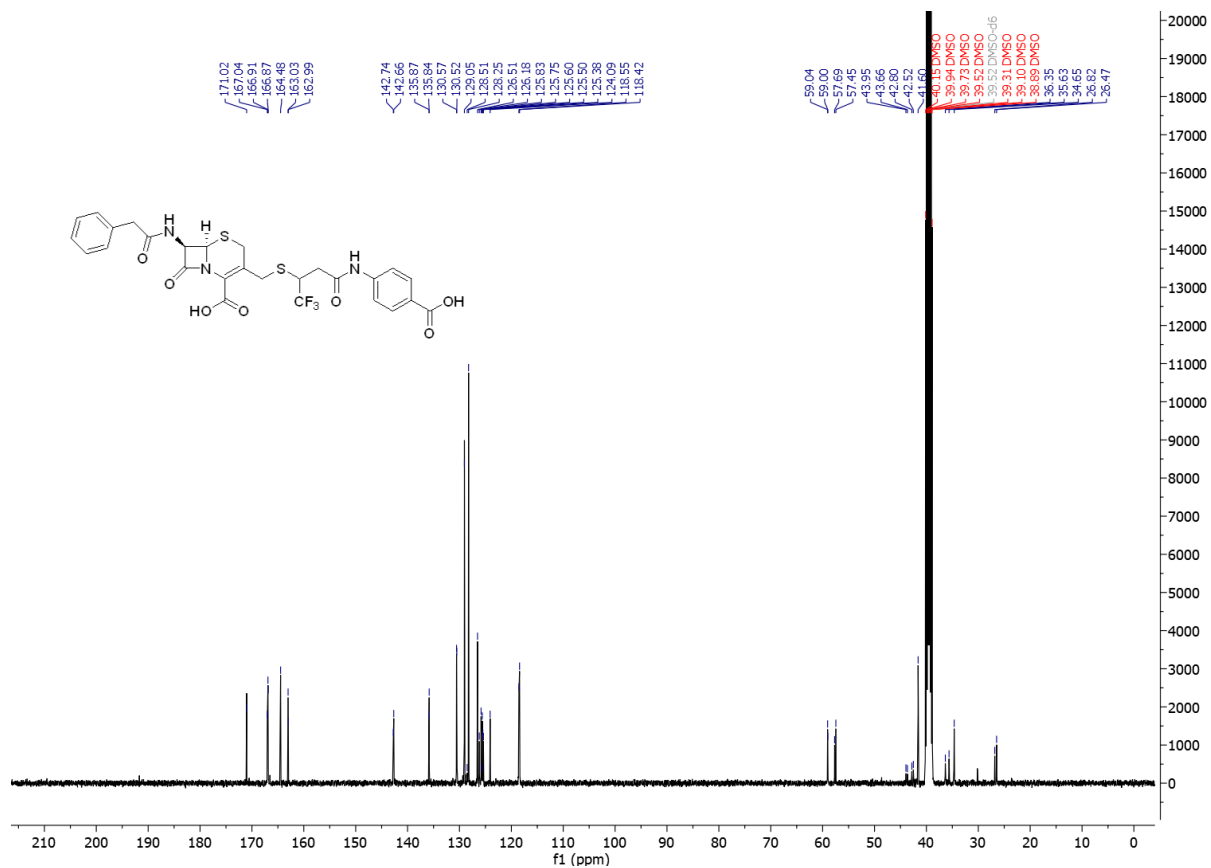
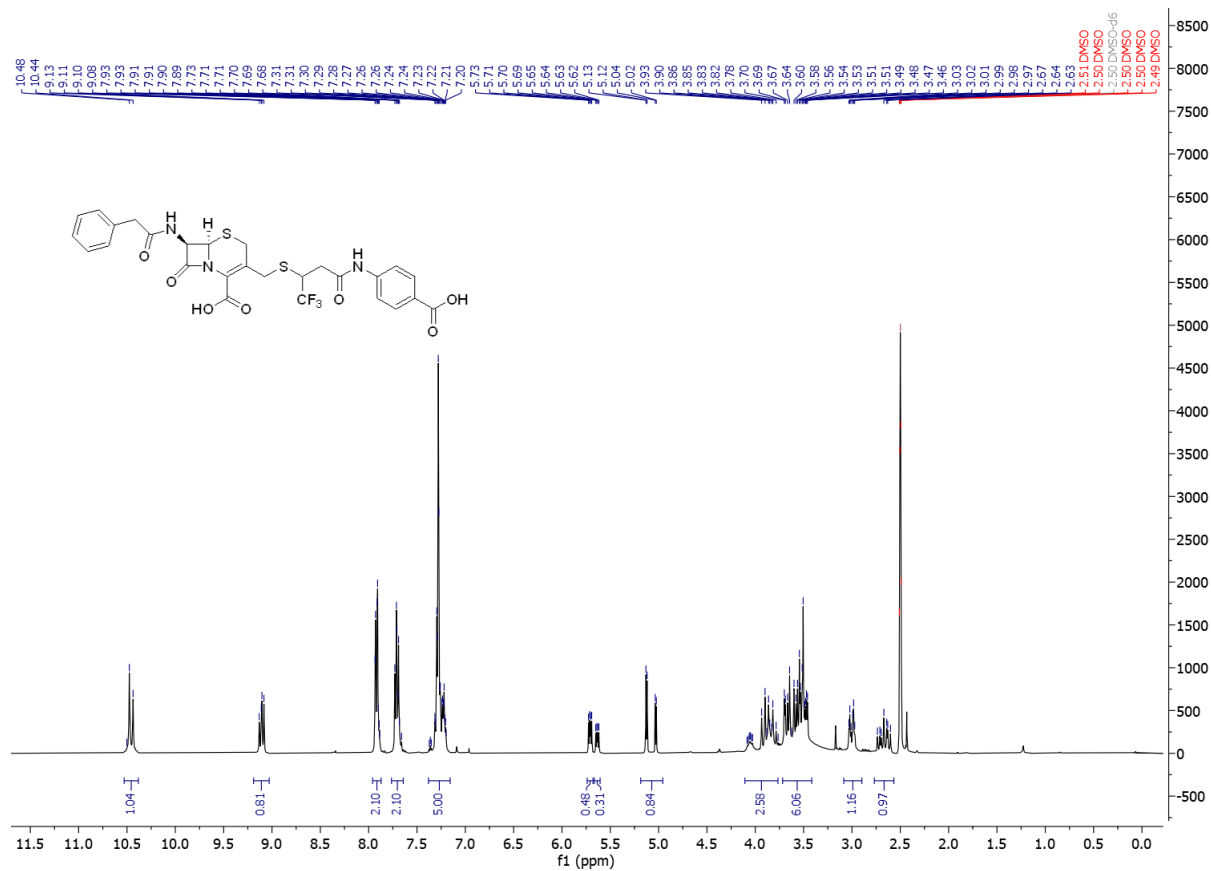*(6R,7R)-3-(((2-(benzylcarbamoyl)-3,3,3-trifluoropropyl)thio)methyl)-8-oxo-7-(2-phenylacetamido)-5-thia-1-azabicyclo[4.2.0]oct-2-ene-2-carboxylic acid* **(3)**
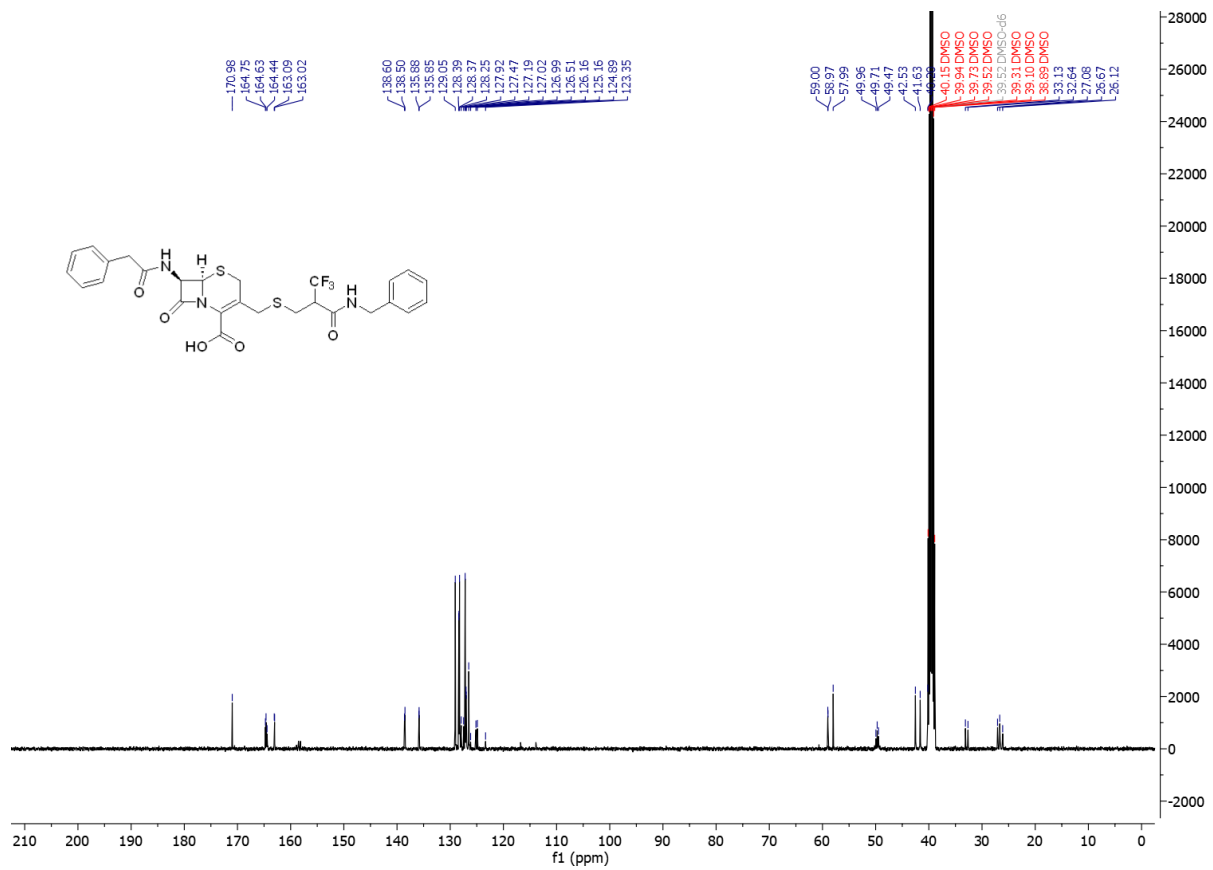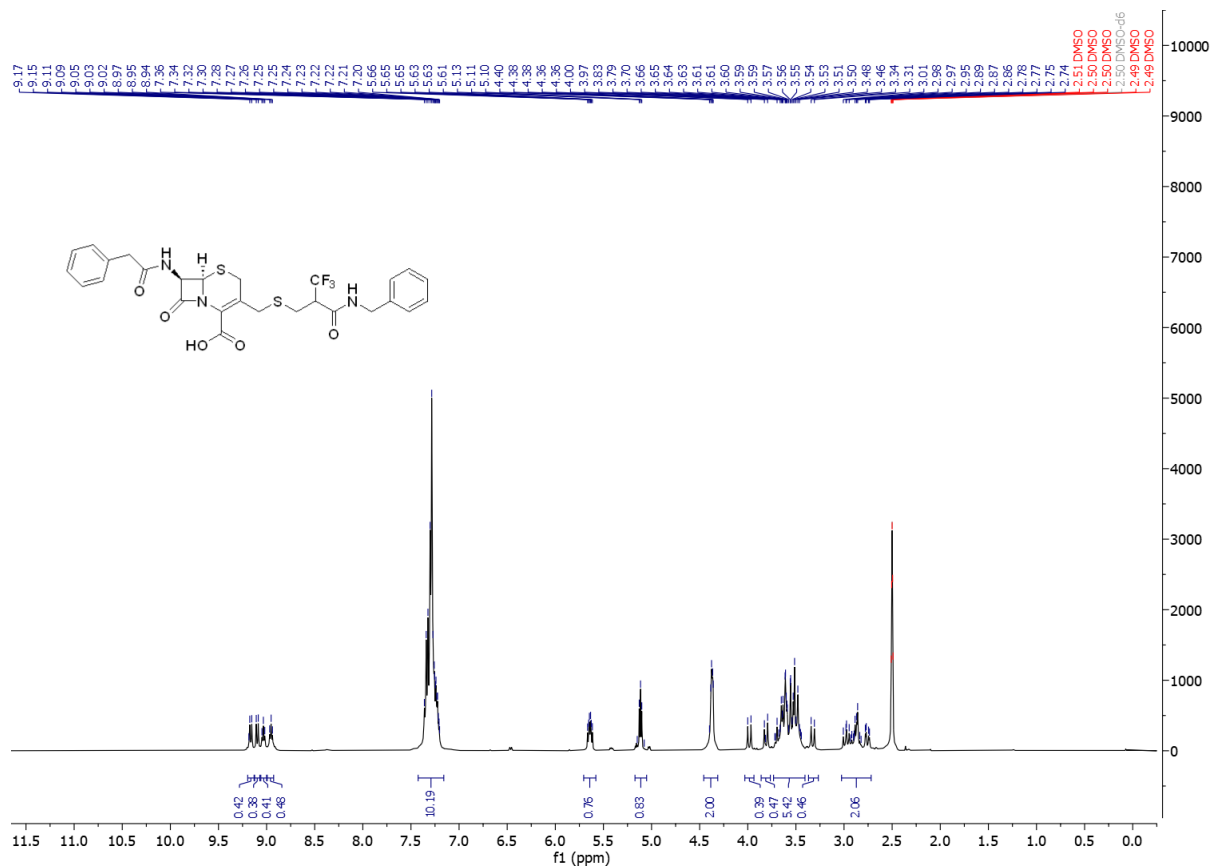
(6R,7R)-8-oxo-7-(2-phenylacetamido)-3-(((3,3,3-trifluoro-2-(phenylcarbamoyl)propyl)thio)methyl)-5-thia-1-azabicyclo[4.2.0]oct-2-ene-2-carboxylic acid **(4)**
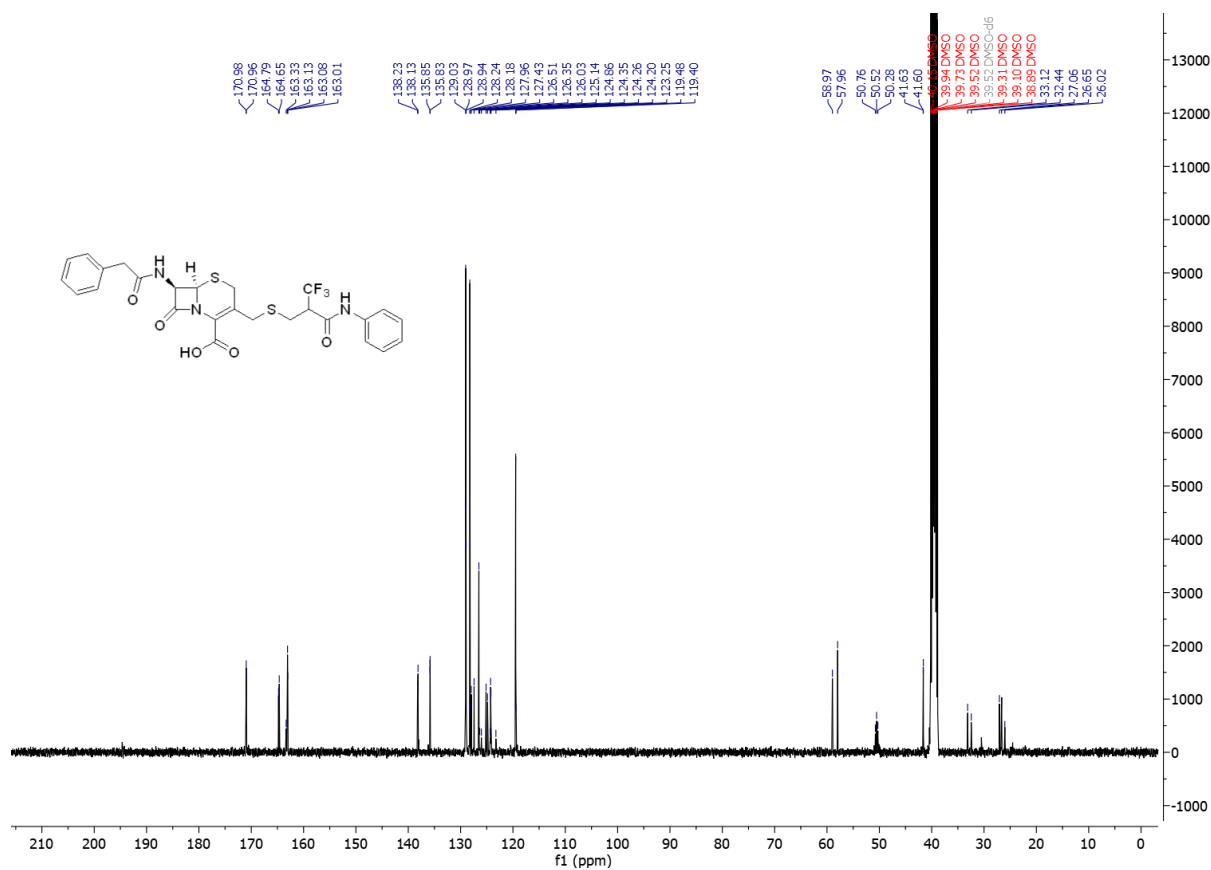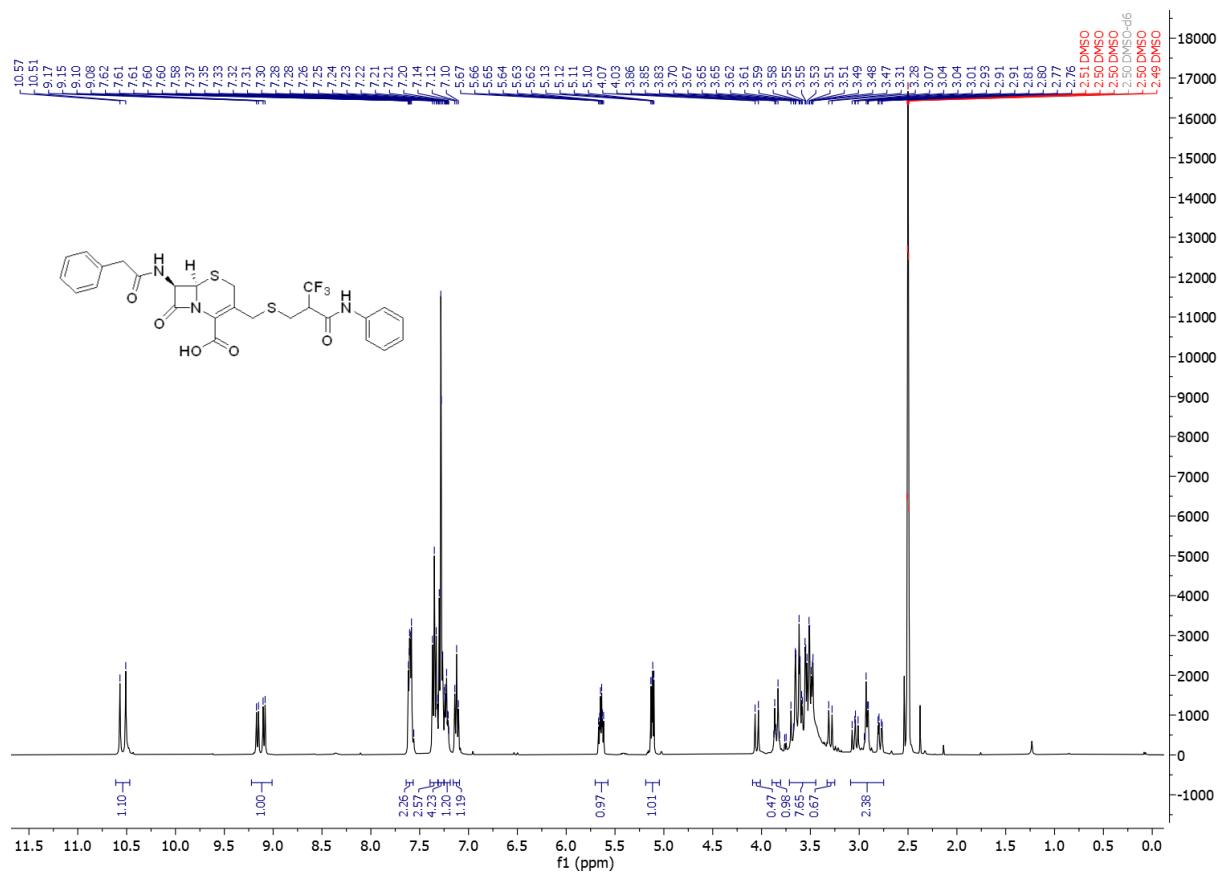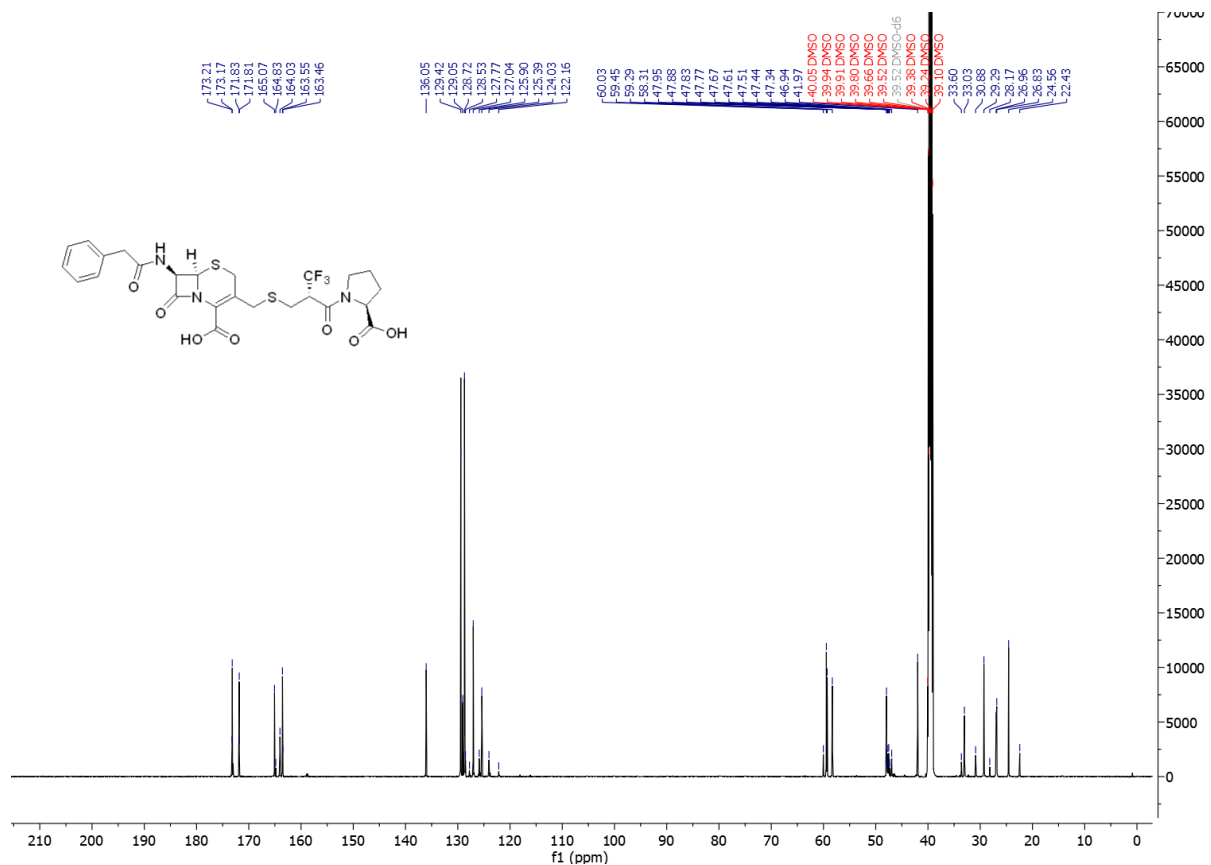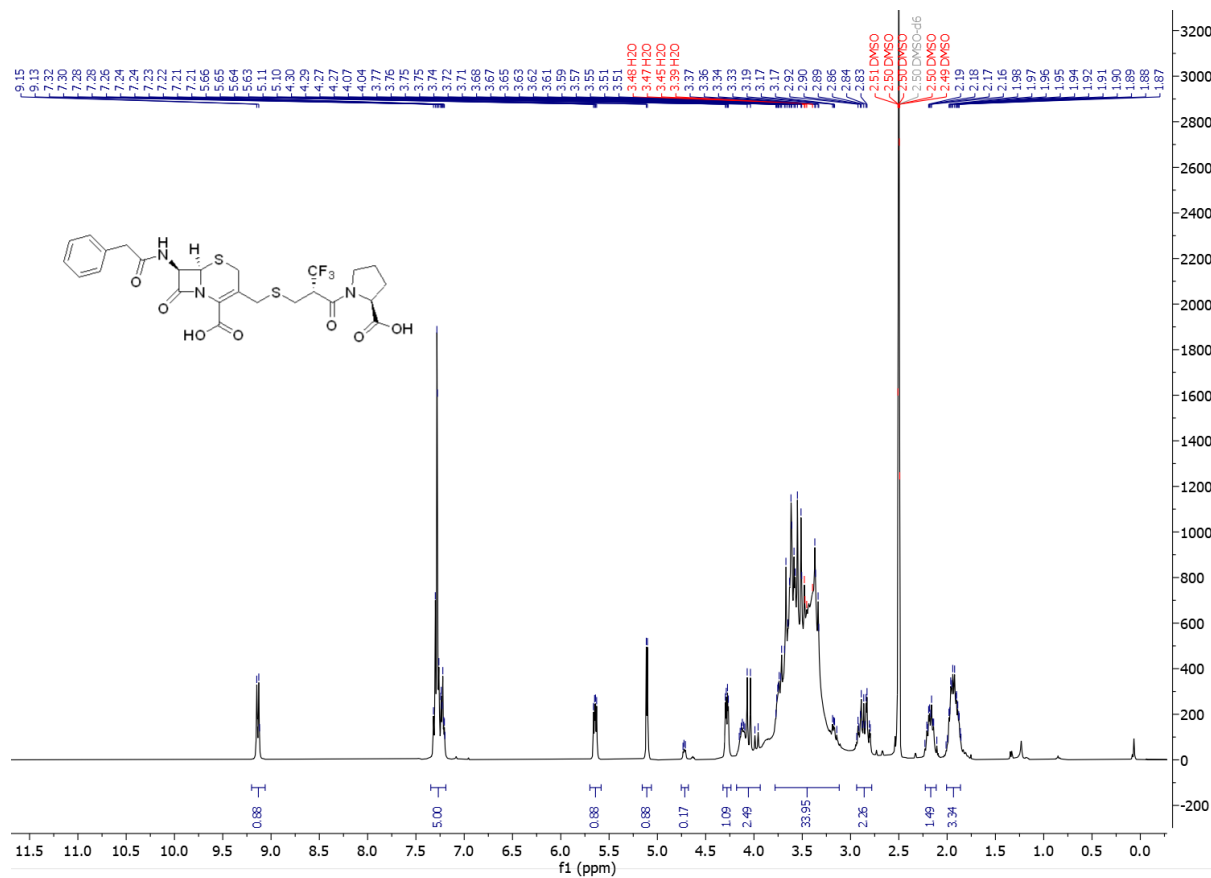
(6R,7R)-8-oxo-7-(2-phenylacetamido)-3-(((1,1,1-trifluoro-4-oxo-4-(phenylamino)butan-2-yl)thio)methyl)-5-thia-1-azabicyclo[4.2.0]oct-2-ene-2-carboxylic acid **(5)**
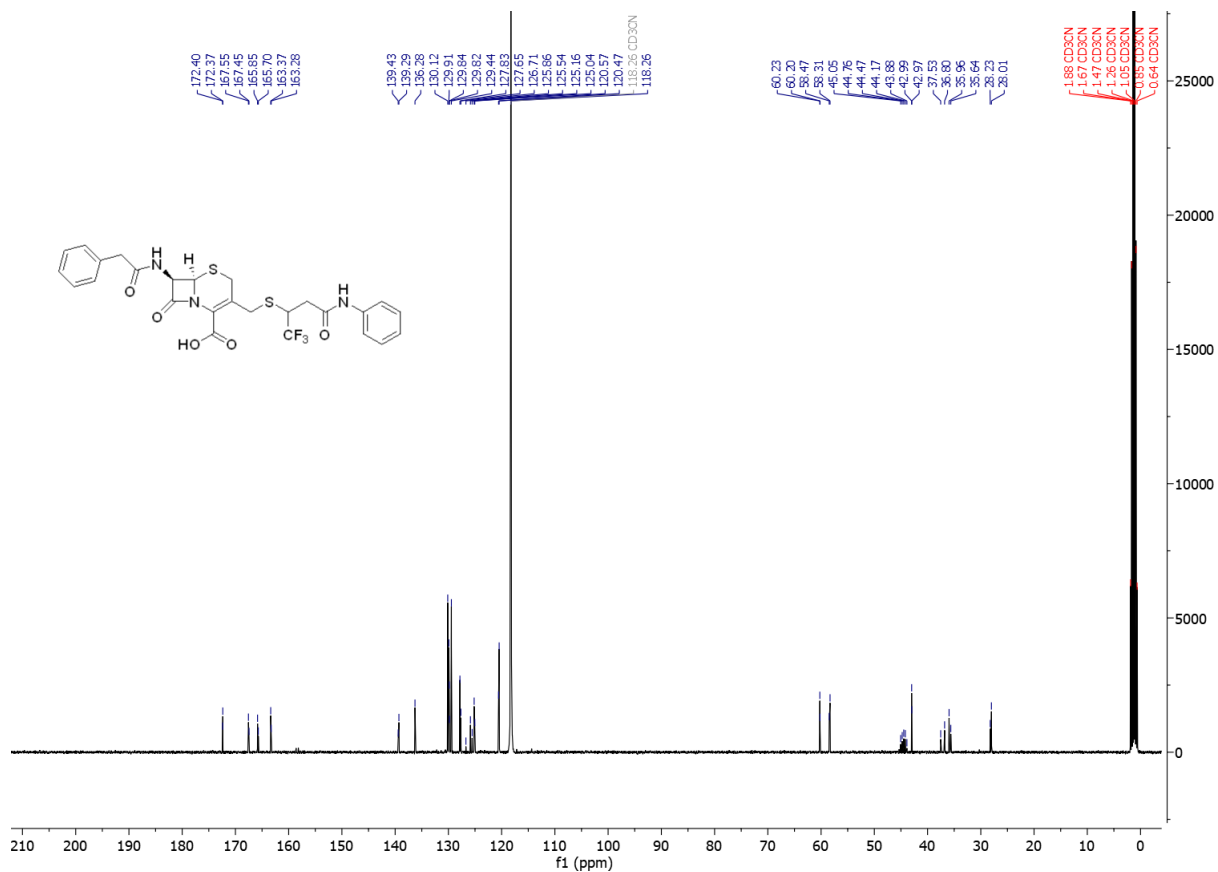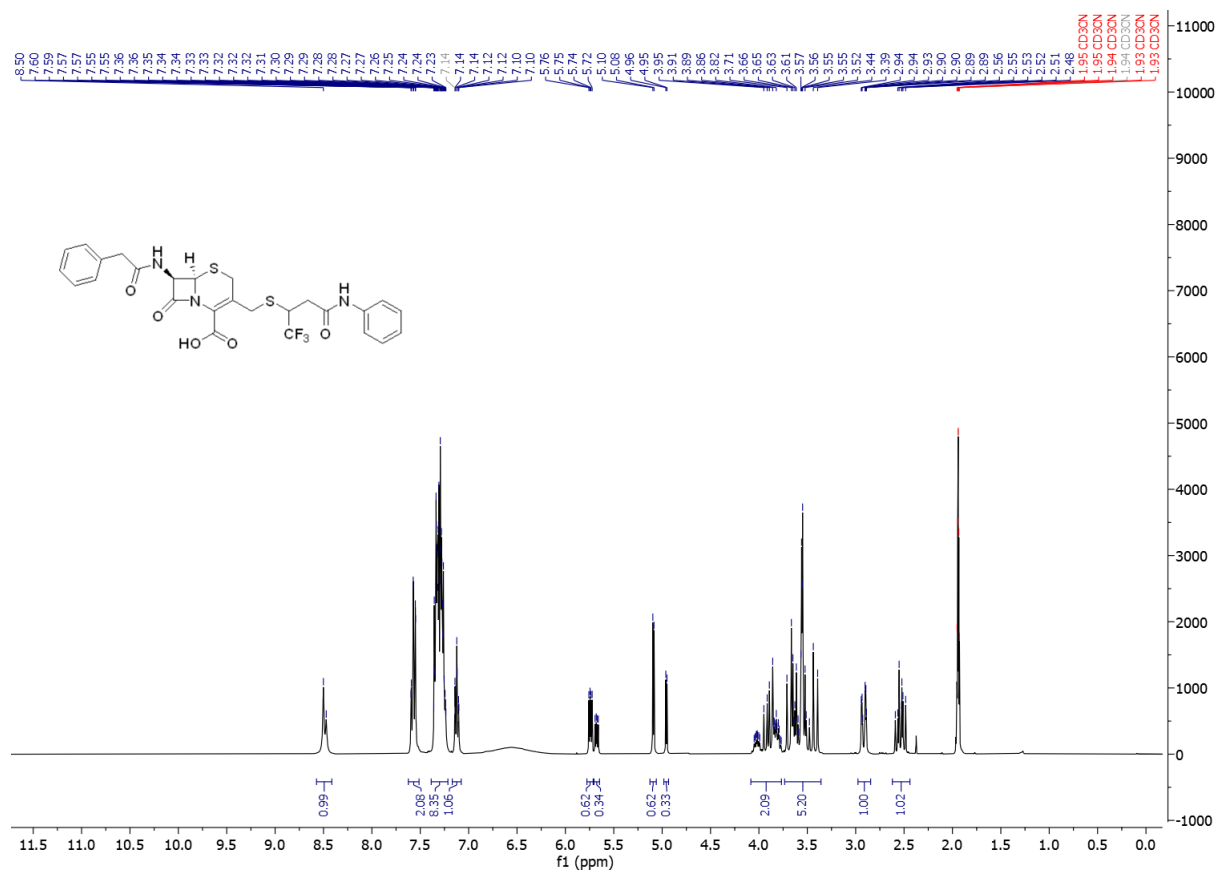
(6R,7R)-3-(((4-((4-carboxyphenyl)amino)-1,1,1-trifluoro-4-oxobutan-2-yl)thio)methyl)-8-oxo-7-(2-phenylacetamido)-5-thia-1-azabicyclo[4.2.0]oct-2-ene-2-carboxylic acid **(6)**

(6R,7R)-3-((((S)-2-((S)-2-carboxypyrrolidine-1-carbonyl)-3,3,3-trifluoropropyl)thio)methyl)-8-oxo-7-
(2-phenylacetamido)-5-thia-1-azabicyclo[4.2.0]oct-2-ene-2-carboxylic acid (**7**)

(6R,7R)-3-((((R)-2-((R)-2-carboxypyrrolidine-1-carbonyl)-3,3,3-trifluoropropyl)thio)methyl)-8-oxo-7-(2-phenylacetamido)-5-thia-1-azabicyclo[4.2.0]oct-2-ene-2-carboxylic acid **(8)**
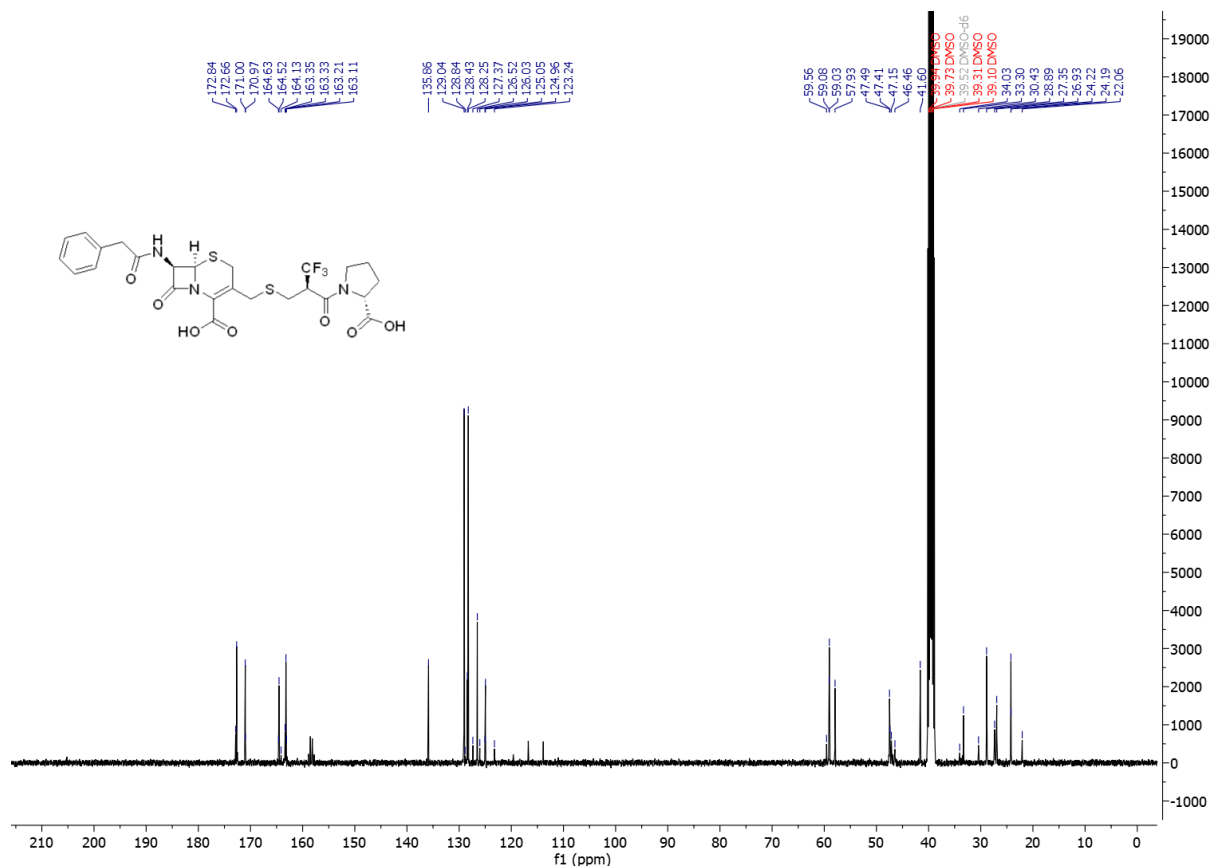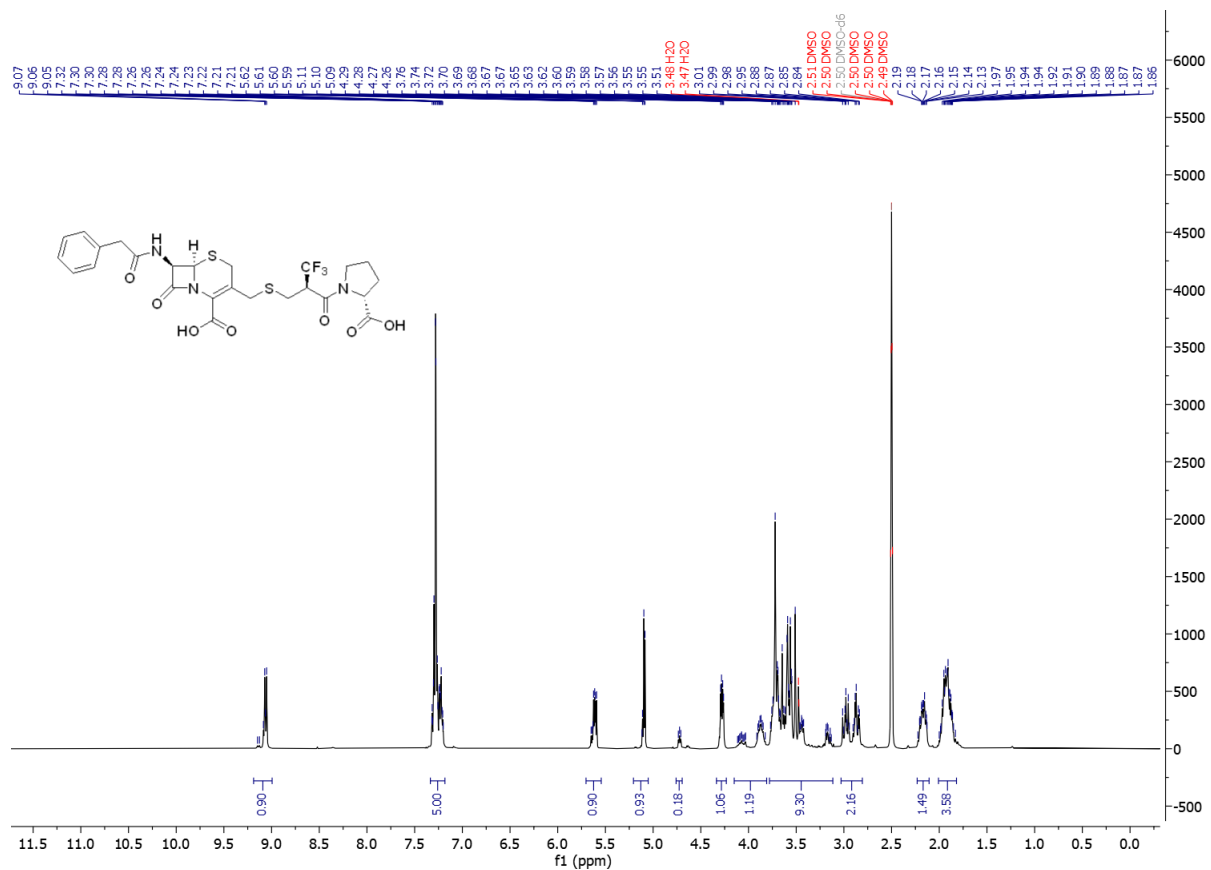
References

[1] Kondratieva, A.; Palica, K.; Frøhlich, C.; Hovd, R. R.; Leiros, H.-K. S.; Erdelyi, M.; Bayer, A., Fluorinated Captopril Analogues Inhibit Metallo-β-Lactamases and Facilitate Structure Determination of NDM-1 Binding Pose. *Eur. J. Med. Chem.* **2024**, *266*, 116140.

[2] van Haren, M. J.; Tehrani, K. H. M. E.; Kotsogianni, I.; Wade, N.; Bruchle, N. C.; Mashayekhi, V.; Martin, N. I., Cephalosporin Prodrug Inhibitors Overcome Metallo-β-Lactamase Driven Antibiotic Resistance. *Chemistry* **2021**, *27*, 3806-3811.

[3] Keltjens, R.; Vadivel, Subramanian K.; de Vroom, E.; Klunder, Antonius J. H.; Zwanenburg, B., A New Convenient Synthesis of 3-Carboxycephems Starting from 7-Aminocephalosporanic Acid (7-ACA). *Eur. J. Org. Chem.* **2001**, *2001*, 2529-2534.

[4] Tehrani, K. H. M. E.; Wade, N.; Mashayekhi, V.; Bruchle, N. C.; Jespers, W.; Voskuil, K.; Pesce, D.; van Haren, M. J.; van Westen, G. J. P.; Martin, N. I., Novel Cephalosporin Conjugates Display Potent and Selective Inhibition of Imipenemase-Type Metallo-β-Lactamases. *J. Med. Chem.* **2021**, *64*, 9141-9151.